UNIVERSIDADE DE LISBOA

INSTITUTO SUPERIOR TÉCNICO

Hydrological Modelling for Portugal

Pedro Chambel Filipe Lopes Leitão

Orientador: Doutor Ramiro Joaquim de Jesus Neves

Co-Orientador: Doutor Tiago Morais Delgado Domingos

Thesis approved in public session to obtain the PhD Degree in:

Environmental Engineering

Jury final classification: Pass with Merit

Jury

Chairperson: Chairman of the IST Scientific Board

Members of the committee:

Doutor Raghavan Srinivasan

Doutor Ramiro Joaquim de Jesus Neves

Doutor Pedro Manuel Hora Santos Coelho

Doutor Gabriel Paulo Alcântara Pita

Doutor Rodrigo de Almada Cardoso Proença de Oliveira

2016

UNIVERSIDADE DE LISBOA
INSTITUTO SUPERIOR TÉCNICO

Hydrological Modelling for Portugal

Pedro Chambel Filipe Lopes Leitão

Orientador: Doutor Ramiro Joaquim de Jesus Neves

Co-Orientador: Doutor Tiago Morais Delgado Domingos

Thesis approved in public session to obtain the PhD Degree in:

Environmental Engineering

Jury final classification: Pass with Merit

Jury

Chairperson: Chairman of the IST Scientific Board

Members of the committee:

Doutor Raghavan Srinivasan, Professor, Texas A&M University, USA;
Doutor Ramiro Joaquim de Jesus Neves, Professor Associado do lnstituto Superior Técnico da Universidade de Lisboa;
Doutor Pedro Manuel Hora Santos Coelho, Professor Auxiliar da Faculdade de Ciências e Tecnologia da Universidade Nova de Lisboa;
Doutor Gabriel Paulo Alcântara Pita, Professor Auxiliar do lnstituto Superior Técnico da Universidade de Lisboa
Doutor Rodrigo de Almada Cardoso Proença de Oliveira, Professor Auxiliar do lnstituto Superior Técnico da Universidade de Lisboa.

Funding institutions: European Union, Instituto Superior Técnico

2016

Abstract

One of the difficulties in the management of water resources within the river basin is knowing the flow in each reach of a stream network. This problem is particularly aggravated by a lack of monitoring, now starting to be felt in Portugal after intensive monitoring in the 80s, 90s and 2000s. With the use of models you can use past data to implement and validate models, and get results for the present. Increasingly available results from the reanalysis of meteorological models allow hydrological models to be more easily forced.

As a general objective, this thesis aims at answering the following question: is it possible to apply a unified modelling strategy to estimate flows throughout the entire continental portion of the country? To prove this, a reach flow forecasting model was implemented in continental Portugal using precipitation data between 1950 and 2003 compiled by IPMA. The ability of the model to simulate the hydrology of watersheds and the limitations arising from the various options of implementation was evaluated. Results show that the model can satisfactorily reproduce flows, for example in Douro, while other watersheds, like Mondego, would need more detailed precipitation data to reproduce flows. The calibrated model was run with precipitation data from the MM5-R and the CSFR meteorological models with respectively 30 and 36 years of reanalysis as input. In general, model performance is reduced when using reanalysis. The decrease in performance is more significant in MM5-R than in CFSR. However some gage stations are an exception in this trend, because they improve their flows when compared with IPMA-GRID.

Finally a national database of runoff and evapotranspiration was generated with the hydrological model. The quality of the results was analysed by the spatial and temporal consistency between the results of the hydrological model and the results of the meteorological model and by comparison with the data of river flows.

KEYWORDS: watershed; flow; reanalysis; water management; evapotranspiration; SWAT; MOHID LAND; CFSR; MM5; rainfall–runoff model

Resumo

Uma das dificuldades na gestão dos recursos hídricos ao nível da bacia hidrográfica é conhecer o caudal em cada trecho da rede de drenagem. Este problema tem sido particularmente sentido pela falta de monitorização que agora se começa a fazer sentir em Portugal, depois da monitorização intensiva nos anos 80, 90 e 2000. Com os modelos é possível usar dados do passado para implementar e validar modelos, e obter resultados para o presente. Hoje em dia estão cada vez mais disponíveis resultados de reanálises de modelos meteorológicos, o que permite gerar o forçamento para modelos hidrológicos com mais facilidade.

Como objetivo geral, esta tese visa responder a seguinte pergunta: é possível aplicar uma estratégia de modelação unificada para estimar os fluxos ao longo de toda a parte continental do país? Para provar isso, foi implementado um modelo de previsão de caudais usando dados de precipitação do período de 1950 a 2003 compilados pelo IPMA. A capacidade do modelo para simular a hidrologia das bacias hidrográficas e as limitações decorrentes das várias opções de implementação, foi avaliada. Os resultados mostram que o modelo pode reproduzir fluxos satisfatoriamente, por exemplo no Douro, enquanto outras bacias, como Mondego, precisaria de mais dados detalhados de precipitação para reproduzir fluxos. O modelo calibrado foi corrido com dados de precipitação do MM5-R e os modelos meteorológicos CSFR com respectivamente 30 e 36 anos de reanálise como entrada. Em geral, o desempenho do modelo é reduzido ao utilizar reanálise. A diminuição no desempenho é mais significativa no MM5-R do que no CFSR. No entanto, algumas estações hidrométricas são uma exceção nessa tendência, porque melhoram os seus caudais, quando comparado com IPMA-GRID.

Foi ainda desenvolvida uma base de dados nacional de escoamento e evapotranspiração gerada com o modelo hidrológico. A qualidade dos resultados foi analisada através da consistência espacial e temporal entre os resultados do modelo hidrológico e os resultados do modelo meteorológico e através de comparação com os dados existentes de caudais fluviais.

Palavras-chave: bacia hidrográfica; caudal; reanálises; gestão de água; evapotranspiração; SWAT; MOHID LAND; CFSR; MM5; modelo de precipitação-escoamento

Agradecimentos

Ao Professor Ramiro Neves, agradeço toda a experiência e conhecimento que me passou para a elaboração desta tese. Agradeço inclusive os “empurrões” que me foi dando para a conclusão da mesma.

Agradeço a todas as pessoas com quem contactei ao longo dos anos no grupo Maretec. Foram muitas e de grande qualidade intelectual, que me é impossível numerá-las. Todas elas, assim como eu, tiveram em comum, a paixão por modelar o meio ambiente, em particular o ciclo hidrológico. Agradeço as longas discussões nos trabalhos que partilhei e desenvolvi com todos.

Ao Professor Tiago Domingos agradeço todo o apoio e tempo que me concedeu na revisão dos textos. Também toda a sua experiência científica foi importantíssima para a realização deste trabalho.

Aos colegas da Hidromod, agradeço o apoio e a visão empresarial que sempre sabem trazer para a modelação.

Finalmente ao Professor Raghavan Srinivasan agradeço o apoio e o contacto que me proporcionou ao longo de vários anos com a comunidade científica internacional do SWAT. Agradeço também a possibilidade que me foi concedida de trabalhar com o seu grupo na Texas A&M University.

Agradeço ainda, de um modo especial, à minha família todo o apoio dado durante a realização deste trabalho.

Overview

Chapter 1

The state of the art of hydrological modeling at the watershed scale is examined. A special emphasis is given to the SWAT.

Chapter 2

In this chapter an overview of the methodology used is shown.

Chapter 3

The methodology used to generate the sub-basin geometry is described. The geometries generated with two levels of detail are presented and justified as being the best to simulate the set of all watersheds in Portugal.

Chapter 4

Inputs of the model are defined with specific information about land use, soil properties and weather which were used as input for modelling the hydrology of Portugal. Special importance is given to the forcing of meteorological models: two reanalysis models, CFSR and MM5-R, with about 30 years of data. Precipitation values from reanalysis are compared with measurements of precipitation available in SNIRH and with IPMA-GRID, a gridded precipitation data set from IPMA.

Chapter 5

This chapter describes the flow data available to evaluate the model results. Then, an evaluation of the modelling results using precipitation inputs from three sources (IPMA-GRID, MM5-R and CFSR) is made followed by an approach to the Calibration/Validation of the model at the national level. Based on the calibration results, a Portugal Hydrological database was produced and described. A temporal and spatial analysis was performed on the database results. An assessment of complementarities with the national monitoring network is also made.

Chapter 6

This chapter presents the main conclusions from this thesis alongside all the future work foreseen based on the results of the thesis.

Appendix

The appendix is divided in two parts.

Appendix A is related with the detailed information on inputs and outputs of the modelling.

Appendix B is an extended Appendix including two papers related with Hydrologic Modeling in Portugal using MOHID LAND.

The first paper has the following title: "MOHID LAND - Porous Media, a tool for modelling soil hydrology at plot scale and watershed scale". It describes MOHID LAND Porous Media, which was the component of the model where the author of this dissertation was mostly involved. Paper compares soil moisture results with results from Hydrus model. Simulation is made in an agriculture field in Sorraia Basin.

The second paper was presented in the 13º Congresso da Água with the flowing title: "Operational System for Streamflow Forecasting to Support Hydroelectric Production Management". It presents an operational system to generate flows based on MOHID LAND and SWAT model.

Table of contents

Figure Index

Table Index

Notation

APA	Agência Portuguesa do Ambiente
ARS	Agricultural Research Service (USDA)
CFSR	Climate Forecast System Reanalysis
CLC	Corine Land Cover
CN	Curve Number (from SCS runoff equation)
DEM	Digital Elevation Model
ECMWF	European Centre for Medium-Range Weather Forecasts
ERA	European Reanalysis
ESDB	European Soil Database
ETRS	European Terrestrial Reference System
EU	European Union
FTP	File Transfer Protocol
GFS	Global Forecast System
GLUE	Generalized Likelihood Uncertainty Estimation
HARP	Harmonised Quantification and Reporting Procedures for Nutrients
HRU	Hydrologic Response Unit
HYPRES	Hydraulic Properties of European Soils
HSG	Hydrologic soil group
IPMA	Instituto Português do Mar e da Atmosfera
IPMA-GRID	Gridded precipitation from IPMA
IST	Instituto Superior Técnico
JRC	Joint Research Centre
MM5	Meteorological Model 5
MM5-R	MM5 reanalysis application to Portugal
MMU	Minimum Mapping Unit
MOHID	MOdelo HIDrodinâmico (“hydrodynamic model” in Portuguese)
NAO	North Atlantic Oscillation
NCDC	National Climatic Data Center (NOAA)
NCEP	National Centers for Environmental Prediction (NOAA)
NOAA	National Oceanic and Atmospheric Administration
NOMADS	National Operational Model Archive and Distribution System (NOAA)
NSE	Nash-Sutcliffe model efficiency
PBIAS	Percent bias

PET	Potential Evapotranspiration
PTRDB	Pedotransfer Rules Database
SCS	Soil Conservation Service
SGDBE	Soil Geographical Database of Eurasia
SMU	Soil Mapping Units
SNIRH	Sistema Nacional de Informação de Recursos Hídricos
SPADE	Soil Profile Analytical Database
SRTM	Shuttle Radar Topography Mission
STU	Soil Typological Unit
SUFI	Sequential Uncertainty Fitting Version
SWAT	Soil and Water Assessment Tool
USDA	U.S. Department of Agriculture
USGS	U.S. Geological Survey

Chapter 1

1 Introduction

1.1 Background

1.1.1 Water managers

Within the Earth system, water is stored in three main reservoirs: oceans, atmosphere and land, and is continuously cycling between these reservoirs (Figure 1). The water stored and continuously flowing on land is the main source of water for human activities. Water is a shared resource that brings together the protection of the environment, food production and energy generation as well as other sectors. Each water-dependent sector has its one water manager.

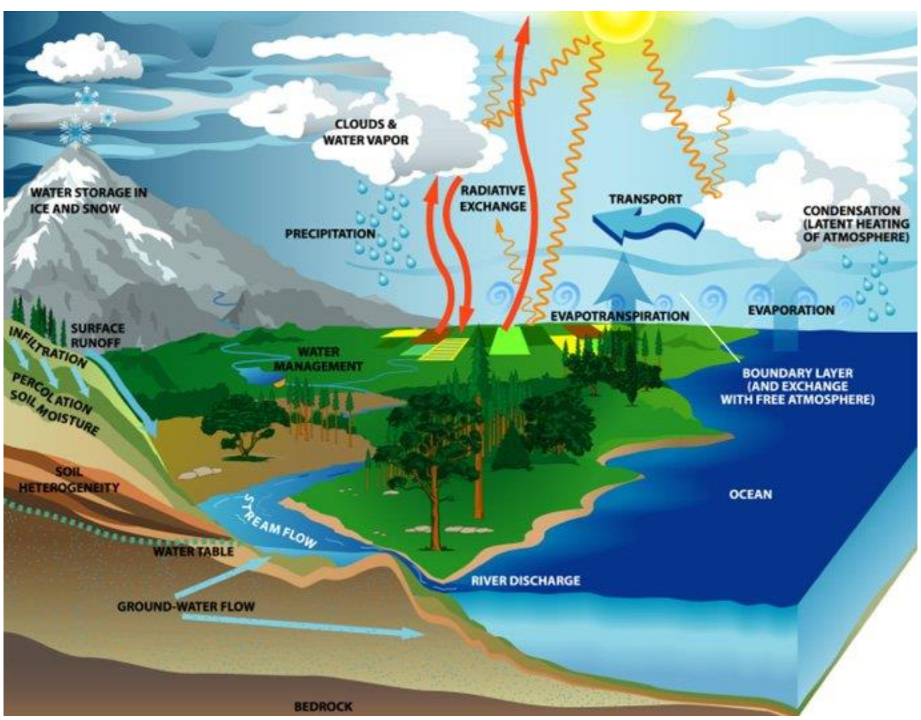

Figure 1 - The water cycle dominates the Earth-climate system. Schematic of the water cycle (UN-Water. and Unesco., 2009)

All of them have to guarantee the quantity and quality of water for their intended use. Water regulators are above the water managers. They have to guarantee that the remaining managers have water. These managers include irrigation water managers, urban water supply managers, managers of water for recreation, industrial water managers, hydro-energy managers. At a lower level the local water managers have to deal with problems of water saving, having to decide when and how to use the water.

Water control managers who regulate multipurpose projects need access to timely and accurate information on which to base decisions. During a flood event, decisions sometimes have to be made within minutes or hours from the onset of rising river stages. During a drought, decisions can affect water availability for months into the future. Water control managers need continuous real-time data observations from field sites, as well as reliable watershed modelling tools, to provide appropriate responses to changing hydrologic and water quality conditions.

1.1.2 World water management

The entire world is experiencing changing patterns of water use as a result of changes in land use. In developing countries the occupation of natural landscapes by agriculture is a major cause, and developed countries are facing changes in crops. In both cases, economic reasons pushed by the globalization of world trade play an important role. Also in both cases further global changes are expected as a result of climate change.

Water availability is essential for socio-economic activities and citizens expect catchment managers to take the necessary measures to assure quantity and quality for direct and indirect human consumption. Kaufman (2012) raises the question of the possible transformation of water into a commodity. From this perspective, the worldwide water budget can become a measure of the prosperity of a country whereas evapotranspiration can become an expense. Knowledge of the processes determining water fate, actual reserves and the capacity to forecast water consumption are essential for a catchment manager's decision-making.

Other authors have named evapotranspiration as green water flow (Falkenmark and Rockström, 2006). These authors associate green water flow to biomass production that is paramount for food production (Figure 2). The proportion of undernourished people is 12.9 per cent in 2014–2016, and the reduction of this percentage is the first Millennium Development Goal (UN, 2015). To obtain this goal, changes to the green water flow might have to happen. The green water flow has two major components, transpiration that is a productive flow, and a nonproductive evaporative flow from soil, ponded water (ex: rice), and intercepted water from foliage surfaces. Green water is mostly stored in unsaturated zone. However part of it could also be stored in the saturated region due to capillary rise or deep root plants. Remaining stored water is blue water, that is stored in aquifers, reservoirs, lakes and streams. Blue water, flows in to the ocean or it can also have a evaporation flux to the atmosphere.

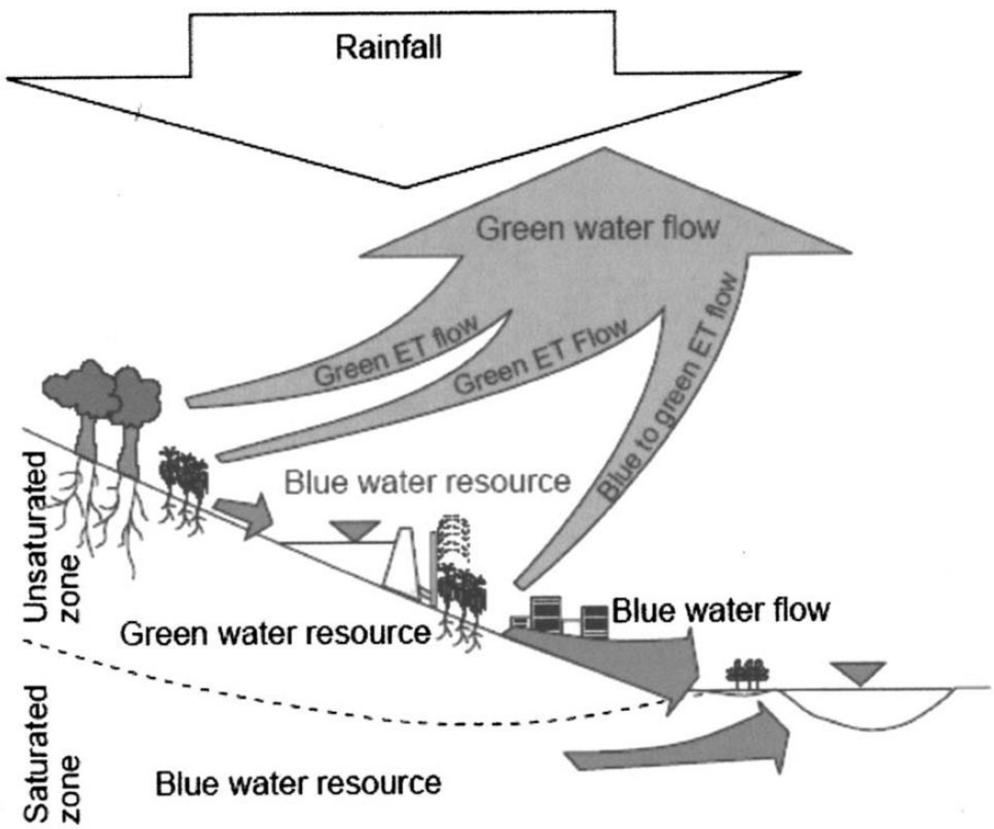

Figure 2 - Conceptualization of green-blue water in the context of water-resource planning and management (Falkenmark and Rockström, 2006)

1.1.3 Numerical models for water managers

Based on the available data and in the simulation models (catchment and reservoir) it is possible to get an early view of the possible evolution of the reservoir and act accordingly. This way it is possible to simulate in real time the effects of an emergency (or accidental) discharge in the reservoir, the potential effects of a decision that involves the modification of the soil use (erosion, nutrient sources, etc.) or the possible effects of different outflow options for reservoir management. An example is the estimation of pollutant loads in Ardila watershed using the SWAT model (Durão et al., 2012).

Models provide forecasts and alternative management scenarios based on technical and scientific information of land use, soil type, weather, etc. In other words the hydrologic models allow the customization of each solution's specificities, allowing the connection between drivers and pressures (agriculture practices, climate changes, etc.) and the state of the water. Some examples include the use of watershed models with hydrodynamic models aiming at integrated coastal water management (Campuzano et al., 2013).

Many hydrologic studies have been successfully accomplished at the Hydrographic Region scale, namely in Portugal, where the Management Plans of the Hydrographic Region have been concluded: the Alentejo and Algarve plans used SWAT for the catchment water budget (LEITÃO et al., 2012a). This approach was possible due to the extensive availability of data in the National SNIRH water web portal. Also, the existence of national-scale weather forecast models allows the implementation of water budget forecasts at the catchment level. In Spain data are not publicly available, which makes the task of implementing and calibrating the models more difficult. The successful application of models to Portugal, using the available data, suggests that this approach can be applied (or extended) throughout the entire continental portion of the country.

Land use change drives the modification of three interdependent global variables of the watershed: evapotranspirated water, biomass production and the organic matter content of soil. The assessment of the consequences of land use changes requires the capacity to study those global variables at an integrated level. Catchment models can simulate those interactions, together with all the processes that determine plant dynamics, and are major tools not only for integrated studies, but also to decision-makers.

Catchment models require field data for validation, but also for the specification of parameters and boundary conditions. Satellite data are inexpensive and are regularly collected at the catchment scale. Together with in-situ point data, they can supply model data needs. The combination of these three sources of data provides a continuous spatial-temporal description of the water path and water quality that allows the forecasting capacity required by managers and optimizes the cost/benefit ratio. A good example on the use of this satellite data to support modelling was MyWater FP7 project (Hartanto et al., 2015).

After implementation and calibration, the model can be used for studying processes and assessing scenarios, but it can also be run operationally in order to generate daily forecasts based on meteorological forecasts. This model can be validated by comparing the model solution with satellite images, whenever they are available, and can generate the data required by catchment managers to assess water availability and water requirements.

The main problems that can be addressed by these types of models are water availability in the soil for agriculture, water availability in reservoirs for water managers and flood dynamics for civil authorities and urban managers. With these users in mind, I have co-supervised 4 theses that have water budget assessments. One included a water budget assessment at the soil scale (Barão, 2007), two included a budget assessment in small scale watersheds (Costa, 2009, Gonçalves, 2006) and the other comprised spatial interpolation methods for rain (Eccel, 2011). The first thesis dealt with difficulties and uncertainties related with the soil. The second with the uncertainties in flow and precipitation measurements and the third with the spatial distribution of the measured precipitation. One of the main challenges today is communicating uncertainty in hydro-meteorological forecasts to water managers (Ramos et al., 2010).

This thesis focuses on a water budget analysis in Continental Portugal Catchments. A catchment water budget is essential for water managers because water consumption is increasing and from the viewpoint of adaptation to climate change it is very important to know the water budget components. It is, however, very expensive to measure all the budget components (precipitation, evapotranspiration, infiltration, aquifer recharge, etc.). However, there are some models that bring together all the processes, and there have been several attempts to validate each of their components.

1.2 State of the art

Two main aspects of this thesis are innovative or different from what has been done in the past: first the application to Continental Portugal of a catchment model using different sources of precipitation as input; and finally, the generation of a seamless database (in time and space) on hydrology for Portugal.

1.2.1 Large scale modelling

Large scale applications of hydrologic models have been described in the bibliography. In particular SWAT has had some applications. The suitability of SWAT for very large-scale applications has been shown in the "Hydrologic Unit Model for the United States" project (HUMUS) (Arnold et al., 1999, Srinivasan et al., 1998). Abbaspour et al. (2015) used SWAT to build a hydrological model of Europe at the subbasin level and with monthly time intervals Abbaspour et al. (2015). In particular, components such as blue water flow (water yield plus deep aquifer recharge), green water flow (evapotranspiration), green water storage (soil moisture), and nitrate concentration of groundwater recharge are quantified. The model estimations at the subbasin level are then aggregated to country and river basin levels for comparison with other studies. At a national level SWAT has been applied, for example to Iran. In this application, results explicitly differentiate between the different freshwater components: blue water flow, green water storage and green water flow (Faramarzi et al., 2009).

An example of implementation of a large scale operational model is EFAS (The European Flood Awareness System). EFAS is a European Commission initiative to generate alerts for riverine floods across Europe. LISFLOOD is the model used in EFAS and it is a spatially distributed, grid-based rainfall-runoff and channel-routing model. LISFLOOD has been specifically designed for large river catchments (Thielen et al., 2009, Van Der Knijff et al., 2010). In a recent paper, other models' suitability to be used with EFAS was evaluated. The SWAT model was one of the possible alternatives (Kauffeldt et al., 2016).

Some efforts have been made in the past to generate worldwide water budget for rivers (Fekete et al., 1999). However the uncertainty of such estimations is high due to low spatial and time detail. Each calculation cell had an area of approximately 2000 km^2 and the input and output were monthly. The author specifies that the correlation between measured and estimated discharge was low. This was because of coarse precipitation distribution and also because the precipitation used had low correlation with measured discharge values. This also means that the error is reduced for bigger watersheds.

Many applications of SWAT were found in the bibliography. None were found where an application was made to continental Portugal, like the one presented in this thesis. However an operational application of MOHID LAND that generates flows to the Portuguese Coast was described in the bibliography (Brito et al., 2015).

1.2.2 Precipitation data

There are many references describing the forcing of hydrological models with reanalysis. Some focus on using reanalysis of relatively coarse resolution global models (Mesinger et al., 2006) and others on the use of high-resolution atmospheric data from downscaling global reanalysis (Kanamaru and Kanamitsu, 2007, Stefanova et al., 2012). In the work of Stefanova et al. (2012) the seasonal cycle of precipitation is particularly well simulated. This is justified by the authors by the ability of the regional model to provide a more accurate representation of the spatial and temporal structure of finer-scale phenomena such as fronts and sea breezes. Because of these results, the scientific community involved with the hydrological modelling of the Earth system is showing a growing demand for reliable high-resolution meteorological data sets that provide fine spatial and temporal detail of near-surface variables.

Trigo et al. (2004) tried to relate reanalysis results with flows in the largest watersheds in Portugal, but did not use a hydrologic model. His study has shown that large inter-annual variability in the flows of Douro, Tejo and Guadiana rivers is largely modulated by North Atlantic Oscillation (NAO). However this study used a reanalysis with a resolution of about 210 km that was developed by Kalnay et al. (1996).

At least one study was found where the author used gridded data from a meteorological institute in Poland (Berezowski et al., 2015). Like the gridded precipitation used in this thesis (IPMA-GRID), this gridded precipitation was obtained with measurements.

No study was found where a hydrologic model was tested with reanalysis and with gridded precipitations simultaneously. Typically the tests are made comparing hydrologic models forced with reanalysis and forced with point measurement data sets.

However references were found comparing directly gridded precipitation datasets with reanalysis (Belo-Pereira et al., 2011).

1.2.3 Databases

Some recent attempts are described in the bibliography to obtain hydrological databases (Tan, 2014, Granato, 2014). The study produced for Malaysia (Tan, 2014) concludes that it was possible to setup such a database based on the statistical analysis of the flows; however, it was limited to monthly simulations rather than daily streamflow modelling. The US database (Granato, 2014), was produced to help water managers to deal with risks of drought. A database and associated decision support system was proven to work on a site with long series of stream flow and with data on water use.

Also, examples on the web focused on databases existing in different countries. In the Iberian peninsula there are two of these systems: SNIRH (Sistema Nacional de Informação de Recursos Hídricos – National Information System of Water Resources) in Portugal and SAIH (Sistema de Informações Hidrológicas Automática – Automatic Hydrological Information System). In Brazil Hidroweb is the name of the National Hydrologic Information System managed by ANA (Agência Nacional das Águas – National Water Agency). The same agency provides real-time data through the DHTR (Dados Hidrológicos em Tempo Real – Hydrological Data System in Real Time). In the US the corresponding system is the National Water Information System (NWIS), which supports the acquisition, processing, and long-term storage of water data. These systems capture, transmit, process (and in some cases validate) the data describing the state of the rivers and hydraulic structures. The aim is to help the management of water resources, forecasting and monitoring floods and droughts. For this, they pursue continuous archiving of hydrological data and its availability to assist the hydrological situation, present and past. However, data is only made available partially through a web filter. This makes data search and analysis more difficult. Presently the main difference between the Portuguese and the Brazilian and US system is that the Portuguese system has a very limited availability of real time data, due to financial restrictions.

An example of a global database of stream flow is the Global Runoff Data Center (GRDC), which operates under the auspices of the World Meteorological Organization (WMO). The GRDC maintains the Global Runoff Database (GRDB). To keep the database up to date, the Center is in touch with national institutions, trans-national organizations and partner data centres. The river flow data is provided through a request form and does not have a web interface to directly download data.

None of these databases appear to provide modelling results. The innovative product of this thesis is a database of modelled flows, at the scale of Continental Portugal.

1.2.4 Watershed models

One important step for this thesis is the choice of watershed model to use. Some of the differences between models will be highlighted to support the choice made.

The major methodological difference between models generally relies in their physical or empirical approach. In this perspective, models are normally separated into mechanistic models (process models) and phenomenological models (empirical models). However, physically-based models can have empirical equations to allow model parameterization in the most unknown processes. The importance of each component normally results in a trade-off on model complexity. MOHID LAND is an example of a very mechanistic model, while SWAT is more empirical (Figure 3).

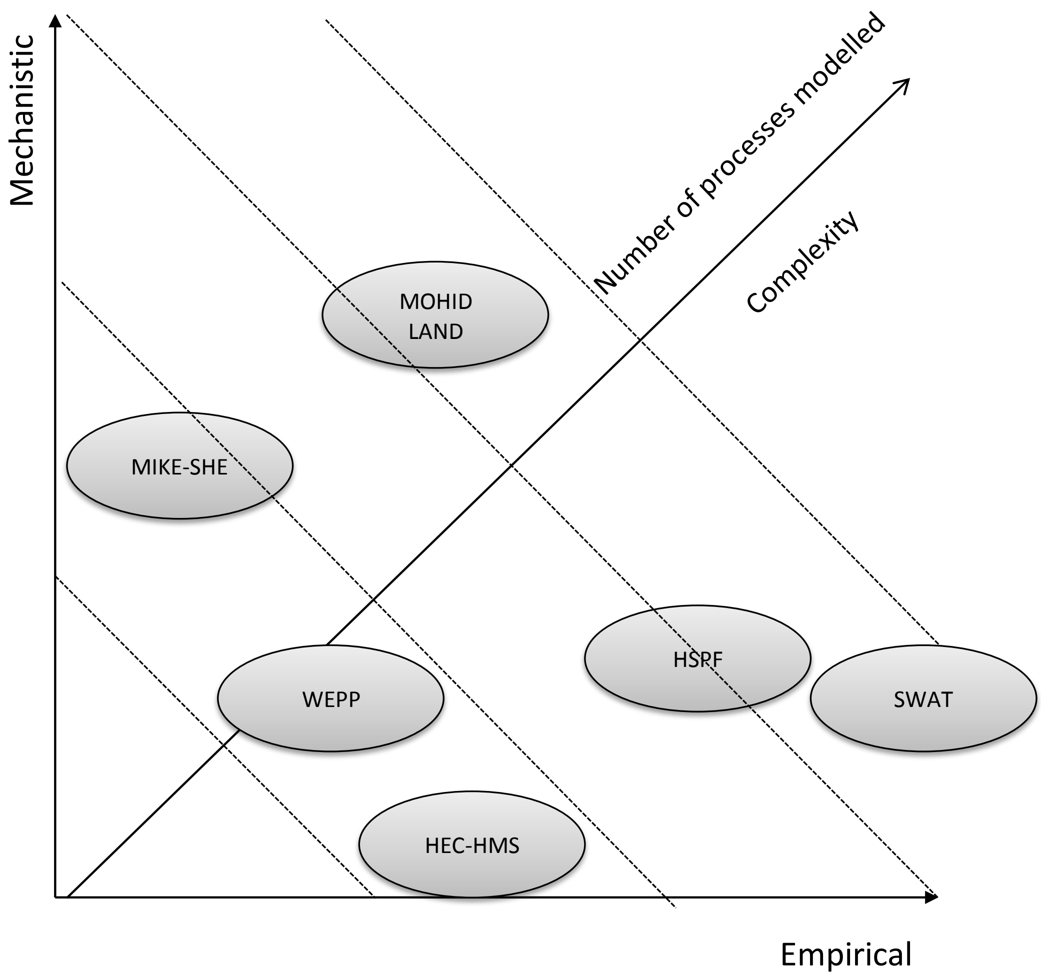

Figure 3 - Graph on the distribution of models in terms of empirical or mechanistic weight of implemented equations

Many papers have been written comparing the different existing models. Some papers compare the models' suitability for specific purposes (Borah and Bera, 2003, Silgram et al., 2009, Daniel et al., 2011). Borah and Bera (2003) made a general comparison between watershed models classifying them and distinguishing their different approaches. Daniel et al. (2011) presents a comparison between different watershed models. In Table 1 some characteristics of the most referenced models in the literature are presented.

Table 1 - Watershed Models. Main Characteristics and Features (adapted Daniel et al. (2011))

Model	Suited Applications	Main Components	Runoff on Overland	Subsurface Flow	Chemical Simulation	Spatial Scale	Temporal Scale	Watershed Representation	Availability
HEC1/ HECHMS	Suited for urban watersheds; widely used for modelling floods and impacts on land use changes	Precipitation, losses, baseflow, runoff transformation & routing	CN, kinematic wave equations	No component	No component	SD	E	Dendritic network or grid	Pu
HSPF	Suited for both agriculture and urban watersheds; diverse water quality and sediment transport at any point on the watershed	Runoff /water quality constituents, simulation of pervious/impervious areas, stream channels & mixed reservoirs	Empirical outflow	outflow, percolation; groundwater	Soil/water temp., DO, CO2, N, NH3, organic N/P, N/P, pesticides	SD	C.	Pervious /impervious land areas, stream channels, & mixed reservoirs; 1-D simulations	Pu
WEPP	watershed and analysing hydrologic and soil erosion in small watersheds	soils, snow accumulation and melt, irrigation, infiltration, overland flow hydraulics, water balance, plant growth, erosion, deposition & residue decomposition	Kinematic wave equations	Green Ampt equation	No component	D	C	Channel segments & impoundments	Pu
MIKE SHE	Wide range of spatial and temporal scales; modular design facilitates integration of other models; advanced capabilities for water quality, parameter estimation and water budget analysis	Interception, overland/channel flow, unsaturated/saturated zone, snowmelt; aquifer/rivers exchange, advection/dispersion of solutes, geochemical processes, plant growth, soil erosion & irrigation	2-D diffusive wave equations	3-D groundwater flow	Dissolved coservative solutes in surface, soil, & ground waters	D	E, C, variable steps	2-D rectangular /square overland grids; 1-D channels; 1-D unsaturated/ 3-D saturated flow	Pr
SWAT	watersheds; excellent for calculating TMDLs and simulating a wide variety of conservation practices and other BMPs; successfully applied across watersheds in several countries	Hydrology, weather, sedimentation, soil temperature and properties, crop growth, nutrients, pesticides, agricultural management and channel & reservoir routing	CN for runoff ; SCS TR-55 for peak flow	Lateral subsurface flow/ ground flow	N, P, pesticides, C	Semi-Distributed (SD)	C, daily steps	Sub-basins based on topography, HRU, ponds, groundwater, & main channel	Pu

Type: F; Agriculture Watershed - A; Urban Watershed - U; Spatial Scale: Semi-Distributed - SD; Distributed - D;

Temporal Scale: Continuous - C; Event-base - E; Availability: Public - Pu; Proprietary - Pr

Many references of watershed models are related to non-point pollution, specifically nitrogen and phosphorous. In particular, these references try to relate land use changes and climate changes with water quality.

For example, Silgram et al. (2009) compares different nutrient export models in their suitability to simulate flows and diffuse sources of nutrients. The only model mentioned in both Silgram et al. (2009) and Daniel et al. (2011) is SWAT. They both conclude that models like SWAT require many parameters (i.e., local knowledge) and model results are sensitive to these parameter values and can significantly influence the results.

SWAT was chosen as the main tool for this dissertation, because it is the one with more references in the literature and because it is freely available.

1.2.4.1 SWAT

SWAT is the acronym for Soil and Water Assessment Tool, a river basin or watershed scale model developed by the USDA Agricultural Research Service (ARS). SWAT was developed to predict the impact of land management practices on water, sediment and agricultural chemical yields in large complex watersheds with varying soils, land use and management conditions over long periods of time.

It intended to be a model for evaluating the impact of agricultural practices at the watershed scale. In fact, it came at a time when there was a need to improve water quality. As point sources were getting more controlled, diffuse sources were the new target for improvements. In order to do that, the origins of the diffuse sources had to be understood using the scarce data available. Hydrology in the watershed is the main driver for the transport of nutrients. Thus hydrology is a minimum requirement to evaluate diffuse sources of nutrients. SWAT appeared as a model that could estimate hydrology from the available data. From the total of 1282 peer reviewed papers on SWAT, 484 were about Hydrology (Table 2). In fact, many peer review references were published in Hydrology Journals (Table 3).

Table 2 - Number of references per year about Hydrology (taken in 4 of June 2013 from https://www.card.iastate.edu/swat_articles/)

Year	Peer review references	Year	Peer review references
<2000	14	2007	21
2000	7	2008	45
2001	7	2009	42
2002	9	2010	54
2003	10	2011	72
2004	13	2012	133
2005	23	2013	25
2006	9	**Total**	**484**

Table 3 - Number of SWAT references per Journal (taken in 4 of June 2013 from https://www.card.iastate.edu/swat_articles/)

Journal	Peer review references
Hydrological Processes	68
Journal of Hydrology	43
Journal of the American Water Resources Association	35
Transactions of the ASABE	29
Hydrology and Earth System Sciences	19
Journal of Hydrologic Engineering	17
Transactions of the ASAE	17
Water Resources Research	13
Agricultural Water Management	11
Hydrological Sciences Journal	10
Water Resources Management	10
Water International	9
Advances in Water Resources	8
Climatic Change	8
Other Journals	187
Total	484

Some of the more frequently studied aspects of hydrology include climate changes, hydrologic assessment, calibration and input effects (Table 4).

Table 4 - Number of SWAT references per application category (taken in 4 of June 2013 from https://www.card.iastate.edu/swat_articles/)

Application category	Peer review references
climate change	86
hydrologic assessment	80
calibration, sensitivity, and/or uncertainty analysis	73
input effects	44
model comparison	30
model interface	27
land use effects	26
climate data effects	17
groundwater and/or soil water impacts	14
crop water productivity or blue/green water	10
irrigation or water allocation impacts	10
Crop growth/yield or plant parameters	9
snowmelt processes	9
evapotranspiration assessment	7
Other Category	42
Total	484

SWAT incorporates features of several previous USDA Agricultural Research Service (USDA-ARS) models and is a direct outgrowth of the SWRRB model (Simulator for Water Resources in Rural Basins) (Arnold et al., 1990, Williams et al., 1985). Specific models that contributed significantly to the development of SWAT were CREAMS (Chemicals, Runoff, and Erosion from Agricultural Management Systems) (Knisel, 1980), GLEAMS (Groundwater Loading Effects on Agricultural Management Systems) (Knisel, 1993), and EPIC (Erosion-Productivity Impact Calculator) (Williams et al., 1985).

In response to the Clean Water Act, the ARS assembled a team of interdisciplinary scientists from across the U.S. to develop a process-based, nonpoint source simulation model in the early 1970s. From that effort CREAMS was developed. CREAMS is a field scale model designed to simulate the impact of land management on water, sediment, nutrients and pesticides leaving the edge of the field. A number of other ARS models such as GLEAMS, EPIC, SWRRB and AGNPS trace their origins to the CREAMS model.

SWRRB is a continuous time step model that was developed to simulate nonpoint source loadings from watersheds.

EPIC (Erosion-Productivity Impact Calculator) was developed to determine the relationship between soil erosion and soil productivity throughout the U.S. (Williams et al., 1984). EPIC continuously simulates the processes involved, simultaneously and realistically, using a daily time step and readily available inputs. Since erosion can be a relatively slow process, EPIC is capable of simulating hundreds of years if necessary. EPIC is generally applicable, computationally efficient and capable of estimating the effects of management changes on outputs. The model must be comprehensive to define the erosion-productivity relationship adequately. EPIC is composed of physically-based components for simulating erosion, plant growth, and related processes and economic components for assessing the cost of erosion, determining optimal management strategies, etc. The EPIC components include weather simulation, hydrology, erosion-sedimentation, nutrient cycling, plant growth, tillage, soil temperature, economics and plant environment control. Typical results are presented for 15 of the 163 tests performed in the continental U.S. and Hawaii. These results generally indicate that EPIC is capable of realistically simulating erosion and crop growth.

GLEAMS (Groundwater Loading Effects of Agricultural Management Systems) is a mathematical model, developed for field-size areas, to evaluate the effects of agricultural management systems on the movement of agricultural chemicals within and through the plant root zone (Knisel, 1993).

SWAT's objective is to predict the long-term impacts in watersheds and also the ideal timing for agricultural practices within a year (i.e., crop rotations, planting and harvest dates, irrigation, fertilization, pesticide application rates and timing). It can be used to simulate, at the basin scale, water and nutrients cycle in landscapes whose dominant land use is agriculture. It can also help in assessing the environmental efficiency of BMP (Best Management Practices) and alternative management policies.

Presently, soil, land use, topographical and meteorological data are widely available, which highly increases SWAT's performance (Romanowicz et al., 2005). Precipitation is a determinant parameter for estimating flows and as Reungsang et al. (2007) showed, good quality precipitation data originated correlations of 0.72 (R2 Parsons coefficient) for monthly flows. Tripathi et al. (2003) showed that SWAT could accurately simulate runoff, sediment yield and nutrient losses, particularly from small agricultural watersheds. Tripathi et al. (2005) suggested BMP and predicted a reduction of sediment yield of 10-20% with the SWAT model as a result of those BMP. Chaplot et al. (2004) also showed, with a similar approach, that winter wheat replacing corn-soybean rotation resulted in a decrease of about 10% in sediment yield.

According to Arnold et al. (1999) cited in Arnold and Fohrer (2005), the model was validated against measured USGS stream flow data across the entire USA and was being validated against measured sediment loads. The model was also linked to national economic models and was used for national planning, addressing scenarios that include: (1) agricultural and municipal water use; (2) tillage trends; (3) fertilizer and animal waste scenarios; (4) flood prevention structures; and (5) cropping systems.

Srinivasan (Srinivasan et al., 1998) made sediment validation by comparing simulated and measured sediment in a watershed for two periods, 1965-68 and 1968-75. Sediment loads predicted by SWAT were 25 000 and 14 000 Mg for these two periods. These predictions were favourably compared with the corresponding measured sediment loads, 29 000 and 14 000 Mg, respectively. FitzHugh (FitzHugh and Mackay, 2001) shows results of SWAT's annual sediment loads calibration.

Arnold (Arnold et al., 2000) applied the SWAT model to the upper Mississippi River Basin, USA (492,000 km^2), in order to estimate recharge. SWAT (surfacewater) and MODFLOW (groundwater) codes have been integrated by Sophocleous (Sophocleous and Perkins, 2000). Huffman (Huffman, 2005) used SWAT to calculate recharges, which were then used as boundary conditions in MODFLOW model.

1.3 Rationale

1.3.1 General objectives

The author of the thesis has provided (over the last few years) model results for different types of water managers. Some examples are:

- Estimating inlet flows to Aveiro Lagoon in the Vouga river;
- Estimating flows for the reservoir manager in Portugal/Douro;
- Providing the irrigation water needs in Sorraia Valey;
- Catchment water budget for the Alentejo and Algarve plans.

Each one of the applications uses different sources of input data. This has the advantage of using the best data available in a tailored solution for each case. However this makes it difficult for inter-comparison of results and ultimately makes it difficult for Hydrography Region-wide or nationwide integrated water management.

As a general objective, this thesis aims at answering the following question: Is it possible to apply a unified modelling strategy to estimate flows throughout the entire continental portion of the country? For this, the quality of precipitation data and the flow modelled results are paramount. The goal will then be achieved if the quality of precipitation used as input can be proven and if resulting model flows compare well with measured flows.

The quality evaluation will be made on a monthly basis and for a few gage stations. This might not fit the requirements of all water managers. The idea is not a solution of one fits all, but a compromise where the time and spatial detail of the model are good enough for it to be used as common ground to discuss water resources shared between different water managers. In the past SNIRH delineated this common ground by providing measurements of water resources nationwide. Presently, financial constraints have forced most of the monitoring activity on water resources to stop. This thesis also tries to evaluate how close we can get to such a system but using model results of flow.

Ultimately a national platform for surface water management could be set up and validated by using direct and indirect methods. Direct methods include the comparison of the model results with real measurements (e.g. flow, soil moisture, etc.), whereas indirect methods involve the comparison with values associated with the water budget (e.g. EO data, energy budgets). In this thesis a nationwide direct validation with flows is made.

The approach presented does not include river flows coming from Spain nor does it calculate the effect of reservoirs in river flows. Because of this, evaluated flows only included gage stations with a drainage area less than 5000 km^2 and larger than 100 km^2.

1.3.2 Specific objectives

- Set up a watershed model for Continental Portugal with seamless data of topography, land use, soil and weather;
- Evaluate the quality of precipitation datasets
- Evaluate model performance in terms of estimated flows, using reanalysis and gridded precipitations as inputs;
- Set up a database of modelled flows, at the scale of Continental Portugal.

Chapter 2

2 Methods

2.1 The water budget

A watershed is the area of land that drains rainfall, snowmelt, sediment and dissolved materials to a particular water body, such as a stream, river, lake, reservoir or marine harbour. Watershed boundaries can be drawn on topographical maps by linking all the surrounding high points in the land, as shown in the diagram below; the dotted lines represent the watershed boundaries or "divides" (Figure 4). All watersheds, regardless of size, consist of the basin within these boundaries and the surface water body (or bodies). The physical characteristics of a watershed – the geology, soil, vegetation and slope, as well as human land uses – influence the quality and quantity of the water that flows through it.

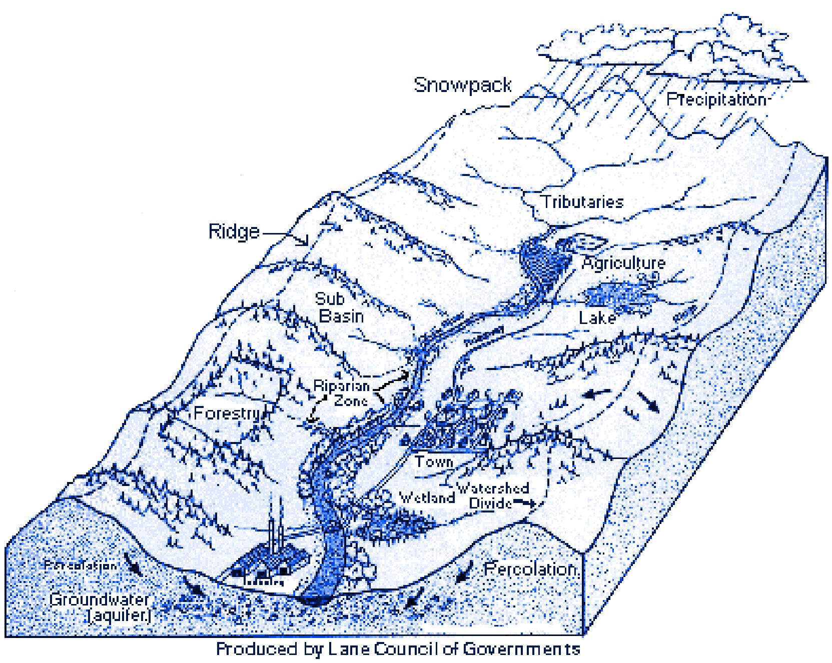

Figure 4 - Watershed model Source: http://water.epa.gov/type/watersheds/whatis.cfm

The volume variation of a watershed ($\partial S/_{\partial t}$ where S is stored volume and t is time) depends on the fluxes of the watershed. The possible fluxes are Precipitation (P), Evapotranspiration (ET), Flow in outlet of watershed (Q_{CH}) and Flow through aquifer in or out of watershed boundaries (Q_{GW}).

$$\frac{\partial S}{\partial t} = P - ET - Q_{ch} - Q_{gw} \qquad \mathbf{1}$$

This means that the stored volume of the watershed at a certain instant depends on the stored volume at the previous instant plus precipitation and minus all the other outgoing volumes:

$$\frac{S_2 - S_1}{\partial t} = P - ET - Q_{ch} - Q_{gw} \Leftrightarrow S_2 = S_1 + \left(P - ET - Q_{ch} - Q_{gw}\right) \cdot \partial t \qquad \mathbf{2}$$

The precipitation falling on the watershed is either transformed into a flux or stored in the watershed. The possible fluxes are Evapotranspiration (ET), Flow in outlet of watershed (Q_{CH}) and Flow through an aquifer in or out of watershed boundaries (Q_{GW}). The possible storage media in the watershed (∂S) are: i) porous media like soils and aquifers; ii) soil surface or vegetation surface; iii) reservoirs and channels; iv) solid water reservoirs like ice and snow. This can be resumed in the following equation

$$P * \partial t = \partial t\left(ET + Q_{ch} + Q_{gw}\right) + \partial S \qquad \mathbf{3}$$

This simple equation will help understand the following balance equation of SWAT.

2.2 SWAT model

SWAT requires specific information about weather, soil properties, topography, vegetation and land management practices occurring in the watershed. The physical processes associated with water movement, sediment movement, crop growth, nutrient cycling, etc. are directly modelled by SWAT using this input data (Figure 5).

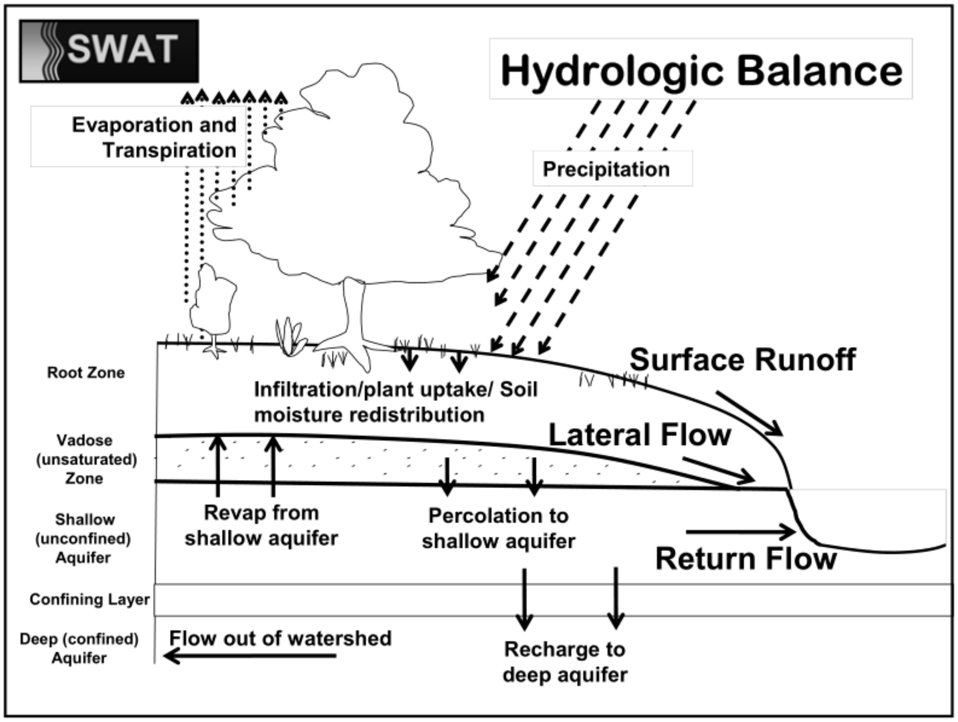

Figure 5 - Water budget fluxes at HRU (source: SWAT course slides)

In SWAT, the simulated basin is divided into several sub-basins. Each sub-basin can be divided into many HRU (Hidrologic Response Units – units with the same land use and soil type) or there can be only one HRU. Each HRU has the soil surface as the superior boundary and the aquifer as the inferior boundary. It receives precipitation (*PRECIP*) from the superior boundary, part of which is converted into runoff ($SURQ\_CNT$) and another part is infiltrated. The part that is converted into runoff is directed to the sub-basin channel, whereas the parcel that infiltrates is carried along the soil profile, being able to evapotranspirate (ET), to be percolated to the aquifer or carried laterally along the soil profile until it reaches the channel ($LATQ$), or it can be stored in the soil (ΔS). The water that reaches the aquifer is lost to the stream (GW_Q), to the deep aquifer (DA_{RCHG}) or, finally, to the atmosphere (*REVAP*). *REVAP* is in fact an indirect way of simulating capillary rise, because the SWAT soil module can only distribute water in the soil profile with a downwards flux. The equation below summarises the water budget for each HRU:

$$PRECIP = ET + DA_{RCHG} + REVAP + LATQ + GW_Q + SURQ\_CNT + \Delta S \quad \mathbf{4}$$

SWAT model fluxes can be compared with the conceptual budget shown in section 2.1 and resumed in equation 3: $ET = ET + REVAP$, $Q_{ch} = LATQ + GW_Q + SURQ\_CNT$, $Q_{gw} = DA_{RCHG}$. SWAT fluxes can also relate with the green and blue water flow mentioned in 1.1.2:

$$GreenWaterFlow = ET + REVAP \quad (5)$$

$$BlueWaterFlow = LATQ + GW_Q + SURQ_{CNT} + DA_{RCHG} \quad (6)$$

Table 5 summarizes the SWAT fluxes presented in equation 4 at the HRU level, shown in the previous equation.

Table 5 – Water budget fluxes at HRU

Variable name	Definition
PRECIP	Total amount of precipitation falling on the HRU during time step (mm H2O).
ET	Actual evapotranspiration (soil evaporation and plant transpiration) from the HRU during the time step (mm H2O).
DA_{RCHG}	Deep aquifer recharge (mm H2O). The amount of water from the root zone that recharges the deep aquifer during the time step. (shallow aquifer recharge = GW_RCHG - DA_RCHG)
REVAP	Water in the shallow aquifer returning to the root zone in response to a moisture deficit during the time step (mm H2O). The variable also includes water uptake directly from the shallow aquifer by deep tree and shrub roots.
SURQ_CNT	Surface runoff contribution to streamflow in the main channel during time step (mm H2O).
LATQ	Lateral flow contribution to streamflow (mm H2O). Water flowing laterally within the soil profile that enters the main channel during time step.
GW_Q	Groundwater contribution to streamflow (mm H2O). Water from the shallow aquifer that enters the main channel during the time step. Groundwater flow is also referred to as baseflow.

Because the evapotranspiration rate is strongly influenced by a number of vegetative surface characteristics, PET is the rate at which evapotranspiration would occur from a large area uniformly covered with growing grass, with uniform height, never short of water and completely shading the ground. The Penman-Monteith method describes the equation to estimate PET. Once total potential evapotranspiration is determined, actual evaporation must be calculated. SWAT first evaporates any rainfall intercepted by the plant canopy. Next, SWAT determines the maximum amount of transpiration and the maximum amount of sublimation/soil evaporation.

Plant growth in SWAT is estimated using the heat unit theory. This theory postulates that plants have heat requirements that can be quantified and linked to the time to reach full maturity. Because a plant will not grow whenever the mean temperature falls below its base temperature, the only portion of the mean daily temperature that contributes towards the plant's development is the amount that exceeds the base value. To measure the total heat requirements of a plant, the accumulation of daily mean air temperatures above the plant's base temperature is recorded over the period of the plant's growth and expressed in terms of heat units.

Runoff in SWAT is based on the SCS runoff equation, which is an empirical model that was the product of more than 20 years of studies involving rainfall-runoff relationships from small rural watersheds across the U.S. The model was developed to provide a consistent basis for estimating the amounts of runoff under varying land use and soil types. Based on those studies the SCS Curve Number (CN) procedure was developed, where CN is an empirical parameter to predict direct runoff from rainfall.

Manning's equation for uniform flow in a channel is used to calculate the rate and velocity of flow in a reach segment and also to estimate overland flow.

Percolation is calculated for each soil layer in the profile. Water is allowed to percolate if the water content exceeds the field capacity for that layer. Water that percolates out of the lowest soil layer enters the vadose zone. The vadose zone is the unsaturated zone between the bottom of the soil profile and the top of the aquifer. An exponential decay weighting function in a precipitation/groundwater response model is used in SWAT to account for the time delay in aquifer recharge once the water exits the soil profile. The baseflow recession constant is a direct index of groundwater flow response to changes in recharge.

The version of ARCSWAT used was 2009.93.7b released on 8-9-2011. ArcSWAT GIS interface, the primary interface to the SWAT model was developed by Stone Environmental in collaboration with Texas A&M University and the Blackland Research Center. The SWAT executable used was revision 481, which corresponds to SWAT2009 released on 16/06/2011 (http://www.public.iastate.edu/~tdc/swat_versions.html).

2.3 Input data

Watershed modelling is data intensive in terms of input but also in terms of the data's calibration and validation. For many users, the process of getting data is so time consuming that they consider modelling watersheds an almost impossible mission. The SWAT model is a watershed model that has made a compromise between the available data and the input required, in such way that it is possible to apply it to almost everywhere in the world, even though there aren't always the best data available. SWAT requires specific information about weather, soil properties, topography, vegetation, presence of ponds or reservoirs, groundwater, the main channel and land management practices to simulate water quality and quantity. SWAT has become an effective tool to evaluate non-point source water resource problems (flow, sediment, nutrients) for a large variety of water quality applications, nationally and internationally.

The Water Framework Directive (WFD) implementation process requires the use of methodologies that generate cause-effect relations between land use/land management and water quality. SWAT is a model that allows the estimation of the nutrients that are exported from a watershed into reservoir models. Reservoir models like CeQualW2 enable the prediction of the water quality's evolution over time. Many studies have produced local results for this kind of coupling (Coelho and Chambel-Leitão, 2010). These studies are data intensive and rely on local available data of difficult access.

With internet and all the new data centers available (WISE for Europe, Africover for Africa, etc.), as well as new directives to make data easily available and searchable (INSPIRE, Metadata ISO, etc.), it is starting to be possible to build a Mosaic of data that makes SWAT application and validation possible in most of the world. This approach has been increasingly used by many researchers (Vu et al., 2011).

Nowadays, water managers have to deal with modified watersheds, mainly due to the reservoirs from which water is pumped, not only for irrigation, but also for urban and industrial water consumption. In some cases most of the pumped water returns to the watershed (as in urban water consumption), while in other cases some of the water will be lost by evapotranspiration (which is mainly the case of irrigation). For water managers, a first step for managing all the water needs is to know the amount of surface water generated by the watershed. SWAT could be a useful tool to make this estimation however the available flows could be influenced by the changes in the reservoirs.

Reservoirs and estuaries can also be used to validate the erosion and water quality of watershed models. In order to do so, the output of the watershed model is used as input for a reservoir and estuary model. A good result obtained with these models validates the overall result of the watershed model. The advantage of this methodology is that reservoirs and estuaries are generally better monitored in terms of sediments and water quality and have a buffer effect on watershed extreme events, which are more difficult to validate with measurements.

Satellites are also of great importance for watershed modelling. Shuttle Radar Topography Mission (SRTM) data is one of the best examples of this. Also all the European GMES effort has shown that is possible to set up many satellite derived products that are of great use for watershed modelling. An example of this is the GSE-Land project that implemented a series of water products based on satellite data. Among the many products, HARP-SWAT was one of those derived (Mateus, 2009).

2.4 Calibration and validation

A primary source of calibration in watershed models are measured flows. This calibration is needed due to many modelling uncertainties. Model uncertainties are due to: i) conceptual simplifications (e.g. ground water flow), ii) processes happening in the catchment but not included in the model (e.g. capillary rise), iii) processes that are included in the model, but which cannot be modelled due to data limitation (e.g. dams and reservoirs and water transfers), iv) input data quality, and v) quality of flows for calibrating (in particular their rating curves). This last uncertainty is important to take into consideration for calibration purposes.

In the calibration process, measured flows are compared with corresponding model estimates. In the first stage, the evaluation is performed mainly qualitatively by visually examining the agreement between observed data and model estimates. In the second stage, the agreement between model and data has to be made quantitatively in terms of misfit of model results. Typically these misfit assessments are functions of the error between measurements and model predictions.

The Nash-Sutcliffe model efficiency (NSE) (Nash and Sutcliffe, 1970) is one of the most used performance evaluators in river flows. NSE indicates how well the plot of observed versus simulated flows fits the 1:1 line (trends) and it is determined as follows:

$$NSE = 1 - \left[\sum_{i=1}^{n} (Y^{obs}{}_i - Y^{sim}{}_i)^2 / \sum_{i=1}^{n} (Y^{obs}i - Y^{mean})^2 \right] \qquad \mathbf{7}$$

where $Y^{obs}{}_i$ = i^{th} observation for the constituent being evaluated, $Y^{sim}{}_i$ = i^{th} simulated value for the constituent being evaluated, Y^{mean} = mean of observed data for the constituent being evaluated, and n = total number of observations. NSE ranges between -∞ and 1.0 (1 inclusive) with NSE = 1 being the optimal value. Values ≤ 0.0 indicate that the mean observed value is a superior predictor than the simulated value, which indicates unacceptable performance.

Another performance evaluator frequently used to evaluate flows is Percent bias (PBIAS) which measures the average tendency of the simulated data to be larger or smaller than their observed counterparts (Gupta et al., 1999). The optimal value of PBIAS is 0.0 with low magnitude values indicating accurate model simulation. Positive values indicate model underestimation bias, and negative values indicate model overestimation bias. PBIAS is computed as:

$$PBIAS = \left[\sum_{i=1}^{n} (Y^{obs}{}_i - Y^{sim}{}_i) * (100) / \sum_{i=1}^{n} (Y^{obs}{}_i) \right] \quad \mathbf{8}$$

where PBIAS is deviation of data being evaluated, expressed as a percentage. In the case of monthly flows Moriasi et al. (2007) suggested performance ratings based on references of flow modelling (Table 6). Estimated flows will be evaluated based on these performance ratings. The same criteria will be used to evaluate monthly precipitation.

Table 6 - General performance ratings for recommended statistics for a monthly time step (Moriasi et al., 2007).

Performance Rating	NSE	PBIAS (%)
Very good	0.75 < NSE < 1.00	PBIAS < ±10
Good	0.65 < NSE < 0.75	±10 < PBIAS < ±15
Satisfactory	0.50 < NSE < 0.65	±15 < PBIAS < ±25
Unsatisfactory	NSE < 0.50	PBIAS > ±25

After the calibration process, it is highly recommended to evaluate the performance criteria on a data set which is independent from the data used for model calibration (Janssen and Heuberger, 1995). We can call this evaluation the validation process. Validation assessment (like calibration) is made, in the first stage, with a qualitative evaluation of performance, mainly by visually examining the agreement between observed data and model estimates. In the second step, the agreement is made quantitatively.

Flow measurements are dependent on the validity stage-discharge relations (rating curves), because what is normally measured are the levels, and they are then transformed into flow. It is easy to understand that stage-discharge relations for stable controls, such as a rock outcrop and man-made structures such as weirs, flumes, and small dams, usually present few problems in their calibration and maintenance (Braca and Futura, 2008). On the other hand, many difficulties can arise when controls are not stable and/or when variable backwater occurs (Figure 6). For unstable controls, segments of a stage-discharge relation may change position abruptly, corresponding to a severe flood, or even continuously. An example is the scour and fill which is the process of first digging out and then refilling a channel instigated by the action of a stream or tide.

Besides changes in section control, a further factor which can affect stage-discharge relations both for stable and unstable channels is variable backwater. Backwater effects occur when disturbances tend to propagate upstream. For example, the effect of a lake (slowing the flow down) or a waterfall (speeding the flow up) is felt upstream.

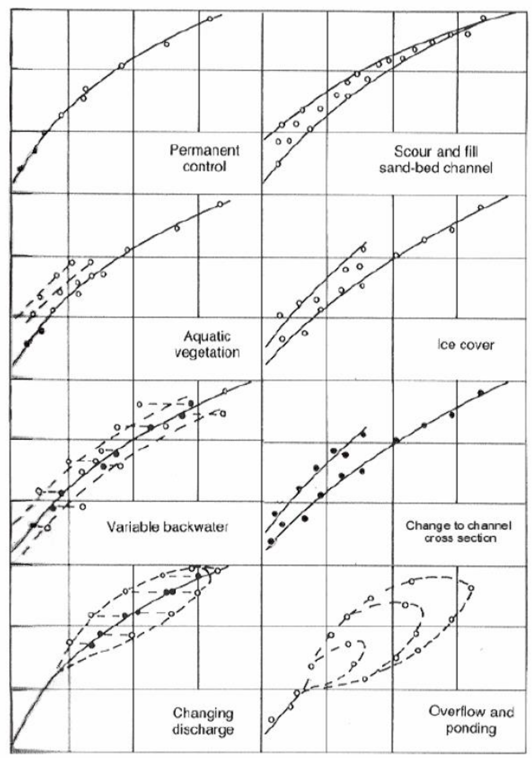

Figure 6 - Effects of different physical processes on rating curves

Chapter 3

3 Model Geometry

In this chapter the methods used to generate a nationwide set of sub-basins and reaches are described (Figure 7). These methods use topography as input and are constrained with the predefined area of Portugal and a river shape file. The geometry generated with different details is presented to justify the best for the present work.

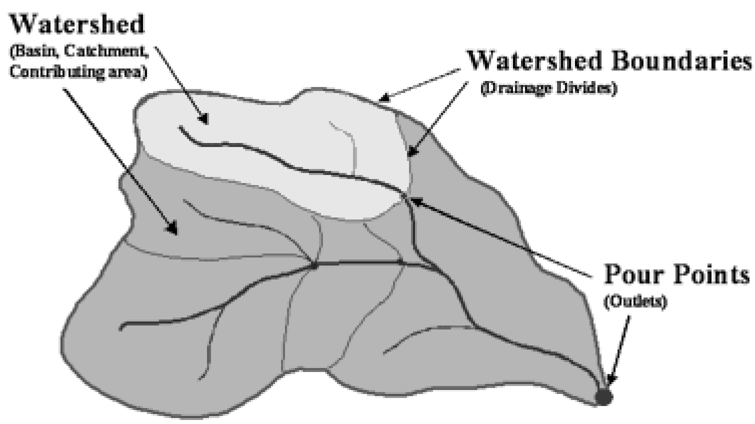

Figure 7 – Watershed divides

Watersheds can be delineated from a Digital Elevation Model (DEM) by calculating the flow direction and using it in the Watershed function. The Watershed function uses a raster of flow direction to determine the contributing area.

The Shuttle Radar Topography Mission (SRTM) obtained a digital elevation model for the entire world (Hounam and Werner, 1999). The SRTM data is accessible as 3 arc seconds with approximately 90 m vertical resolution and 70 m horizontal resolution. This topography has become a reference in its area. The original data distributed by NASA/USGS (finished product) contains "no-data" holes where water or substantial shadow barred the quantification of elevation. More recent databases of SRTM have further processed the original DEMs to fill in these no-data voids. The database used in this work was SRTM 90 m Digital Elevation Database v4.1 (Jarvis et al., 2008).

3.1 Methods used

ArcGis 3D analyst and Spatial Analyst provides analysis tools that were used for the determination of raster surface properties, such as slope. The Hydrology tools of ArcGis Spatial Analyst were used to generate flow direction and accumulation. These ArcGis tools are combined in an ArcGis extension called ArcSWAT. Flow accumulation in its simplest form is the accumulated number of upslope cells that flow into each cell, or, in terms of flow, it is the accumulated m^3/s of flow from upslope cells that flow into each cell, assuming that each cell generates 1 m^3/s. By applying a threshold value to the results of the Flow Accumulation function, a stream network is delineated.

The Stream Definition function of the ArcGis Watershed Delineator uses the threshold method to delineate the watershed and stream network. For this, slope, flow direction and accumulation need to be calculated. A shape file from SNIRH of the rivers was also provided ("burned in") in the DEM, which can improve the accuracy of generated streams. This burn-in consists of adding a constant value to all grid cells that are not in the predefined stream. This creates an auxiliary topography called "Target DEM" that is then used to generate the streams. The Target DEM maintains the slope between cells, changing only the slope with adjacent cells. Among river cells the slope is also maintained. Target DEM is only used to generate the streams and is not used by the model in any other way.

The output of Flow Accumulation is a raster of accumulated flow in each cell, determined by summing the unit flow of all the upstream cells. Output cells with a big flow accumulation, are used to identify stream channels. The stream raster is created using a threshold on Flow Accumulation, which represents where a permanent stream or stream channel begins. With this, a raster stream network is created for which directionality is known. At the same time, output cells with a flow accumulation of zero are local topographic highs and can be used to identify ridges. Threshold plays an important role in determining the detail of the stream network and the size and number of sub-basins created.

Once created, the raster stream network is further analysed using the Stream Link, and Stream to Feature functions, for ordering (ranking) the streams, assigning unique IDs to stream links, and creating a feature dataset. This vectorization algorithm is designed for vectorization of raster stream networks for which directionality is known.

Links are the sections of a stream channel connecting two successive junctions (Figure 8). The area that drains to each junction is denominated the subbasin.

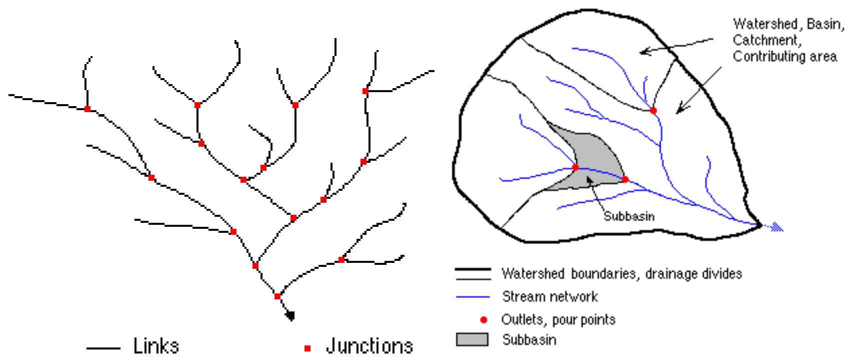

Figure 8 – Watershed delineation of channels and sub-basins

By selecting the main watershed Outlet(s), the watershed area of interest and the stream network of interested is defined.

Basic watershed characteristic parameters are calculated for each subbasin using the DEM and sub-watershed themes. Each subbasin is identified with a number. The Flow Length tool is also used to calculate the length of the longest flow path within a given basin. This measure is used to calculate the time of concentration of each subbasin. Stream ordering is a method of assigning a numeric order to links in a stream network. The results of the calculations, stream ordering, etc. are stored in the streams and sub-basins tables of the database produced in this thesis.

3.2 Projection

To make the data produced in this thesis comparable and convertible with other datasets, all the geographic layers were converted in to ETRS PT-TM06. European Terrestrial Reference System 1989 (ETRS89) is the EU-recommended frame of reference for geodata for Europe. It is the only geodetic datum to be used for mapping and surveying purposes in Europe. Portuguese institutions use a coordinate system based on ETRS89, the PT-TM6, with the following parameters: i) Datum: ETRS89, ii)Ellipsoid: GRS80, iii) Projection: Transverse Mercator, iv) Longitude of the 1st meridian: 08º 07' 59.19"W, v) Latitude of central point: 39º 40' 05.73"N, vi) Scale factor: 1.0000, vii) Origin translation: X=0 m, Y=0. The local system PT-TM06, based on ETRS89, produces projected coordinates similar to those obtained with Datum 73 and Lisbon Datum (previously used Datum). This also explains the option followed by Portugal in adopting the described parameters.

3.3 Data used to define watershed area of interest

The digital elevation model (DEM) used is in a raster format with a grid of approximately 90 m vertical resolution and 70 m horizontal resolution which was clipped from the Shuttle Radar Topography Mission (SRTM) DEM data (Jarvis et al., 2008, Hounam and Werner, 1999). This generated a file with 4358 * 9356 cells (Figure 9) with a regular grid of 82 by 82 meters. Figure 9 shows the average slope for each of the represented sub-basins. The highest slopes are located in the sub basins in the north-east of Portugal, and the lowest in the south and west of Portugal.

An official APA dataset was used to define the watershed (Figure 10). This dataset identifies the outlets in the coastal area and restricts the simulation to Portuguese territory only. Stream networks were delineated from a digital elevation model (DEM) using the output from the Flow Accumulation function. The use of this APA dataset guarantees that geometry definition is focused on the interest areas defined by national institutions.

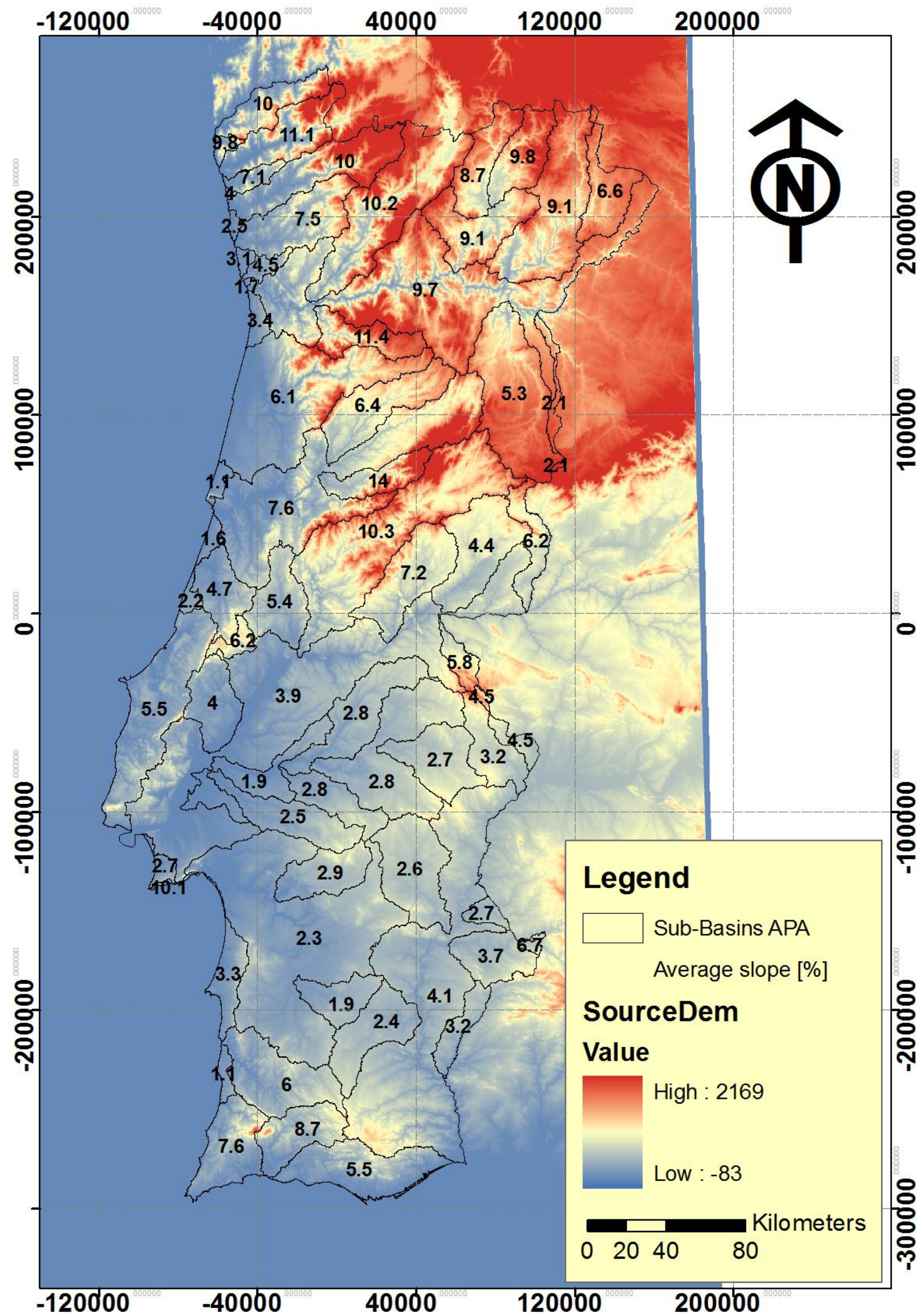

Figure 9 - Shuttle Radar Topography Mission (SRTM) DEM data (source: NASA)

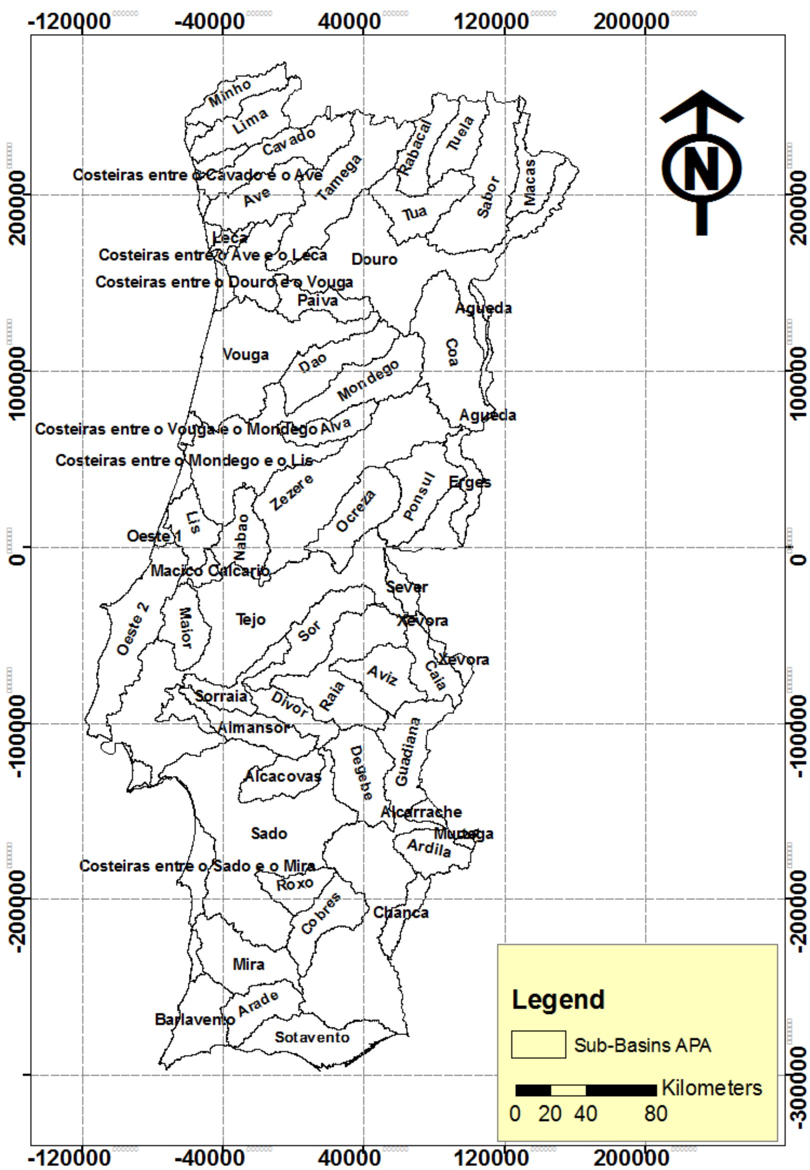

Figure 10 – APA shape file on Portuguese watersheds (source: APA)

3.4 Sensitivity tests

The flow accumulation threshold and the pour points were used to delineate watersheds. The thresholds were used to define the watershed and the outlets for the watershed will be the junctions of a stream network derived from flow accumulation. A minimum number of cells that constitute a stream (the threshold value) have to be used. Two values were tested: 2868 cells (20 km^2) and 717 (5 km^2). The resulting sub-basins and streams are represented in Figure 11 and Figure 12.

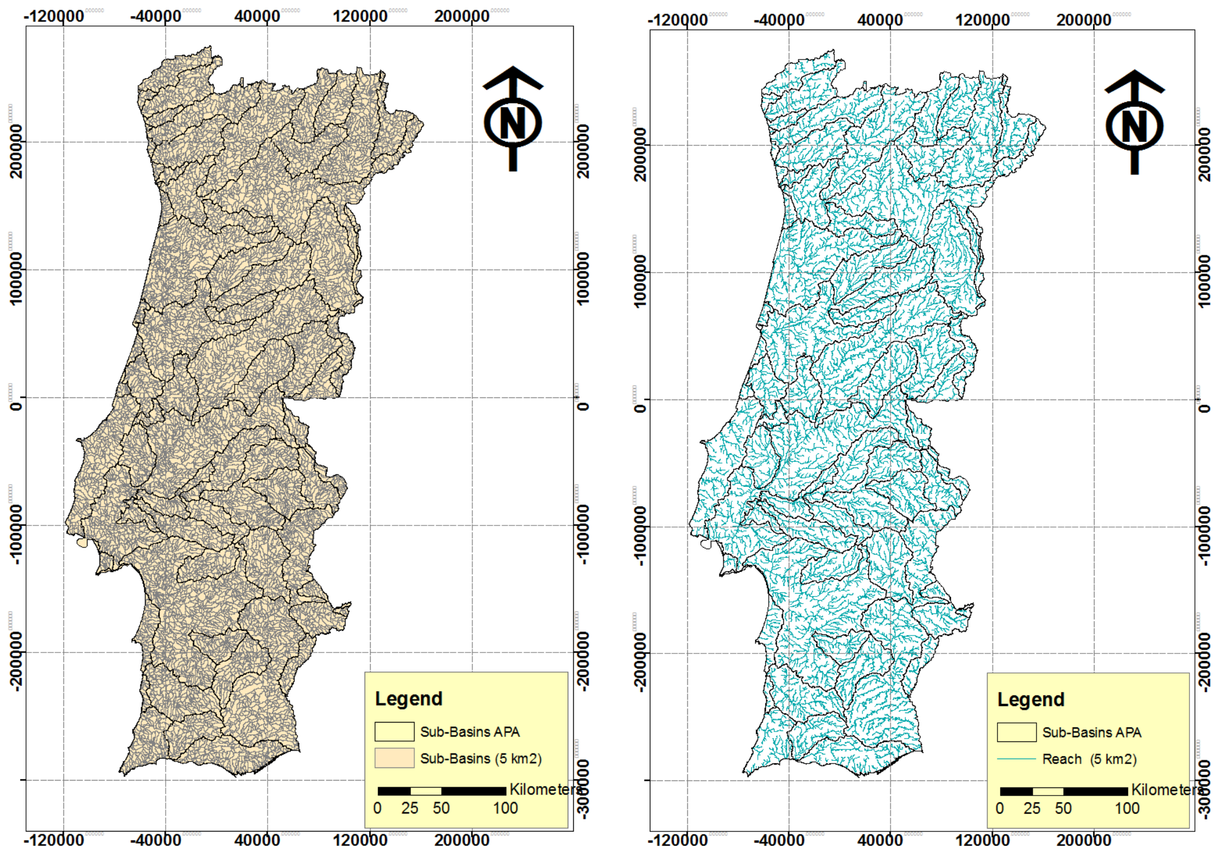

Figure 11 – Sub-basins and stream network generated with a 5-km² threshold

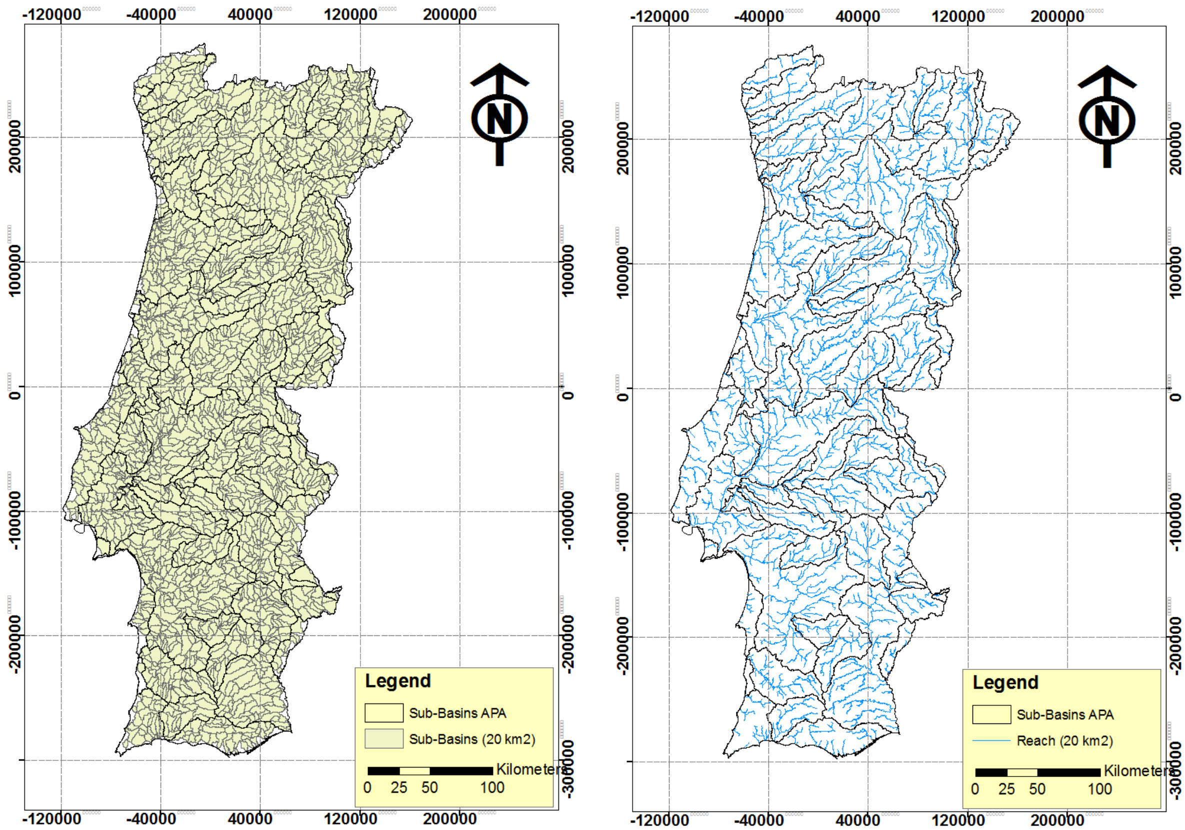

Figure 12 – Sub-basins and stream network generated with a 20-km² threshold

For the 500-hectare threshold an overall coverage of 98% of territory was obtained (Table 7). This means that 2% of the cells are sub-basins of less than 500 hectares. These sub-basins either drain directly into the sea or drain to Spain or from Spain. The number of sub-basins generated was 9455. This number of sub-basins generates ascii outputs of 10 GB that are not easily handled.

For the 2000-hectare threshold an overall coverage of 96% was obtained with a total number of sub-basins of 2288 (Table 7). This generated outputs of 2.5 GB that were more easily converted to an operational database.

Table 7 – Simulated area per watershed

APA watershed	Area [km²]	% of Area simulated		APA watershed	Area [km²]	% of Area simulated	
		20-km² threshold	5-km² threshold			20-km² threshold	5-km² threshold
Agueda	248	25%	60%	Lima	1220	93%	96%
Alcacovas	895	100%	100%	Leca	191	99%	99%
Alcarrache	207	88%	88%	Lima	1220	93%	96%
Almansor	1080	100%	100%	Lis	850	100%	100%
CAB Alva	708	100%	100%	Macas	901	88%	95%
Arade	979	100%	100%	Macico Calcario	233	100%	100%
Ardila	855	95%	95%	Maior	923	100%	100%
Ave	1391	99%	100%	Minho	818	74%	85%
Aviz	1135	100%	100%	Mira	1576	100%	100%
Barlavento	1184	82%	88%	Mondego	4570	100%	100%
Caia	816	96%	98%	Murtega	59	72%	72%
Cavado	1592	98%	99%	Nabao	997	100%	100%
Chanca	485	68%	83%	Neiva, CAB Lima & Neiva	248	97%	97%
Coa	2522	100%	100%	Ocreza	1430	100%	100%
Cobres	1156	100%	100%	West 1	119	44%	72%
CAB Ave & Leca	89	55%	75%	West 2	2390	88%	93%
CAB Cavado & Ave	68	4%	68%	Paiva	796	100%	100%
CAB Douro & Vouga	207	51%	83%	Ponsul	1495	100%	100%
CAB Leca & Douro	12	5%	47%	Rabacal	946	96%	97%
CAB Minho & Lima	123	63%	79%	Raia	2303	100%	100%
CAB Mira & Barlavento	152	30%	74%	Roxo	689	100%	100%
CAB Mondego & Lis	145	31%	68%	Sabor	2410	99%	99%
CAB Neiva & Cavado	20	3%	47%	Sado	6149	100%	100%
CAB Sado & Mira	594	68%	80%	Sever	327	79%	84%
CAB Tagus & Sado 1	163	66%	72%	Sor	1393	100%	100%
CAB Tagus & Sado 2	30	2%	3%	Sorraia	1063	100%	100%
CAB Vouga & Mondego	138	41%	76%	Sotavento	1583	82%	90%
Dao	1381	100%	100%	Tamega	2648	97%	98%
Degebe	1538	100%	100%	Tejo	7288	98%	99%
Divor	756	100%	100%	Tua	1256	100%	100%
Douro	6004	94%	97%	Tuela	921	98%	98%
Erges	595	62%	87%	Vouga	3685	98%	99%
Guadiana	6185	96%	98%	Xevora	297	59%	84%
Leca	191	99%	99%	Zezere	4007	100%	100%
				Total	**89237**	**96%**	**98%**

*CAB - Coastal Areas Between

3.5 Discussion

Two watershed geometries for Continental Portugal generated with two levels of detail were developed. The coarser one was the best suited to simulate all the watersheds in Portugal. The reason was that the simulated area of Continental Portugal only increased from 2% (96% to 98%) by increasing four times the spatial detail.

The area of model application was restricted only to that within Portugal's borders. This can be justified either from the perspective of the input or the output. For the input the advantage of this option is the possibility of using and harmonizing a set of data that exists for the country. If the area of interested delineated was done on a purely hydrologic perspective, the entire Iberian peninsula should be simulated. In that case, data like that from SNIRH, IPMA-GRID and MM5-R would cover only part of the simulation area. Even an intermediate solution, extending a little into Spain to complete some smaller watersheds, would generate data availability problems. From the output perspective, the result restricted to the national level can be easily compared with other national data sets. It can also be used as a national database on the Portuguese territory.

On the other hand a transboundary simulation database would be of great use not only for managing water between Portugal and Spain, but also to help National institutions to manage water coming from Spain. In the context of the European Union this type of approach has been stimulated by the development of transboundary datasets.

The definition of geometry in the case of SWAT allowed generating shape files of rivers and sub-basins. These shape files have associated information that are used to run the SWAT model. The most important attributes generated from topography that will be associated with each subbasin are: subbasin area, subbasin average slope length, average slope (Figure 13) , longest tributary channel length, average slope and width of tributary channels.

These parameters will be used to estimate concentration time of each subbasin. Concentration time will be used to estimate runoff in the subbasin, which will contribute to the reaches. Concentration time is the travel time of a drop of water between the remotest point of the subbasin to its outlet (Neitsch et al., 2011).

Topography resolution has a direct impact on these parameters. For example in two papers describing the sensitiveness of the SWAT model to topography, the authors found that a finer grid resolution resulted in a higher slope and hence a higher simulated flow volume (Cho and Lee, 2001, Cotter et al., 2003). Both papers also agree on the importance of having the right subbasin area to get the right flow, and that also depends on the topography resolution. However, while the slope has more impact on daily flows and less on monthly flows, the area has the same impact on any time resolution flow. An increase or decrease in area of subbasin will be accompanied by the corresponding increase or decrease of the flow. Because of this, it is important to use the most detailed topography available.

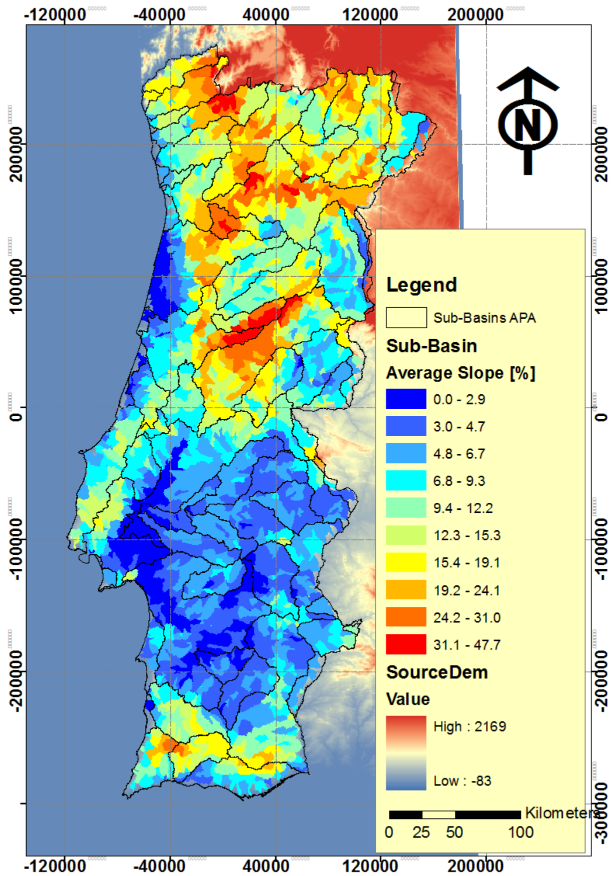

Figure 13 - Sub-basin average slope

The fact that SWAT lumps the flows to just one unit (the sub-basin) allows an estimate of the flow for a relatively small amount of computation units (in this case the topography units of 4358*9356 cells were transformed into 2288 sub-basins, the computation units).

Chapter 4

4 Definition of model input

It was described in Chapter 2 that each SWAT HRU is characterized by a type of soil, a land use and a weather time series. The HRU also inherits the properties of the sub-basins described in the previous chapter. This chapter presents the input of the model defined with specific information about land use, soil properties and weather which were used as input for modelling Portugal Hydrology. The physical processes associated with water movement, sediment movement, crop growth, nutrient cycling, etc. are directly modelled by SWAT using this input data. Special emphasis is given to the forcing of meteorological models: Two reanalysis models, CFSR and MM5-R, with about 30 years of data are presented. Precipitation values from reanalysis are compared with measurements of precipitation.

4.1 Soil

Soil data is a very important input for modelling water. Normally available soil maps show the distribution of different soil types in terms of their main empirical characteristics: colour, parent material, etc. These characteristics indicate a lot about soil pedogenesis (processes that lead to the formation of soil). Physical properties are needed for running hydrological models. Due to soil complexity it is difficult to have maps of physical properties (the USA being one of the few exceptions). The usual methodology is to have soil profiles to obtain the texture for each soil type and then use pedotransfer functions to obtain physical properties associated with the soil-type maps such as texture and depth. There are a number of continental and regional scale databases available, which can be associated with soil maps to support catchment water modelling. Pedotransfer rules at a continental scale have been developed around the world for these datasets: HYPRES (Wösten et al., 1999) and ROSETTA (Schaap et al., 2001) are among the most used databases. Pedotransfer rules or pedotransfer functions are predictive functions of soil properties like porosity using soil data obtained in surveys, such as soil texture.

Measurements of soil in Portugal are becoming increasingly frequent. However, data is dispersed and heterogeneous. Moreover, there is no soil map that covers all the country, except for low resolution maps. There is no national map of basic soil characteristics like soil depth, soil texture and soil organic matter. This is probably related to the spatial heterogeneity of soils in Portugal, due to the highly variable topography. In terms of soil classification, the only detailed map covers merely the south of Portugal, using the Portuguese classification system. For this work we chose to use the coarser grid map because it covers all the Portuguese territory and also because (considering it is a map covering many countries of EU) it will allow testing of the methodology described herein for other study sites in Europe (Figure 14).

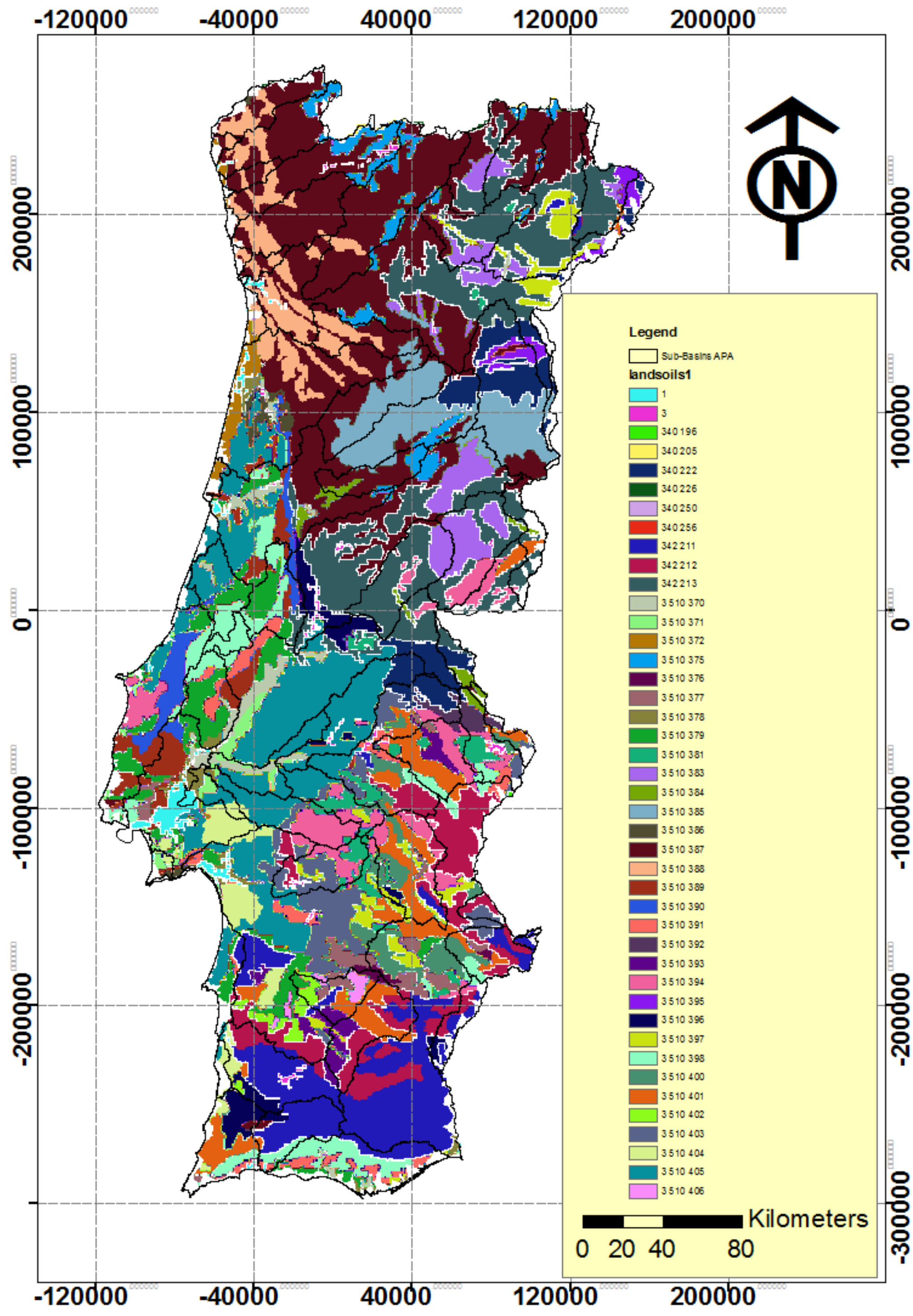

Figure 14 – Soil type (source: Joint Research Centre - JRC)

The Soil Geographical Database of Eurasia (SGDBE) provides a harmonised set of soil parameters covering Eurasia and Mediterranean countries at scale 1:1,000,000 (EC, 2003). It is part of the European Soil Database (ESDB), along with the Pedotransfer Rules Database (PTRDB), the Soil Profile analytical Database (SPADE) and the Database of Hydrological Properties of European Soils (HYPRES Wösten et al., 1999). Information in SGDBE is available at the Soil Typological Unit (STU) level, characterised by attributes specifying the nature and properties of soils (Figure 15). For mapping purposes, the STUs are grouped into Soil Mapping Units (SMU) since it is not possible to delineate each STU at the 1:1,000,000 scale (EC, 2003).

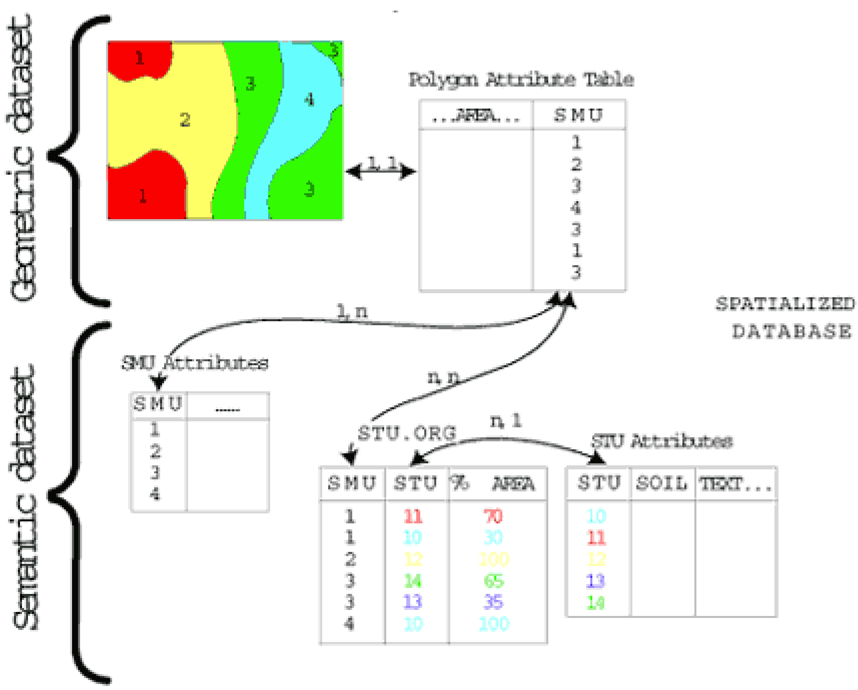

Figure 15 – Soil Geographical Database of Eurasia SMU vs. STU (source: JRC)

The attributes needed at the soil layer level could either be retrieved from the estimated profile database or from the pedotransfer rules (PTR). The former gives a more detailed account of a representative profile for the STU, but it is not available for all STUs. The latter gives rough categorical estimations for the topsoil and the subsoil of each STU. In order to provide homogeneous data, only attributes derived from the STU properties or from PTR were used.

The soils for Portugal are characterized in Table 8, as well as the area occupied by each soil type. From all the properties in the database the most important parameters for infiltration and evapotranspiration are shown. Hydrologic soil groups (HSG) range from A with low runoff potential to D with high runoff potential. HSG, along with land use, management practices, and hydrologic conditions, define an associated runoff curve number (CN) to each HRU, The most frequent group displayed for Portugal is C. Soils were defined with one or two layers. The first layer has between 200 and 300 mm depth while the second layer can reach a depth of 1200 mm. The higher the soil depth, the higher the water available for evapotranspiration. Three of the soils make up almost 40% of Portugal: 3510387, 342213, and 3510405. Soil 3510387 occupies about 19% of the area, has a depth of 200 mm and its HSG is C. Soil 342213 occupies about 10% of the area, has a depth of 500 mm and the HSG is C. Soil 3510405 has about 9% of area, a depth of 1000 mm and is HSG A.

Table 8 – Soils for Portugal according with soil data base developed by JRC. Most important parameters for infiltration and evapotranspiration.

SOIL code (SMU)	Number of Layers	TEXTURE*	Hydrologic soil group	First layer Depth [mm]	Second layer Depth [mm]	Area [km^2]	Area [%]
1	1	C	D	300	0	598	0.70%
3	1	C	D	300	0	27	0.03%
340222	2	C-C	A	300	500	2394	2.81%
342211	2	M-M	C	300	500	5777	6.77%
342212	2	M-M	C	300	500	3291	3.86%
342213	2	M-M	C	300	500	9328	10.94%
3510370	2	M-M	C	300	1200	769	0.90%
3510371	2	C-C	A	300	1000	398	0.47%
3510372	2	C-C	A	300	1000	419	0.49%
3510375	1	M	C	200	0	971	1.14%
3510376	2	F-F	C	300	1000	145	0.17%
3510377	2	F-F	C	300	1000	820	0.96%
3510378	1	F	C	200	0	324	0.38%
3510379	2	C-C	A	300	600	2697	3.16%
3510381	1	C	A	200	0	1252	1.47%
3510383	1	C	A	200	0	2398	2.81%
3510384	1	C	A	200	0	294	0.34%
3510385	1	C	A	200	0	3548	4.16%
3510386	2	C-C	A	300	600	357	0.42%
3510387	1	M	C	200	0	16486	19.33%
3510388	1	M	C	200	0	2522	2.96%
3510389	2	M-M	C	300	1000	1423	1.67%
3510390	2	C-C	A	300	1000	1092	1.28%
3510391	2	F-F	C	300	1000	1003	1.18%
3510392	1	M	C	200	0	373	0.44%
3510393	1	M	C	200	0	833	0.98%
3510394	1	C	C	200	0	2696	3.16%
3510395	1	M	C	200	0	523	0.61%
3510396	1	M	C	200	0	1420	1.66%
3510397	1	M	C	200	0	1262	1.48%
3510398	1	F	C	200	0	2727	3.20%
3510400	2	M-F	C	300	1000	1654	1.94%
3510401	1	M	C	200	0	2946	3.46%
3510402	2	C-M	C	300	1000	454	0.53%
3510403	1	C	D	200	0	2162	2.54%
3510404	2	C-C	A	300	1000	1312	1.54%
3510405	2	C-C	A	300	1000	8434	9.89%
3510406	2	C-C	B	300	400	143	0.17%
Total						85270	100.00%

*C-Coarse, M-Medium, F-Fine

The dominant soils in each Hydrographic Region of Portugal are described in Table 9. Soil 3510387 is dominant in all the north Hydrographic Region. For the South, soil 312211 is the most important one. Finally for the Tejo Hydrographic Region, soil 3510405 is dominant.

Table 9 – Dominant soils in each Hydrographic Region of Portugal

Code	Hydrographic Region	SOIL	Percent of total area
PTRH1	Lima and Minho	3510387	62%
PTRH2	Cavado and Leça	3510387	73%
PTRH3	Douro	3510387	45%
PTRH4	Mondego and Vouga	3510387	35%
PTRH5	Tejo	3510405	19%
PTRH6	Sado and Mira	342211	14%
PTRH7	Guadiana	342211	25%
PTRH8	Algarve	342211	43%

4.2 Land use

Land use changes are very important for water regulators because they have a direct impact on the quantity and quality of the water. Most of the current land use maps were obtained based on satellite images, either by visual interpretation or by automatic or semi-automatic methods. These maps are currently used to estimate hydrology and diffuse loads using watershed models (Mateus, 2009). Maps that delineate burned areas can also be used to complement land use maps to estimate diffuse sources using watershed models (Yarrow and Chambel-Leitão, 2008, Yarrow and Chambel-Leitão, 2007, Chambel-Leitão, 2008, Canas et al., 2010). The vegetation present in each land use has characteristics like Leaf Area Index – LAI (area of leaves per area of soil), height and root depth. LAI determines evapotranspiration through precipitation interception and transpiration and plant height determines evapotranspiration through the wind. Finally root depth determines evapotranspiration through the availability of water in the different soil layers.

Corine Land Cover 2006 represents the main land use-land cover of Europe with a legend of 50 classes. In terms of agricultural practices it distinguishes between cold season annuals from warm season annuals but it does not differentiate the kind of crop (Figure 16). It uses a Minimum Mapping Unit (MMU) of 25 hectares for rural areas, which means it is prone to errors where we have high variability of land-use inside 25-hectare units. Tests were made with new maps like M2.1 from the GMES initiative, where the existing MMU of 5 hectares has been shown to be more accurate than CLC 2006, even though it does not differentiate between cold season annuals and warm season annuals.

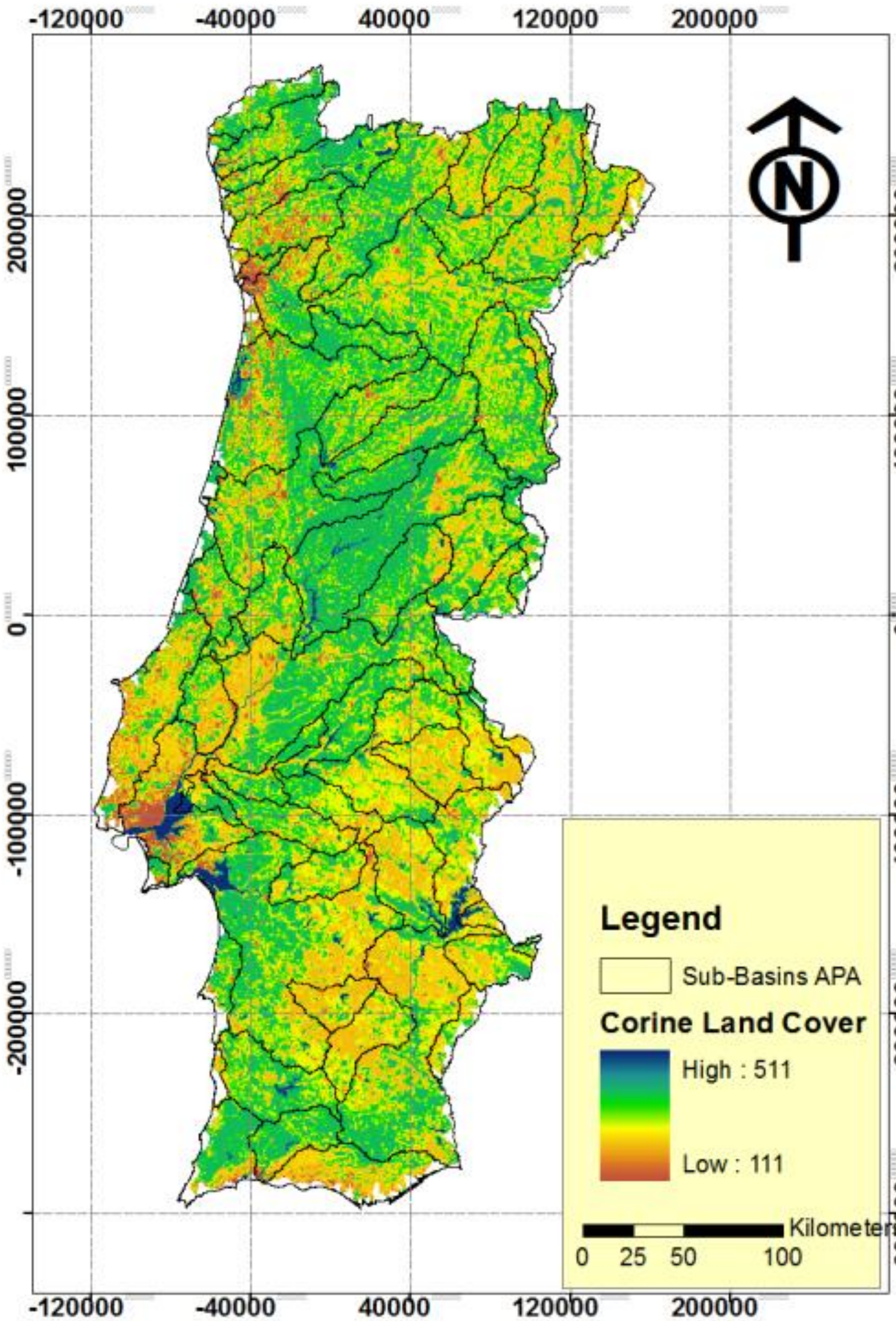

Figure 16 – Corine Land cover (source: IGP)

The CORINE land cover classification codes were converted to the SWAT land cover/plant codes (Table 10).

Table 10 – Correspondence between Corine Land Cover and SWAT land cover/plant codes

CLC code	SWAT LANDUSE	Corine Land Cover Sub-Classification	Corine Land Cover Class
111	URHD	Continuous urban fabric	Built-up area
112	URML	Discontinuous urban fabric	
121	UIDU	Industrial or commercial units	
122	UTRN	Road and rail networks and associated land	
123	UIDU	Port areas	
124	UIDU	Airports	
131	UIDU	Mineral extraction sites	
132	UIDU	Dump sites	
133	UIDU	Construction sites	
141	URLD	Green urban areas	
142	URLD	Sport and leisure facilities	
211	AGRC	Non-irrigated arable land	Agricultural area
212	AGRR	Permanently irrigated land	
213	RICE	Rice fields	
221	ORCD	Vineyards	
222	ORCD	Orchard	
223	ORCD	Olive trees	
231	PAST	Pastures	
241	AGRC	Annual crops associated with permanent crops	
242	AGRC	Complex cultivation patterns	
243	AGRC	Land principally occupied by agriculture, with significant areas of natural vegetation	
244	OAK	Agro-forestry areas	
311	FRSD	Broad-leaved forest	Forest and natural area
312	PINE	Coniferous forest	
313	PINE	Mixed forest	
321	RNGE	Natural grassland	
322	PINE	Moors and heathland	
323	PINE	Sclerophyllous vegetation	
324	PINE	Transitional woodland-shrub	
331	PINE	Beaches, dunes, and sand plains	
332	PINE	Bare rock	
333	PINE	Sparsely vegetated areas	
334	PINE	Burnt areas	
411	PINE	Inland wetlands	Inland marshes
421	PINE	Salt marshes	Wetland, salt
422	PINE	Salines	
423	WETN	Intertidal flats	
511	WATR	Water courses	Water

The aggregated land use data set was made indicating that 31% of the whole basin belongs to the "Agricultural Land-Close-grown" class (AGRC), 1% to the "Agricultural Land-Row Crops" class (AGRR), 12% to the "Forest-Deciduous" class (FRSD), 5% to the "Oak" class (OAK), 4% to the "Orchard" class (ORCD), 0.05% to the "Pasture" class (PAST), 44.39% to the "Pine" class (PINE), 0.12% to the "Rice" class (RICE), 0.51% to the "Range-Grasses" class (RNGE), 0.04% to the "Industrial" (UIDU) class), less than 0.01% to the "Residential-High Density" class (URHD), 0.94% to the "Residential-Med/Low Density" class (URML) and 0.83% to the "Water" class (WATR) (Table 11)

Table 11 - Dominant SWAT land cover per Hydrographic Region (HR)

Code	Hydrographic Region	LANDUSE	Area	Percent of total area
PTRH1	Lima and Minho	PINE	4056	92%
PTRH2	Cavado and Leça	PINE	3895	60%
PTRH3	Douro	PINE	17582	54%
PTRH4	Mondego and Vouga	PINE	18225	89%
PTRH5	Tejo	PINE	19088	38%
PTRH6	Sado and Mira	AGRC	7167	42%
PTRH7	Guadiana	AGRC	9920	51%
PTRH8	Algarve	PINE	2064	39%

4.3 Weather

The SWAT model uses daily values of daily precipitation, maximum and minimum temperatures, solar radiation, wind speed, and relative humidity. The GIS interface selects the weather station closest to the centroid of each subbasin. This spatial integration approach is one of the simplest approaches and is similar to Thiessen's method [(Thiessen, 1911) referenced in (Galván et al., 2014)], which assigns the record from the closest weather station to the unsampled location.

Rainfall is generally considered as the most important input that drives runoff production in watershed models (Shen et al., 2012). However, rainfall data often exhibits irregular occurrence, duration and magnitude across a catchment due to the variation of nature conditions. Fu et al. (2011) found that the effect of rainfall spatial resolution on discharge modelling is relatively low for catchment sizes above 250 km^2, and even negligible for watersheds larger than 1000 km^2. However, these types of conclusions are very dependent on local conditions. For example, in the North of Portugal there is a high spatial variability of precipitation which is mainly related with the uneven distribution of orography (Trigo and DaCamara, 2000). This means that at least in this region simulated flows should be worse in smaller watersheds due to precipitation resolution. But that is not the case. This thesis shows a similar conclusion to that of Fu et al. (2011), i.e., whatever the precipitation used, bigger watersheds do not have any tendency to have better results than small watersheds.

4.3.1 Reanalysis

Reanalysis data provide a seamless and coherent record of the global atmospheric circulation (Dee et al., 2011). Unlike weather analyses from operational forecasting systems, a reanalysis is produced with a single version of a data assimilation system and is therefore not affected by changes in method. The development of reanalysis was possible thanks to the Global Weather Experiment. In 1978-1979 an unprecedented analysis of the atmosphere of planet Earth started with the involvement of over 140 countries in the Global Weather Experiment. At the time it was considered the largest international scientific experiment yet attempted (Fleming et al., 1979).

Developments in numerical atmosphere modelling and atmosphere remote sensing have resulted in a readily available suite of meteorological products for water professionals. The national weather service offers model output time series and images directly, e.g. through File Transfer Protocol (FTP), to water management agencies that can automatically process and forward these time series as input to hydrological models for decision support. For example, in Portugal weather forecasts are produced by the numerical model MM5 running at IST for Portugal in a 9 km^2 grid (Sousa, 2002) and converted to a format that can be read by the MOHID and SWAT model. Using this input, the SWAT model is running in forecast mode using meteorological data from the previous week and forecasts for the next week (precipitation, temperature, relative humidity, wind speed and solar radiation). Estimated values of evapotranspiration are sent to the users (Chambel-Leitão et al., 2011).

The downscaling techniques are supposed to retain all the large-scale information that has been resolved by the global reanalysis data assimilation, and to add smaller-scale information that the coarse-resolution global data assimilation models could not resolve. Regional models, however, have to deal with the problem of lateral boundary conditions that often produce undesirable noise, which often results in instabilities (Kanamaru and Kanamitsu, 2007).

Mass et al. (2002) evaluated the importance of horizontal resolution in the quality of forecasts. A study was presented of 2-year forecast results obtained with the MM5 grid with spatial resolution of 36-km, 12-km and 4-km grids for the United States. The main conclusions are that the quality of rainfall forecasts improves with the change of horizontal resolution from 36 km to 12 km because the 36-km mesh does not adequately define the phenomena associated with the resulting precipitation of orographic barriers. However, transition from 12 to 4 km features results which are more difficult to assess, with the exception of heavy rainfall events upstream of the mountains where 4 km represents an improvement in quality. These findings are in agreement with Zhang et al. (2002) who concluded that an increase to a 10-km horizontal scale represents a significant improvement in the estimates of the amount of precipitation but that a finer resolution no longer justifies the additional computational time.

4.3.1.1 CFSR

In the present work, the NCEP Climate Forecast System Reanalysis (CFSR) was used as an example of a global reanalysis. The NCEP Climate Forecast System Reanalysis (CFSR) was designed and executed as a global, high resolution, coupled atmosphere-ocean-land surface-sea-ice system to provide the best estimate of the state of these coupled domains over the 36-year period of record from January 1979 to March 2014. This product is continuously extended as an operational real time product into the future.

The CFSR data was developed by NOAA's National Centers for Environmental Prediction (NCEP). The data for this study are from NOAA's National Operational Model Archive and Distribution System (NOMADS) which is maintained at NOAA's National Climatic Data Center (NCDC).

The CFSR weather includes rainfall, maximum and minimum temperature, wind speed, relative humidity, and solar radiation (Figure 18, Figure 19, Figure 20 and Figure 21). In Portugal there are 218 cells of CFSR. Figure 17 shows the center of the cells.. The CFSR weather is produced using cutting-edge data-assimilation techniques (both conventional meteorological gage observations and satellite irradiances) as well as highly advanced (and coupled) atmospheric, oceanic, and surface-modelling components at ~38 km grid (Saha et al., 2014). This indicates that the production of CFSR data involves various spatial and temporal interpolations.

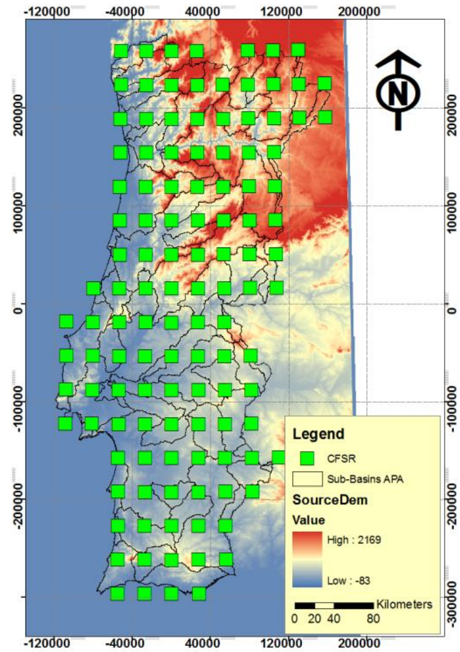

Figure 17 – Centre of cells CFSR over continental Portugal.

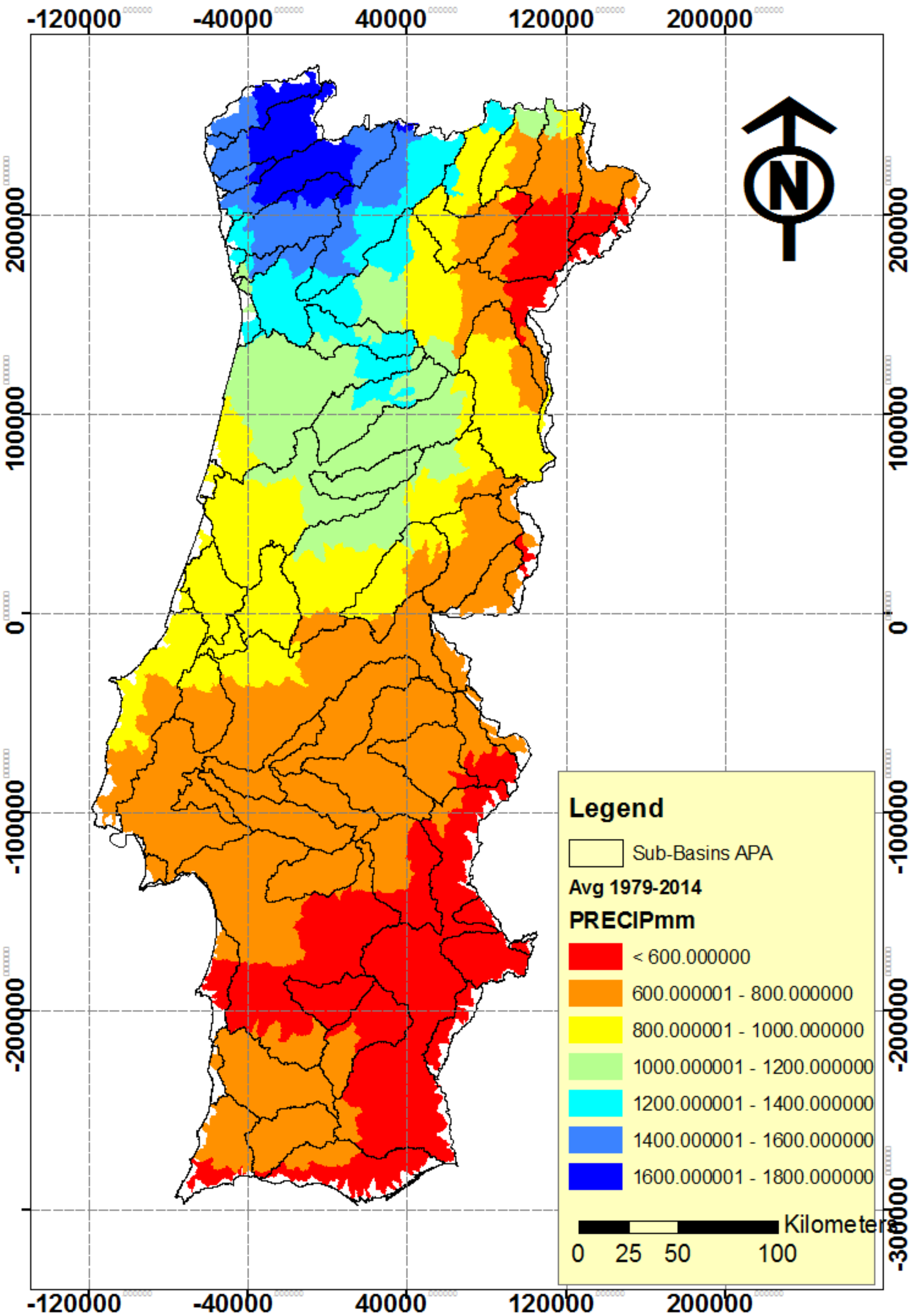

Figure 18 – CFSR model 36-year average (1979-2014) per subbasin for precipitation

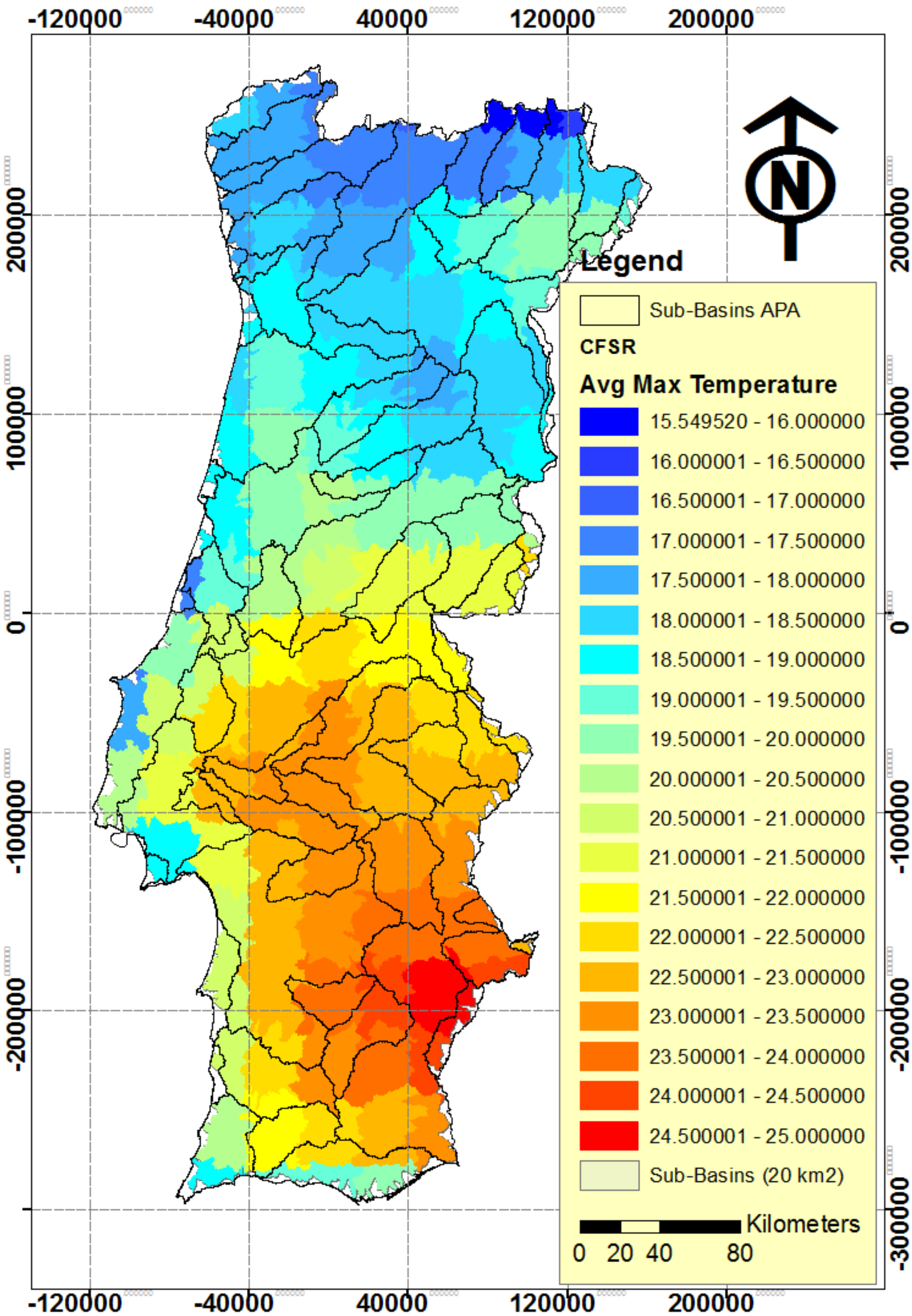

Figure 19 – CFSR model 36-year average (1979-2014) per subbasin for maximum temperature

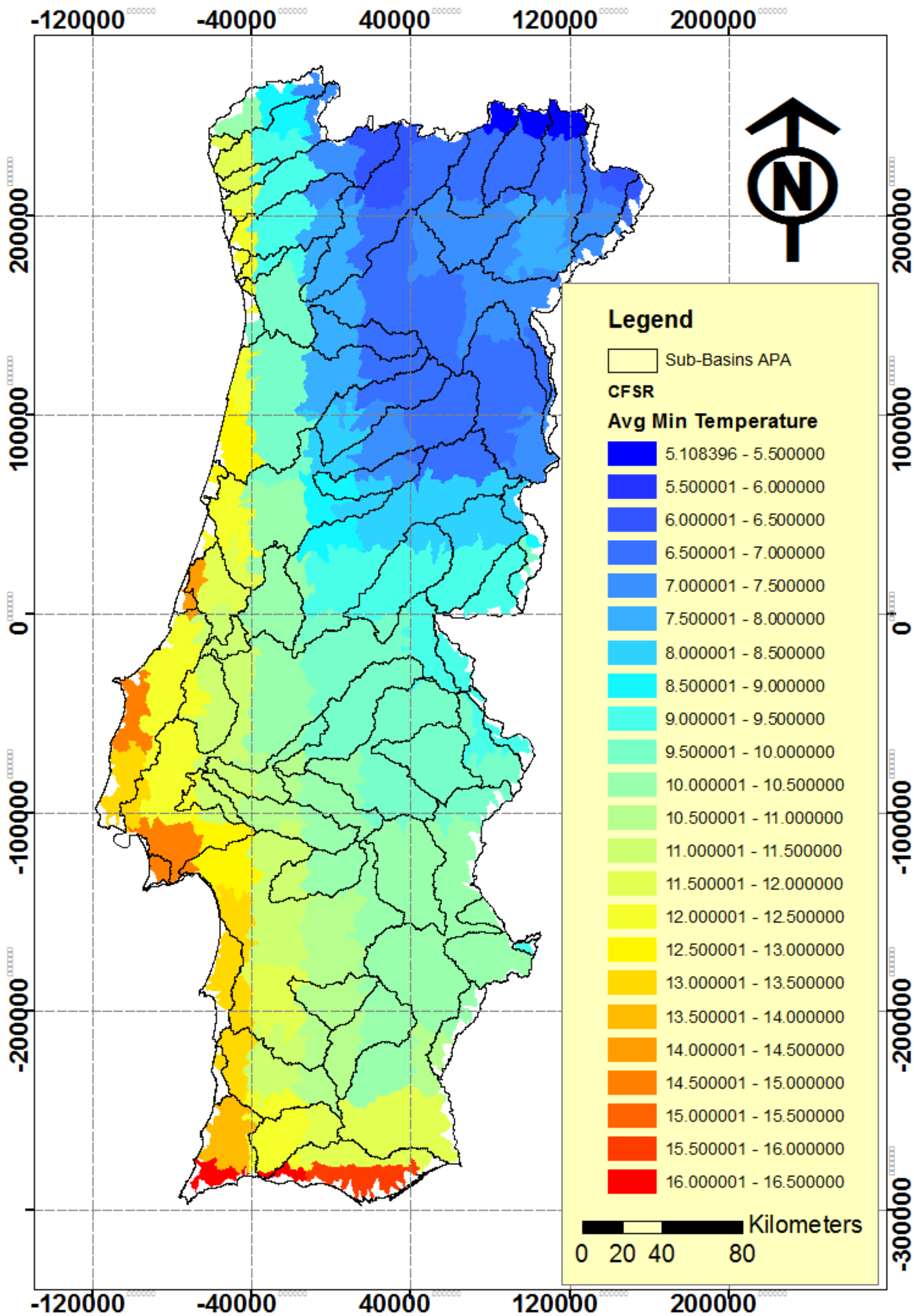

Figure 20 – CFSR model 36-year average (1979-2014) per subbasin for minimum temperature

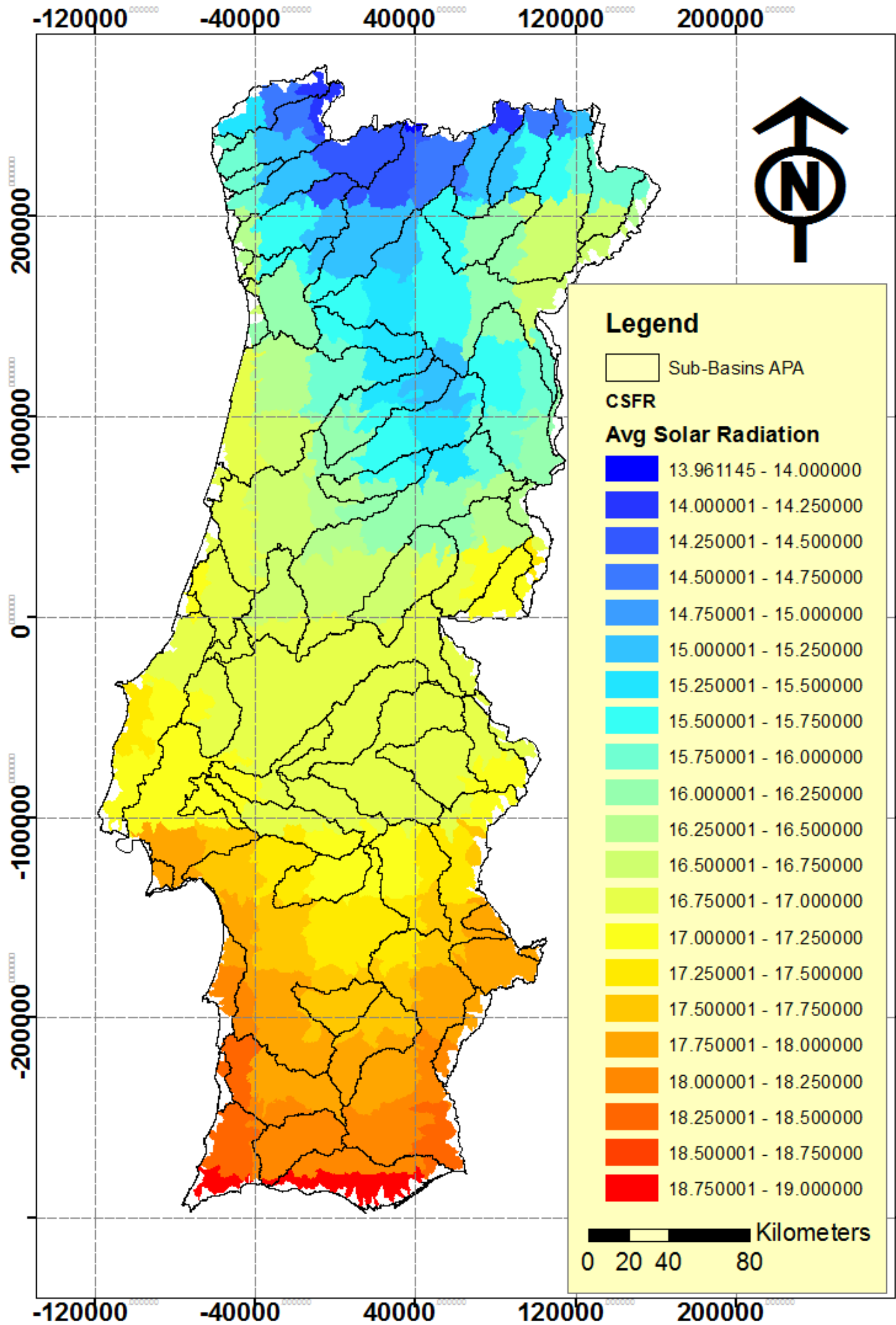

Figure 21 – CFSR model 36-year average (1979-2014) per subbasin for solar radiation

4.3.1.2 MM5-R

An MM5 application for Continental Portugal was used as an example of a local reanalysis. A 30-year period of records from January 1979 to March 2010 was made available for this thesis. This product is not continuously extended. However, it has a twin MM5 application that was implemented on a forecast mode with a ~9 km grid and described by Sousa (2002) and is still used to provide weather predictions (http://meteo.tecnico.ulisboa.pt/). It was this same model and grid that was forced with global reanalysis results from GFS. As such it was possible to retain all the large-scale information that has been resolved by the global reanalysis data assimilation, and to add smaller-scale information that the coarse-resolution global data assimilation models could not resolve. Based on this application a set of precipitation data was generated.

4.3.1.3 Model results inter-comparison

Both reanalysis, CFSR and MM5-R, are well correlated. Monthly averages have a R^2 correlation of 0.71 while annual averages have a correlation of 0.84 (Figure 22).

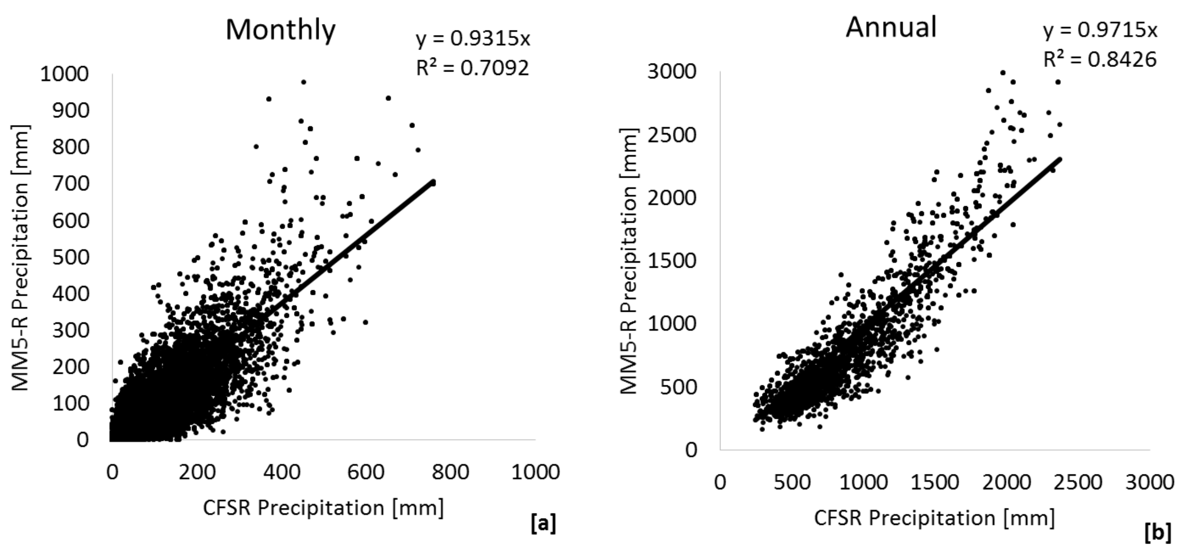

Figure 22 Comparison of precipitation obtained from CFSR and obtained from MM5-R: [a] monthly and [b] annual results.

4.3.2 Measurements

Precipitation is traditionally measured by weather gages. In Portugal two main monitoring networks exist: SNIRH and IPMA. In the last few years SNIRH has reduced its monitoring network. On the other hand the number of private weather gages has multiplied in the last 10 years. Many of these private gages are freely available in sites like *Weather Unground*. Precipitation Radar monitoring also covers the whole of Portugal, but no published work was found on correlating of radar measurements with local precipitation measurements. On the other hand there are a few studies on spatial integration of precipitation. A number of techniques are available for rainfall spatial integration (Galván et al., 2014). One of the most used is the inverse square distance technique, but it does not allow factors such as topography to improve integration. Kriging methods are currently very much used and allow the effect on rainfall of factors like elevation, slope and orientation to be taken into account. An example of the application of rainfall spatial integration for Portugal is (Nicolau, 2002) where a map was created for precipitation between 1960 to 1990 for Continental Portugal (Nicolau, 2002).

The first precipitation dataset that we will designate as SNIRH was obtained from 96 weather stations. The second dataset designated as IPMA-GRID is a gridded precipitation dataset that resulted from an interpolation of 806 weather stations. Finally the third dataset is a map of average annual precipitation in Portugal obtained from APA "Atlas da água", which we named after the Thesis reference.

4.3.2.1 SNIRH

Precipitation data was obtained from National System of Water Resources Information (Sistema Nacional de Informação de Recursos Hídricos - SNIRH), managed by the Portuguese Institute for Water, and are available through downloads from the SNIRH website (http://snirh.inag.pt). This data has been used for weather studies (Costa and Soares, 2009) and hydrologic studies (Durão et al., 2012, Chambel-Leitão et al., 2007b).

Precipitations stations were filtered for Portugal according to data availability and reliability. We assumed that stations with more years operating are the most reliable ones. The number of stations available for altitudes lower than 600 m is abundant, while for altitudes higher than 600 m they are less frequent. Because of that a more demanding filtering was done for stations below 600 m, accepting stations with a minimum of 80 years of data. With this filter we obtained 47 precipitation stations for altitudes lower than 600 m. For stations above 600 m, they needed to have a minimum of 60 years of data. With this filter we obtained a total of 49 stations for altitudes higher than 600 m. Figure 23 shows the location of the precipitation stations obtained.

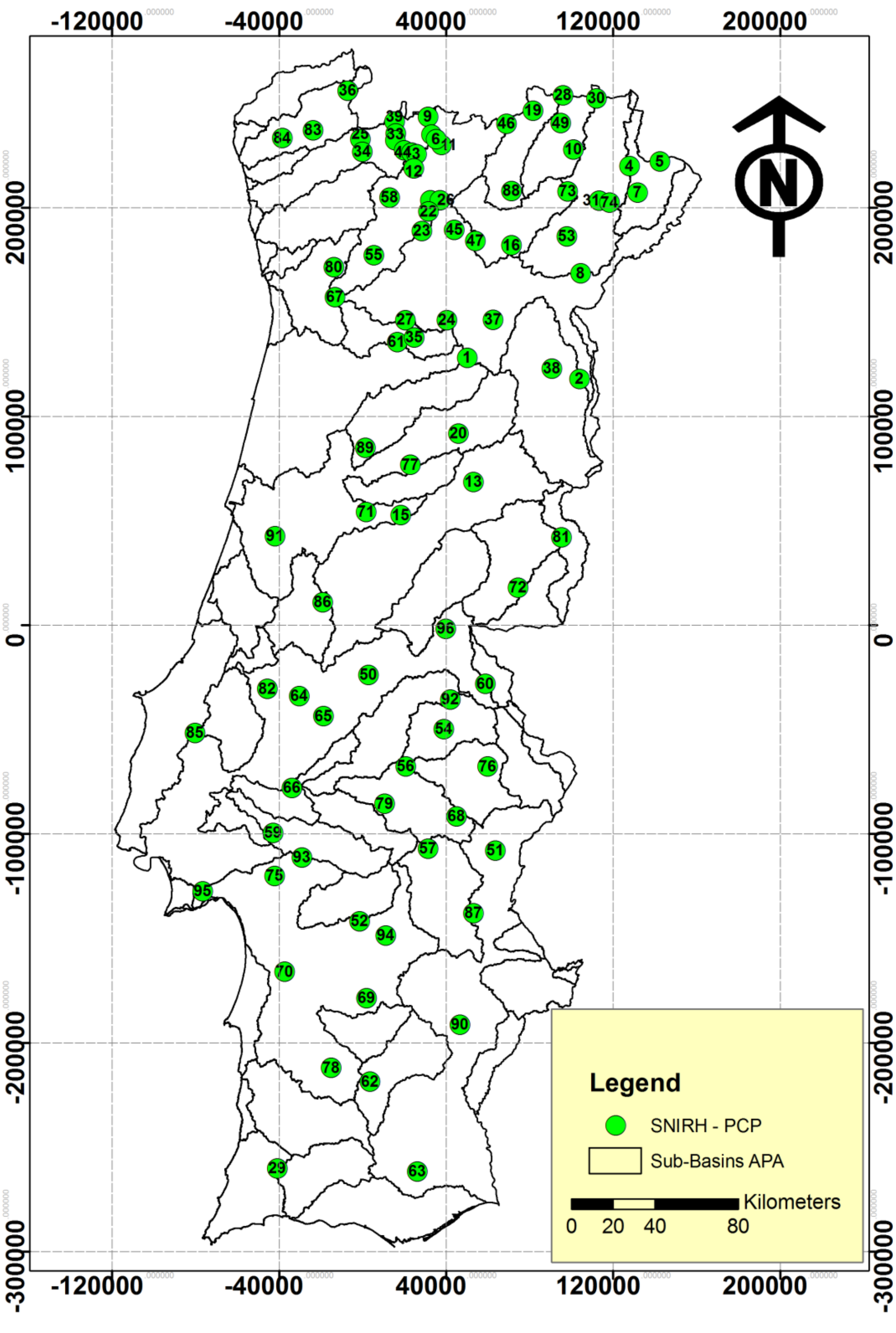

Figure 23 – Precipitation stations obtained from SNIRH.

With this data it was possible to compare precipitation obtained from SNIRH and obtained from CFSR and MM5-R (Figure 24). Each point refers to the annual sum of precipitation for each weather station compared with the same value of each calculation cell of the CFSR model where the station is located. This means that no spatial interpolation was made. In Figure 25 and Figure 26 comparison is made in the same perspective as Figure 24 but results are organized per station and parameters analysed are average precipitation, NSE and PBIAS. Sado and Tejo tend to have better results than Douro.

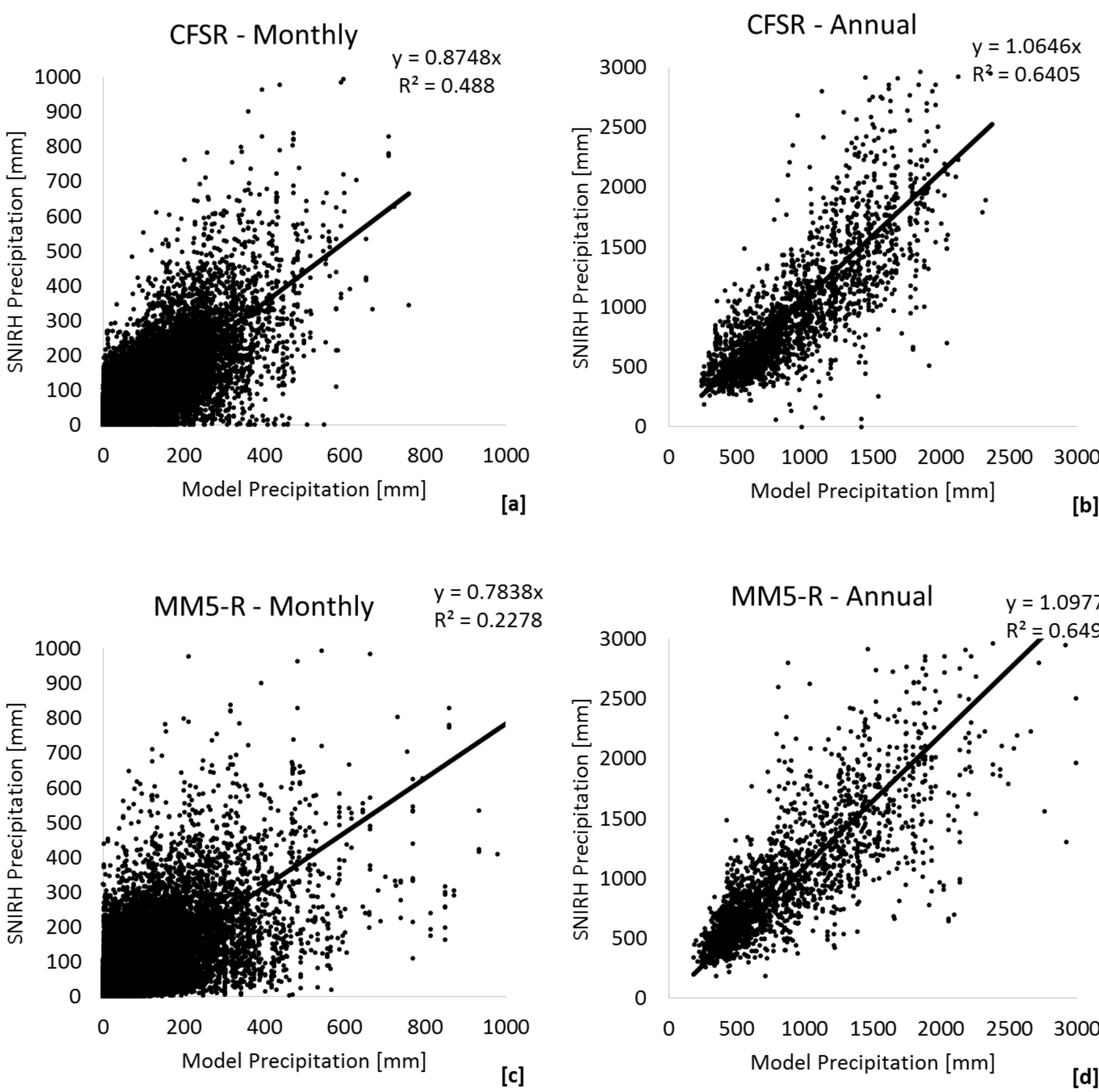

Figure 24 Comparison of precipitation obtained from SNIRH and from CFSR.

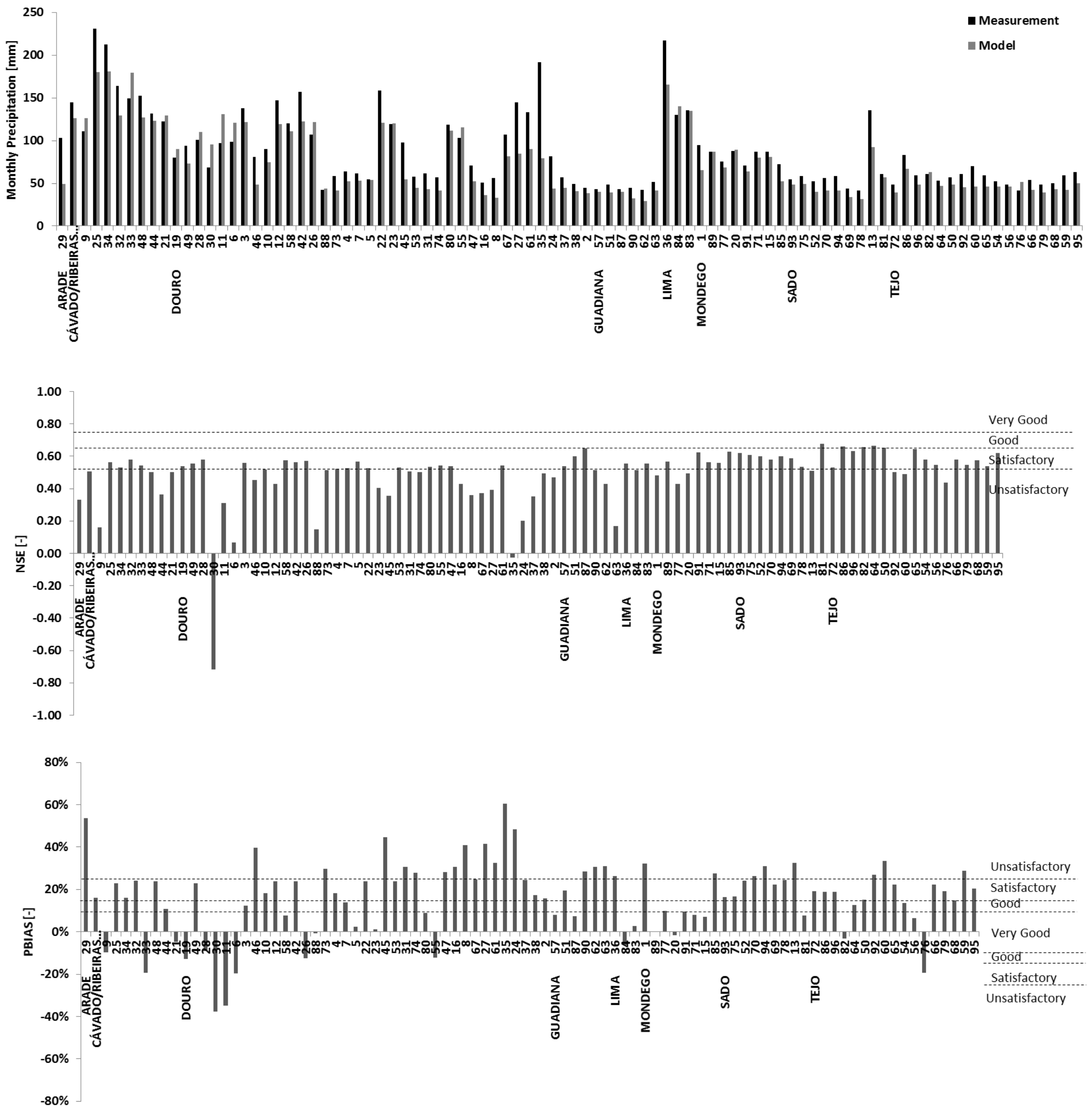

Figure 25 Average values of MM5-R and SNIRH monthly precipitation and NSE and PBIAS.

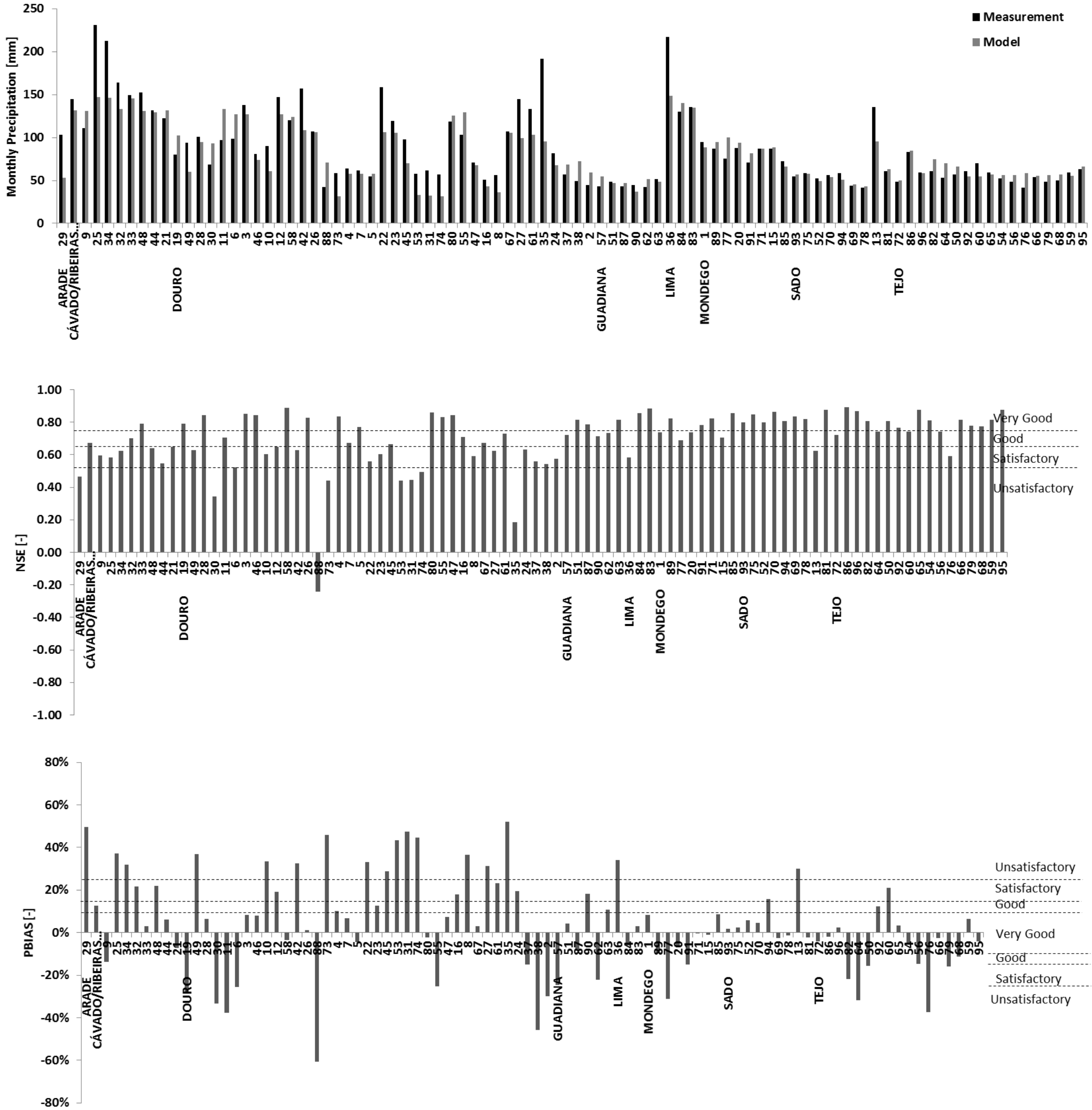

Figure 26 Average values of CFSR and SNIRH monthly precipitation and NSE and PBIAS.

4.3.2.2 IPMA-GRID

Belo - Pereira et al. (2011) developed a dataset called PT02 which is a daily gridded (~20 km grid) precipitation dataset over mainland Portugal. We will call this the IPMA-GRID. This dataset spans the period from 1950 to 2003 and is based on 806 stations, 188 meteorological stations from the

Portuguese Meteorological Service (IPMA) and 618 rain gages from the National System of Water Resources (SNIRH) from the National Environment Agency (APA). This dataset was obtained by Belo - Pereira et al. (2011) using a Kriging method to evaluate two ECMWF reanalyses (ERA40 and ERA Interim). Figure 27 shows the grid from IPMA-Grid to compare with precipitation from CFSR.

With this data it was possible to compare gridded precipitation obtained from IPMA and obtained from CFSR (Figure 28). Each point refers to annual sum of precipitation for each grid cell compared with the same value of each calculation cell of the CFSR model where the station is located. This means that no spatial interpolation was made. Monthly values show a correlation of 0.85 while annual values show a correlation of 0.76. On the other hand, the relation between CFSR and IPMA-GRID is closer to one in the case of annual values (0.9669) than in the case of monthly values (0.9159).

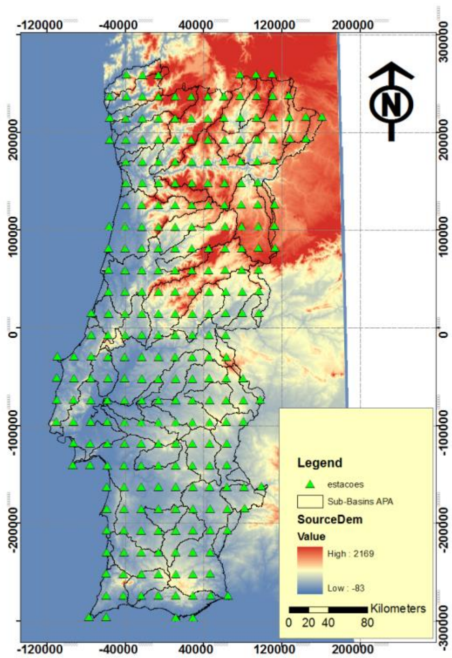

Figure 27 – Grid from gridded precipitation from Belo-Pereira (Belo-Pereira et al., 2011).

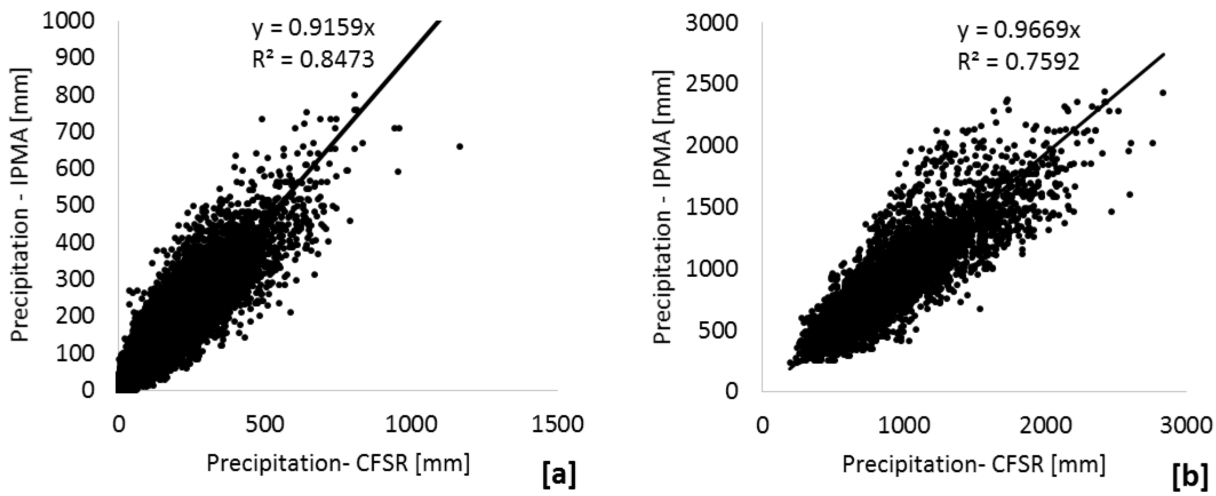

Figure 28 Comparison of precipitation obtained from IPMA-GRID and obtained from CFSR: [a] monthly and [b] annual results.

4.3.2.3 Nicolau, 2002

Nicolau (2002) applied a spatial integration of local precipitation measurements between 1960 and 1990 for Continental Portugal (Nicolau, 2002). This map is shown in Figure 29, and an extra source is presented to evaluate precipitation data that will be used as input for the model.

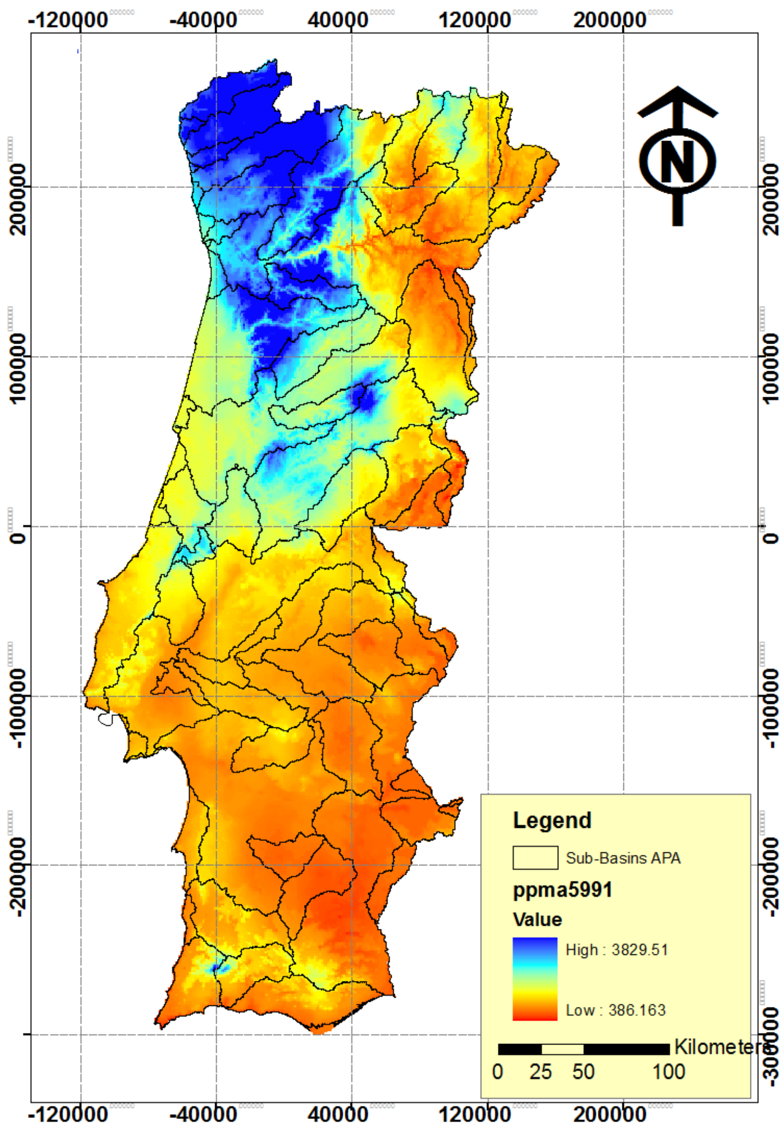

Figure 29 – Total annual precipitation for the period 1960 - 1990 (source: http://geo.snirh.pt/AtlasAgua/)

4.3.2.4 Inter-comparison of measurement data

Average annual precipitation was made for each APA watershed (Figure 10) using data from three sources: IPMA (Figure 18), SNIRH (Figure 23) and Nicolau (2002) (Figure 29). The result of inter-comparison between the three sources of data is shown in Figure 30. One can find differences at the watershed level. For example in the Cavado river, precipitation has an average value of 2094 mm in Nicolau (2002), while for IPMA-GRID the value is 1535 mm.

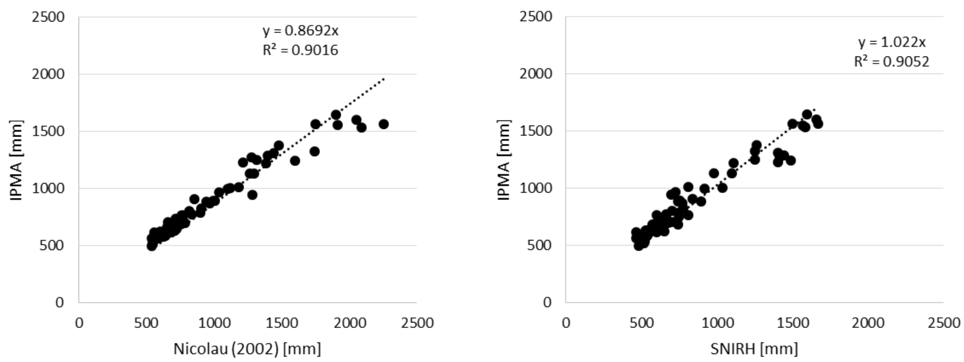

Figure 30 – Comparisons between precipitation from IPMA-GRID with SNIRH and precipitation from Figure 29

Another comparison can be made statistically analysing the correlation between the monthly precipitation data of SNIRH with the monthly precipitation data from IPMA-GRID (Figure 31). Data from SNIRH was used to generate the IPMA-GRID. However IPMA-GRID includes more precipitation stations from SNIRH and also includes stations from IPMA. An interpolation is also made. Thus, datasets are expected to be different. This comparison can show how different they are and also if there is any bias. Figure - 32 shows that agreement between SNIRH and IPMA-GRID was made quantitatively in terms of misfit of model results. This evaluation was done using two performance evaluators: Nash-Sutcliffe model efficiency (NSE) and Percent bias (PBIAS). Overall result show that IPMA-GRID is well correlated with SNIRH gage station. Biggest differences were found in Arade, Cavado and Lima.

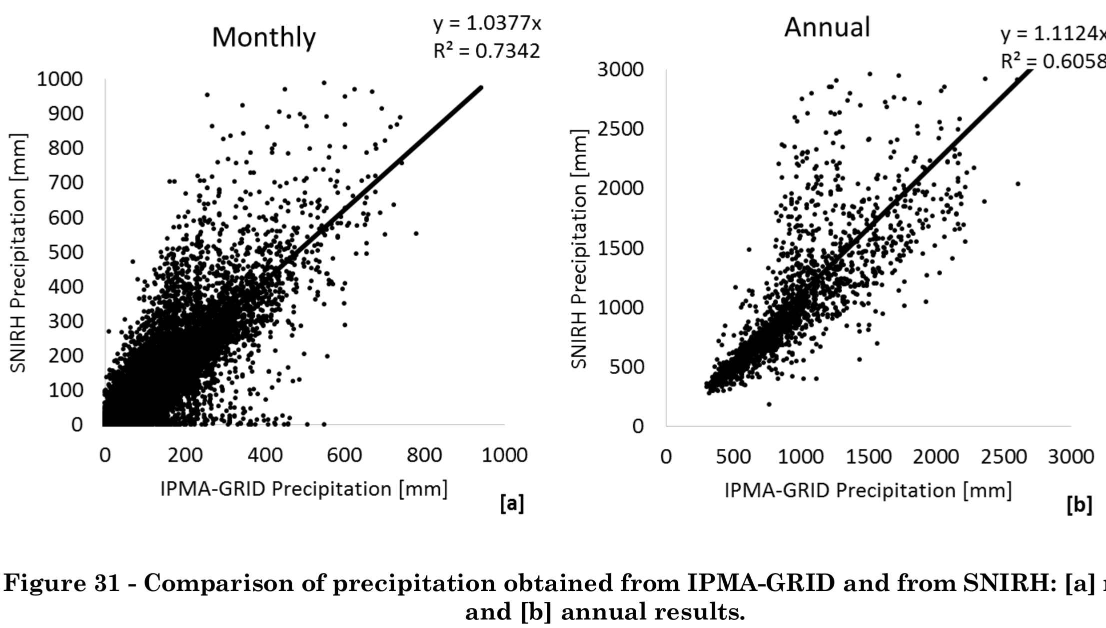

Figure 31 - Comparison of precipitation obtained from IPMA-GRID and from SNIRH: [a] monthly and [b] annual results.

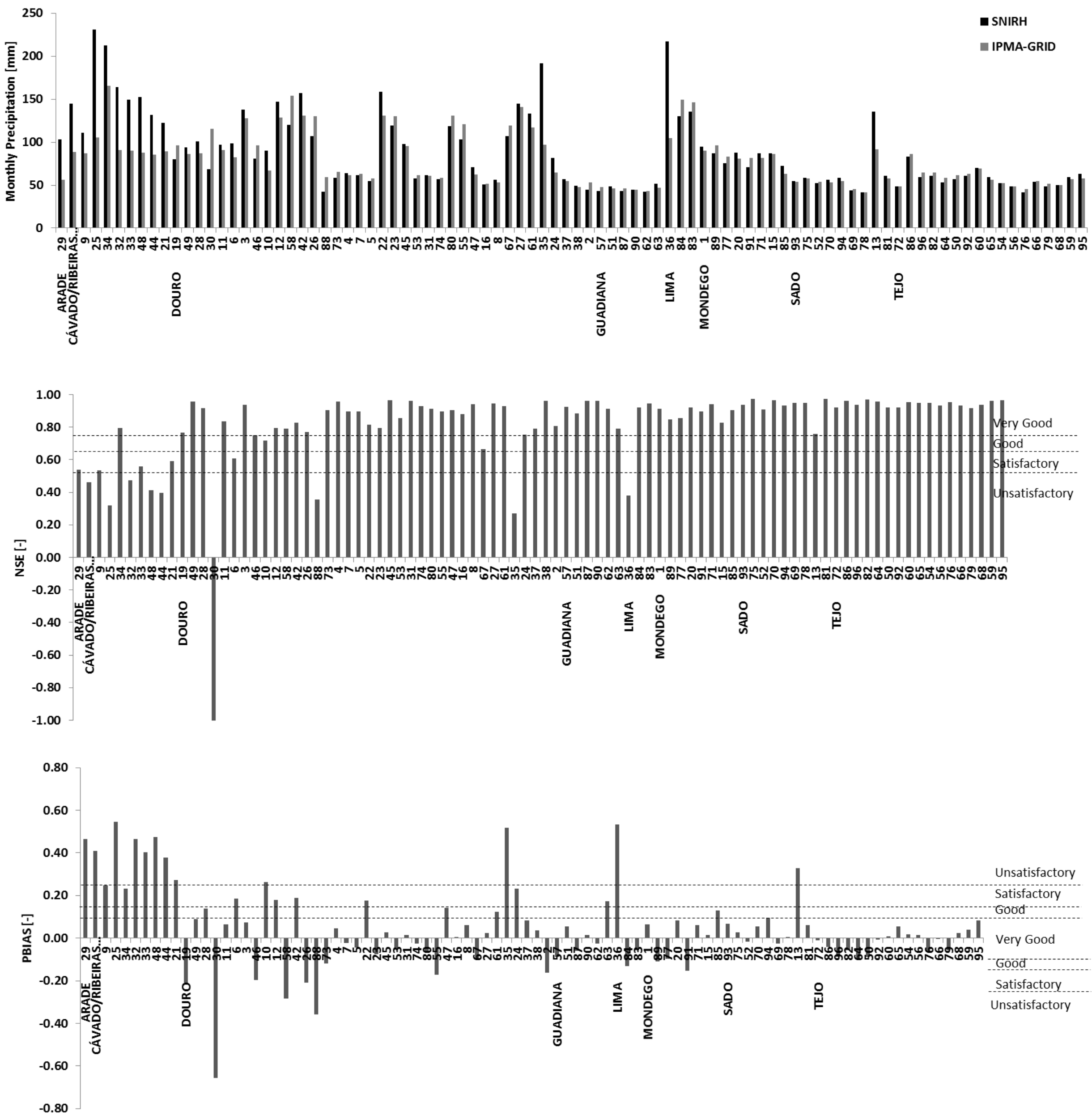

Figure - 32 Average values of IPMA-GRID and SNIRH monthly precipitation and NSE and PBIAS.

4.4 Discussion

4.4.1 Model heterogeneity

One of the major difficulties in watershed models is the inclusion of the inherent heterogeneity of real watersheds. This heterogeneity regards both flow paths and geometry (Beven, 1996). An example of a heterogeneous (complex) flow path is soil infiltration. Infiltrated water depends, among other things, on micro topography and the saturated conductivity of the soil. The first retains the water giving it more time to infiltrate and the second increases the velocity of infiltration. Bedford (Bedford, 2008) has found that these two parameters vary with vegetation in semi-arid shrubland and grassland landscapes. The best example of geometry heterogeneity is the porous media of the watershed (which comprises the soil, aquifer and river beds). As a result it is generally accepted that there isn't just one set of perfect parameter values in the logic of one fits all, but instead there is the perception of a range of parameter values that originate multiple results. These results include the measurements, which themselves have errors that justify the non-uniqueness of model results. Monte Carlo methods are used to deal with this range of parameter values and consist of a class of computational algorithms that rely on repeated random sampling to compute their results. Some examples of codes are GLUE (Beven and Binley, 1992) and SUFI (Abbaspour et al., 2007). These methods were not used in this thesis but can be in the future a valuable tool to obtain the best set of parameters needed to reproduced measured flows with the model.

Watershed models lump the heterogeneities one way or the other. However, different models can reproduce the hydrology of the same watershed, even if they have different lumping procedures, and because of that they are called equifinal. Two models are equifinal if they lead to an equally acceptable or behavioural representation of the observed natural processes, though they have different equations and different parameters.

In the present application of SWAT, it was also not possible to include all the heterogeneity of available data. The first lumping was described in the previous chapter by creating sub-basins that had a slope generated from a very detailed topography. However these sub-basins were generated at the maximum possible detail that is adequate for this thesis. A second lumping was necessary on the definition of input of land use and soil. This lumping consisted of attributing a dominant HRU to each sub-basin. As a consequence some land use areas gain importance (ex: coniferous forests) while some others reduced their importance (ex: wetlands). However land use has a limited impact on the monthly hydrology of the model. This happens because i) even with no plants (and consequently with no transpiration) there are losses by evaporation, ii) the impact of land use on runoff is less apparent in monthly flows, and iii) because evapotranspiration is mostly limited by soil depth and reference evapotranspiration (which depends only on climate). In fact, the physical properties of soil determine the actual amount of evapotranspirated water. The depth of the soil, its field capacity and wilting point determine the water available to be evapotranspirated. Taking this into consideration one could say that the use of the dominant soil could bias the results. However, the soil map available is coarse and as a result there is either only one soil per sub-basin or there is a clearly dominant one.

One must not think that land use is not important to understand hydrology. In fact land use has the potential to change runoff, infiltration and evapotranspiration. For example, the water available for transpiration is dependent on root depth. This root depends on the soil but also on plant type. While some trees can reach many metres deep, annual crops typically reach less than 1 metre. To be able to determine the root depth, more information would be necessary about the soil and plants than that available.

4.4.2 Weather

4.4.2.1 Model Input data

From all the datasets presented the only one that is not adequate to be used as SWAT input is the one from Nicolau (2002), because it does not have daily precipitation values. The remaining datasets have daily time step, although SNIRH dataset has missing values. These missing values are typically below 15% but rarely lower than 5% (see 8.1). To use this dataset as input for SWAT implies that these missing values would have to be filled with values from other sources. Another drawback of the SNIRH dataset is its non-uniform spatial distribution. So, SNIRH was used only to validate the IPMA-GRID, CFSR and MM5-R.

Table 12 summarises the coefficient of determination (R^2) and slope obtained in the previous figures for monthly results: Figure 22, Figure 24, Figure 28 and Figure 31. These results show a good correlation between IPMA-GRID and SNIIRH and between IPMA-GRID and CFSR. It also shows a slope close to 1 (1.04) in the case of IPMA-GRID vs. SNIRH.

Table 12 – Correlation between monthly precipitations: R^2 and m slope ($Y=m*X$)

Y \ *X*	SNIRH	IPMA-GRID	MM5-R	CFSR
	R^2 / m			
SNIRH	1.00 / 1.00	0.73 / 1.04	0.23 / 0.78	0.48 / 0.87
IPMA-GRID		1.00 / 1.00	0.49 / 0.90	0.85 / 0.91
MM5-R	-	-	1.00 / 1.00	0.71 / 0.93
CFSR	-	-	-	1.00 / 1.00

IPMA-GRID was chosen has the reference dataset to run SWAT models because the best correlation obtained was between SNIRH and IPMA-GRID. This means that IPMA-GRID was used to calibrate and validate the model. Calibration was done for a period similar to the period where reanalysis data were available: 1979-2003. For the validation, a previous period from IPMA-GRID was used: 1950-1978. Daily values of temperature, solar radiation, wind and relative humidity used were from the CFSR dataset.

Subsequently the model was run using the reanalysis data (CFSR and MM5-R). For CFSR 36 years of data (1979-2014) were used, and for MM5-R 30 years of input (1979-2010). Each model has a different grid. To easily compare both results, the grid from CFSR was used as the reference grid. This means that precipitation was obtained from the centre of the CFSR cells not only for the CFSR model (which was the natural thing to do) but also for MM5-R where precipitation was obtained from those points. This means that the precipitation obtained from MM5-R was from the grid cells that were closer to the centre of the CFSR cells. So no interpolation was used to obtain precipitation values of MM5-R. This also means that this thesis did not use the full spatial detail of MM5-R.

4.4.2.2 Precipitation measured vs. model reanalysis

The local SNIRH values have lower correlations with the weather reanalysis probably because local values have very local trends that in reality do not represent the average of the cell and so do not compare well with the model results that represent average sub basin results.

The IPMA-GRID models could be operationalized allowing production of a result on precipitation for the near pass. In theory, this result could replace the weather reanalysis. In practice, now such a product exists. Moreover, the weather reanalysis has the advantage of generating a value that takes into account the topography and the use of soil. The IPMA-GRID uses only a spatial interpolation. This means that, in the future, reanalysis results have more potential to improve the accuracy of precipitation results. For the present work it was assumed that IPMA-GRID was the most accurate precipitation dataset and it was because of this it was used for the model calibration. For example Dile and Srinivasan (2014) had a different approach. They had precipitation from CFSR and from conventional precipitation station. The model was run with no calibration for both datasets.

As mentioned previously IPMA-GRID precipitation was obtained with a Kriging method . The fact that the IPMA-GRID is well correlated with CFSR precipitation means that the spatial interpolation of IPMA-GRID picks up an average result that is similar in CFSR.

Chapter 5

5 Model calibration and validation

The present chapter describes the flow data available in SNIRH to evaluate the model results. This data was then used to calibrate the model using precipitation data from IPMA-GRID between 1979 and 2003. Daily values of temperature, solar radiation, wind and relative humidity used were from the CFSR dataset. The model was validated using precipitation data from IPMA-GRID between 1950 and 1978. For temperature, solar radiation, wind and relative humidity, again CFSR data had to be used. The calibrated model is then used to generate flows using MM5-R and CFSR precipitation as input. The flows thus obtained were then compared with measured flows. Model results were then exported to a Portugal Hydrological database. The database structure and are described in appendix 8.6. Database was used to retrieve the water budget for continental Portugal in terms of blue and green water flow (based on model results).

5.1 Model runs

A first model run was produced using all the previously described inputs. Some parameters of the model area not dependent on input. A first run of the model was produced using IPMA-GRID precipitation and no changes were made to the default parameters of SWAT. A second calibrated run was produced and finally a third validated run was made. Calibration and validation process are described in next sections. Based on the calibrated run, a fourth run was produced using precipitation from CFSR and a fifth run was produced using MM5-R precipitation. In this chapter the results of all runs (except the first) are compared with measured flows.

5.2 Gage station data gathering

Data on measured flows was obtained from the Portuguese web data system on water resources (SNIRH). SNIRH has filters to sort the most relevant data to download. These filters were used to choose the most adequate gage station to evaluate results obtained in the present work.

Two periods were considered: one after 1979 that was used for model calibration and anther period before 1979 and until 1950 for model validation. The IPMA-GRID precipitation dataset exists for both periods with no gaps in time and space. Flows from SNIRH exist but in less quantity before

1979 and in higher quantity after 1979. However, flow data has random gaps. SNIRH gage stations were selected based on number of data years. The chosen criteria a minimum of 15 years of data.

Drainage area is the area of the watershed that contributes to the gage station. The bigger the drainage area the bigger the probability of having drainage areas in Spain. Also rivers with larger drainage areas are more influenced by reservoir management. Reservoirs typically change flow regimes by reducing flood peaks and enhancing summer low flows. Because of this an upper limit for drainage area of 5000 km^2 was imposed on retrieving gage stations. On the other hand, considering that the minimum drainage area of the model was 20 km^2 (and that in average each sub-basin about 40 km^2 drains), the lower limit of 100km^2 was imposed.

Model geometry was restricted to national territory. Because of this, some rivers' drainage area is smaller than the reality. Especially those with a relevant contribution from Spain. Another restriction was the size of the sub-basins. This means that the drainage area of the gage station was compared with the correspondent drainage area of the model reach. Stations that had a drainage area 10% bigger or smaller than the one in the model were excluded. Thus we were sure that geometry model restrictions do not affect comparison with measurements.

Typically, two types of station were excluded: i) stations with a relevant contribution from Spain; ii) stations with low drainage area that were positioned in the middle of the model sub-basin and not at its outlet. Figure 33 shows the number of values available for each watershed and for each hydrologic year. Until 1974 there is a constant increase of measurements. After 1974 values start decreasing and monitoring almost disappears in 1976, 1977 and 1978. This happened after the Portuguese revolution of 1974 during the period of political regime change. In 1979 the number of values sharply increases in all watersheds. Finally all watersheds have a sharp decrease in measurements between 2000 and 2010, some more at the beginning of the decade and others more towards the end. Appendix 8.2 shows the description of the chosen stations and Figure 34 shows their location on a map. SNIRH has 715 hydrometric stations, so the group chosen for this thesis was about 10% of the total hydrometric stations.

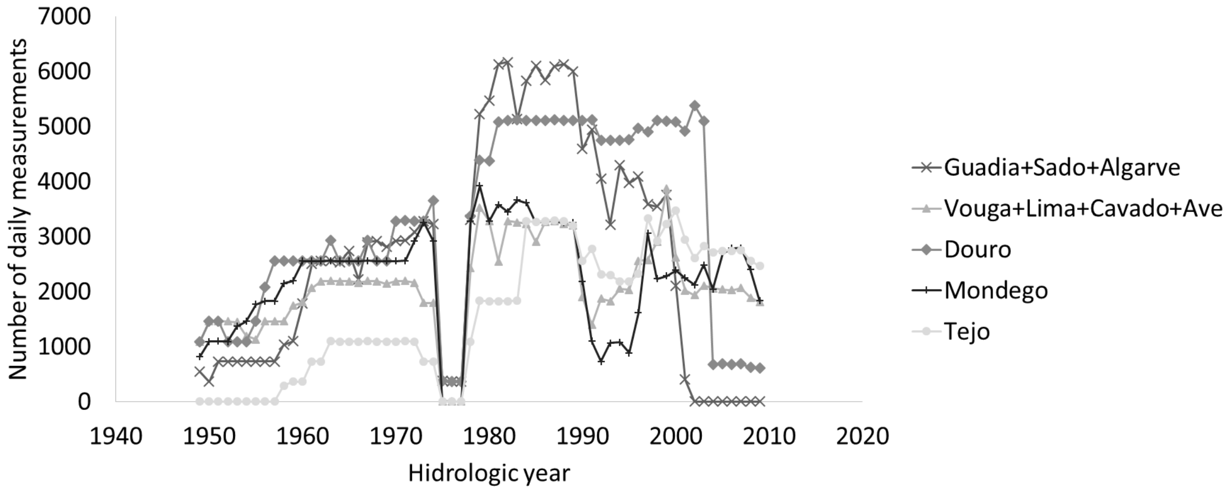

Figure 33 – Available SNIRH flow measurements

Two types of flows were retrieved: i) flow in river and ii) flow affluent to reservoir. The gage stations that have affluent flow to reservoir have their name marked with "(EDP)" (appendix 8.2). The remainder are all river flows.

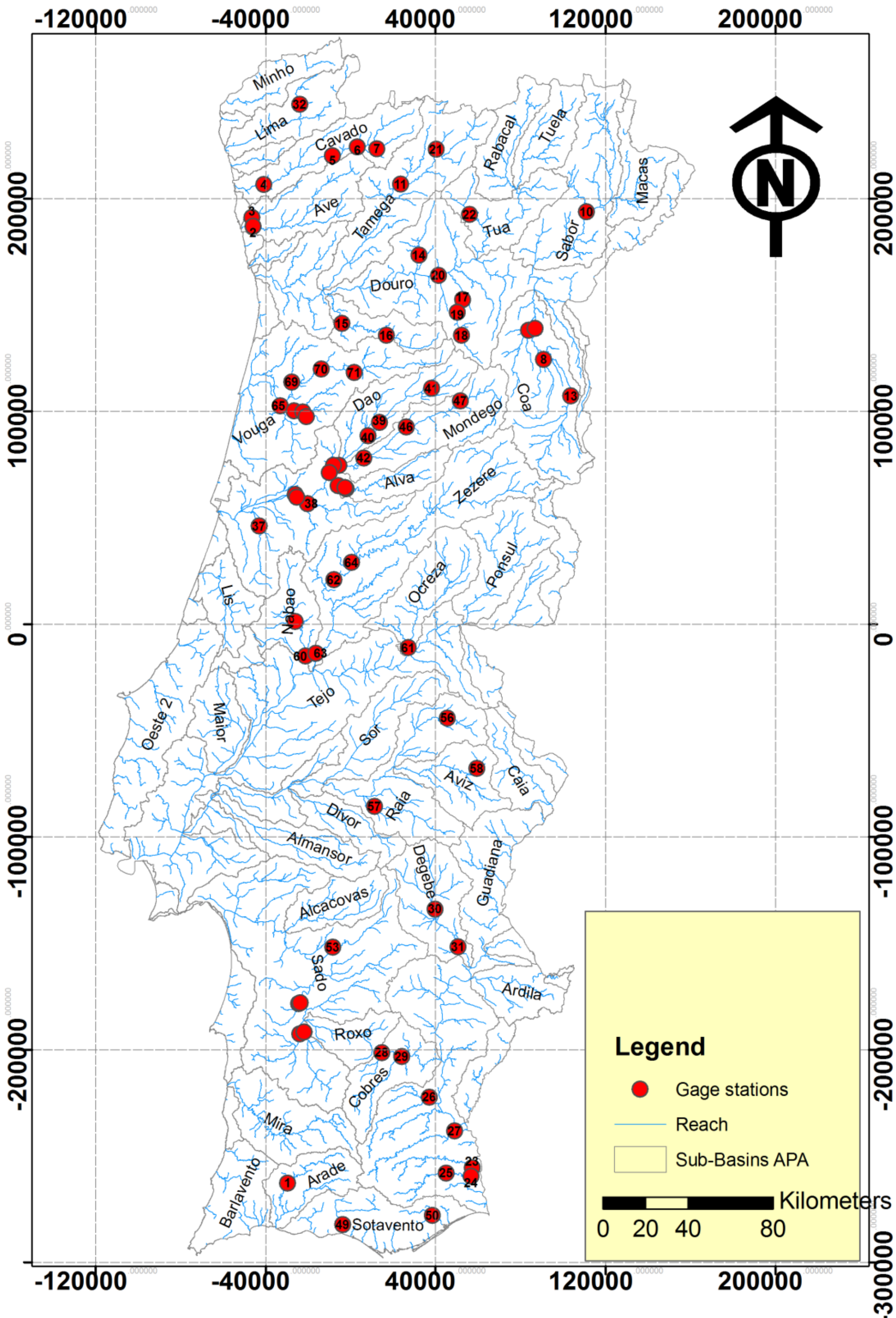

Figure 34 – Location of gage stations used to evaluate model (correspondent ID in Appendix 8.2)

5.3 Reservoir data gathering

SNIRH describes the available reservoirs in Continental Portugal. The data on 233 reservoirs was retrieved. Of these reservoirs only 163 had information on year of construction (Figure 35), either because it was not known or because they were not yet built. The number of reservoirs with a drainage area smaller than 5000 km^2 is 151, of which only 111 have information on active storage volume. Most of the reservoirs with no information on active storage volume have a drainage area smaller than 100 km^2 (only 11 have a drainage area bigger than 100km^2).

Reservoirs have an impact on the gage station results. The effect of these reservoirs is not simulated in the model. The effect they have on the gage station measurements are also not filtered out. This means that some of the bad results could be related to the reservoirs. However, the relation between the bad results and the reservoirs is not clear. Figure 35 shows the location of gage stations in relation to reservoirs. One should note that the image shows reservoirs that were created in the fifties and others created after the year 2000.

The approach presented does not calculate the effect of reservoirs in river flows. Because of this, evaluated flows only included gage stations with a drainage area less than 5000 km^2 and larger than 100 km^2. This filters out the rivers with a higher drainage area like the Douro, Tejo and Guadiana, that have a flow completely regulated by the reservoirs.

Still there are some reservoirs that can potentially have an impact on flows of gage stations with less than 5000 km^2 of drainage area. Reservoirs can change flow regimes by reducing flood peaks and enhancing summer low flows. Table 13 shows the reservoirs with more than 200 hm^3 that are in the gage station drainage areas analysed. Alto Lindoso reservoir in the Lima watershed and Santa Clara in the Mira watershed have a capacity higher than 200 hm^3, but they are not shown because they were not in the drainage area of any of the gage stations analysed. The table shows that Alto Rabagão, Cabril and Castelo de Bode were built before the calibration period while Aguieira was built before the calibration period.

Table 13 – Reservoirs with high storage capacity and with a drainage area smaller than 5000 km^2 (source: SNIRH)

Reservoir	Watershed	Year	Active storage [hm^3]	Total area [km^2]
Alto Rabagão	CÁVADO	1964	557	103
Aguieira	MONDEGO	1981	216	3069
Cabril	TEJO	1954	615	2416
Castelo de Bode	TEJO	1951	902	3965

The Ave watershed's many reservoirs do not seem responsible for differences, because both the capacity of reservoirs and drained area are relatively small. Guilhofrei is the biggest reservoir with 18 hm^3 of volume and a drainage area of 121 km^2.

On the other hand Cávado has many reservoirs that were constructed before the monitored period that could justify the very high base flow in its rivers. In particular, Alto Rabagão reservoir has a very high storage capacity (557 hm^3) and a very small drainage basin (103 km^2). Because of that the outflow of this reservoir has much lower peak flows and much higher base flow than the natural regime.

Guadiana watershed is an interesting example, where a first glance could lead to the conclusion that the reservoir significantly changes the flows: gage station 30 has two reservoirs before the gage station, and the result is bad. However, gage station (which is s after gage station 30) has a much better result.

Finally the Mondego watershed reservoir, built in 1985 affects results; however, the model underestimates high flows. Station 44 should not be considered due to the construction of Aguieira in 1981.

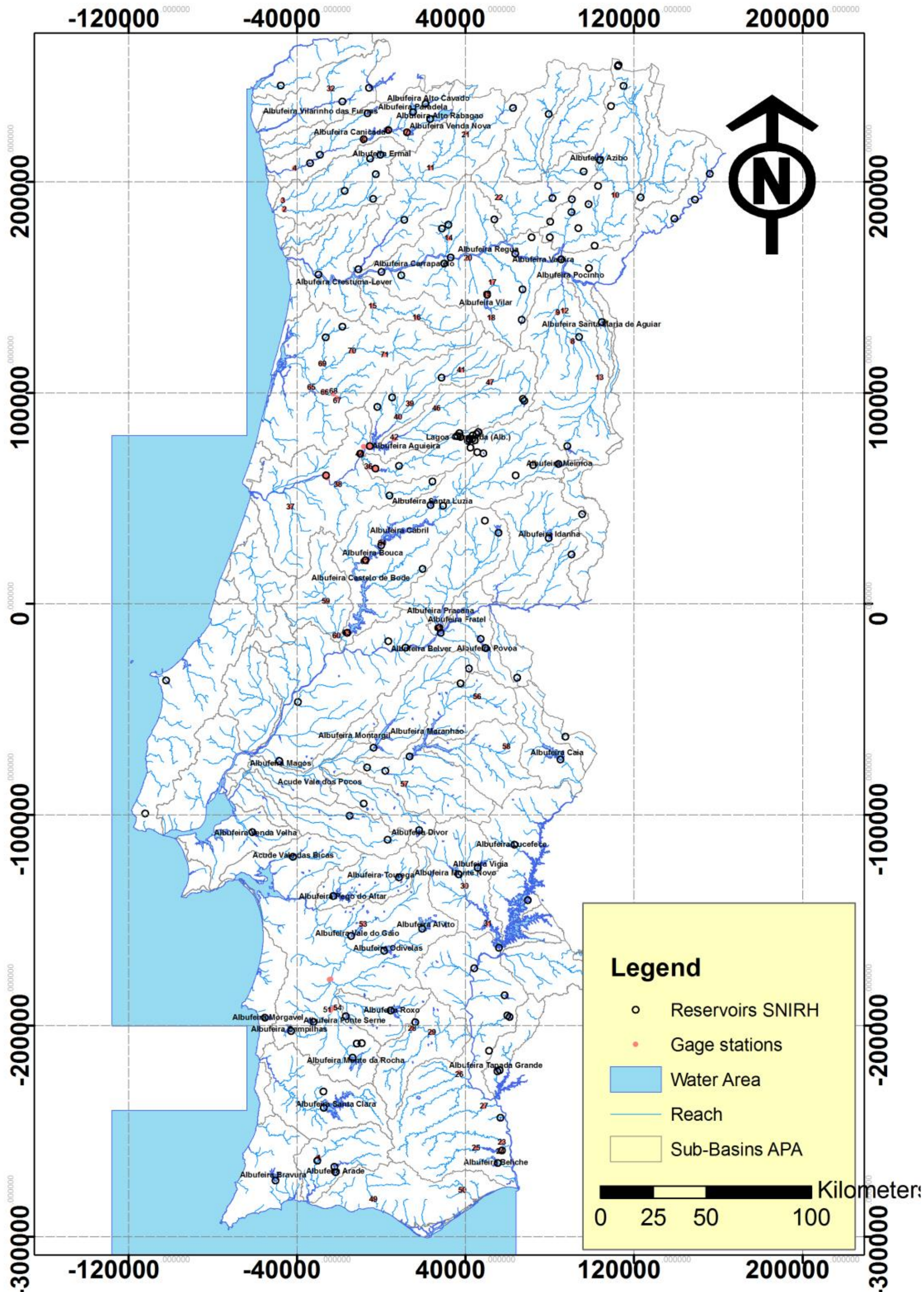

Figure 35 – Location of gage stations in relation to reservoirs (source: INAG, SNIRH).

5.4 Model calibration

The SWAT model does not have GIS input data on aquifers. In fact is very difficult to find seamless data on aquifers across the watershed. Normally ground water measurements are mostly performed in aquifers with higher water productivities. For areas with low productivity aquifers there is no data. Because of this the ground input data was used to calibrate model river flows. Table 14 shows the groundwater parameters and their values before and after calibration. Each of the parameters is described next, as well as its impact on simulation results.

The first year was used for spin-up (warming-up) of the model to minimise the influence of the initial states. This means that the calibration produced only began in 1980. This allows the model to get the water cycling properly before any comparisons between measured and simulated data are made. Because of this, the initial depth of water in the shallow aquifer parameter (SHALLST) was unchanged because this value only has impact on the beginning of the simulation.

The initial depth of water in the deep aquifer (DEEPST) was also left unchanged. In the SWAT model, the water stored in the deep aquifer can only be removed by including a pumping operation. In this implementation there was no water pumping from the deep aquifer. This variable will store the water lost from the percolation to the deep aquifer. Thus the initial condition has no impact on flow results.

Groundwater delay time (GW_DELAY) is the number of days that water moves past the lowest depth of the soil profile by percolation or bypass flow enters and flows through the vadose zone before becoming shallow aquifer recharge. This time will depend on the depth to the water table and the hydraulic properties of the vadose zone. A value of 6 was set for this parameter.

The baseflow recession constant, ALPHA_BF, accounts for groundwater flow response to changes in recharge. Values vary from 0.1-0.3 (1/days) for land with slow response to recharge to 0.9-1.0 for land with a rapid response. This parameter has a considerable impact on streamflow during periods of no recharge in the watershed. A value of 0.8 was set for this parameter.

Water may move from the shallow aquifer into the overlying unsaturated zone. In periods when the material overlying the aquifer is dry, water in the capillary fringe that separates the saturated and unsaturated zones will evaporate and diffuse upward. As water is removed from the capillary fringe by evaporation, it is replaced by water from the underlying aquifer. Water may also be removed from the aquifer by deep-rooted plants which are able to uptake water directly from the aquifer. This process is significant in watersheds where the saturated zone is not very far below the surface or where deep-rooted plants are growing. To account for this effect groundwater "revap" coefficient

(GW_REVAP) is used. As GW_REVAP approaches 0, movement of water from the shallow aquifer to the root zone is restricted. As GW_REVAP approaches 1, the rate of transfer from the shallow aquifer to the root zone approaches the rate of potential evapotranspiration. The value for GW_REVAP should be between 0.02 and 0.20. For the current implementation 0.2 was the selected value.

REVAPMN is the threshold depth of water in the shallow aquifer for “revap” or percolation to the deep aquifer to occur (mm H2O). Movement of water from the shallow aquifer to the unsaturated zone is allowed only if the volume of water in the shallow aquifer is equal to or greater than REVAPMN. A value of zero means that all water from shallow aquifer can be lost by evapotranspiration. This value was unchanged.

RCHRG_DP is the fraction of percolation from the root zone which recharges the deep aquifer. The value for RCHRG_DP should be between 0.0 and 1.0. For the overall budget this water does not contribute to flow or evapotranspiration unless there is pumping considered in the model. This value was unchanged.

GWQMN is the threshold depth of water in the shallow aquifer required for return flow to occur (mm H2O). Groundwater flow to the reach is allowed only if the depth of water in the shallow aquifer is equal to or greater than GWQMN. The higher the value, the higher the capacity to retain the first peak flows and the higher the evaporative capacity in the dry period. Low values lead to higher peak flows and lower evapotranspiration in drier periods. A value of 200 mm was set for this parameter.

Table 14 – SWAT groundwater hydrologic parameters

Name	Description	Default value	Calibrated value
SHALLST	Initial depth of water in the shallow aquifer [mm]	0.5	0.5
DEEPST	Initial depth of water in the deep aquifer [mm]	1000	1000
GW_DELAY	Groundwater delay [days]	31	6
ALPHA_BF	Baseflow alpha factor [days]	0.048	0.8
GWQMN	Threshold depth of water in the shallow aquifer required for return flow to occur [mm]	1	200
GW_REVAP	Groundwater "revap" coefficient	0.02	0.2
REVAPMN	Threshold depth of water in the shallow aquifer for "revap" to occur [mm]	1	1
RCHRG_DP	Deep aquifer percolation fraction	0.05	0.05
GW_SPYLD	Specific yield of the shallow aquifer [m^3/m^3]	0.003	0.003

Calibration evaluation was made, in the first stage, with a qualitative evaluation of performance, mainly by visually examining the agreement between observed data and model estimates. Graphs used for visual inspection are available in the appendix. An example of this visual examination is presented in Figure 36. Comparison was made between measurements (black line) and three modelling results. The blue line is a model using IPMA-GRID precipitation, the green line is a model with CFSR precipitation and finally the red line is a model with MM5-R precipitation. Figure 36 shows results for the Castro Daire gage station (SNIRH code: 08J/01H) located on the River Paiva, which is a part of the Douro watershed. In this case the IPMA-GRID result tends to overestimate the peak flows and to underestimate the base flow (when compared with measurements). It is also possible to see that the model with MM5-R precipitation overestimates also the peak flows in some years. The year 1979 was used as spin-up, because default initial conditions were used. However, the model results for this year were included in the graph.

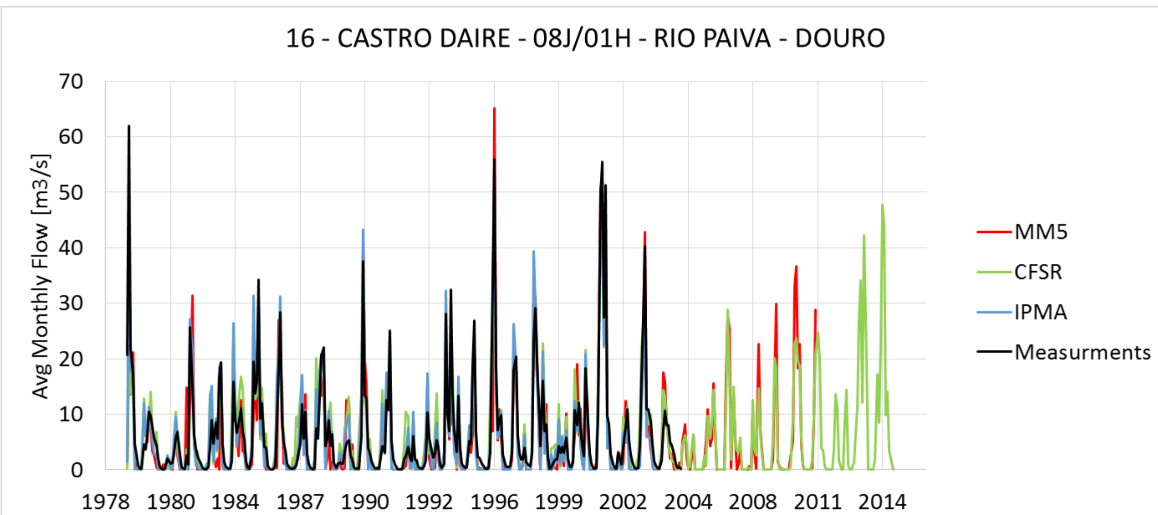

Figure 36 – Flow measured and simulated for the Castro Daire gage station of Paiva River in Douro watershed

In the second stage, the agreement between model and data was made quantitatively in terms of misfit of model results (Figure 37, Figure 38 and Figure 39). This evaluation was done using two performance evaluators: Nash-Sutcliffe model efficiency (NSE) and Percent bias (PBIAS).

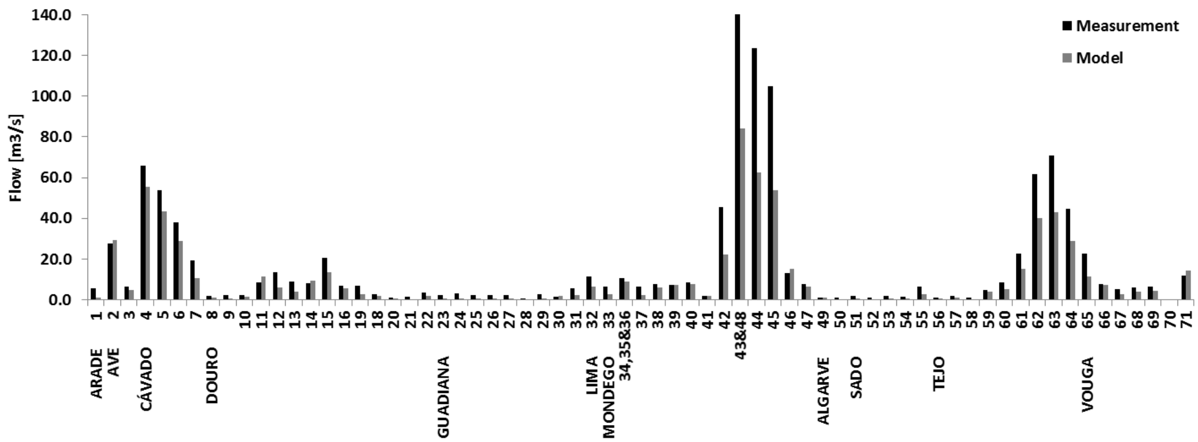

Figure 37 – Flow measured and simulated with IPMA-GRID (1979-2003)

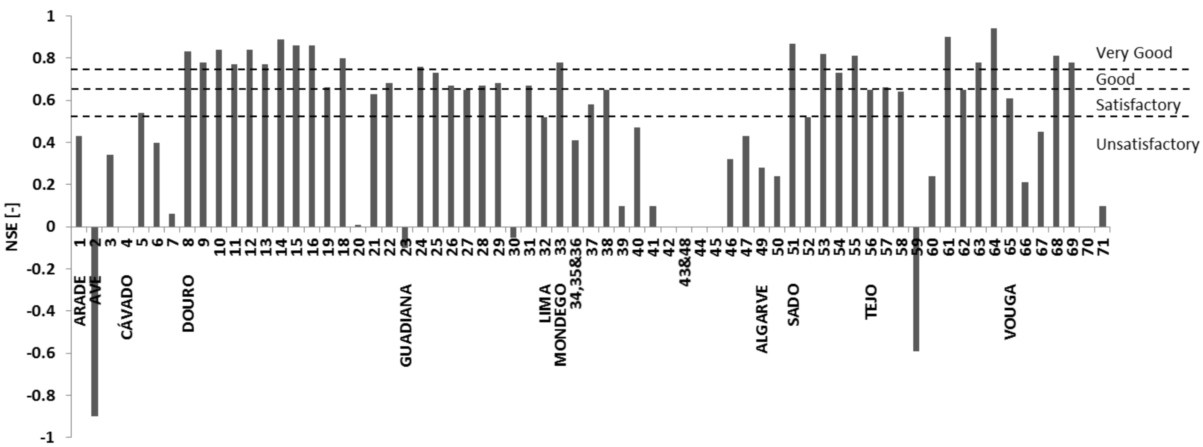

Figure 38 – NSE for simulation with IPMA-GRID (1979-2003)

PBIAS shows that the obtained calibration works mostly for Douro, Sado, Tejo and Vouga (Figure 39). For Cávado and Guadiana, the model tends to underestimate. In the case of Cávado the underestimation is mostly related to precipitation, while for Guadiana the present calibration is responsible for the model’s underestimation. This is to say that with a different calibration in Guadiana that decreased the amount of evapotranspiration, it would bring PBIAS to satisfactory values. On the other hand in Mondego, there is no clear tendency to under- or overestimation. This means that part of the gage stations would have to have a decrease of evapotranspiration (on the gage station drainage area) to increase PBIAS. Other gage station drainage areas would have to increase evapotranspiration to reduce PBIAS to satisfactory values. Finally the drainage area of some gage stations would have to maintain the same evapotranspiration rate, because PBIAS already has satisfactory values. This new calibration could get more complicated if there are gage station drainage areas that overlap. In this case drainage areas marked to increase evapotranspiration could overlap with areas marked to decrease evapotranspiration.

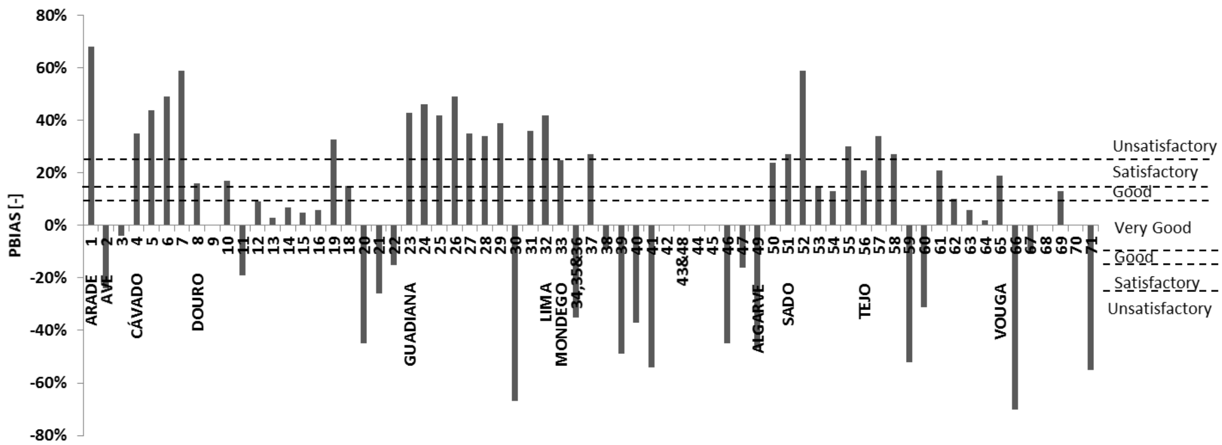

Figure 39 – PBIAS for simulation with IPMA-GRID (1979-2003)

5.4.1 Arade

In Arade only one gage station was analysed. Figure 40 shows the model runed using the SWAT model with IPMA-GRID with a blue line, while the black line shows the measurements made in Pachecos Gage station in Ribeira de Odelouca (station number 1 is the red dot and is also described in appendix 8.2). Figure 41 shows the location of the gage station as well as the streams that drain to the gage station. The black line in Figure 40 shows some gaps in the measurements that correspond to the unmonitored period. The comparison of the blue and black line shows that the model underestimates high flows, though the base flow returns reasonable results. The very high difference in the high flows explains why Arade gage station scored an unsatisfactory value of NSE (Figure 38) and also an unsatisfactory 70% PBIAS (Figure 39). This is probably related to an underestimation of precipitation of IPMA-GRID in the Arade watershed that was detected for SNIRH precipitation station of Monchique in Figure - 32. Figure 41 shows the location of that precipitation station, in relation to the total annual precipitation that was described in 4.3.2.3 (Nicolau, 2002). The total annual precipitation is represented by a rainbow colour scale where blue is the highest precipitation of the scale and red is the lowest. Even though the area with high precipitation is low when compared with the remaining watersheds, the precipitation is very high, which can generate high values of runoff and consequently the high flows that are visible in the flow measurements.

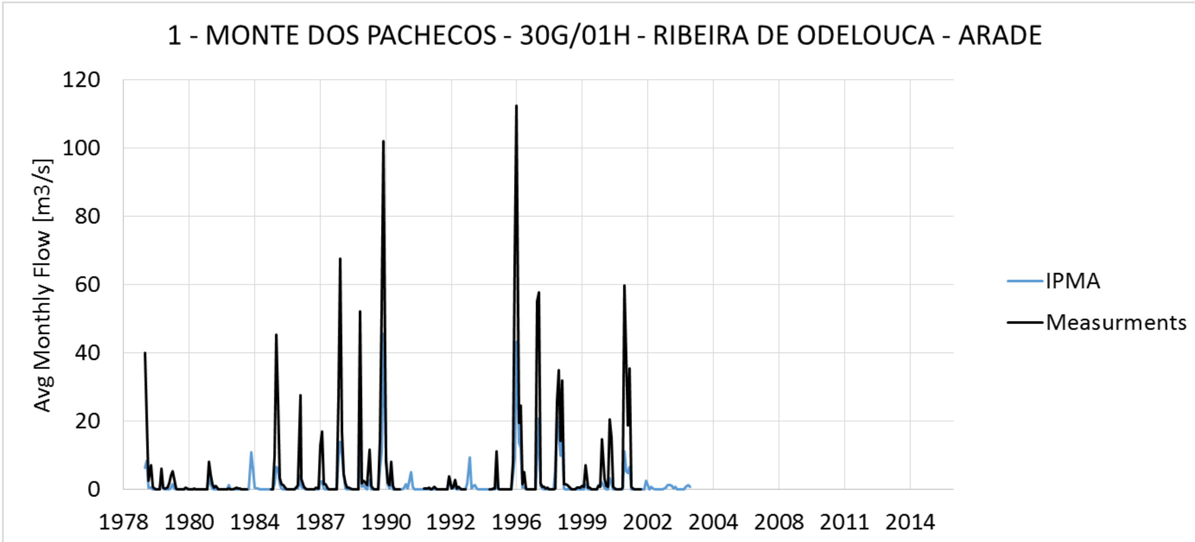

Figure 40 – Flow measured and simulated for the Monte dos Pachecos gage station of Arade River in Algarve

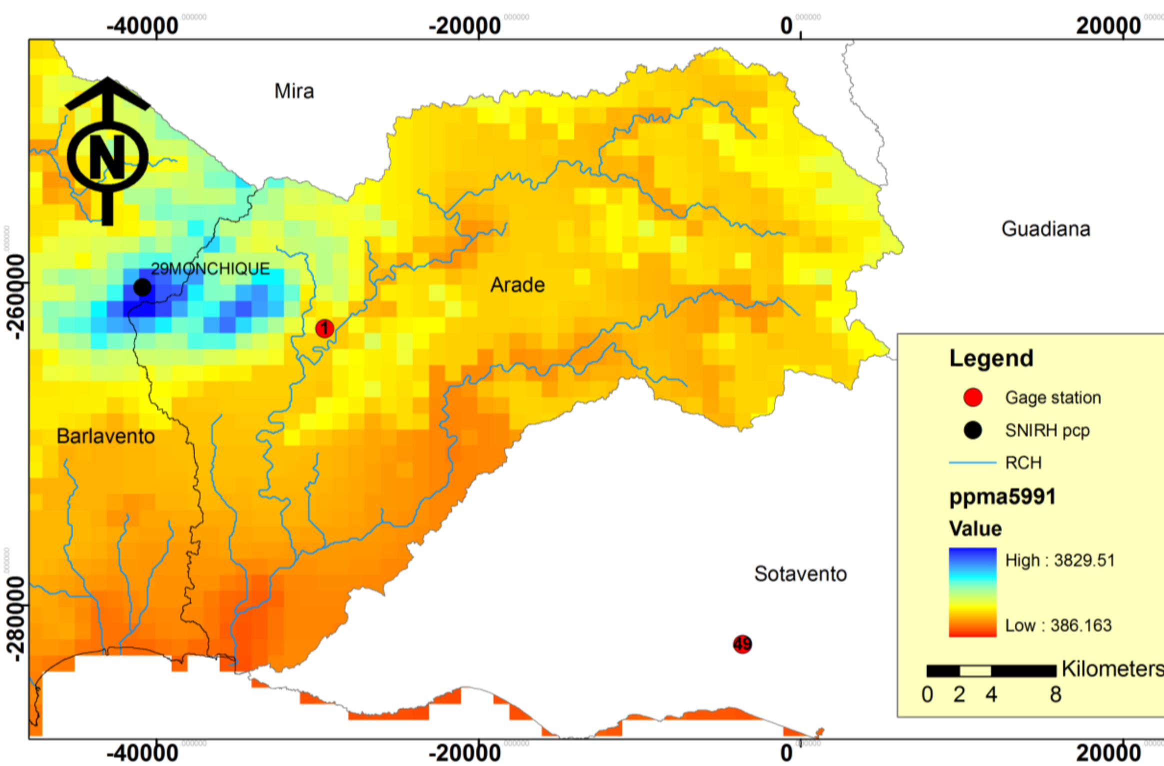

Figure 41 – Location of SNIRH precipitation stations and flow gage stations in relation to total annual precipitation in Arade watershed (source: Nicolau, 2002 and SNIRH).

5.4.2 Ave

Two gage stations were analysed in the Ave watershed (Figure 42 and Figure 43). Ponte Ave Gage station includes most of the drainage area of the Ave watershed (Figure 44). On the other hand, Ponte Junqueira Gage station drains a smaller area closer to the coast and with lower precipitation variability. Variability of precipitation in the Ponte Ave drainage area is as high as in the Cávado watershed. Ponte Junqueira has more satisfactory results than Ponte Ave, probably because of this difference of precipitation distribution. Nevertheless, the model overestimates high flows and underestimates base flows in both stations. One should note that in Ponte Ave, flow measurements are missing in at least three peak periods.

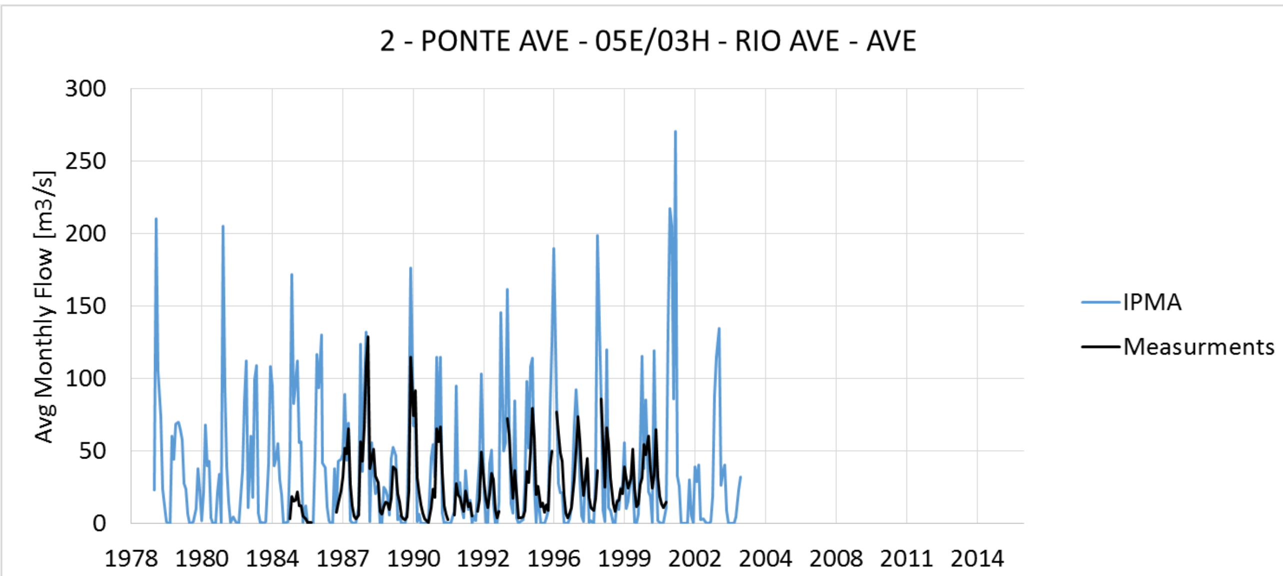

Figure 42 – Flow measured and simulated for the Ponte Ave gage station of Rio Ave in Ave watershed

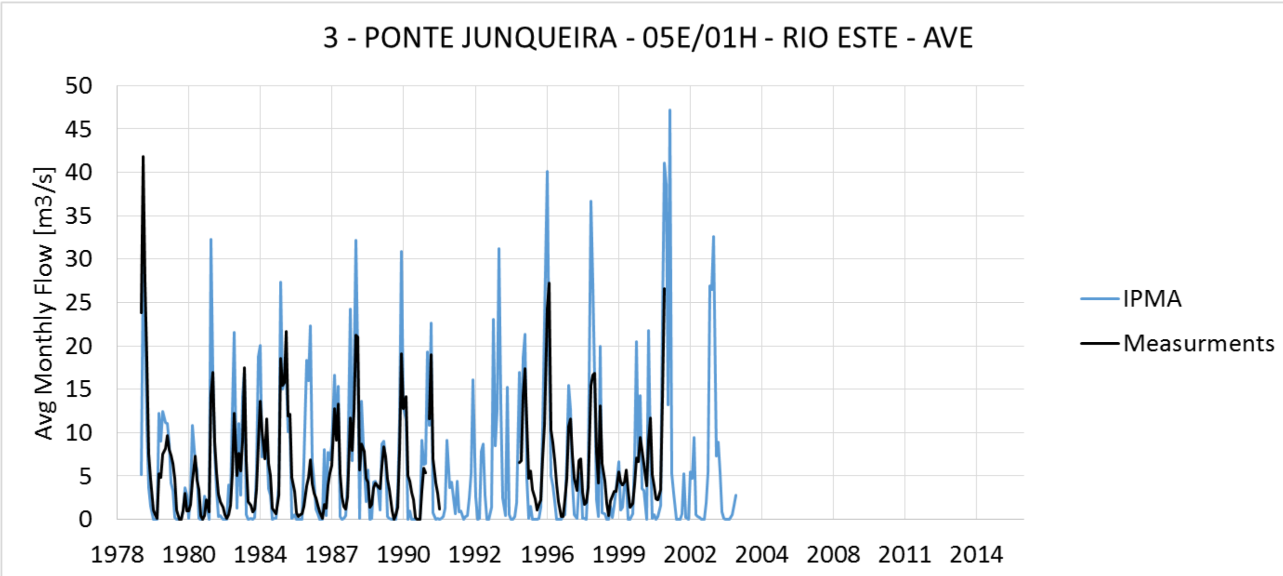

Figure 43 – Flow measured and simulated for the Ponte Junqueira gage station of Rio Este in Ave watershed

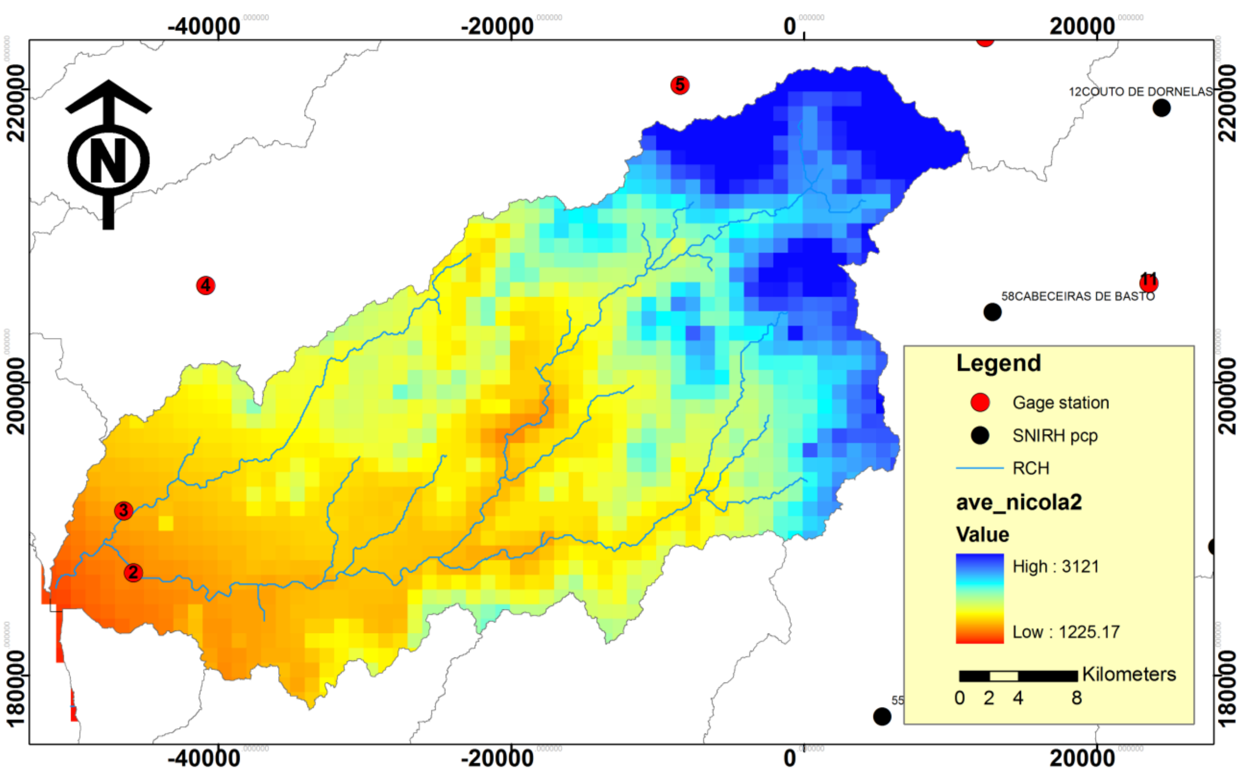

Figure 44 – Location of SNIRH precipitation stations and flow gage stations in relation to total annual precipitation in Ave watershed (source: Nicolau, 2002 and SNIRH).

5.4.3 Cávado

Four gage stations were obtained for the Cávado watershed (Figure 45). The model underestimates high flows and underestimates base flow. As an example, measured and simulated flows for gage Venda Nova and Salomonde stations are presented in Figure 46 and Figure 47. For the other two gage stations (4-Barcelos and 5-Caniçada), measured and simulated flows are presented in appendix 8.4.3. The underestimation of high flows is probably related to the underestimation of precipitation (Figure - 32). On the other hand, the base flow measured is very irregular and much higher than the model base flow. This is probably due to the reservoir Alto Rabagão that has a storage capacity of 557 hm^3. Flow station 7 shows the high base flow values, which are similar in downstream station 6. The cascade of reservoirs along the river might also increase this irregular and high base flow.

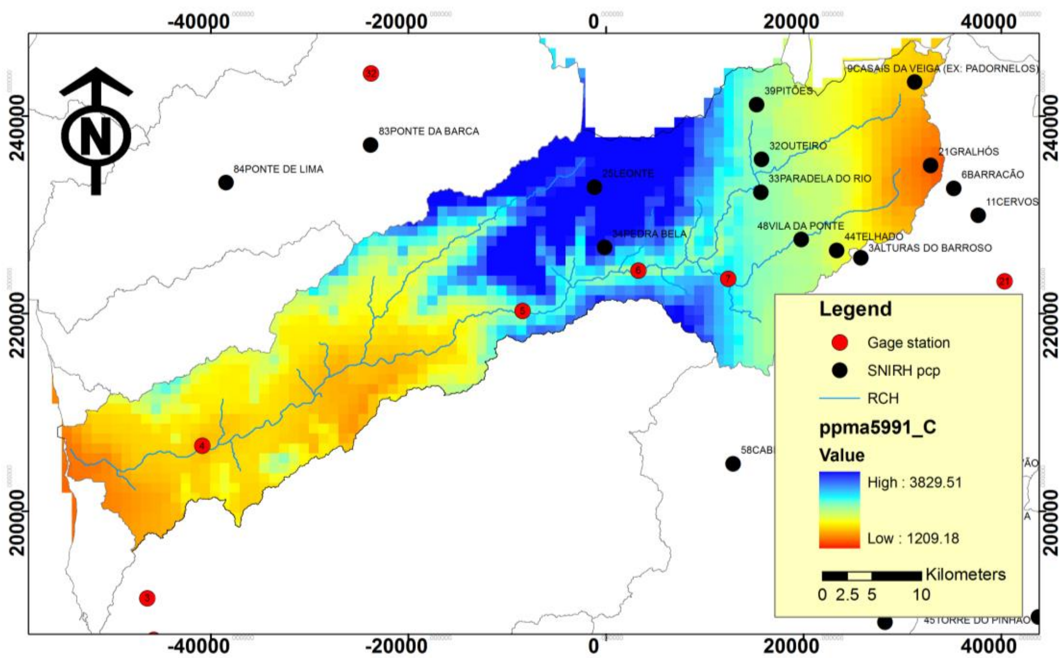

Figure 45 – Location of SNIRH precipitation stations and flow gage stations in relation to total annual precipitation in Cávado watershed (source: Nicolau, 2002 and SNIRH).

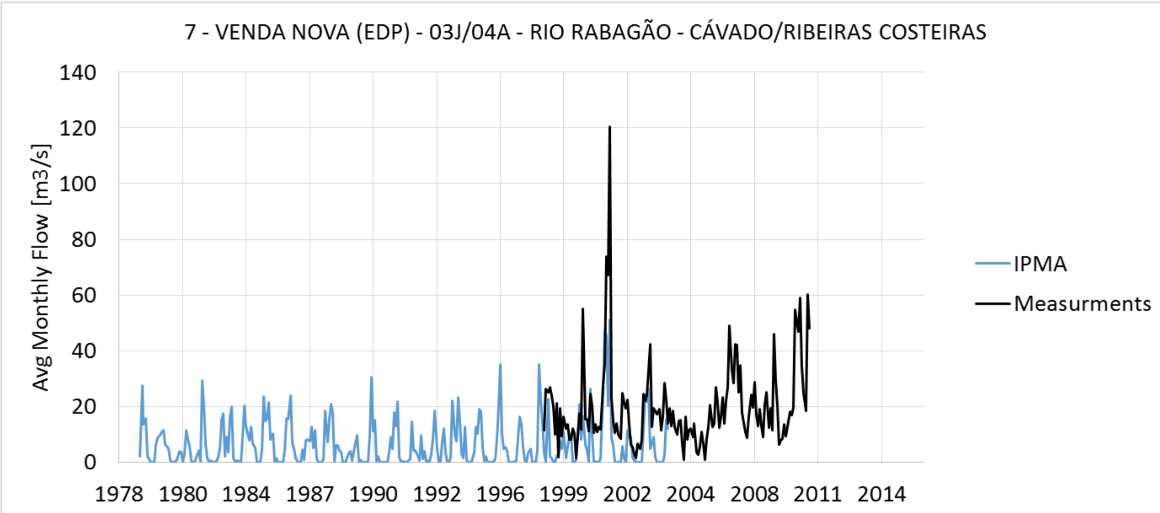

Figure 46 – Flow measured and simulated for the Venda Nova gage station of Rio Rabagão in Cávado watershed

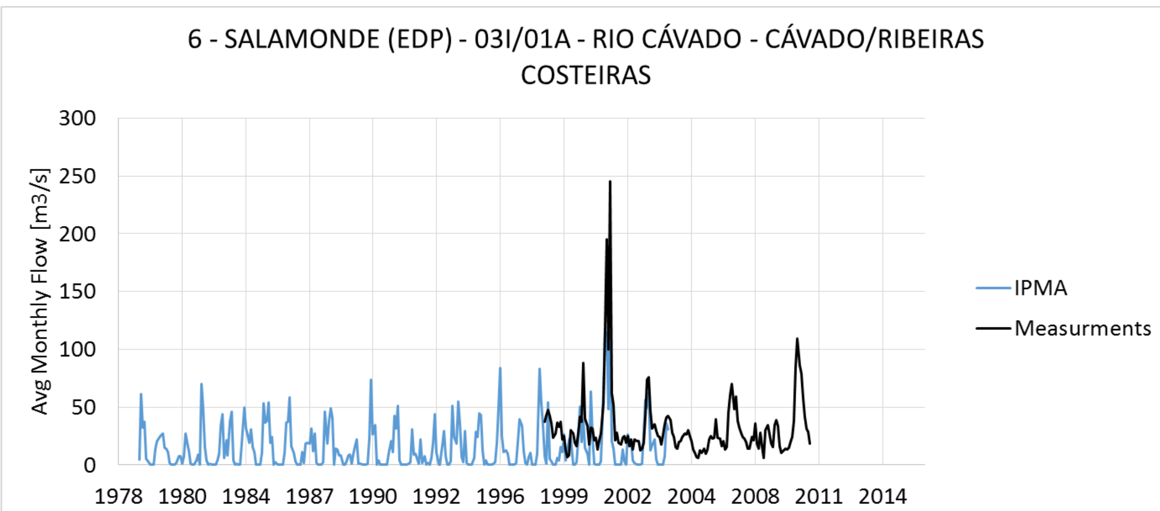

Figure 47 – Flow measured and simulated for the Salamonde gage station of Rio Cávado in Cávado watershed

5.4.4 Douro

In Douro 15 gage stations were retrieved, and Figure 38 and Figure 39 show that they either had very good or good results in terms of NSE and PBIAS. Figure 48 shows one of the gage stations with worse results in Douro, where is possible to see that the model overestimates flow, but where it is also possible to see that in the period of 1999 and 2002 there is missing data. On the other hand, Figure 49 shows an example of a good result in the Paiva river. The comparison of the 13 remaining gage stations between simulated and measured flow is presented in appendix 8.4.4. Overall model results are in accordance with measurements. In this watershed IPMA-GRID precipitation had a good correlation with SNIRH precipitation stations. Only few precipitation stations revealed unsatisfactory results for Douro. In general, in the case of Douro, gage stations have a long period and completeness of data. This also contributes to a good result. Figure 50 shows all the flow and precipitations stations analysed in Douro.

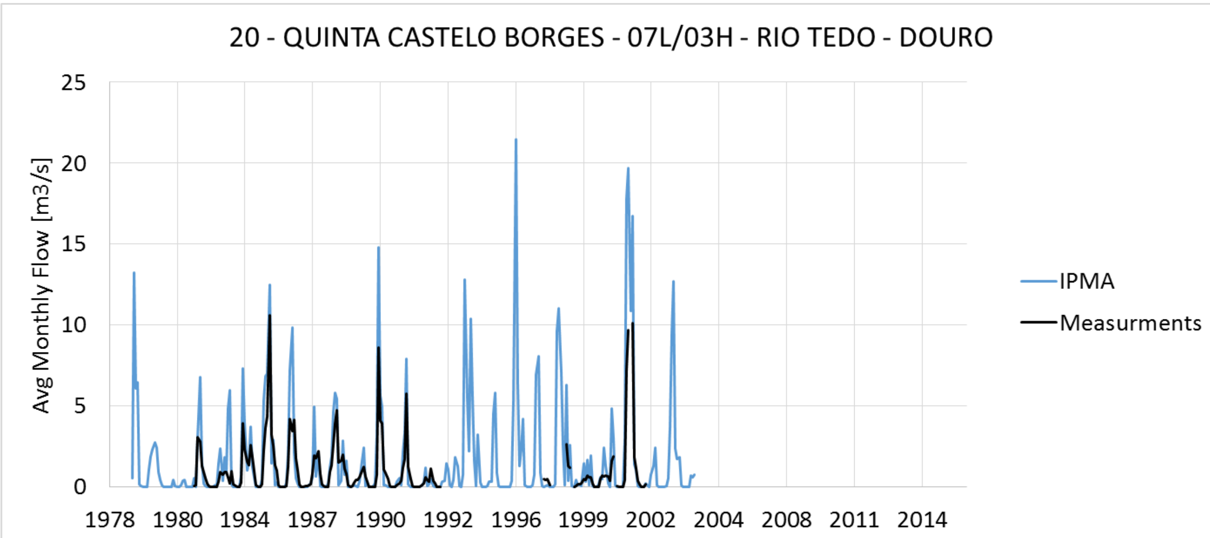

Figure 48 – Flow measured and simulated for the Quinta Castelo Borges gage station of Rio Tedo in Douro watershed

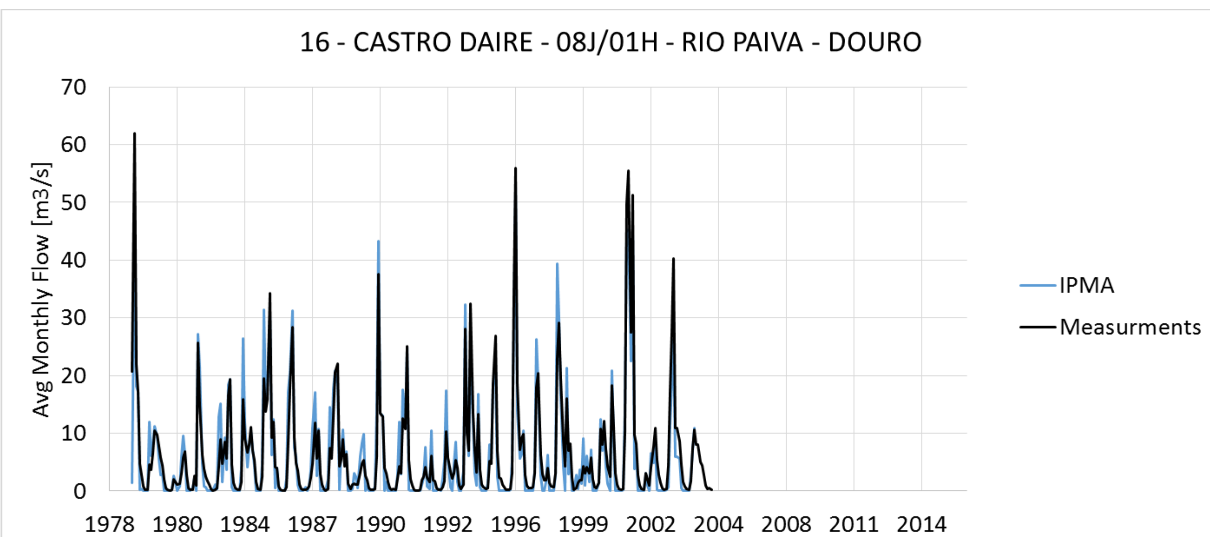

Figure 49 – Flow measured and simulated for the Castro Daire gage station of Rio Paiva in Douro watershed

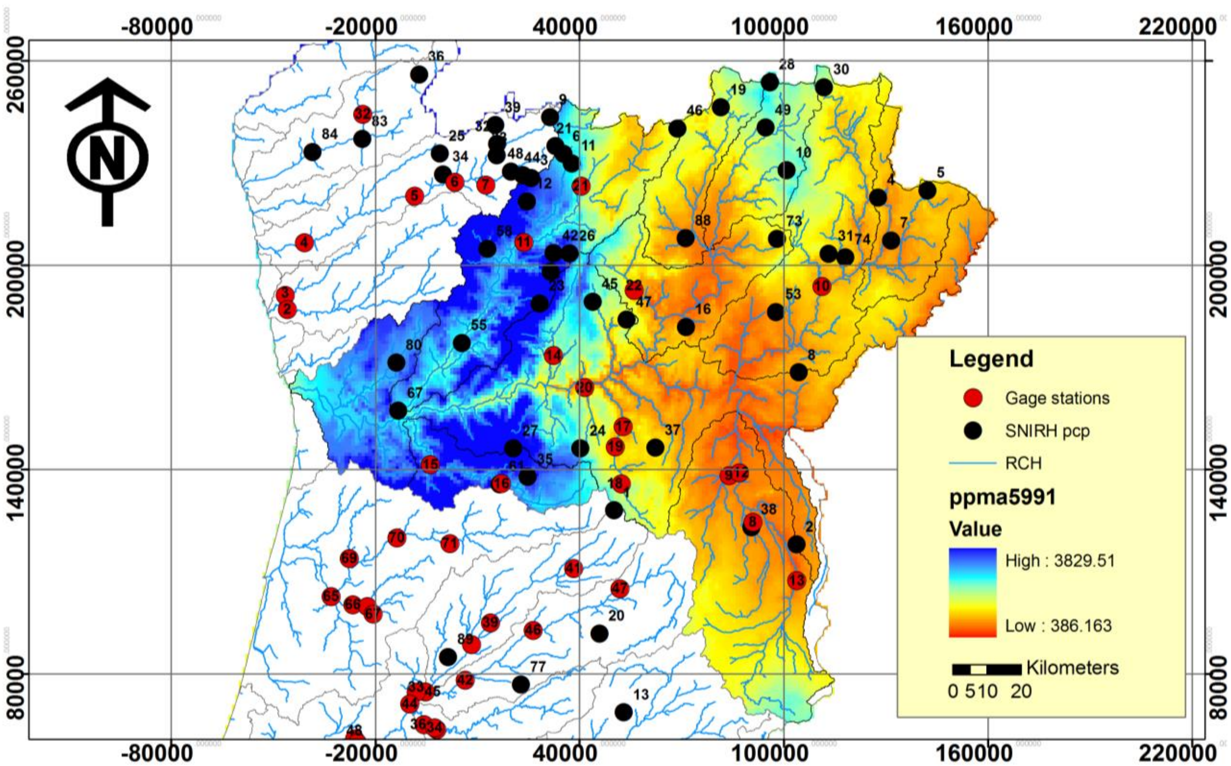

Figure 50 – Location of SNIRH precipitation stations and flow gage stations in relation to total annual precipitation in Douro Watershed (source: Nicolau, 2002 and SNIRH).

5.4.5 Guadiana

Guadiana returned a satisfactory or good result for the NSE in 7 out of the 9 gage stations analysed (Figure 38). On the other hand, in terms of PBIAS (Figure 39), all stations have unsatisfactory results. In general, the model tends to underestimate flows (PBIAS is close to 40%). Good results in terms of NSE means that IPMA-GRID precipitation is good enough for the model to reproduce the flow variability. This is confirmed by the good correlation of IPMA-GRID with the precipitation stations of SNIRH. Moreover, Figure 53 shows that each SNIRH precipitation station is in an area of very different precipitation intensity from the others. PBIAS results mean that peak flows have to be increased by a specific calibration in Guadiana.

The monthly comparison between measured and modelled flows in the 9 gage stations is available in appendix 8.5.3. Vendinha gage station has a drainage area of 821 km^2 while Amieira gage station as an area of about 1477 km^2. However the peak flows in Vendinha are many times less than a quarter of the flow in Amieira (compare Figure 51 and Figure 52) while the distribution of precipitation is not that different between the drainage areas of the two gage stations. This means that measured flows from Vendinha gage station are probably biased.

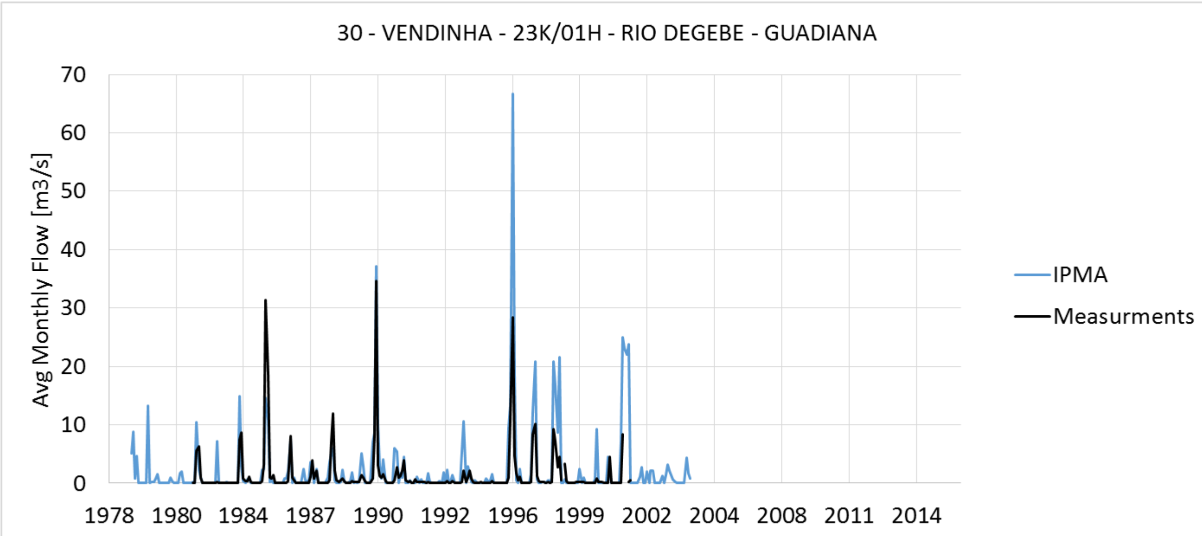

Figure 51 – Flow measured and simulated for the Vendinha gage station of Rio Degebe in Guadiana watershed

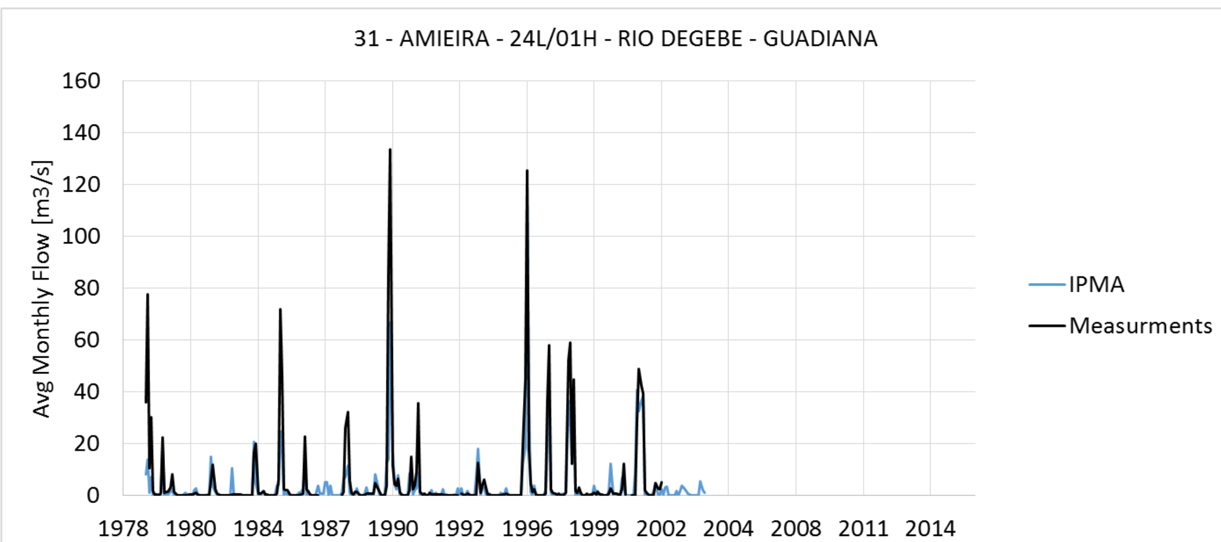

Figure 52 – Flow measured and simulated for the Amieira gage station of Rio Degebe in Guadiana watershed

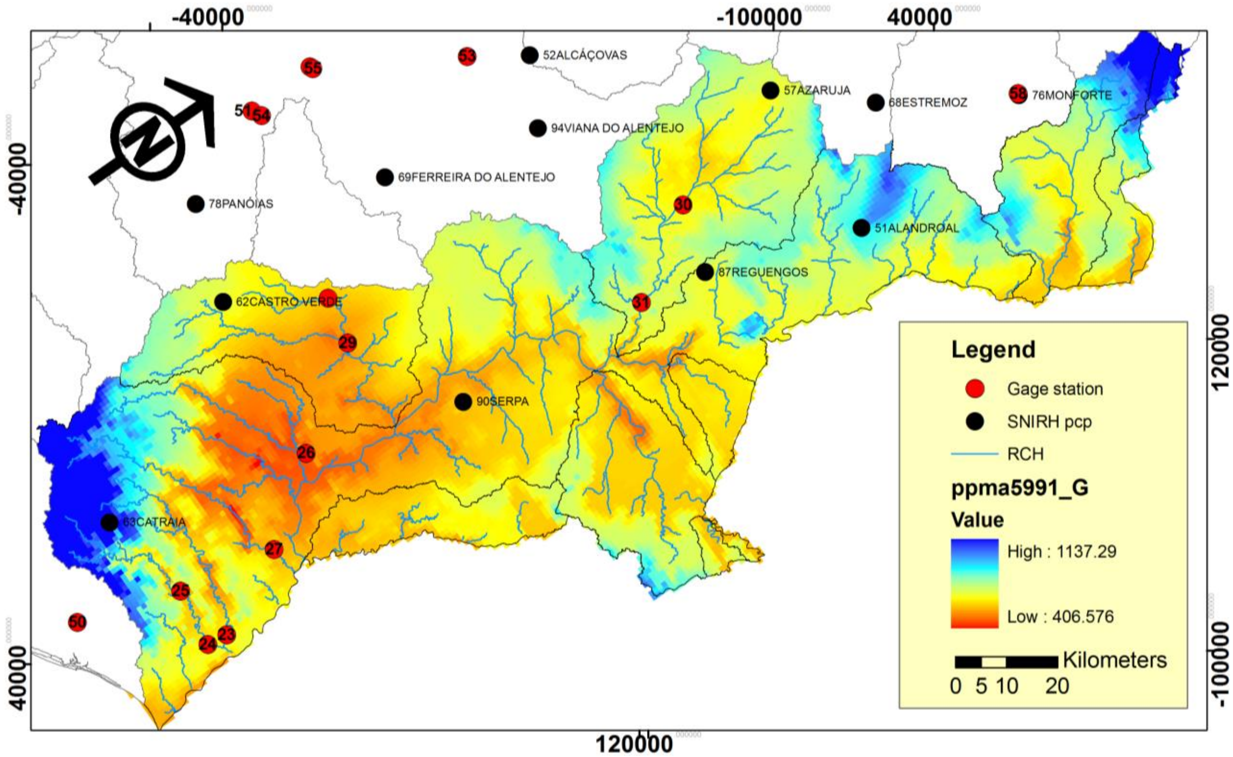

Figure 53 – Location of SNIRH precipitation stations and flow gage stations in relation to total annual precipitation in Guadiana Watershed (source: Nicolau, 2002 and SNIRH).

5.4.6 Lima

Only one gage station is available and with a small drainage area (170km^2). Modelled and measured flow of this gage station is shown in Figure 54. Precipitation station 83 and 84 from SNIRH had a good correlation with IPMA-GRID precipitation (Figure - 32). However, IPMA-GRID underestimated precipitation in station 36. From Figure 55 we can see that part of the watershed of the gage station has a significant influence from an area with precipitation similar to that of station 36, which is not reproduced by IPMA-GRID. Consequently the modelled flow in gage station 36 is lower than the flow measured.

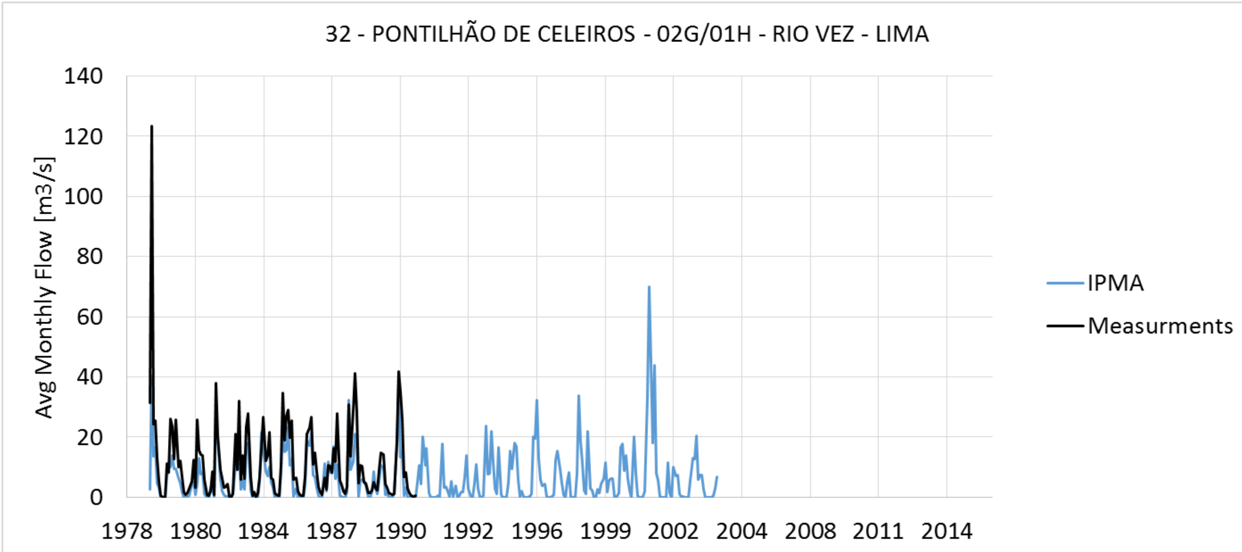

Figure 54 – Flow measured and simulated for the Pontilhão de Celeiros gage station of Rio Vez in Lima watershed

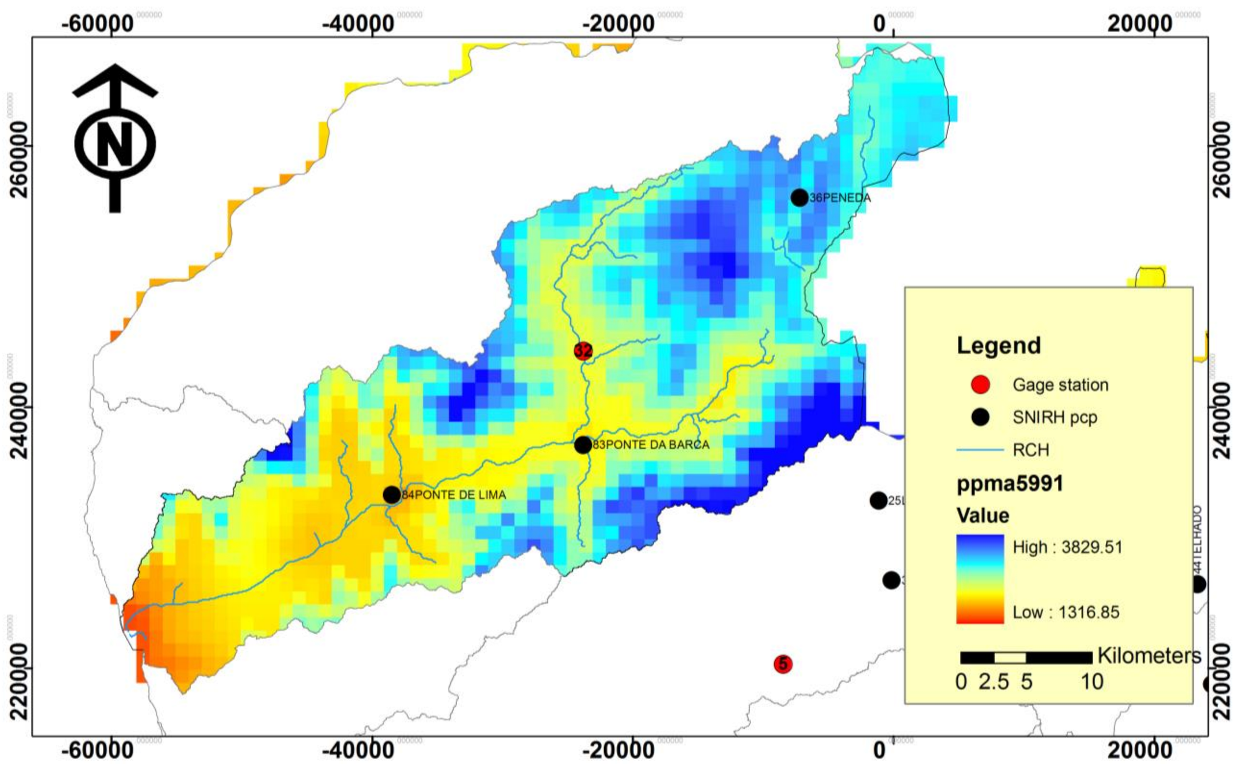

Figure 55 – Location of SNIRH precipitation stations and flow gage stations in Lima watershed in relation to total annual precipitation (source: Nicolau, 2002 and SNIRH).

5.4.7 Mondego

In Mondego 16 gage stations were retrieved (Figure 58). A group of 3 gage stations (34,35 and 36) and a group of 2 gage stations (43 and 48) had almost equal results (see monthly measured and modelled results in appendix 8.4.7). In general, in the case of Mondego, gage stations are either incomplete or measurements showed inconsistencies. For example in Aguieira gage station (Figure 56) there are two periods with different hydrologic behaviour. A first period with an abnormally high base flow and a second period with a more regular base flow. This could be justified by the way the affluent flow is calculated. Aguieira reservoir has a reversible turbine/generator that can act as pump and turbine. At times of low electrical demand, it is used to pump water from Raiva reservoir to Aguieira. When there is higher demand, water is released back into Raiva reservoir through a turbine, generating electricity. The pumped water has to be taken into consideration to get the right water balance in the reservoir and thus calculate the amount of water that is arriving from the watershed.

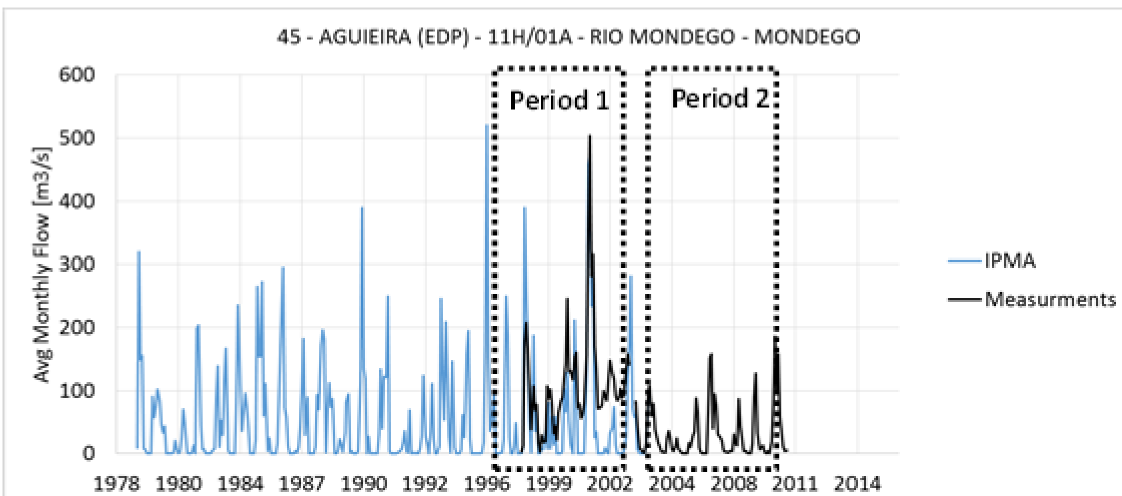

Figure 56 – Example of inconsistent flow measurements for the Aguieira gage station of Mondego watershed

Another example is Fronhas gage station (Figure 57) where it is possible to identify three distinct periods. A first period with regular results followed by a second period with an atypically low base flow. Finally a third period where the base returns to values similar to the first period.

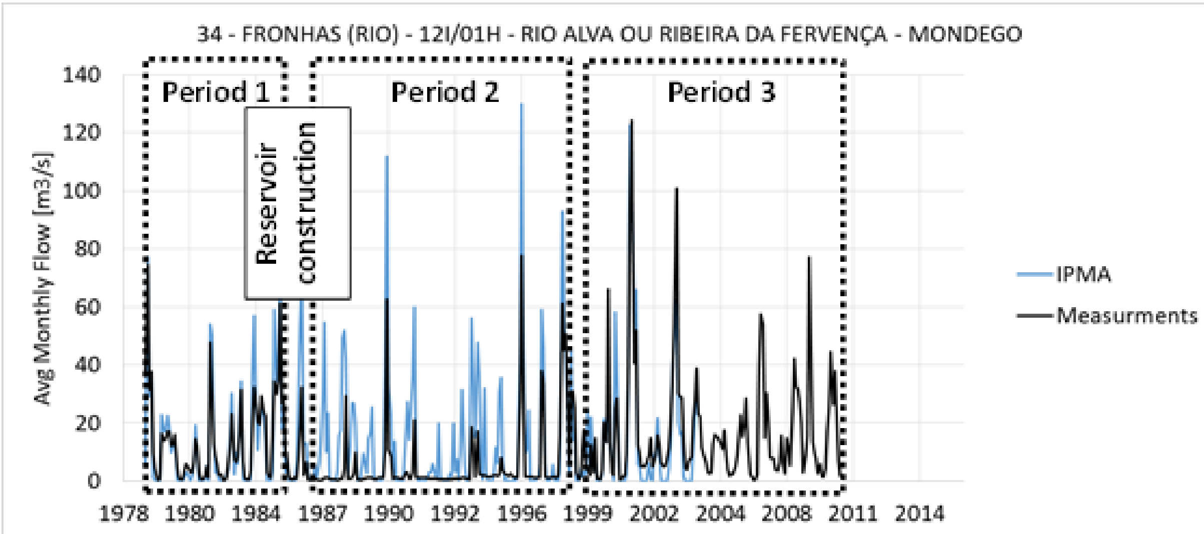

Figure 57 – Example of inconsistent flow measurements for Fronhas gage station of Mondego watershed

To all this it should be added that precipitation is very variable in Mondego. There is high concentration of precipitation on the north ridge of the watershed and on the south ridge of the watershed (Figure 58). The grid of IPMA-GRID is very coarse when compared with the spatial changes in precipitation, from the north and south ridges to the lower part of watershed. Variability of precipitation could be in the origin of bad results in Mondego. In chapter 4.3.2, a good correlation was established between the gathered precipitation stations and the IPMA-GRID results. However, a closer look shows that the precipitation stations are in areas with higher precipitation. On the other hand the flows of the model (that use precipitation of IPMA-GRID) tend to overestimate the peaks. If precipitation stations were obtained for areas with lower precipitation, the correlation would be worse. So, IPMA-GRID precipitation is overestimated for the Mondego watershed.

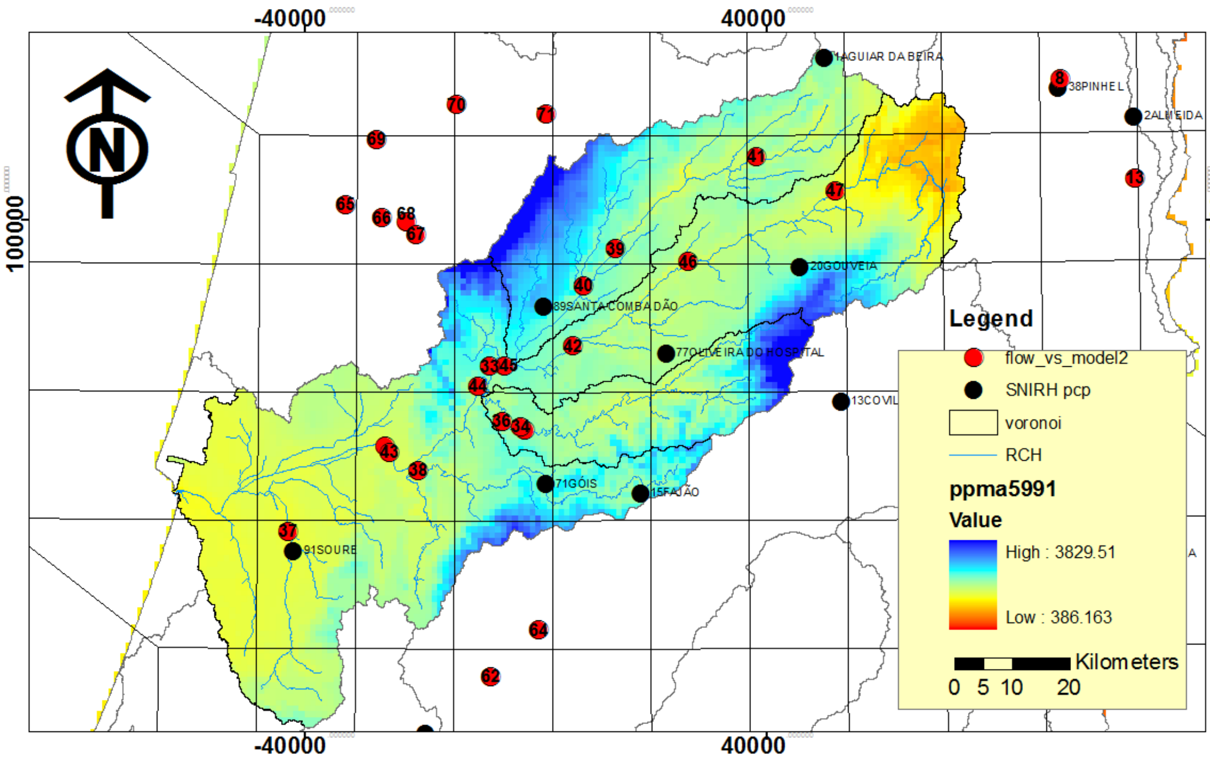

Figure 58 – Location of SNIRH precipitation stations and flow gage stations in Mondego watershed in relation to total annual precipitation (source: Nicolau, 2002 and SNIRH).

5.4.8 Ribeiras do Algarve

Results in both gage stations in Algarve have bad results in terms of NSE and PBIAS (Figure 38 and Figure 39). Peak flow is Probably being overestimated because IPMA-GRID overestimates precipitation on the south part of Ribeiras do Algarve (Figure 59 and appendix 8.4.8). For Ribeiras do Algarve a SNIRH precipitation station was not obtained to validate the results. However, precipitation station 63 (CATRAIA) in Guadiana is close, and is located in Serra do Algarve where there is more precipitation (Figure 60). This station presented a good correlation with IPMA-GRID, but it is located in a higher precipitation area. Probably in the southern part, IPMA-GRID overshoots precipitation resulting in the modelled high flows.

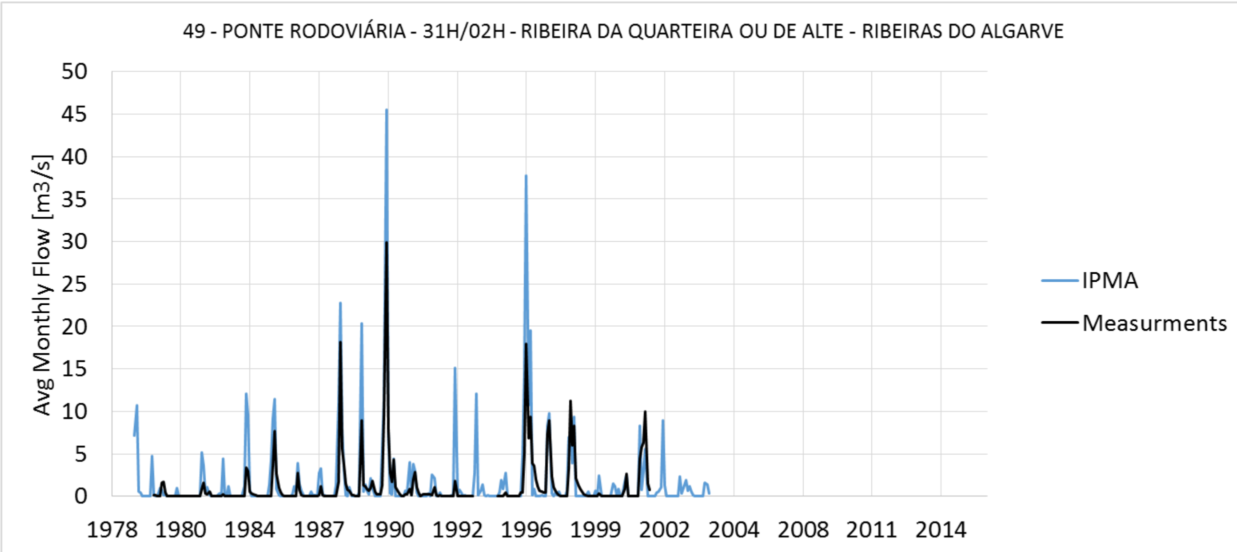

Figure 59 – Flow measured and simulated for the Ponte Rodoviária station of Ribeiras do Algarve watershed

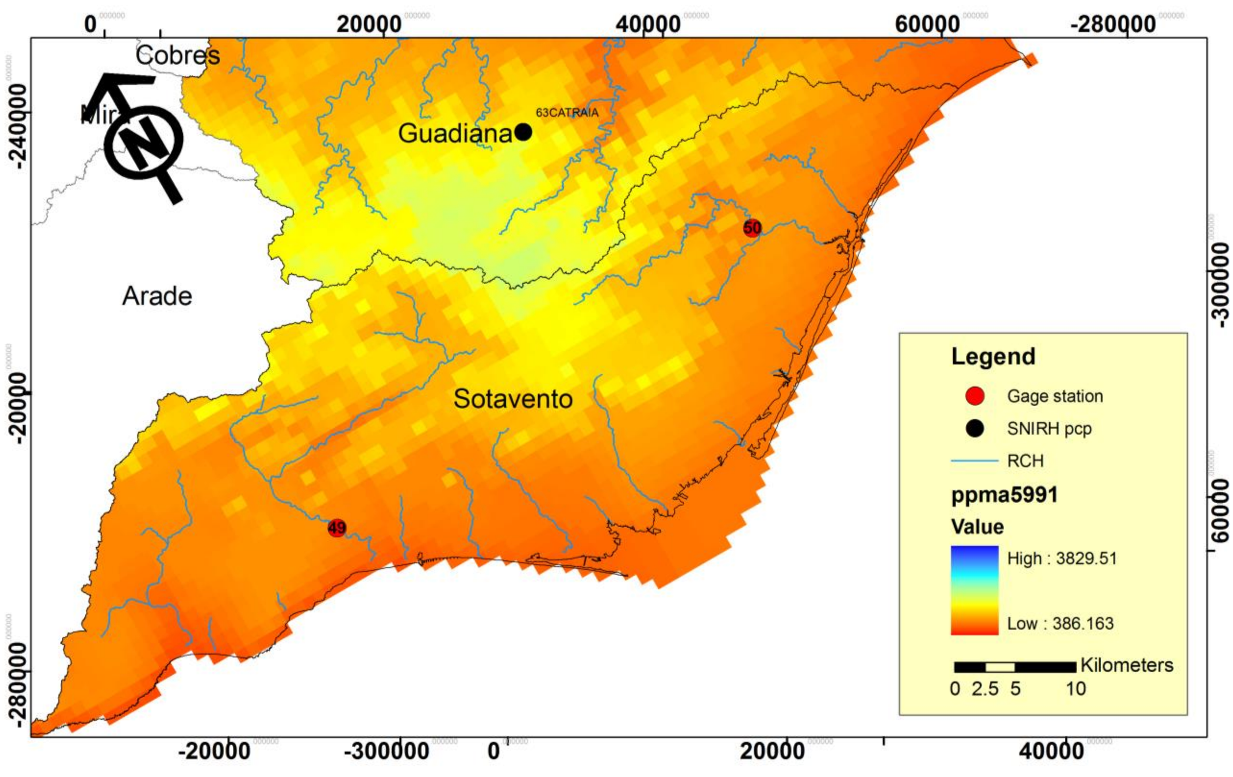

Figure 60 – Location of SNIRH precipitation stations and flow gage stations in Ribeiras do Algarve watershed in relation to total annual precipitation (source: Nicolau, 2002 and SNIRH).

5.4.9 Sado

Five gage stations were retrieved for the Sado watershed (Figure 63). Flow peaks in gage station 52 are frequently underestimated by the model (Figure 61). Comparing the drainage area with the nearby drainage area of gage station 51 (which retuned better results) one can see that precipitation distributions look similar in both gage stations (Figure 62). However, the drainage area of gage station 52 is almost a quarter of the area of station 51, but on the other hand, the peak flow of station 52 is about half the flow in gage station 51. This shows that precipitation is more concentrated in the drainage area of gage station 52, and that concentration is probably not obtained in the IPMA-GRID precipitation data set. Remaining stations have either very good or good NSE, but some PBIAS results show that a local calibration should be developed for the Sado watershed.

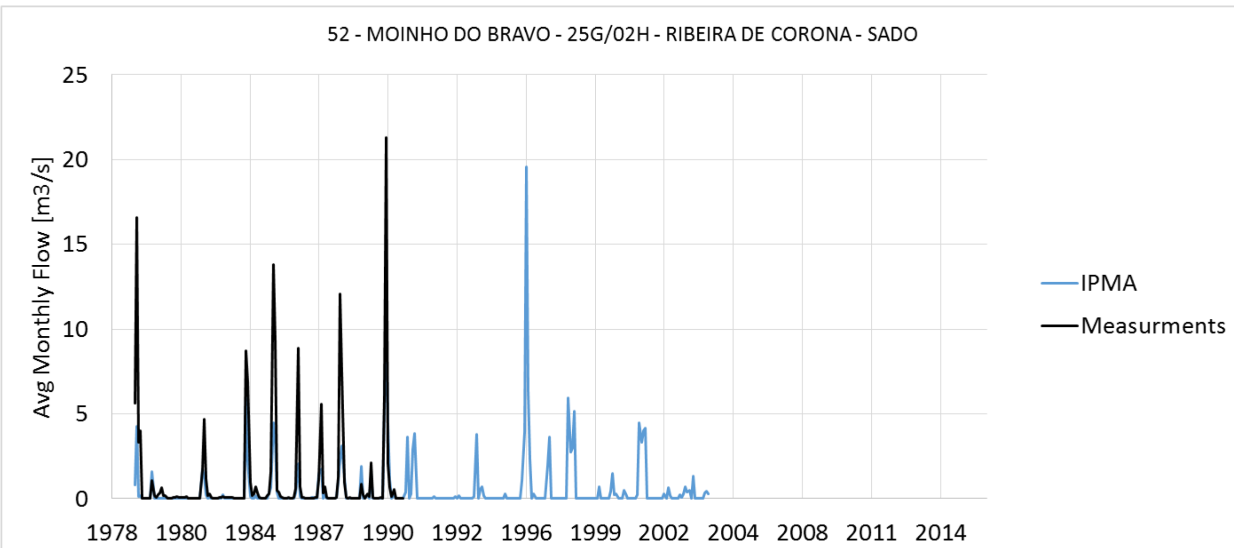

Figure 61 – Flow measured and simulated for the Moinho Bravo gage station of Ribeira de Corona in Sado watershed

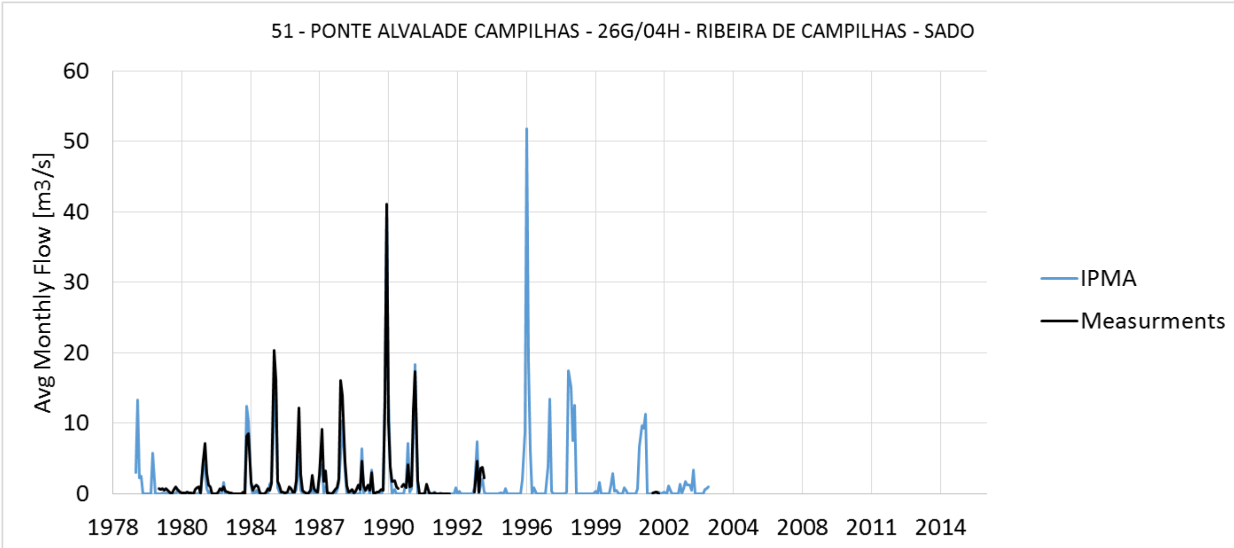

Figure 62 – Flow measured and simulated for the Ponte Alvalade Campilhas gage station of Ribeira de Campilhas in Sado watershed

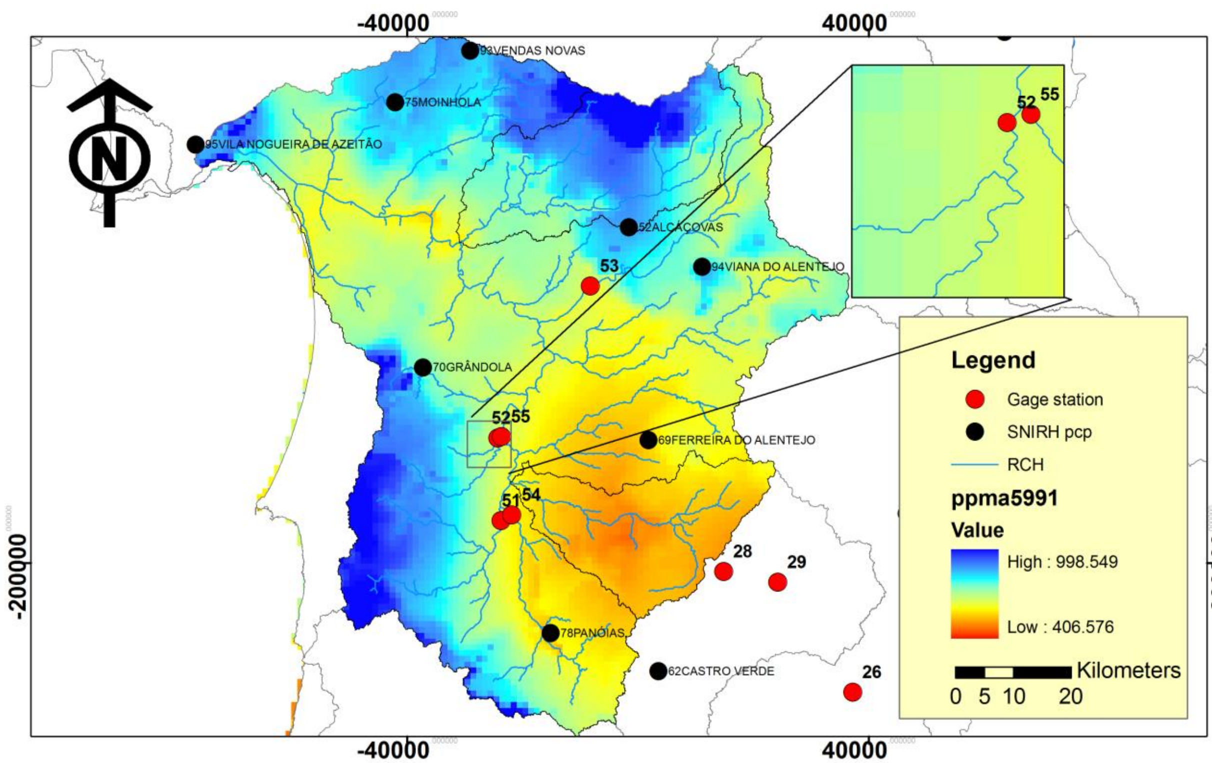

Figure 63 – Location of SNIRH precipitation stations and flow gage stations in Sado watershed in relation to total annual precipitation (source: Nicolau, 2002 and SNIRH).

5.4.10 Tejo

A total of 9 gage stations were evaluated in Tejo (Figure 64). Results in both gage stations of Rio Nabão (59 and 60) are bad. The remainder range from satisfactory to very good in terms of NSE. One should note that even though Castelo de Bode (gage station 63) had a very good NSE and PBIAS, the base flow period is clearly affected by the Cabril reservoir (Figure 65). In fact, the Cabril reservoir has an active storage of 615 hm^3 (Table 13). On the other hand, the impact of upstream reservoirs on the inflow to Cabril reservoir (Figure 66) is almost negligible, showing a very good fit between simulated and measured results (where Santa Luzia with 50 hm^3 is the biggest active storage).

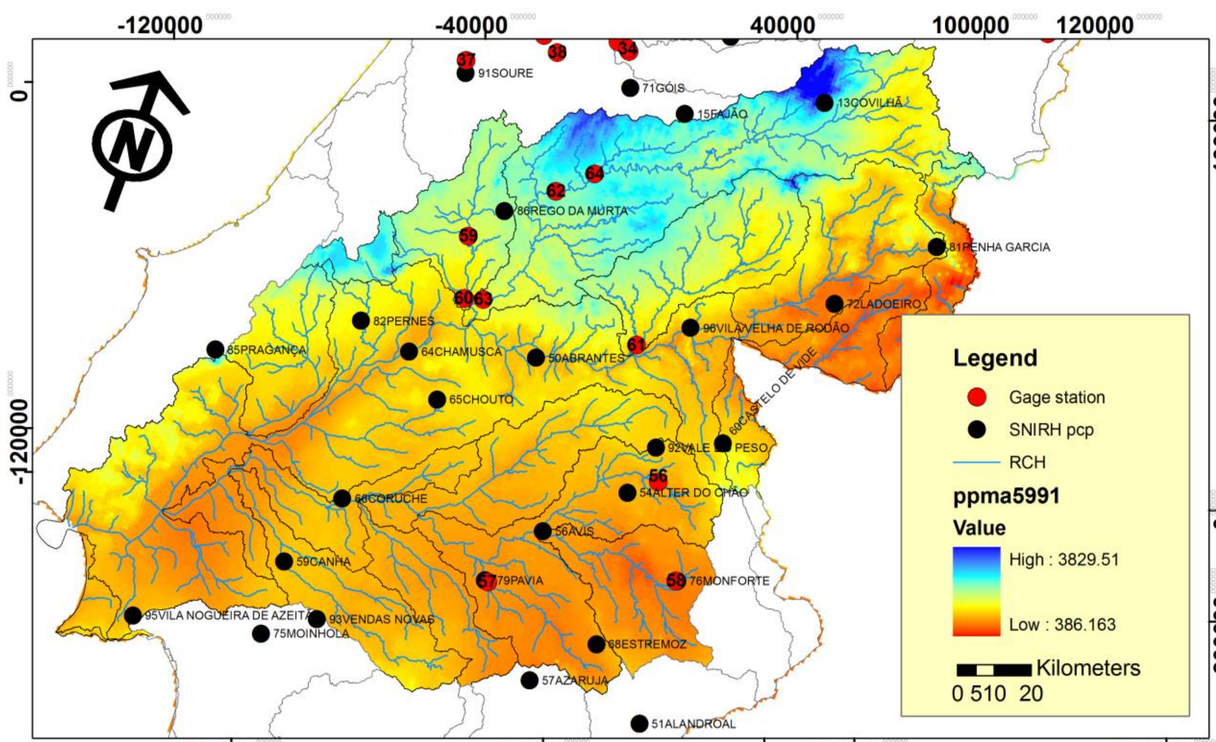

Figure 64 – Location of SNIRH precipitation stations and flow gage stations in Tejo watershed in relation to total annual precipitation (source: Nicolau, 2002 and SNIRH).

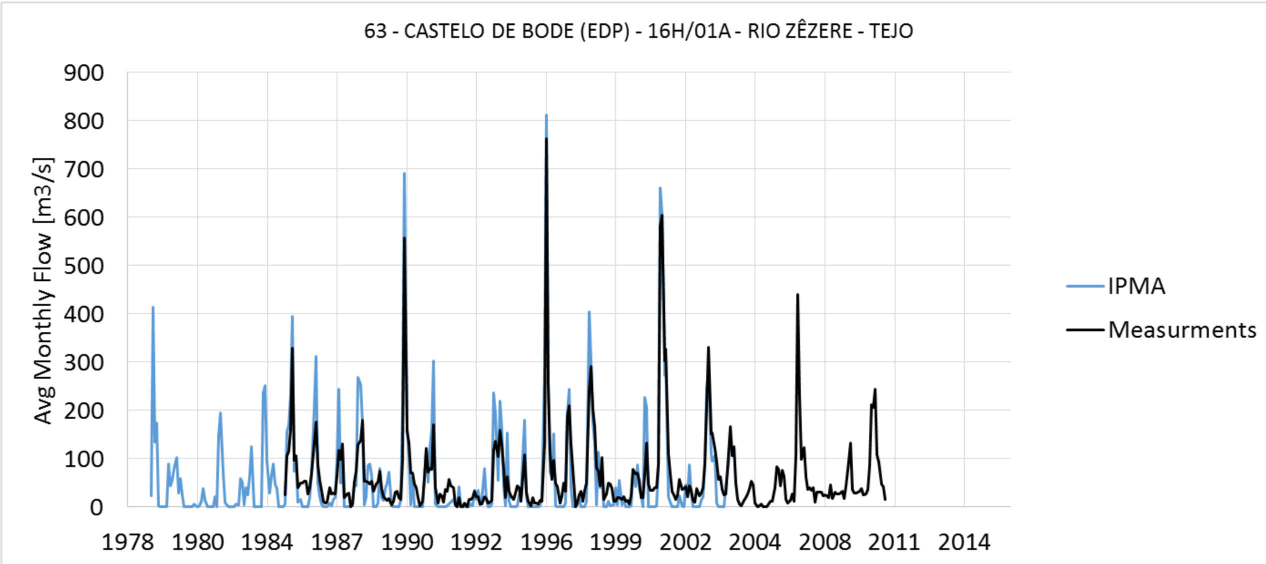

Figure 65 – Flow measured and simulated for the Castelo de Bode gage station of Rio Zêzere in Tejo watershed

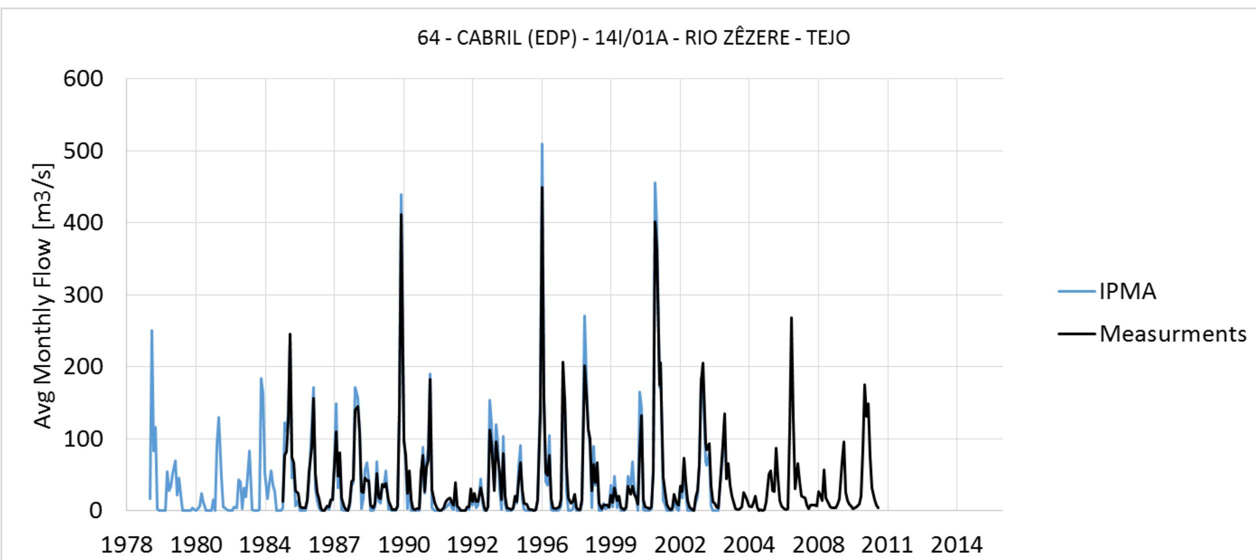

Figure 66 – Flow measured and simulated for the Cabril gage station of Rio Zêzere in Tejo watershed

5.4.11 Vouga

Four out of seven gage stations have satisfactory results. Model tends to overestimate peak flow. No precipitation data was retrieved for Vouga. However, results show that in some parts of the watershed, IPMA-GRID does not represent the spatial precipitation variability (Figure 69). Station

67 and 68 have an apparently similar precipitation distribution (Figure 67 and Figure 68). However, station 67 modelling overestimates probably because the whole watershed is associated with the higher precipitation region. Gage stations 66 and 71 have much better NSE and PBIAS results in both CFSR and MM5-R (see 5.6) than flows obtained with IPMA-GRID. This shows that a change in the precipitation input improves the model results, supporting again the idea that IPMA-GRID does not represent the spatial precipitation variability at least in some parts of the Vouga watershed.

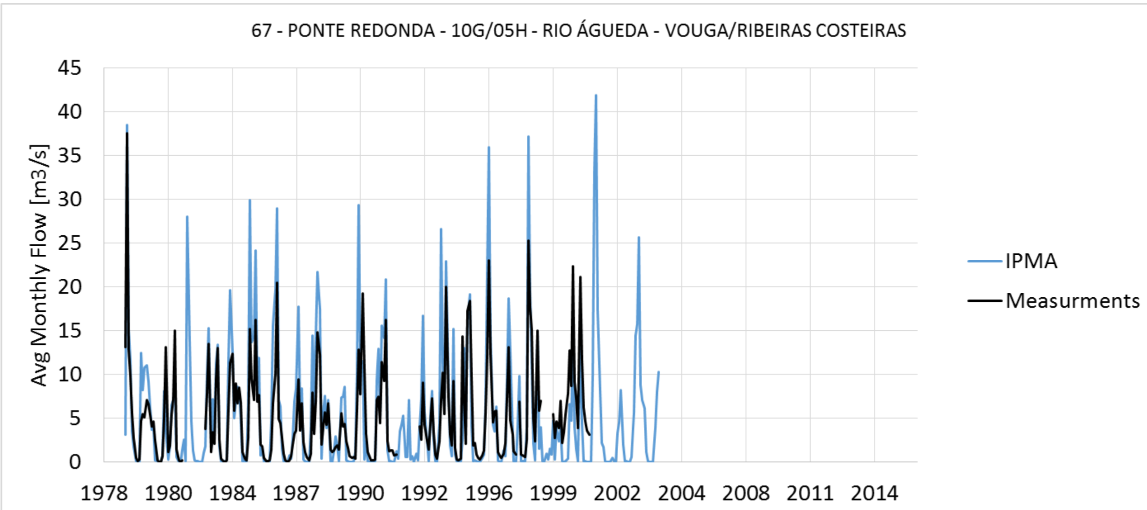

Figure 67 – Flow measured and simulated for the Ponte Redonda gage station of Rio Águeda in Vouga watershed

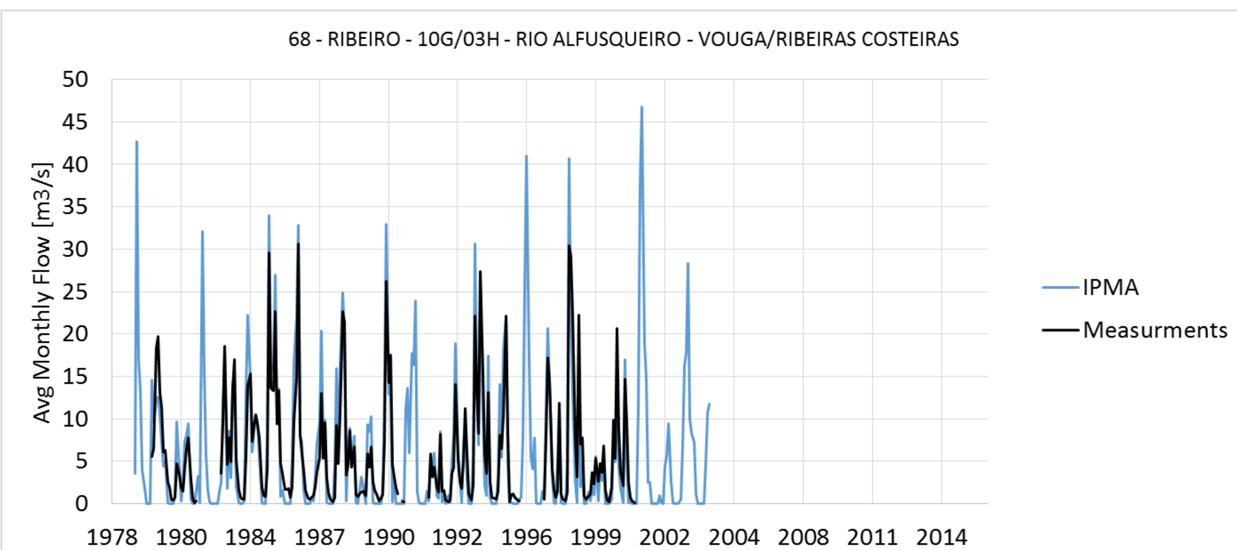

Figure 68 – Flow measured and simulated for the Ribeiro gage station of Rio Alfusqueiro in Vouga watershed

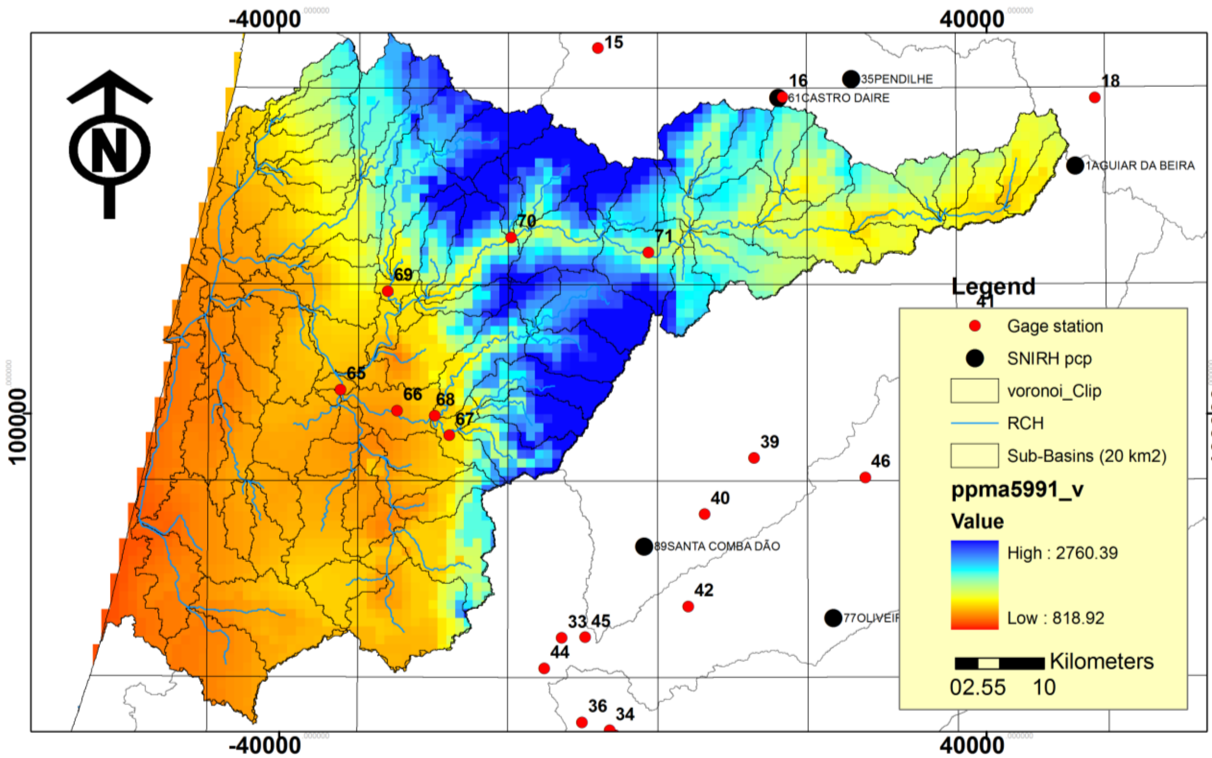

Figure 69 – Location of SNIRH precipitation stations and flow gage stations in Vouga watershed in relation to total annual precipitation (source: Nicolau, 2002 and SNIRH).

5.5 Model validation

An attempt to validate the model is done using precipitation data from IPMA-GRID between 1950 and 1978. Validation assessment was made, in the first stage, with a qualitative evaluation of performance, mainly by visually examining the agreement between observed data and model estimates. Graphs used for visual inspection are available in the appendix 8.5.

Figure 70 shows an overall comparison of calibrated and validated flow. The calibration period results have more dispersion and the model results tend to be 10% below the measurements. On the other hand, the validation period has less dispersion and the model results tend to be 25% above measurements. However, Figure 71 show that watersheds like Mondego and Tejo have very few results in the validation period and Cávado data is missing, while for the calibration period there is data for all those watersheds (Figure 37).

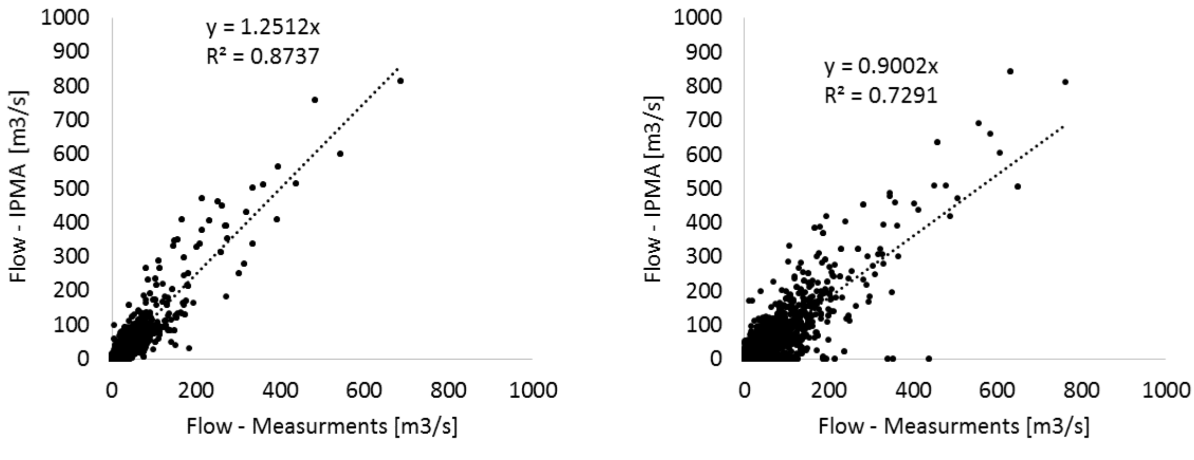

[a] [b]

Figure 70 – Correlation between measured flows and validated [a] and calibrated [b] flows

Similarly to calibration, in the second stage the evaluation of agreement between model and data was made quantitatively in terms of misfit of model results. This evaluation was done using two performance evaluators: Nash-Sutcliffe model efficiency (Figure 72) and Percent bias (Figure 73).

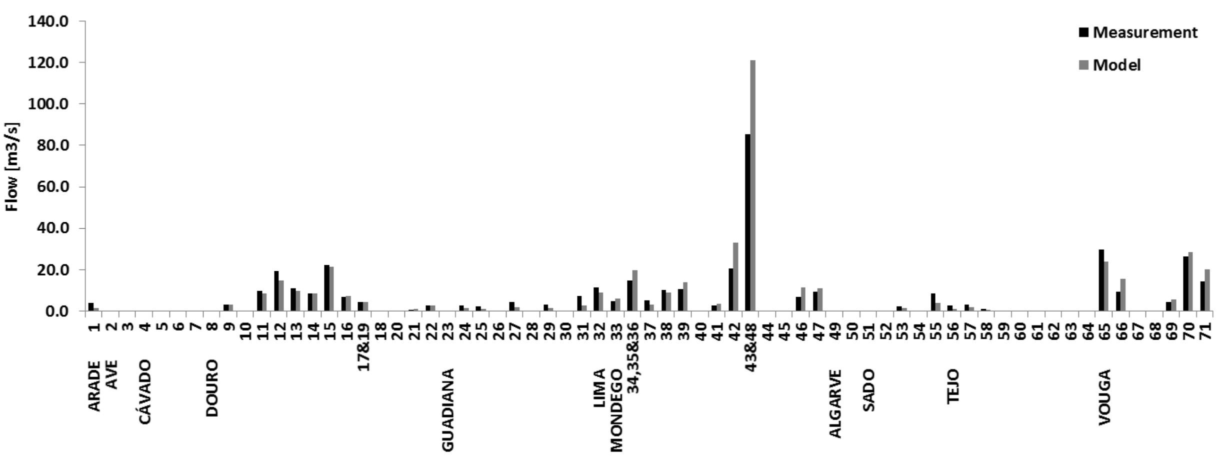

Figure 71 – Flow measured and simulated with IPMA-GRID (1950-1978)

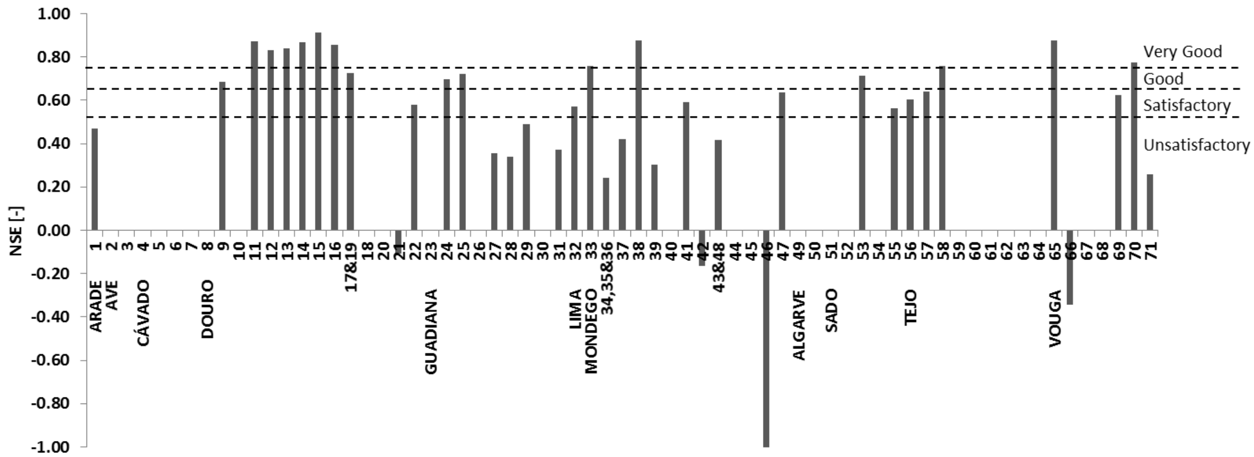

Figure 72 – NSE for simulation with IPMA-GRID (1950-1978)

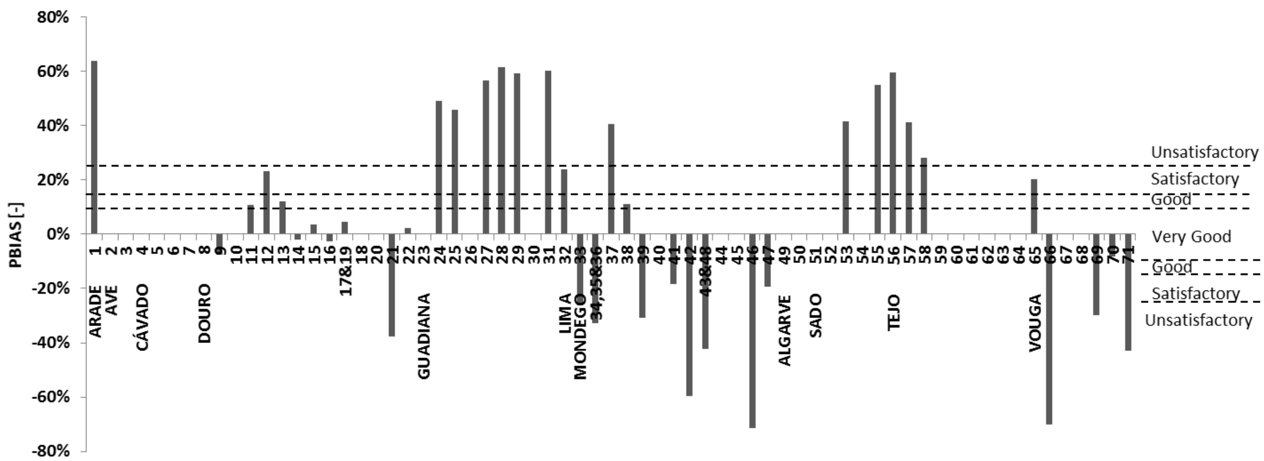

Figure 73 – PBIAS for simulation with IPMA-GRID (1950-1978)

Gage station Monte dos Pachecos in the Arade watershed showed that model was underestimating flow (Figure 74). For the validation period, the tendency seems to be the same, maintaining the unsatisfactory results in terms of NSE and PBIAS. Figure 76 shows the monthly flows measured and simulated for the validation period.

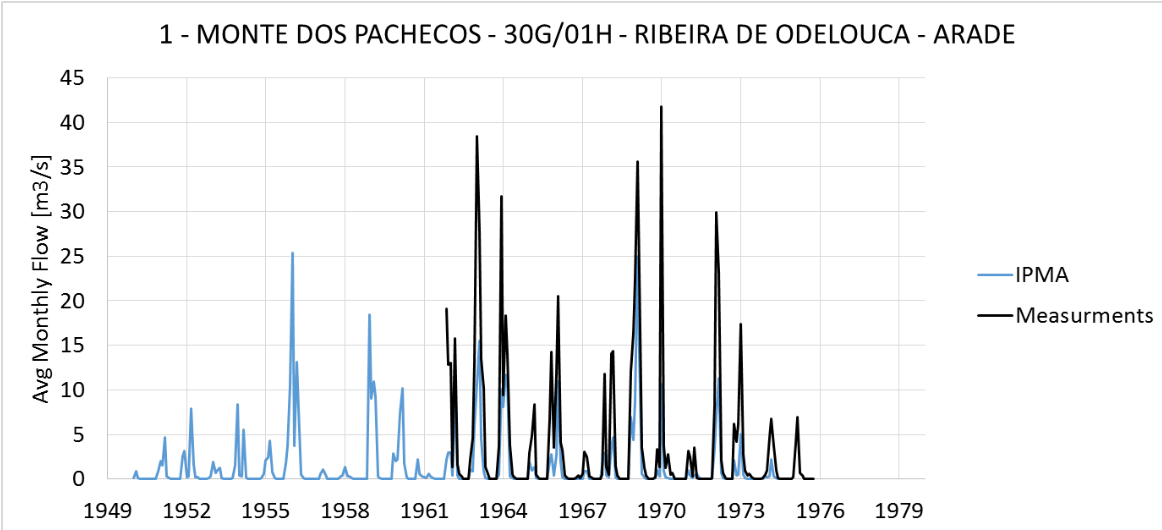

Figure 74 – Flow measured and simulated for the Monte dos Pachecos gage station of Ribeira de Odelouca in Arade watershed

Figure 75 shows the monthly flows measured and simulated in one of the gage stations. This gage station returned a very good result in terms of NSE and PBIAS during the calibration period. For the validation period this station showed also very good values of NSE and PBIAS. Model flows are validated for this gage station. Table 15 presents appreciation of validation results per watershed.

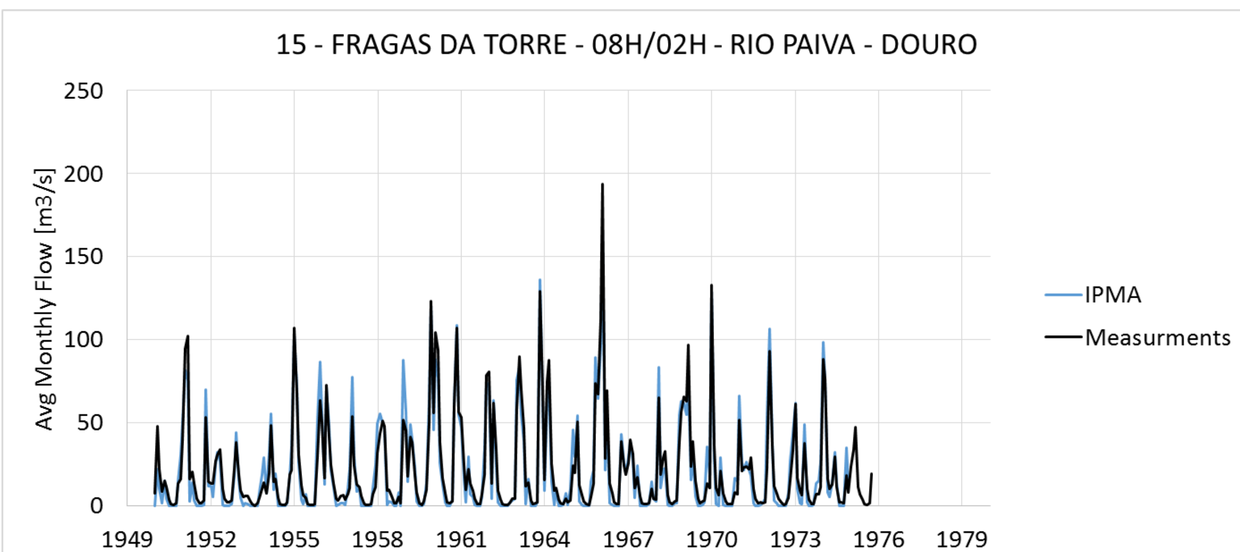

Figure 75 – Flow measured and simulated for the Fragas da Torre gage station of Rio Paiva in Douro watershed

Table 15 – Validation statistics for a monthly time step in IPMA-GRID (1950-1978).

Watershed	Comments
ARADE	Result with same tendencies as in calibration
AVE	No data available
CÁVADO	No data available
DOURO	Result with same tendencies as in calibration
GUADIANA	Result with similar tendencies as in calibration, but overall the result is worse.
LIMA	Result with same tendencies as in calibration
MONDEGO	Result with similar tendencies as in calibration, but overall the result is worse. Station 41 has a better result in the validation period. Results confirm that in Mondego IPMA-GRID overestimates precipitation.
RIBEIRAS DO ALGARVE	No data available
SADO	Result with same tendencies as in calibration but only two gage stations available.
TEJO	Result with same tendencies as in calibration. No data available for Rio Nabão.
VOUGA/RIBEIRAS COSTEIRAS	Result with same tendencies as in calibration

5.6 Evaluation of CFSR and MM5-R reanalysis

The calibrated model was used to generate flows with input precipitation from reanalysis of two forecasting models: CFSR and MM5-R. CFSR has 36 years of reanalysis (1979-2014) and MM5-R has 30 years of reanalysis (1979-2010). The flows thus obtained were then compared with measured flows. Flows simulated with CFSR and MM5-R can also be compared with IPMA-GRID results. Overall CFSR flow results correlate well with IPMA-GRID flow results (Figure 76[a]). Flows from MM5-R have a lower correlation, but still correlate well with IPMA-GRID flows (Figure 76[b]).

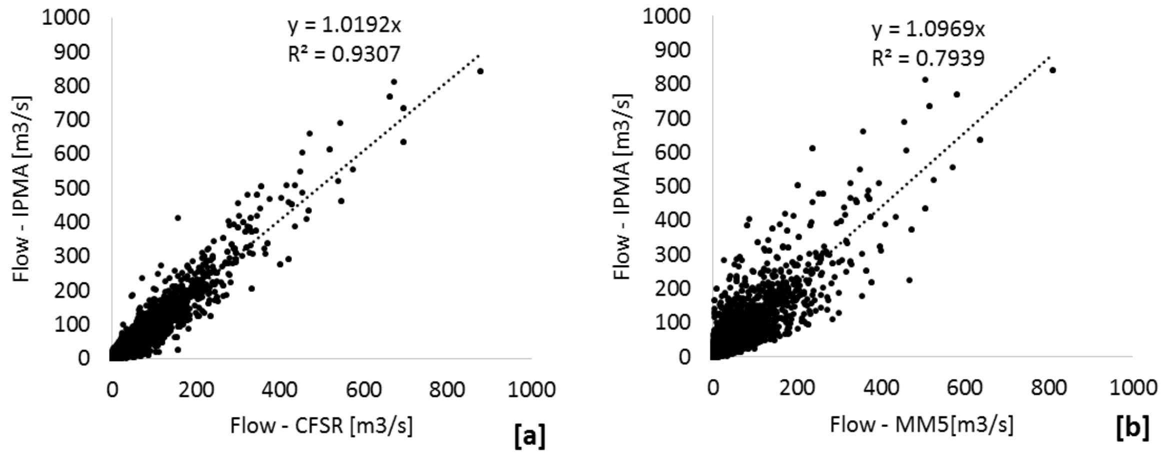

Figure 76 – Correlation between IPMA-GRID modelled flows and CFSR [a] and MM5-R [b] modelled flows

A comparison with IPMA-GRID flows (Figure 37) can be made per gage station with Figure 77 and Figure 78. In the case of Mondego and Cávado, CFSR and MM5-R average modelled flows are higher (and closer to the measured values) than IPMA-GRID. On the other hand in the Tejo watershed average modelled flow is lower than IPMA-GRID flows. The lower simulated flow of CFSR and MM5-R in Tejo resulted in a higher difference to the average measured flow, than the difference that existed between measured and simulated flow in IPMA-GRID flows.

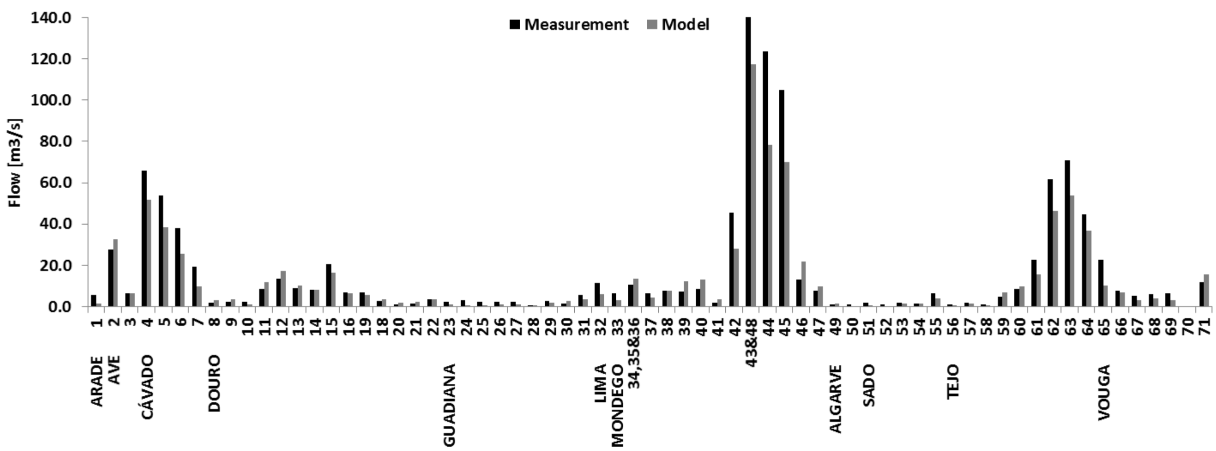

Figure 77 – Flow measured and simulated with CFSR (1979-2003)

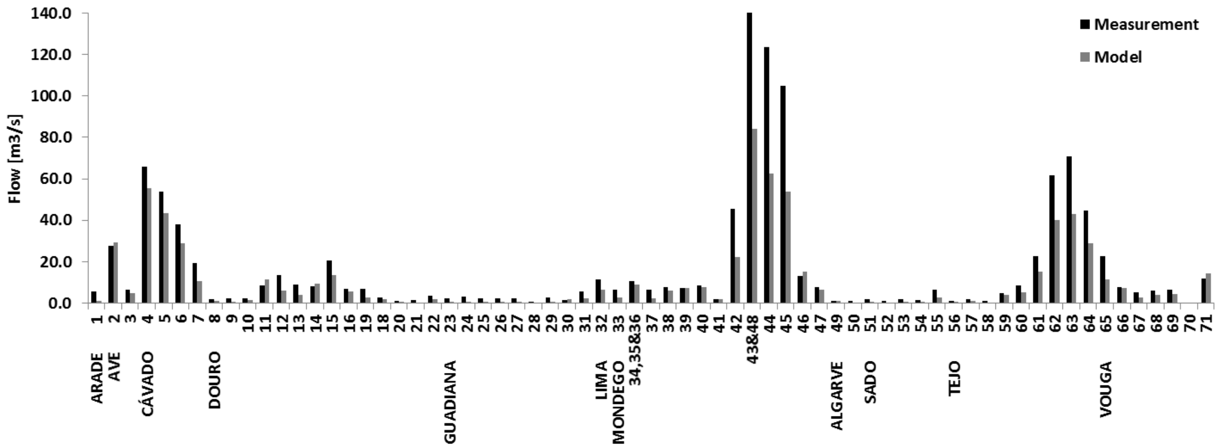

Figure 78 – Flow measured and simulated with MM5-R (1979-2003)

Statistical evaluation of CFSR and MM5-R model flows is made in Figure 81 with NSE and in Figure 82 with PBIAS. In general, model performance is reduced when using precipitation from CFSR and from MM5-R. The decrease in performance is more significant in MM5-R than in CFSR. However, some gage stations are an exception in this trend, because they maintain results of IPMA-GRID or because they improve their result when compared with IPMA-GRID. These results are confirmed by the results shown in Figure 25 and Figure 26, where the MM5-R and CFSR precipitation was compared with precipitation from SNIRH. Statistical analysis shows worse results than the comparison between IPMA-GRID and SNIRH (Figure - 32). Figure 25 and Figure 26 also show that MM5-R and CFSR precipitation correlate better with SNIRH precipitation in the case of Cavado.

Douro is the watershed where most gage stations maintained satisfactory flow results. For example Castro Daire gage station flows (Figure 79) maintain a status that ranges between good and very good (Figure 81 and Figure 82).

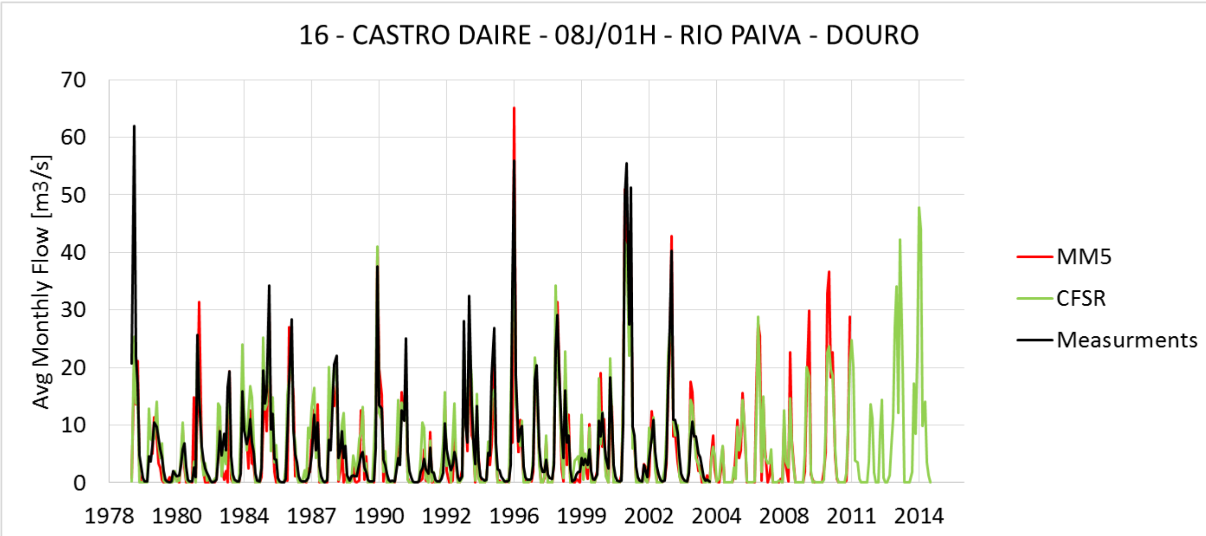

Figure 79 – Flow measured and simulated (CFSR and MM5-R) for the Castro Daire gage station of Rio Paiva in Douro watershed

Some examples can be found where a significant improvement was obtained in the flows using precipitation reanalysis. For example Vouga gage stations 66 (Figure 80) and 71 have much better NSE and PBIAS results in both CFSR and MM5-R, with results ranging from very good to satisfactory. The only exception in those two stations is PBIAS for gage station 71 in CFSR, which is still unsatisfactory (though much closer to satisfactory than the result of IPMA-GRID for flow in gage station 71). In the Tejo watershed, gage stations 59 and 60 also have improved flow results. However, these improvements only get satisfactory values in MM5-R for the NSE of gage station 60 and for PBIAS of gage station 59, while for CFSR it only gets satisfactory results for PBIAS of gage station 60. Finally in Mondego and Algarve watersheds, gage stations 46, 47 and 49 have a significant improvement, special in MM5-R, where NSE and PBIAS range between very good and satisfactory.

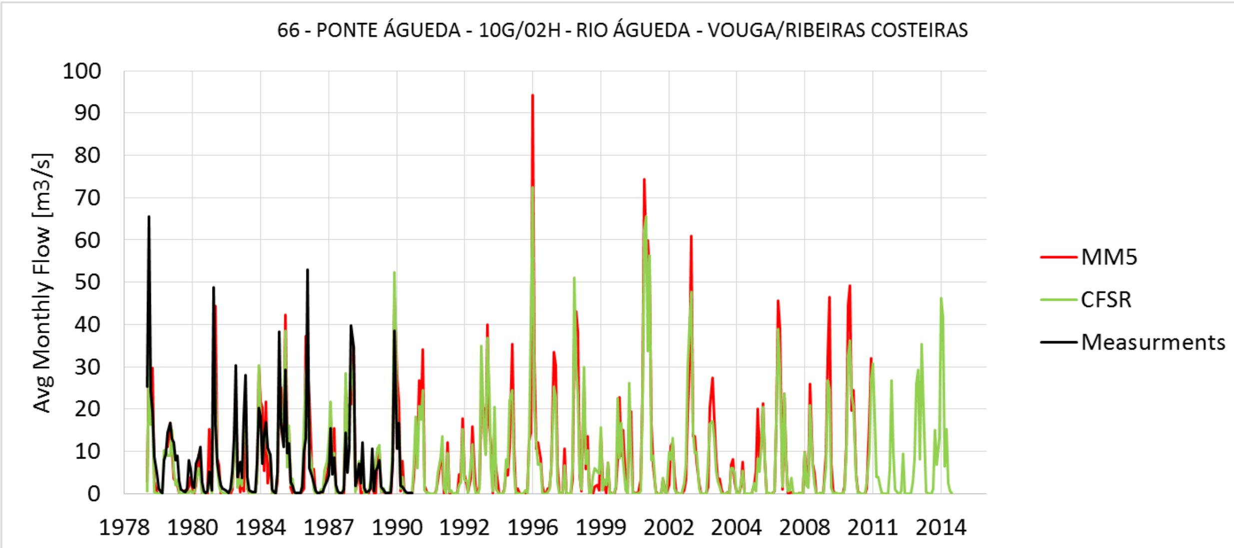

Figure 80 – Flow measured and simulated for the Ponte Águeda gage station of Rio Agueda in Vouga watershed

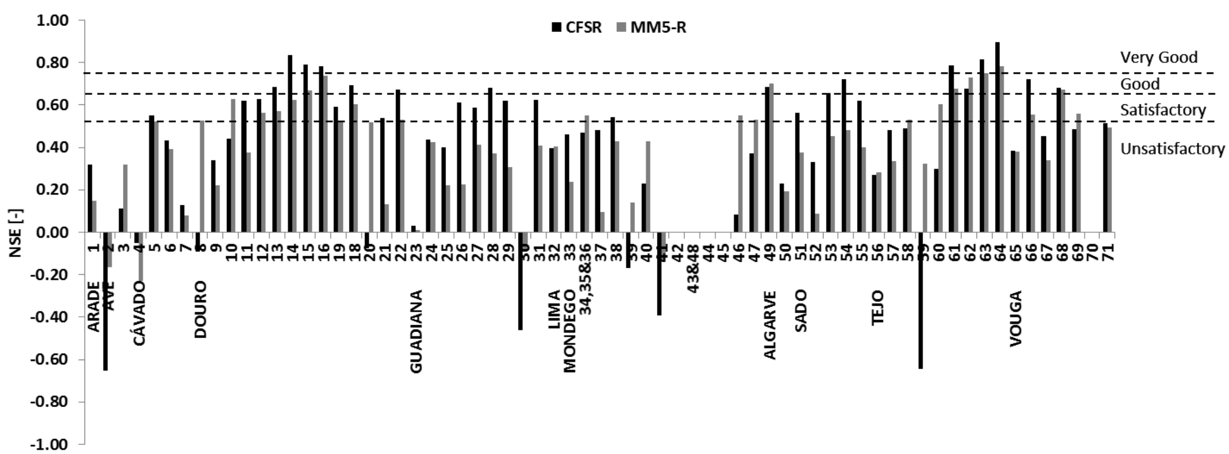

Figure 81 – NSE for simulation with CFSR and MM5-R (1979-2003)

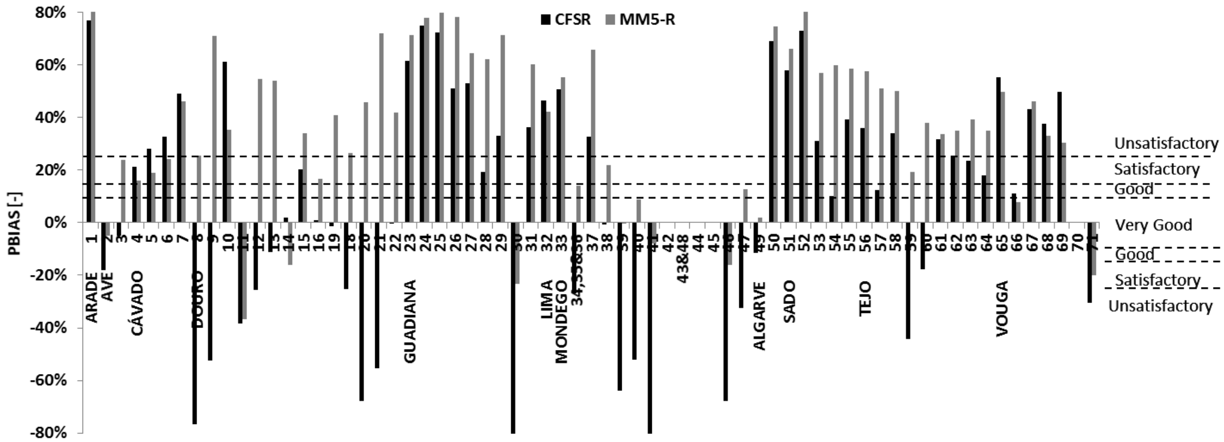

Figure 82 – PBIAS for simulation with CFSR and MM5-R (1979-2003)

5.7 Discussion

The model was run with four precipitation periods. Two periods from IPMA-GRID used for the calibration and validation process, one from MM5-R and another from CFSR. One of the questions that arises from these results is the difference in results obtained with the different data sets. In terms of validation per gage station, results show considerable differences. Are these differences maintained for bigger areas?

Overall precipitation for the total area simulated (see Table 7), for each of the precipitation data sets, is presented in Figure 83. Results are shown per hydrologic year. Each year in the figure is the first year of the hydrologic year, for example 1979 is the hydrologic year 1979-1980 (from 1 of October 1979 to 30 of September 1980). Again, it is possible to see that IPMA-GRID is more similar to CFSR than MM5-R. The volume of precipitation per year is 72 km^3 for IPMA-GRID, 71 km^3 for CFSR and of 60 km^3 for MM5-R. According with Table 7 these volumes correspondent to 96% of continental Portugal.

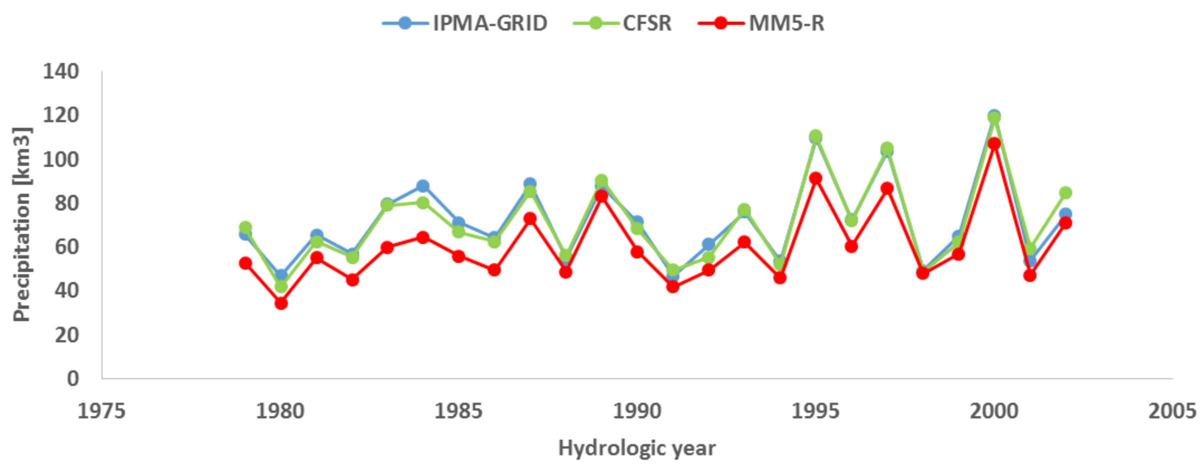

Figure 83 – Volume of precipitation for Continental Portugal

According with equations 5 and equation 6, watershed simulated fluxes for Continental Portugal can be divided in blue water flow (Figure 84) and green water flow. Values of modelled blue water flow using reanalysis, tend to be lower than IPMA-GRID especially in the 80s. For more recent years blue water flow results are more similar to the IPMA-GRID dataset. Never the less blue water flow obtained with CFSR are the ones more similar to the flow obtained with IPMA-GRID. The average volume of blue water flow per year is 28 km^3 for IPMA-GRID, 27 km^3 for CFSR and of 21 km^3 for MM5-R.

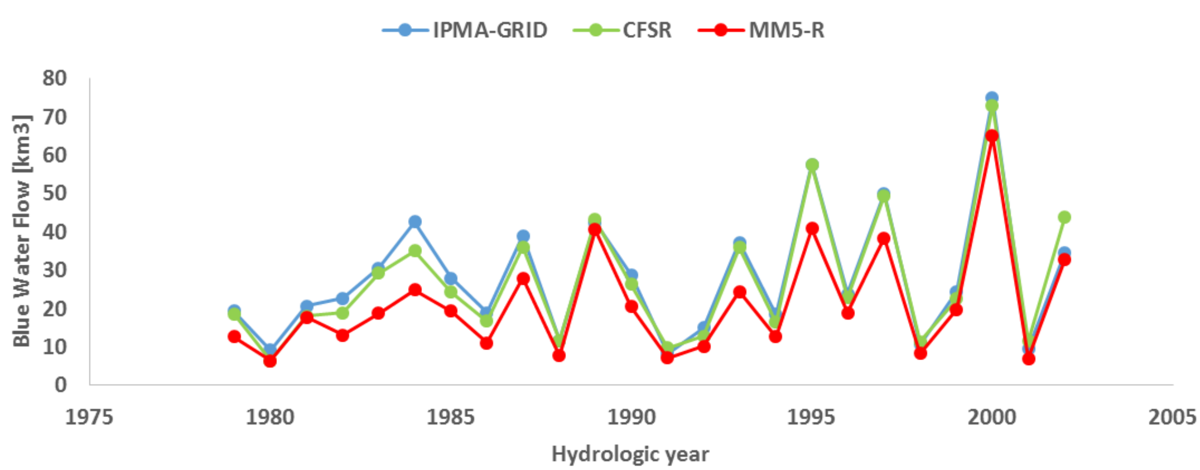

Figure 84 – Volume of simulated blue water flow for Continental Portugal

Similar comparison can be made for each Hydrologic Region. Table 16 shows the accumulated volumes of water flow from precipitation, green water, blue water and the water storage variation on the soil and shallow aquifer. The volumes result from the sum of the period 1 October 1979 to 30

September 2003, while the storage variation takes into consideration the volume available at the beginning and end of this period. The error column shows that the model has an error on mass conservation, but is always smaller than 0.5%. This error was calculated based on equation 4. For example in the case of Algarve, to obtain a error of zero the ΔS should be -0.06 km^3 which was the difference between accumulated precipitation, green water flow and blue water flow. However, the model generated a bigger reduction of the storage volume with a value of -0.18 km^3. This means the model is losing water, that is not accounted for.

Table 16 – Water budget per Hydrographic Region from 1 October 1979 to 30 September 2003 for model run with IPMA-GRID (values in km^3 in 24 years)

Hydrographic Region	Code	PRECIP	Green Water Flow	Blue Water Flow	ΔS	Error
Lima and Minho	PTRH1	80.45	24.21	56.30	-0.13	0.09%
Cavado and Leça	PTRH2	111.07	36.67	74.61	-0.27	0.05%
Douro	PTRH3	411.79	206.67	205.47	-0.78	0.10%
Mondego e Vouga	PTRH4	292.56	142.80	149.98	-0.75	0.18%
Tejo	PTRH5	494.37	356.25	138.35	-2.08	0.38%
Sado and Mira	PTRH6	140.73	118.44	22.45	-0.59	0.31%
Guadiana	PTRH7	144.85	123.61	21.47	-0.58	0.24%
Algarve	PTRH8	51.73	41.25	10.54	-0.18	0.23%

Based on the global volumes presented Table 16, the proportion of each of the HR in each flow can be shown (Figure 85). For example HR 1, 2 and 3 account for only for 35% of precipitation, but it accounts for 49% of all the blue water flow. Considering the results shown in calibration of the modeled flows for Cávado and Lima (5.4.3 and 5.4.6), the amount of flow generated in these HR could be even bigger if precipitation input to the model was higher. On the other hand HR 6, 7 and 8 account for 19% of precipitation but only contribute for 8% of blue water flow. However improved calibration on these watersheds could make the model estimate a bigger contribution from blue water flow (see evaluation of current calibration in 5.4.5 and 5.4.9).

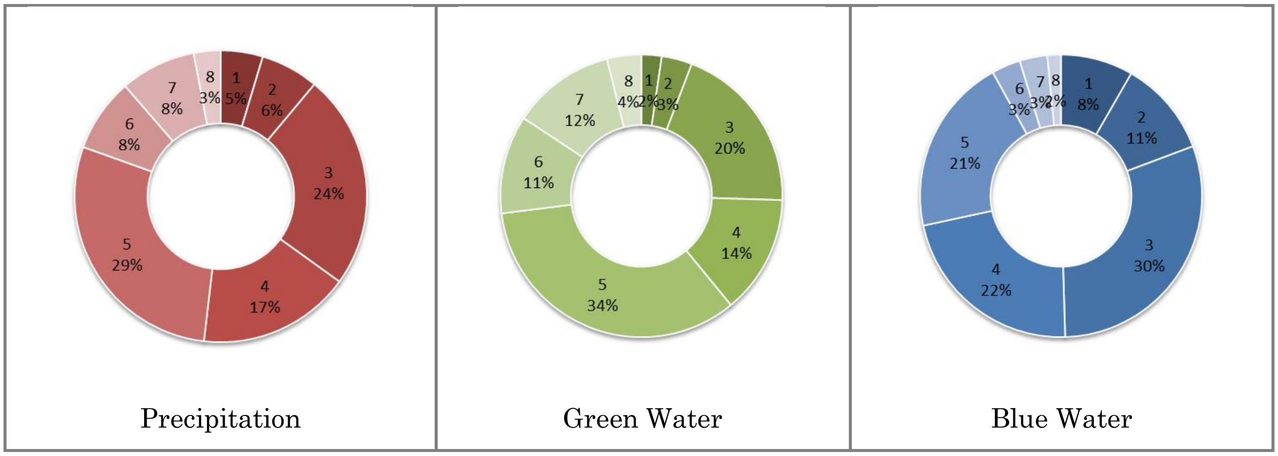

1-Lima and Minho, 2-Cavado and Leça, 3-Douro, 4-Mondego e Vouga, 5-Tejo, 6-Sado and Mira, 7-Guadiana, 8-Algarve

Figure 85 – Accumulated volumes of water flow from precipitation, green water, blue water per HR

Differences between model flows using different precipitation sources, can be seen in Table 17 and are bigger for Algarve and Cávado e Leça Hydrographic Regions. This means that differences that were detected for gage stations in this regions can be extrapolated for the Hydrographic Regions.

Table 17 - Water budget per Hydrographic Region from 1 October 1979 to 30 September 2003 for IPMA-GRID, CFSR and MM5-R (values in mm/year)

	CFSR			IPMA-GRID			MM5-R		
Hydrographic Region	PRECIP	Green Water Flow	Blue Water Flow	PRECIP	Green Water Flow	Blue Water Flow	PRECIP	Green Water Flow	Blue Water Flow
Algarve	618	520	98	663	529	135	538	453	86
Cavado and Leça	1577	502	1076	1458	482	980	1533	501	1034
Douro	927	470	457	954	479	476	777	441	337
Guadiana	531	462	69	550	469	81	419	376	43
Lima and Minho	1665	507	1157	1627	490	1139	1674	516	1160
Mondego and Vouga	1077	543	535	1084	529	556	944	524	422
Sado and Mira	607	517	90	602	506	96	463	410	54
Tejo	762	569	193	768	553	215	620	496	126

To evaluate the model flow, gage station data was obtained from SNIRH. Also data on reservoirs was obtained from SNIRH to evaluate any eventual impact on the flows. Some gage stations returned poor results after calibration. To improve results some actions can be undertaken in the future. First to increase the spatial detail of precipitation data. Watersheds influenced by very localized precipitation like in Serra de Monchique and Serra da Estrela, need more spatially detailed precipitation. Second, instead of a overall calibration, to have watershed specific calibration. The best option is to try to improve input data that could improve flow results. As was shown, the depth of soil and root depth can have a large impact on the results. Improvements in these inputs will improve significantly modelling results. One must not forget that porous media includes all the media below the soil surface, not only the normally saturated region studied with ground water models, but also the region between the soil and the normally saturated region. This last region and its interaction with the soil is poorly studied. In the future more information obtained on this region between soil and aquifer will be valuable for model input.The model calibration that was done in this thesis, changing aquifer parameters, can disguise processes other than the ones related to groundwater. Table 18 shows the proportion of each of the calculated fluxes for each Hydrography Region, including evaporation from soil (ET) and evaporation directly from aquifer (REVAP). For example, the increase in direct transpiration from aquifers could be related to an underestimation of evapotranspiration from the soil. If one concludes this, the calibration should be done for the soil parameters and not the aquifer. This was not the case in the present work because we had no data that pointed to this. In any case, the point we want to make in this thesis is that is possible to implement a unified modelling strategy to estimate flows in Portugal. This means that the centre is not the calibration process but how well model can perform in generating flows using different sources of precipitation.

Major components of flow are GW_Q (Groundwater contribution to streamflow) and SURQ (Surface runoff contribution to streamflow). GW_Q is water flowing through a shallow aquifer. GW_Q is much bigger than SURQ in HR where blue water flow dominates. The reason for this is the green flow that removes water from the green water compartment (soil and aquifer), preventing this water to contribute to the river and deep aquifer, i.e., preventing the infiltrated water to transform in to blue water flow.

For flow calibration the proportion of GW_Q and SURQ is not very important. The big difference between both flows is that GW_Q flow results from infiltrated water that eventually enters the main channel, while SURQ is non infiltrated direct runoff. However for studies related with nutrient and sediment transport, the knowledge of the right infiltration is essential. Water that infiltrate promotes nitrate lixiviation, while direct runoff promotes erosion. In this perspective blue water flow in Guadiana promotes more lixiviation of nitrate than it promotes erosion while Minho and Lima blue water flow promotes more erosion than lixiviation.

Table 18 – Water budget per Hydrographic Region using IPMA-GRID

Hydrographic Region	Code	PRECIP [mm]	ET [mm]	DA_RCHG [mm]	REVAP [mm]	LATQ [mm]	GW_Q [mm]	SURQ [mm]
Algarve	PTRH8	663	366	11	163	9	38	78
Cavado and Leça	PTRH2	1458	296	43	186	23	636	277
Douro	PTRH3	954	295	26	184	24	307	120
Guadiana	PTRH7	550	350	7	119	2	22	49
Lima and Minho	PTRH1	1627	300	51	189	36	777	275
Mondego e Vouga	PTRH4	1084	320	33	209	25	421	77
Sado and Mira	PTRH6	602	360	10	147	2	36	48
Tejo	PTRH5	768	365	17	188	12	136	49

Figure 86 shows the water budget per basin, with the partition of the different water components: Evapotranspiration (ET+REVAP), deep aquifer recharge (DA_RCHG) and flow (SURQ, LTQ and GW_Q). The calibration chosen increased the amount of REVAP and decreased the amount of flow. For example in the case of Guadiana, a new calibration should be made to decrease the REVAP and consequently increase flow. On the other hand Cavado watershed should have a higher flow, although not by reducing evapotranspiration but by increasing the input precipitation.

LATQ (Lateral flow contribution to streamflow) has typically a small contribution to stream flow. LATQ depends on slope and soil water conductivity. Figure 86 shows that in fact it has the bigger contributions in the watersheds with higher slopes (Figure 13). In the centre of Portugal, Zêzere and Alva (both including Serra da Estrela) and in the north Minho, Lima, Cávado, Paiva and Douro.

Deep aquifer recharge (DA_RCHG) is 5% percentage of GW_Q+REVAP (see calibration parameters in Table 14). This is the same to say that DA_RCHG is 5% of all he water that percolates from the soil to the shallow aquifer. Because of that it has the bigger contributions in watersheds with the highest GW_Q+REVAP contribution and is almost negligible in watersheds with low GW_Q+REVAP.

How well is evapotranspirated water simulated in this simulation? A lot of water comes from the aquifer. In the model this is the consequence of very shallow soils – many of them only 20 cm deep. Does this happen in reality? If so, this could be because roots are taking up water directly, or that there is capillary rise from the aquifer to the soil? These questions remain to be answered, and should be address in future research.

Finally the amount of water lost directly from the reservoirs to the atmosphere is also not differentiated in the presented water budget. In the present simulation results, we could say this evaporative loss is included in the green water flow, because evapotranspiration was increased, during calibration process, to obtain gage station flows. However, considering that this evaporation is not directly associated with biomass production, it should be separately calculated and included in the blue water flow. For that SWAT model should be runned in the future including reservoir simulation. For a accurate simulation of evaporation from the reservoirs, the area of water of the reservoir has to be accurately simulated. For that it has to be known for each reservoir the relation between volume and water area. Reservoir operation has also to be known including not only the turbinated and discharged water but also water pumped out of the reservoirs for irrigation, urban and industrial consumption.

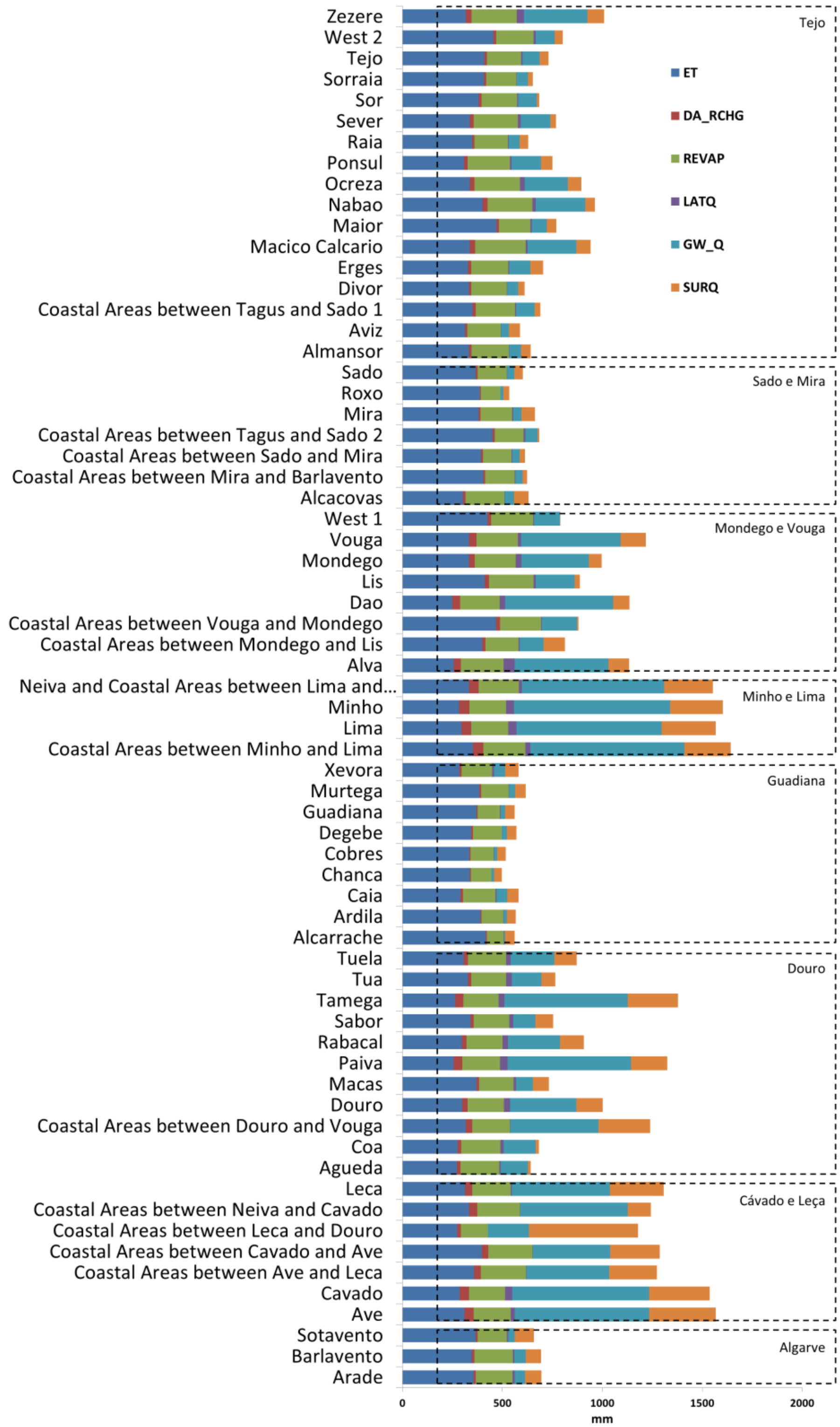

Figure 86 – Water budget per basin (table in Appendix 8.3)

Chapter 6

6 Conclusions & Future work

The SNIRH monitoring system was a common platform for water managers to obtain and exchange data. Presently, budget constraints have forced most of the monitoring activity on water resources associated with SNIRH to stop. This thesis has addressed the question of whether it is possible to mimic the SNIRH nationwide database on flow using hydrologic models. This thesis shows the implementation of a unified modelling strategy to estimate flows in Portugal. For some watersheds this methodology was even validated. This suggests that this approach can be applied throughout the entire continental portion of the country for monthly data. However, it has to be constantly improved with new input data and new local calibrations.

6.1 Model geometry

Two watershed geometries for Continental Portugal, generated with two levels of detail, were developed. The coarser one (20 km^2 threshold) was the best suited to simulate all the watersheds in Portugal. The reason was that the simulated area of Continental Portugal only increased from 2% (96% to 98%) by increasing four times the spatial detail. It was possible to produce output results with 2.5 GB with all the HRU water budget components as well as the flows in the rivers, and for all precipitation inputs. The finer geometry (5 km^2 threshold) would make model results 4 times larger.

The area of model application was restricted only to that within Portugal's borders. This can be justified either from the perspective of the input or the output. For the input the advantage of this option is the possibility of using and harmonizing a set of data that exists for the country. If the area of interested delineated was done on a purely hydrologic perspective, the entire Iberian peninsula should be simulated. In that case, data like that from SNIRH, IPMA-GRID and MM5-R would cover only part of the simulation area. Even an intermediate solution, extending a little into Spain to complete some smaller watersheds, would generate data availability problems. From the output perspective, the result restricted to the national level can be easily compared with other national data sets. It can also be used as a national database on the Portuguese territory.

On the other hand a transboundary simulation database would be of great use not only for managing water between Portugal and Spain, but also to help National institutions to manage water coming from Spain. In the context of the European Union this type of approach has been stimulated by the development of transboundary datasets. Future work should include the creation of a geometry for the entire Iberian Peninsula with the subsequent development of an Iberian model.

6.2 Definition of model input

Inputs of the model were defined with specific information about land use, soil properties and weather which were used as input for modelling the Hydrology of Portugal. The most explored input in this thesis was the precipitation.

Three datasets of precipitation were compared with data from 96 SNIRH precipitation stations. The result of the comparison was that the best available precipitation dataset was IPMA-GRID. This dataset was proven to be well correlated with SNIRH gage station data with a correlation of 0.73 for the monthly averages. The biggest differences between IPMA-GRID and SNIRH were found in Ave, Cavado, Lima, Mondego and Arade and the smallest in Douro, Tejo, Sado and Vouga. Precipitation should be improved for these watersheds.

Reanalysis datasets were also used as input to SWAT model, CFSR and MM5-R, and their monthly averages are well correlated, with a R^2 correlation of 0.71. CFSR and IPMA-GRID show a good correlation (R^2=0.85), but a poor correlation between MM5-R and IPMA-GRID (R^2=0.49). Finally both MM5-R and CFSR show a poor correlation with SNIRH, with a R^2 of 0.23 for MM5-R and a R^2 of 0.48 for CFSR. However, in the case of Cávado, CFSR and MM5-R average modelled flows are higher (and closer to the SNIRH values) than IPMA-GRID. Values of precipitation from reanalysis tend to be lower than IPMA-GRID especially in the 80s. For more recent years precipitation results are more similar to the IPMA-GRID dataset. A future work could include a precipitation dataset using all the SNIRH precipitations stations and fill in the gaps with the IPMA-GRID data set. This could remove most of the bias introduced by the spatial interpolation of the rain.

Part of the shortcomes in the calibration are related to water storage available for evapotranspiration. This storage is given through the soil data. However this data was coarse, and there is an additional available storage of water in the groundwater that is not included in that data. Instead this storage was used to calibrate the model for the whole country. However, this storage is specific to each area and is difficult to estimate. It depends not only on the proportion of the porous media below the soil but also on the type of vegetation and its roots and from what depth they can retrieve water. Also the possibility of capillary rise of the porous media can have a considerable impact on the availability of water to be evapotranspirated from deeper layers of the unsaturated and saturated layers.

Improved input on vegetation rooting depths associated with more information on soil and aquifer to store water can reduce the need for additional model calibration.

6.3 Model calibration and validation

Calibration of the model was made using precipitation inputs from IPMA-GRID. The calibrated model was also run with CFSR and MM5-R precipitation. Validation was made for a different period of data from the IPMA-GRID dataset. IPMA-GRID was proven to be the precipitation dataset that allowed to better reproduce flows with SWAT model. However some regions still need improved precipitation input for the model.

SNIRH has 715 hydrometric stations. In 1979 the number of measured flows sharply increases in all watersheds. Finally all watersheds have a sharp decrease in measurements between 2000 and 2010, some more at the beginning of the decade and others more towards the end. Only 10% of the hydrometric stations available in SNIRH were used to evaluate model results. The model should be further evaluated with the remaining stations, particularly in watersheds with poor calibration/validation. A future work could include testing for homogeneity and consistency of the chosen hydrometric stations, which could eventually remove low quality gage stations.

The ability of the model to simulate the hydrology of watersheds and the limitations arising from the various options of implementation was evaluated. Results show that the model can satisfactorily reproduce flows, for example in Douro, while other watersheds, like Mondego, would need more detailed precipitation data to reproduce flows. Calibration was performed by changing only aquifer parameters, because is very difficult to find seamless data on aquifers across the watershed

The calibrated model was run with precipitation data from the MM5-R and the CSFR meteorological models with respectively 30 and 36 years of reanalysis as input. In general, model performance is reduced when using reanalysis. The decrease in performance is more significant in MM5-R than in CFSR. However some gage stations are an exception in this trend, because they improve their flows when compared with IPMA-GRID.

Flow simulation was restricted to the Portuguese part of the Iberian Peninsula. Because of that, all the transboundary watersheds (even the small ones) are not fully simulated. The results presented here show that for future work it makes sense to apply the SWAT model to the entire Iberian Peninsula using CFSR as input. An application like this can be used as a transnational uniform data provider on flows generated. This could be useful for managing water between Portugal and Spain.

The approach presented does not calculate the effect of reservoirs in river flows. Because of this, evaluated flows only included gage stations with a drainage area less than 5000 km^2 and larger than

100 km^2. Still there are some reservoirs that can potentially have an impact on flows of gage stations with less than 5000 km2 of drainage area. The reservoirs that showed a bigger control on flows on downstream rivers were Alto Rabagão and Aguieira.

The accumulated volumes of water flow from precipitation, green water, blue water and the water storage variation shows that the model has an error on mass conservation, but is always smaller than 0.5%.

Volume of precipitation for the simulated area is 72 km^3/year for IPMA-GRID, 71 km^3/year ^{3} for CFSR and of 60 km^3/year for MM5-R. The average volume of accumulated blue water flow is 28 km^3/year ^{3} for IPMA-GRID, 27 km^3/year ^{3} for CFSR and of 21 km^3/year ^{3} for MM5-R. For the IPMA-GRID simulation, HR 1, 2 and 3 account for only for 35% of precipitation, but it accounts for 49% of all the blue water flow. On the other hand HR 6, 7 and 8 account for 19% of precipitation but only contribute for 8% of blue water flow.

GW_Q (Groundwater contribution to streamflow) is much bigger than SURQ (Surface runoff contribution to streamflow) in HR where blue water flow dominates. The reason for this is the green flow that removes water from the green water compartment (soil and aquifer), preventing this water to contribute to the river and deep aquifer. For flow calibration the proportion of GW_Q and SURQ is not very important but for studies related with nutrient and sediment transport, the knowledge of the right infiltration is essential, and should be calibrated and validated.

Modelled results of flow using the three sources of precipitation were compiled in a relational database. The developed database and models are complementary to the national monitoring network. However, only average monthly flows were evaluated. In the future, the model should be calibrated for daily flows, and a similar database should be compiled.

7 References

ABBASPOUR, K., ROUHOLAHNEJAD, E., VAGHEFI, S., SRINIVASAN, R., YANG, H. & KLØVE, B. 2015. A continental-scale hydrology and water quality model for Europe: Calibration and uncertainty of a high-resolution large-scale SWAT model. *Journal of Hydrology,* 524, 733-752.

ABBASPOUR, K., VEJDANI, M. & HAGHIGHAT, S. SWAT-CUP calibration and uncertainty programs for SWAT. MODSIM 2007 International Congress on Modelling and Simulation, Modelling and Simulation Society of Australia and New Zealand, 2007.

ALLEN, R. G., PEREIRA, L. S., RAES, D. & SMITH, M. 1998. Crop evapotranspiration-Guidelines for computing crop water requirements-FAO Irrigation and drainage paper 56. *FAO, Rome,* 300, 6541.

ALLEN, R. G., PRUITT, W. O., WRIGHT, J. L., HOWELL, T. A., VENTURA, F., SNYDER, R., ITENFISU, D., STEDUTO, P., BERENGENA, J. & YRISARRY, J. B. 2006. A recommendation on standardized surface resistance for hourly calculation of reference ET< sub> o</sub> by the FAO56 Penman-Monteith method. *Agricultural Water Management,* 81, 1-22.

ARAKAWA, A. & LAMB, V. R. 1977. Computational design of the basic dynamical processes of the UCLA general circulation model. *Methods in computational physics,* 17, 173-265.

ARNOLD, J., MUTTIAH, R. S., SRINIVASAN, R. & ALLEN, P. 2000. Regional estimation of base flow and groundwater recharge in the Upper Mississippi river basin. *Journal of Hydrology,* 227, 21-40.

ARNOLD, J. G. & FOHRER, N. 2005. SWAT2000: current capabilities and research opportunities in applied watershed modelling. *Hydrological processes,* 19, 563-572.

ARNOLD, J. G., SRINIVASAN, R., MUTTIAH, R. S. & ALLEN, P. M. 1999. Continental scale simulation of the hydrologic balance1. Wiley Online Library.

ARNOLD, J. G., WILLIAMS, J., NICKS, A. & SAMMONS, N. 1990. *SWRRB; a basin scale simulation model for soil and water resources management*, Texas A & M University Press.

BARÃO, L. 2007. *Modelação do transporte do ciclo do Azoto no solo utilizando o modelo Mohid e RZWQM.* Mestrado em Engenharia do Ambiente., Universidade Técnica de Lisboa.

BARÃO, L., LEITÃO, P. C., BRAUNSCHWEIG, F., NEVES, R., GONÇALVES, M., RAMOS, T. & CASTANHEIRA, N. 2010. Simulation of water dynamics in two irrigated soils. *Revista de Ciências Agrárias,* 33, 346-357.

BEDFORD, D. R. 2008. *Effects of vegetation-related soil heterogeneity on runoff, infiltration, and redistribution in semi-arid shrubland and grassland landscapes.* UNIVERSITY OF COLORADO AT BOULDER.

BELO - PEREIRA, M., DUTRA, E. & VITERBO, P. 2011. Evaluation of global precipitation data sets over the Iberian Peninsula. *Journal of Geophysical Research: Atmospheres (1984–2012),* 116.

BEREZOWSKI, T., SZCZEŚNIAK, M., KARDEL, I., MICHAŁOWSKI, R., OKRUSZKO, T., MEZGHANI, A. & PINIEWSKI, M. 2015. CPLFD-GDPT5: high-resolution gridded daily precipitation and temperature dataset for two largest Polish river basins. *Earth Syst. Sci. Data Discuss.,* 8**,** 1021–1060.

BEVEN, K. & BINLEY, A. 1992. The future of distributed models: model calibration and uncertainty prediction. *Hydrological processes,* 6**,** 279-298.

BEVEN, K. J. 1996. *A discussion of distributed hydrological modelling*, Springer.

BORAH, D. & BERA, M. 2003. Watershed-scale hydrologic and nonpoint-source pollution models: Review of mathematical bases. *Transactions of the ASAE,* 46**,** 1553-1566.

BRACA, G. & FUTURA, G. 2008. *Stage-discharge relationships in open channels: Practices and problems*, Università di Trento. Dipartimento di ingegneria civile e ambientale.

BRAUNSCHWEIG, F., LEITAO, P. C., FERNANDES, L., PINA, P. & NEVES, R. J. J. 2004. The object-oriented design of the integrated water modelling system MOHID. *Computational Methods in Water Resources, Vols 1 and 2,* 55**,** 1079-1090.

BRITO, D., CAMPUZANO, F., SOBRINHO, J., FERNANDES, R. & NEVES, R. 2015. Integrating operational watershed and coastal models for the Iberian Coast: Watershed model implementation–A first approach. *Estuarine, Coastal and Shelf Science,* 167**,** 138-146.

CAMPUZANO, F., FERNANDES, R., LEITÃO, P., VIEGAS, C., DE PABLO, H. & NEVES, R. 2012. Implementing local operational models based on an offline downscaling technique: The Tagus estuary case. *2. as Jornadas de Engenharia Hidrográfica***,** 105-108.

CAMPUZANO, F. J., MATEUS, M. D., LEITÃO, P. C., LEITÃO, P. C., MARÍN, V. H., DELGADO, L. E., TIRONI, A., PIERINI, J. O., SAMPAIO, A. F. & ALMEIDA, P. 2013. Integrated coastal zone management in South America: A look at three contrasting systems. *Ocean & Coastal Management,* 72**,** 22-35.

CANAS, A., CHAMBEL-LEITÃO, P. & BRAUNSCHWEIG, F. Study of runoff variability in a forest fire scenario for the Trancão River basin. . 5º Congresso Internacional sobre Ordenamento do Território., 2010 Lisboa, Portugal.

CARSEL, R. F. & PARRISH, R. S. 1988. Developing joint probability distributions of soil water retention characteristics. *Water Resources Research,* 24**,** 755-769.

CELIA, M. A. & BINNING, P. 1992. A mass conservative numerical solution for two‐phase flow in porous media with application to unsaturated flow. *Water Resources Research,* 28**,** 2819-2828.

CHAMBEL-LEITÃO, P. 2008. Load and flow estimation: HARP-NUT guidelines and SWAT model description. *In:* NEVES, R., BARETTA, J MATEUS, M (ed.) *In Perspectives on Integrated Coastal Zone Management in South America* Lisbon, Portugal.: IST Press.

CHAMBEL-LEITÃO, P., ALMEIDA, C., JAUCH, E., TRANCOSO, R., NEVES, R. & LEITÃO, J. Evapotranspiration forecast using SWAT model and weather forecast model. . 2011 International SWAT Conference, 2011 Toledo, Spain.

CHAMBEL-LEITÃO, P., BRAUNSCHWEIG, F., FERNANDES, L., NEVES, R. & GALVÃO, P. Integration of MOHID model and tools with SWAT model. 4th International SWAT Conference Delfi, The Netherlands, 2007a. Citeseer.

CHAMBEL-LEITÃO, P., BRAUNSCHWEIG, F., FERNANDES, L., NEVES, R. & GALVÃO, P. Integration of MOHID model and tools with SWAT model. 4th International SWAT Conference Delft, The Netherlands, 2007b.

CHAPLOT, V., SALEH, A., JAYNES, D. & ARNOLD, J. 2004. Predicting water, sediment and NO3-N loads under scenarios of land-use and management practices in a flat watershed. *Water, Air, and Soil Pollution,* 154**,** 271-293.

CHO, S. M. & LEE, M. 2001. Sensitivity considerations when modeling hydrologic processes with digital elevation model. *Journal of the american water resources association,* 37**,** 4.

COELHO, H. & CHAMBEL-LEITÃO, P. 2010. Integrated modelling of watershed and reservoirs: Pocinho and Enxoés cases. . *Revista Recursos Hídricos,* 31**,** 77-85.

COSTA, A. C. & SOARES, A. 2009. Trends in extreme precipitation indices derived from a daily rainfall database for the South of Portugal. *International Journal of Climatology,* 29**,** 1956-1975.

COSTA, A. C. D. L. 2009. *Aplicação do Modelo SWAT ao estudo hidrológico das Ribeiras da Costa do Estoril.* . Mestrado em Engenharia do Ambiente. , Universidade Técnica de Lisboa.

COTTER, A. S., CHAUBEY, I., COSTELLO, T. A., SOERENS, T. S. & NELSON, M. A. 2003. Water quality model output uncertainty as affected by spatial resolution of input data1. *Journal of the american water resources association,* 39**,** 10.

DANIEL, E. B., CAMP, J. V., LEBOEUF, E. J., PENROD, J. R., DOBBINS, J. P. & ABKOWITZ, M. D. 2011. Watershed modeling and its applications: A state-of-the-art review. *Open Hydrology Journal,* 5.

DEE, D., UPPALA, S., SIMMONS, A., BERRISFORD, P., POLI, P., KOBAYASHI, S., ANDRAE, U., BALMASEDA, M., BALSAMO, G. & BAUER, P. 2011. The ERA - Interim reanalysis: Configuration and performance of the data assimilation system. *Quarterly Journal of the Royal Meteorological Society,* 137**,** 553-597.

DILE, Y. T. & SRINIVASAN, R. 2014. Evaluation of CFSR climate data for hydrologic prediction in data - scarce watersheds: an application in the Blue Nile River Basin. *JAWRA Journal of the American Water Resources Association,* 50**,** 1226-1241.

DURÃO, A., MORAIS, M., BRITO, D., CHAMBEL LEITÃO, P., FERNANDES, R. M. & NEVES, R. 2012. Estimation of Pollutant Loads in Ardila Watershed Using the SWAT Model. *Journal of Environmental Science and Engineering***,** 1179-1191.

EC 2003. *Soil geographical database for Eurasia & the Mediterranean: instructions guide for elaboration at scale 1: 1,000,000 version 4.0*, Office for Official Publications of the European Communities.

ECCEL, F. 2011. *Develop tools and adapt watershed models to simulate water quantity and quality based on satellite images.* Mestrado em Engenharia do Ambiente., Universidade Técnica de Lisboa.

FALKENMARK, M. & ROCKSTRÖM, J. 2006. The new blue and green water paradigm: Breaking new ground for water resources planning and management. *Journal of water resources planning and management,* 132**,** 129-132.

FARAMARZI, M., ABBASPOUR, K. C., SCHULIN, R. & YANG, H. 2009. Modelling blue and green water resources availability in Iran. *Hydrological Processes,* 23**,** 486.

FEKETE, B. M., VÖRÖSMARTY, C. J. & GRABS, W. 1999. Global, composite runoff fields based on observed river discharge and simulated water balances. Fed. Inst. of Hydrology.

FITZHUGH, T. & MACKAY, D. 2001. Impact of subwatershed partitioning on modeled source-and transport-limited sediment yields in an agricultural nonpoint source pollution model. *Journal of soil and water conservation,* 56**,** 137-143.

FLEMING, R., KANESHIGE, T. & MCGOVERN, W. 1979. The Global Weather Experiment 1. The observational phase through the first special observing period. *Bulletin of the American Meteorological Society,* 60**,** 649-661.

FOLEY, J. A., DEFRIES, R., ASNER, G. P., BARFORD, C., BONAN, G., CARPENTER, S. R., CHAPIN, F. S., COE, M. T., DAILY, G. C., GIBBS, H. K., HELKOWSKI, J. H., HOLLOWAY, T., HOWARD, E. A., KUCHARIK, C. J., MONFREDA, C., PATZ, J. A., PRENTICE, I. C., RAMANKUTTY, N. & SNYDER, P. K. 2005. Global consequences of land use. *Science,* 309**,** 570-574.

FORKUTSA, I., SOMMER, R., SHIROKOVA, Y. I., LAMERS, J. P. A., KIENZLER, K., TISCHBEIN, B., MARTIUS, C. & VLEK, P. L. G. 2009. Modeling irrigated cotton with shallow groundwater in the Aral Sea Basin of Uzbekistan: I. Water dynamics. *Irrigation Science,* 27**,** 331-346.

FU, S., SONNENBORG, T. O., JENSEN, K. H. & HE, X. 2011. Impact of precipitation spatial resolution on the hydrological response of an integrated distributed water resources model. *Vadose Zone Journal,* 10**,** 25-36.

GALVÁN, L., OLÍAS, M., IZQUIERDO, T., CERÓN, J. & DE VILLARÁN, R. F. 2014. Rainfall estimation in SWAT: An alternative method to simulate orographic precipitation. *Journal of Hydrology,* 509**,** 257-265.

GALVÃO, P., CHAMBEL LEITÃO, P., NEVES, R. & LEITAO, P. C. 2004. A different approach to the modified Picard method for water flow in variably saturated media. *Developments in Water Science,* 55**,** 557-567.

GONÇALVES, F. 2006. *Quantificação das cargas de azoto e de fósforo afluentes à albufeira da Aguieira, na Bacia Hidrográfica do Mondego.* . Licenciatura em Engenharia do Ambiente. , Universidade Técnica de Lisboa. .

GONÇALVES, M., RAMOS, T., NEVES, M., MARTINS, J., PIRES, F. P. & LEITÃO, P. 2007. Modelação da dinâmica da água e dos sais num Aluviossolo regado com águas de diferente qualidade: ensaio de validação do modelo HYDRUS-1D com observações em monólitos. *Revista de Ciências Agrárias,* 30**,** 38-52.

GRANATO, G. E. 2014. Hydrologic Drought Decision Support System (HyDroDSS). US Geological Survey.

GUPTA, H. V., SOROOSHIAN, S. & YAPO, P. O. 1999. Status of Automatic Calibration for Hydrologic Models: Comparison with Multilevel Expert Calibration. *Journal of Hydrologic Engineering,* 4**,** 135-143.

HARTANTO, I. M., ALMEIDA, C., ALEXANDRIDIS, T. K., WEYNANTS, M., TIMOTEO, G., CHAMBEL-LEITÃO, P. & ARAUJO, A. 2015. MERGING EARTH OBSERVATION DATA, WEATHER PREDICTIONS, IN-SITU MEASUREMENTS AND HYDROLOGICAL MODELS FOR WATER INFORMATION SERVICES. *Environmental Engineering & Management Journal (EEMJ),* 14.

HOUNAM, D. & WERNER, M. The shuttle radar topography mission (SRTM). Proceedings of ISPRS workshop-Sensors and Mapping from Space, 1999. Citeseer.

HUFFMAN, J. H. 2005. *Impacts of estimating recharge on groundwater modeling for arid basins.* PhD Baylor University Waco, Texas.

JANSSEN, P. & HEUBERGER, P. 1995. Calibration of process-oriented models. *Ecological Modelling,* 83**,** 55-66.

JARVIS, A., REUTER, H., NELSON, A. & GUEVARA, E. 2008. Hole-filled SRTM for the globe Version 4, available from the CGIAR-CSI SRTM 90m Database. htt p. *srtm. csi. cgiar. org*.

KALNAY, E., KANAMITSU, M., KISTLER, R., COLLINS, W., DEAVEN, D., GANDIN, L., IREDELL, M., SAHA, S., WHITE, G. & WOOLLEN, J. 1996. The NCEP/NCAR 40-year reanalysis project. *Bulletin of the American Meteorological Society,* 77**,** 437-471.

KANAMARU, H. & KANAMITSU, M. 2007. Scale-selective bias correction in a downscaling of global analysis using a regional model. *Monthly Weather Review,* 135**,** 334-350.

KAUFFELDT, A., WETTERHALL, F., PAPPENBERGER, F., SALAMON, P. & THIELEN, J. 2016. Technical review of large-scale hydrological models for implementation in operational flood forecasting schemes on continental level. *Environmental Modelling & Software,* 75**,** 68-76.

KAUFMAN, F. 2012. Futures market: Wall Street's thirst for water. *Nature,* 490**,** 469-471.

KNISEL, W. G. 1980. CREAMS: A field-scale model for chemicals, runoff and erosion from agricultural management systems. *USDA Conservation Research Report*.

KNISEL, W. G. 1993. *GLEAMS: Groundwater Loading Effects of Agricultural Management Systems: Version 2.10*, University of Georgia Coastal Plain Experiment Station, Bio. & Ag. Engineering.

LEITÃO, J. C., CHAMBEL-LEITÃO, P., COUTINHO, P. B., FULGÊNCIO, C., COTA, T., ALMEIDA, C., SIMÃO, M. & GRADE, M. DISPONIBILIDADES DE ÁGUA, EM REGIME NATURAL E MODIFICADO, NAS REGIÕES HIDROGRÁFICAS DO ALENTEJO E ALGARVE. 11.º Congresso da Água, 2012a Porto.

LEITÃO, P., GALVÃO, P., AIRES, E., ALMEIDA, L. & VIEGAS, C. 2012b. FECAL CONTAMINATION MODELING IN COASTAL WATERS USING A WEB SERVICE APPROACH. *Environmental Engineering & Management Journal (EEMJ),* 11.

MARTINEZ, G., PACHEPSKY, Y. A., VEREECKEN, H., HARDELAUF, H., HERBST, M. & VANDERLINDEN, K. 2013. Modeling local control effects on the temporal stability of soil water content. *Journal of Hydrology,* 481**,** 106-118.

MASS, C. F., OVENS, D., WESTRICK, K. & COLLE, B. A. 2002. Does increasing horizontal resolution produce more skillful forecasts? *Bulletin of the American Meteorological Society,* 83**,** 407-430.

MATEUS, V., D. BRITO, CHAMBEL-LEITÃO P E M. CAETANO. Produção e utilização de cartografia multi-escala derivada através dos sensores LISSIII, AWiFS e MERIS para modelação da qualidade da água para a Bacia Hidrográfica do Rio Tejo. Cartografia e Geodesia 2009, 2009. 230-243.

MESINGER, F., DIMEGO, G., KALNAY, E., MITCHELL, K., SHAFRAN, P. C., EBISUZAKI, W., JOVIC, D., WOOLLEN, J., ROGERS, E. & BERBERY, E. H. 2006. North American regional reanalysis. *Bulletin of the American Meteorological Society,* 87**,** 343-360.

MIRANDA, R., BRAUNSCHWEIG, F., LEITAO, P., NEVES, R., MARTINS, F. & SANTOS, A. 2000a. MOHID 2000 - A coastal integrated object oriented model. *Hydraulic Engineering Software Viii,* 7**,** 393-401.

MIRANDA, R., BRAUNSCHWEIG, F., LEITAO, P., NEVES, R., MARTINS, F. & SANTOS, A. 2000b. MOHID 2000, a coastal integrated object oriented model. *Southampton, UK: WIT Press, Hydraulic Engineering Software VIII.*

MORIASI, D., ARNOLD, J., VAN LIEW, M., BINGNER, R., HARMEL, R. & VEITH, T. 2007. Model evaluation guidelines for systematic quantification of accuracy in watershed simulations. *Trans. Asabe,* 50**,** 885-900.

NASH, J. & SUTCLIFFE, J. 1970. River flow forecasting through conceptual models part I—A discussion of principles. *Journal of Hydrology,* 10**,** 282-290.

NEITSCH, S., AMOLD, J., KINIRY, J., SRINIVASAN, R. & WILLIAMS, J. 2011. Soil and Water Assessment Tool SWAT Theoretical documentation. Version 2009. *In:* UNIVERSITY, T. A. M. (ed.). Version.

NEVES, R., CHAMBEL-LEITÃO, P. & LEITÃO, P. 2000a. Modelação Numérica Da Circulação Da água no solo-o modelo MOHID. *Pedologia,* 28.

NEVES, R., CHAMBEL-LEITÃO, P. & LEITÃO, P. 2000b. Numerical modeling of water circulation in the soil - MOHID model. Modelação Numérica Da Circulação Da água no solo-o modelo MOHID. *Pedologia,* 28.

NICOLAU, M. R. R. C. 2002. *Modelação e mapeamento da distribuição espacial de precipitação: uma aplicação a Portugal Continental.* Doutor em Engenharia do Ambiente, Universidade Nova de Lisboa.

OBERMANN, M. 2007. *Nutrient dynamics in temporary waters of Mediterranean catchments*, ISAH, Inst. für Siedlungswasserwirtschaft und Abfalltechnik der Univ. Hannover.

RAMOS, M. H., MATHEVET, T., THIELEN, J. & PAPPENBERGER, F. 2010. Communicating uncertainty in hydro‐meteorological forecasts: mission impossible? *Meteorological Applications,* 17**,** 223-235.

RAMOS, T. B., GONCALVES, M. C., CASTANHEIRA, N. L., MARTINS, J. C., SANTOS, F. L., PRAZERES, A. & FERNANDES, M. L. 2009. Effect of sodium and nitrogen on yield function of irrigated maize in southern Portugal. *Agricultural Water Management,* 96**,** 585-594.

RAMOS, T. B., SIMUNEK, J., GONCALVES, M. C., MARTINS, J. C., PRAZERES, A. & PEREIRA, L. S. 2012. Two-dimensional modeling of water and nitrogen fate from sweet sorghum irrigated with fresh and blended saline waters. *Agricultural Water Management,* 111**,** 87-104.

REUNGSANG, P., KANWAR, R. S., JHA, M., GASSMAN, P. W., AHMAD, K. & SALEH, A. 2007. Calibration and validation of SWAT for the Upper Maquoketa River watershed. *International Agricultural Engineering Journal,* 16**,** 35-48.

ROMANOWICZ, A., VANCLOOSTER, M., ROUNSEVELL, M. & LA JUNESSE, I. 2005. Sensitivity of the SWAT model to the soil and land use data parametrisation: a case study in the Thyle catchment, Belgium. *Ecological Modelling,* 187**,** 27-39.

SAHA, S., MOORTHI, S., WU, X., WANG, J., NADIGA, S., TRIPP, P., BEHRINGER, D., HOU, Y.-T., CHUANG, H.-Y. & IREDELL, M. 2014. The NCEP climate forecast system version 2. *Journal of Climate,* 27**,** 2185-2208.

SCANLON, B. R., CHRISTMAN, M., REEDY, R. C., PORRO, I., SIMUNEK, J. & FLERCHINGER, G. N. 2002. Intercode comparisons for simulating water balance of surficial sediments in semiarid regions. *Water Resources Research,* 38**,** 59-1-59-16.

SCHAAP, M. G., LEIJ, F. J. & VAN GENUCHTEN, M. T. 2001. ROSETTA: a computer program for estimating soil hydraulic parameters with hierarchical pedotransfer functions. *Journal of Hydrology,* 251**,** 163-176.

SHEN, Z., CHEN, L., LIAO, Q., LIU, R. & HONG, Q. 2012. Impact of spatial rainfall variability on hydrology and nonpoint source pollution modeling. *Journal of Hydrology,* 472**,** 205-215.

SILGRAM, M., ANTHONY, S., COLLINS, A., STRŐMQVIST, J., BOURAOUI, F., SCHOUMANS, O., PORTO, A. L., GROENENDIJK, P., ARHEIMER, B. & MIMIKOU, M. 2009. Evaluation of diffuse pollution model applications in EUROHARP catchments with limited data. *Journal of Environmental Monitoring,* 11**,** 554-571.

SIMUNEK, J. & VAN GENUCHTEN, M. T. 2008. Modeling nonequilibrium flow and transport processes using HYDRUS. *Vadose Zone Journal,* 7**,** 782-797.

SOPHOCLEOUS, M. & PERKINS, S. P. 2000. Methodology and application of combined watershed and ground-water models in Kansas. *Journal of Hydrology,* 236**,** 185-201.

SOUSA, T. 2002. *Previsão Meteorológica em Portugal Continental utilizando o modelo operacional e de investigação MM5* Dissertação para obtenção do grau de Mestre em Ecologia, Gestão e Modelação dos Recursos Marinhos, Instituto Superior Técnico.

SRINIVASAN, R., ARNOLD, J. & JONES, C. 1998. Hydrologic modelling of the United States with the soil and water assessment tool. *International Journal of Water Resources Development,* 14**,** 315-325.

STEFANOVA, L., MISRA, V., CHAN, S., GRIFFIN, M., O'BRIEN, J. J. & SMITH III, T. J. 2012. A proxy for high-resolution regional reanalysis for the Southeast United States: assessment of precipitation variability in dynamically downscaled reanalyses. *Climate dynamics,* 38**,** 2449-2466.

TAN, M. Free internet datasets for streamflow modelling using SWAT in the Johor river basin, Malaysia. IOP Conference Series: Earth and Environmental Science, 2014. IOP Publishing, 012193.

THIELEN, J., BARTHOLMES, J., RAMOS, M.-H. & ROO, A. D. 2009. The European flood alert system–Part 1: concept and development. *Hydrology and Earth System Sciences,* 13**,** 125-140.

THIESSEN, A. H. 1911. Precipitation averages for large areas. *Monthly Weather Review,* 39**,** 1082-1089.

TRANCOSO, A. R., BRAUNSCHWEIG, F., CHAMBEL-LEITAO, P. C., OBERMANN, M. & NEVES, R. 2009. An advanced modelling tool for simulating complex river systems. *Science of the Total Environment,* 407**,** 3004-3016.

TRIGO, R. M. & DACAMARA, C. C. 2000. Circulation weather types and their influence on the precipitation regime in Portugal. *International Journal of Climatology,* 20**,** 1559-1581.

TRIGO, R. M., POZO ‐ VÁZQUEZ, D., OSBORN, T. J., CASTRO ‐ DÍEZ, Y., GÁMIZ ‐ FORTIS, S. & ESTEBAN ‐ PARRA, M. J. 2004. North Atlantic Oscillation influence on precipitation, river flow and water resources in the Iberian Peninsula. *International Journal of Climatology,* 24**,** 925-944.

TRIPATHI, M., PANDA, R. & RAGHUWANSHI, N. 2003. Identification and prioritisation of critical sub-watersheds for soil conservation management using the SWAT model. *Biosystems Engineering,* 85**,** 365-379.

TRIPATHI, M., PANDA, R. & RAGHUWANSHI, N. 2005. Development of effective management plan for critical subwatersheds using SWAT model. *Hydrological processes,* 19**,** 809-826.

UN-WATER. & UNESCO. 2009. *Water in a changing world,* Paris, London, UNESCO Publishing; Earthscan.

UN 2015. The Millennium Development Goals Report. http://www.un.org/millenniumgoals/.

VALIPOUR, M. 2014. Investigation of Valiantzas' evapotranspiration equation in Iran. *Theoretical and Applied Climatology***,** 1-12.

VALIPOUR, M. 2015. Importance of solar radiation, temperature, relative humidity, and wind speed for calculation of reference evapotranspiration. *Archives of Agronomy and Soil Science,* 61**,** 239-255.

VAN DER KNIJFF, J., YOUNIS, J. & DE ROO, A. 2010. LISFLOOD: a GIS ‐ based distributed model for river basin scale water balance and flood simulation. *International Journal of Geographical Information Science,* 24**,** 189-212.

VANGENUCHTEN, M. T. 1980. A Closed-Form Equation for Predicting the Hydraulic Conductivity of Unsaturated Soils. *Soil Science Society of America Journal,* 44**,** 892-898.

VITHANAGE, M., VILLHOLTH, K., ENGESGAARD, P. & JENSEN, K. H. 2010. Vulnerability Analysis of the Coastal Sandy Aquifers in the East Coast of Sri Lanka with Recharge Change Consideration. *Open Hydrology Journal*.

VU, M., RAGHAVAN, S. & LIONG, S. 2011. Simulating stream flow over data sparse areas–an application of internet based data. *Hydrology and Earth System Sciences Discussions,* 8**,** 11015-11037.

WILLIAMS, J., JONES, C. & DYKE, P. 1984. Modeling approach to determining the relationship between erosion and soil productivity. *Transactions of the American Society of Agricultural Engineers,* 27.

WILLIAMS, J. R., NICKS, A. & ARNOLD, J. G. 1985. Simulator for water resources in rural basins. *Journal of Hydraulic Engineering,* 111**,** 970-986.

WÖSTEN, J., LILLY, A., NEMES, A. & LE BAS, C. 1999. Development and use of a database of hydraulic properties of European soils. *Geoderma,* 90**,** 169-185.

YARROW, M. & CHAMBEL-LEITÃO, P. 2007. Calibration of the SWAT model to the Aysén basin of the Chilean Patagonia: Challenges and Lessons. *Proceedings of the Watershed Management to Meet Water Quality Standards and TMDLS (Total Maximum Daily Load) 10-14 March 2007, San Antonio, Texas 701P0207.*

YARROW, M. & CHAMBEL-LEITÃO, P. 2008. Estimation of loads in the Aysén Basin of the Chilean Patagonia: SWAT model and Harp-Nut guidelines. *In:* NEVES, R., BARETTA, J. & MATEUS, M. (eds.) *Perspectives on Integrated Coastal Zone Management in South America.* Lisbon, Portugal: IST Press.

ZHANG, G., VIVEKANANDAN, J. & BRANDES, E. 2002. Effects of random inhomogeneity on radar measurements and rain rate estimation. *IEEE transactions on geoscience and remote sensing,* 40**,** 223-227.

8 Appendix A

8.1 Precipitations stations

Nº	BACIA	CÓDIGO	NOME	Nº Values	Begin	End	Elevation (m)	Nº Days	Values /Days*100	LAT (ºN)	LON (ºW)
29	ARADE	30F/01C	MONCHIQUE	12053	01-01-1979	01-02-2015	792	13180	91%	37.32	-8.59
39	CÁVADO/RIBEIRAS COSTEIRAS	02J/01G	PITÕES	10057	01-01-1979	01-12-2010	1077	11657	86%	41.84	-7.95
9	CÁVADO/RIBEIRAS COSTEIRAS	02K/01UG	CASAIS DA VEIGA (EX: PADORNELOS)	9246	01-01-1979	24-12-2009	1065	11315	82%	41.86	-7.76
25	CÁVADO/RIBEIRAS COSTEIRAS	03I/03UG	LEONTE	8742	01-01-1979	11-12-2003	874	9110	96%	41.77	-8.15
34	CÁVADO/RIBEIRAS COSTEIRAS	03I/06UG	PEDRA BELA	10407	01-01-1979	01-12-2010	714	11657	89%	41.71	-8.14
32	CÁVADO/RIBEIRAS COSTEIRAS	03J/02UG	OUTEIRO	10771	01-01-1979	08-12-2010	845	11664	92%	41.79	-7.94
33	CÁVADO/RIBEIRAS COSTEIRAS	03J/03UG	PARADELA DO RIO	11201	01-01-1979	01-12-2010	834	11657	96%	41.76	-7.95
48	CÁVADO/RIBEIRAS COSTEIRAS	03J/05G	VILA DA PONTE	12256	01-01-1979	01-02-2015	745	13180	93%	41.72	-7.90
44	CÁVADO/RIBEIRAS COSTEIRAS	03J/06UG	TELHADO	9815	01-01-1979	03-12-2009	1042	11294	87%	41.71	-7.85
21	CÁVADO/RIBEIRAS COSTEIRAS	03K/02UG	GRALHÓS	11126	01-01-1979	01-12-2010	910	11657	95%	41.78	-7.74
19	DOURO	02O/01UG	GESTOSA	10981	01-01-1979	01-12-2010	706	11657	94%	41.88	-7.15
49	DOURO	02O/02UG	VINHAIS	10627	01-01-1979	23-12-2009	636	11314	94%	41.83	-6.99

Nº	BACIA	CÓDIGO	NOME	Nº Values	Begin	End	Elevation (m)	Nº Days	Values /Days*100	LAT (ºN)	LON (ºW)
28	DOURO	02P/01C	MOIMENTA DA RAIA	11024	01-01-1979	02-12-2010	837	11658	95%	41.95	-6.98
30	DOURO	02Q/01UG	MONTEZINHO	3122	01-01-1979	05-12-2008	1159	10931	29%	41.93	-6.79
11	DOURO	03K/05UG	CERVOS	11236	01-01-1979	01-12-2010	842	11657	96%	41.74	-7.68
6	DOURO	03K/06UG	BARRACÃO	8271	01-01-1979	07-12-2009	801	11298	73%	41.76	-7.71
3	DOURO	03K/07UG	ALTURAS DO BARROSO	7358	01-01-1979	02-12-2009	1068	11293	65%	41.70	-7.82
46	DOURO	03N/01G	TRAVANCAS	12117	01-01-1979	01-02-2015	884	13180	92%	41.83	-7.31
10	DOURO	03P/01UG	CELAS	10379	01-01-1979	05-12-2008	905	10931	95%	41.71	-6.92
12	DOURO	04J/03UG	COUTO DE DORNELAS	8808	01-01-1979	29-12-2009	679	11320	78%	41.64	-7.84
58	DOURO	04J/06UG	CABECEIRAS DE BASTO	8557	01-01-1979	29-12-2009	263	11320	76%	41.51	-7.98
42	DOURO	04K/02G	SANTA MARTA DA MONTANHA	11772	01-01-1979	30-11-2014	866	13117	90%	41.50	-7.75
26	DOURO	04K/03UG	LIXA DO ALVÃO	10357	01-01-1979	01-02-2015	939	13180	79%	41.50	-7.69
88	DOURO	04N/01C	RIO TORTO	10433	01-01-1979	01-02-2015	322	13180	79%	41.54	-7.28
73	DOURO	04P/06UG	MACEDO DE CAVALEIROS	9355	01-01-1979	22-12-2009	551	11313	83%	41.53	-6.96
4	DOURO	04R/01UG	ARGOZELO	10853	01-01-1979	01-02-2015	685	13180	82%	41.64	-6.60
7	DOURO	04R/03UG	CAMPO DE VÍBORAS	10329	01-01-1979	01-08-2010	654	11535	90%	41.52	-6.56
5	DOURO	04S/01UG	AVELANOSO	10285	01-01-1979	01-08-2010	713	11535	89%	41.66	-6.43
22	DOURO	05K/02UG	LAMAS DE ALVADIA	8393	01-01-1979	03-12-2009	964	11294	74%	41.45	-7.76
23	DOURO	05K/03UG	LAMAS DE OLO	9302	01-01-1979	30-12-2009	984	11321	82%	41.37	-7.80
45	DOURO	05L/03UG	TORRE DO PINHÃO	10717	01-01-1979	01-12-2010	661	11657	92%	41.37	-7.61

Nº	BACIA	CÓDIGO	NOME	Nº Values	Begin	End	Elevation (m)	Nº Days	Values /Days*100	LAT (ºN)	LON (ºW)
53	DOURO	05P/04UG	ALFÂNDEGA DA FÉ	9189	10-01-1983	09-12-2009	558	9830	93%	41.34	-6.97
31	DOURO	05Q/01UG	MORAIS	11273	01-01-1979	01-07-2010	626	11504	98%	41.49	-6.78
74	DOURO	05Q/03UG	MOGADOURO	10364	01-01-1979	22-12-2009	537	11313	92%	41.48	-6.72
80	DOURO	06H/01UG	PENAFIEL	9985	01-01-1979	02-12-2010	175	11658	86%	41.21	-8.30
55	DOURO	06I/01G	AMARANTE	10544	01-01-1979	03-12-2010	146	11659	90%	41.26	-8.07
47	DOURO	06M/01G	VILA CHÃ (ALIJÓ)	10405	01-01-1979	01-12-2009	770	11292	92%	41.32	-7.49
16	DOURO	06N/01C	FOLGARES	10780	01-01-1979	01-02-2015	739	13180	82%	41.30	-7.28
8	DOURO	06P/02UG	CARVIÇAIS	10492	01-01-1979	01-06-2010	611	11474	91%	41.18	-6.89
67	DOURO	07H/01UG	ENTRE-OS-RIOS	10513	01-01-1979	01-12-2010	18	11657	90%	41.08	-8.29
27	DOURO	08J/02G	MEZIO (PAIVA)	10362	01-01-1979	08-12-2007	611	10568	98%	40.98	-7.89
61	DOURO	08J/04G	CASTRO DAIRE	8309	01-01-1979	09-12-2001	584	8378	99%	40.89	-7.94
35	DOURO	08J/05UG	PENDILHE	8313	01-01-1979	09-12-2007	737	10569	79%	40.91	-7.84
24	DOURO	08L/03UG	LEOMIL	9187	01-01-1979	30-12-2009	704	11321	81%	40.98	-7.66
37	DOURO	08M/01UG	PENEDONO	7548	01-01-1979	31-12-2001	957	8400	90%	40.98	-7.39
38	DOURO	09O/01G	PINHEL	13026	01-01-1979	01-02-2015	606	13180	99%	40.77	-7.06
2	DOURO	09P/02UG	ALMEIDA	10337	01-01-1979	03-12-2009	742	11294	92%	40.72	-6.91
57	GUADIANA	21K/01UG	AZARUJA	12540	01-01-1979	01-02-2015	270	13180	95%	38.70	-7.77
51	GUADIANA	21M/02UG	ALANDROAL	11626	01-01-1979	01-02-2015	302	13180	88%	38.69	-7.40
87	GUADIANA	23L/01G	REGUENGOS	12397	01-01-1979	01-02-2015	218	13180	94%	38.42	-7.53
90	GUADIANA	26L/01UG	SERPA	12120	01-01-1979	11-12-2013	209	12763	95%	37.94	-7.60
62	GUADIANA	27I/01G	CASTRO VERDE	12556	01-01-1979	01-02-2015	217	13180	95%	37.70	-8.09
63	GUADIANA	30J/02G	CATRAIA	4151	03-01-2001	01-02-2015	475	5142	81%	37.31	-7.84
36	LIMA	02H/03UG	PENEDA	10807	01-01-1979	01-12-2010	697	11657	93%	41.97	-8.22

Nº	BACIA	CÓDIGO	NOME	Nº Values	Begin	End	Elevation (m)	Nº Days	Values /Days*100	LAT (ºN)	LON (ºW)
84	LIMA	03F/01G	PONTE DE LIMA	12708	01-01-1979	01-02-2015	18	13180	96%	41.77	-8.60
83	LIMA	03G/02C	PONTE DA BARCA	11387	01-01-1979	01-02-2015	39	13180	86%	41.80	-8.42
1	MONDEGO	09L/01UG	AGUIAR DA BEIRA	10673	01-01-1979	31-12-2009	776	11322	94%	40.82	-7.54
89	MONDEGO	11I/01G	SANTA COMBA DÃO	11123	01-01-1979	01-02-2015	289	13180	84%	40.43	-8.12
77	MONDEGO	11J/02C	OLIVEIRA DO HOSPITAL	11586	01-01-1979	30-11-2014	468	13117	88%	40.36	-7.87
20	MONDEGO	11L/01UG	GOUVEIA	7515	01-01-1979	01-11-2007	671	10531	71%	40.49	-7.59
91	MONDEGO	13F/01G	SOURE	11104	01-01-1979	01-02-2015	18	13180	84%	40.05	-8.63
71	MONDEGO	13I/01G	GÓIS	9300	01-01-1979	05-12-2010	190	11661	80%	40.16	-8.11
15	MONDEGO	13J/01UG	FAJÃO	11040	01-01-1979	02-12-2010	700	11658	95%	40.14	-7.92
85	RIBEIRAS DO OESTE	18C/01G	PRAGANÇA	11977	01-01-1979	10-12-2011	183	12031	100%	39.20	-9.06
93	SADO	21G/01UG	VENDAS NOVAS	9914	10-01-1980	01-12-2010	135	11283	88%	38.67	-8.47
75	SADO	22F/03C	MOINHOLA	12672	01-01-1979	01-02-2015	41	13180	96%	38.58	-8.62
52	SADO	23I/01C	ALCÁÇOVAS	11691	01-01-1979	11-12-2014	218	13128	89%	38.39	-8.15
70	SADO	24F/01C	GRÂNDOLA	11483	01-01-1979	01-02-2015	95	13180	87%	38.17	-8.56
94	SADO	24I/01C	VIANA DO ALENTEJO	10277	10-01-1984	01-02-2015	314	11345	91%	38.33	-8.01
69	SADO	25I/01UG	FERREIRA DO ALENTEJO	10893	01-01-1979	03-12-2011	143	12024	91%	38.06	-8.11
78	SADO	27H/01CG	PANÓIAS	10591	01-01-1979	08-12-2013	164	12760	83%	37.76	-8.31
13	TEJO	12L/03G	COVILHÃ	11712	01-01-1979	02-12-2014	719	13119	89%	40.28	-7.51
81	TEJO	13O/01UG	PENHA GARCIA	9342	01-01-1979	21-12-2009	495	11312	83%	40.04	-7.02
72	TEJO	14N/02UG	LADOEIRO	12987	01-01-1979	01-02-2015	215	13180	99%	39.83	-7.27

Nº	BACIA	CÓDIGO	NOME	Nº Values	Begin	End	Elevation (m)	Nº Days	Values /Days*100	LAT (ºN)	LON (ºW)
86	TEJO	15G/02G	REGO DA MURTA	12453	01-01-1979	01-02-2015	241	13180	94%	39.77	-8.36
96	TEJO	16K/01G	VILA VELHA DE RODÃO	10566	01-01-1979	01-02-2015	84	13180	80%	39.65	-7.67
82	TEJO	17F/01UG	PERNES	11271	01-01-1979	18-12-2009	81	11309	100%	39.39	-8.66
64	TEJO	17G/02G	CHAMUSCA	11727	01-01-1979	01-02-2015	18	13180	89%	39.36	-8.49
50	TEJO	17H/01C	ABRANTES	12931	01-01-1979	01-02-2015	105	13180	98%	39.45	-8.10
92	TEJO	17L/02UG	VALE DO PESO	12721	01-01-1979	25-12-2014	285	13142	97%	39.35	-7.65
60	TEJO	17M/01G	CASTELO DE VIDE	11565	01-01-1979	01-02-2015	552	13180	88%	39.41	-7.45
65	TEJO	18G/01G	CHOUTO	11812	01-01-1979	01-09-2013	126	12662	93%	39.27	-8.35
54	TEJO	18L/01UG	ALTER DO CHÃO	10937	01-01-1979	02-12-2010	224	11658	94%	39.22	-7.68
56	TEJO	19J/03UG	AVIS	10952	01-01-1979	02-12-2010	151	11658	94%	39.06	-7.90
76	TEJO	19M/01UG	MONFORTE	11176	01-01-1979	01-02-2015	259	13180	85%	39.06	-7.44
66	TEJO	20F/01UG	CORUCHE	11074	01-01-1979	15-12-2009	73	11306	98%	38.97	-8.52
79	TEJO	20I/01G	PAVIA	10981	01-01-1979	01-02-2015	189	13180	83%	38.90	-8.01
68	TEJO	20L/01G	ESTREMOZ	10911	01-01-1979	07-12-2010	333	11663	94%	38.84	-7.62
59	TEJO	21F/01UG	CANHA	11404	01-01-1979	01-02-2015	52	13180	87%	38.77	-8.63
95	TEJO	22C/02UG	VILA NOGUEIRA DE AZEITÃO	13055	01-01-1979	01-02-2015	126	13180	99%	38.52	-9.01

8.2 Flow gage station

Table 19 – SNIRH flow gage stations used to evaluate model results

ID	Code	Name	Watershed	River	LON ETRS	LAT ETRS	Drained Area (KM²)	Period
1	30G/01H	MONTE DOS PACHECOS	ARADE	RIBEIRA DE ODELOUCA	-29577	-262838	386	1979 - 2001
2	05E/03H	PONTE AVE	AVE	RIO AVE	-45852	187004	1107.72	1984 - 2000
3	05E/01H	PONTE JUNQUEIRA	AVE	RIO ESTE	-46494	191229	233.88	1979 - 2000
4	04F/02H	BARCELOS	CÁVADO	RIO CÁVADO	-40887	206633	1434.3	1979 - 2002
5	04H/01A	CANIÇADA (EDP)	CÁVADO	RIO CÁVADO	-8488	220294	774.66	1997 - 2010
6	03I/01A	SALAMONDE (EDP)	CÁVADO	RIO CÁVADO	3256	224399	615.05	1997 - 2010
7	03J/04A	VENDA NOVA (EDP)	CÁVADO	RIO RABAGÃO	12351	223546	239.35	1997 - 2010
8	09O/02H	PONTE FIGUEIRA	DOURO	RIBEIRA DAS CABRAS	90919	124449	273.33	1981 - 2003
9	08O/01H	VALE TREVO	DOURO	RIBEIRA DE MASSUEIME	83841	138138	405.4	1979 - 2004
10	05Q/01H	AZIBO (RIO)	DOURO	RIO AZIBO	111137	193820	282.68	1979 - 2004
11	04J/04H	CUNHAS	DOURO	RIO BEÇA	23544	206778	337.28	1979 - 2004
12	08O/02H	CIDADELHE	DOURO	RIO CÔA	86949	138951	1743.1	1979 - 2004
13	10P/01H	CASTELO BOM	DOURO	RIO CÔA	103738	107290	944.16	1979 - 2004
14	06K/01H	ERMIDA CORGO	DOURO	RIO CORGO	32204	173492	294.22	1979 - 2004
15	08H/02H	FRAGAS DA TORRE	DOURO	RIO PAIVA	-3949	141327	646.74	1979 - 2004
16	08J/01H	CASTRO DAIRE	DOURO	RIO PAIVA	16948	135793	288.17	1979 - 2004
17	07L/01H	MOINHO DA PONTE NOVA	DOURO	RIO TÁVORA	52814	152510	439.92	1979 - 2004
18	08L/01H	QUINTA RAPE	DOURO	RIO TÁVORA	52261	135736	171.55	1979 - 2004
19	08L/01A	VILAR TABUAÇO (EDP)	DOURO	RIO TÁVORA	50332	146607	357.39	2002 - 2010
20	07L/03H	QUINTA CASTELO BORGES	DOURO	RIO TEDO	41397	163987	172.4	1981 - 2001
21	03L/01H	BOTICAS	DOURO	RIO TERVA	40310	223290	100.42	1979 - 2004
22	05M/01H	MURÇA	DOURO	RIO TINHELA	56037	192629	261.4	1979 - 2004
23	29M/01H	TENÊNCIA (PORTO DAS AREIAS)	GUADIANA	RIBEIRA DA FOUPANA	57325	-255591	396.89	1979 - 2001
24	30M/01H	ODELEITE (PONTE)	GUADIANA	RIBEIRA DE ODELEITE	56733	-259701	346.12	1979 - 1990
25	29L/01H	MONTE DOS FORTES	GUADIANA	RIBEIRA DE ODELEITE	45113	-258107	284.29	1979 - 2001
26	28K/02H	OEIRAS	GUADIANA	RIBEIRA DE OEIRAS	37155	-222408	467.53	1981 - 2002
27	28L/02H	VASCÃO	GUADIANA	RIBEIRA DO VASCÃO	48984	-238329	409.89	1979 - 2000
28	26J/01H	ALBERNOA	GUADIANA	RIO COBRES OU RIBEIRA DE TERGES	14795	-201500	169.84	1979 - 1997
29	27J/01H	MONTE DA PONTE	GUADIANA	RIO COBRES OU RIBEIRA DE TERGES	24129	-203365	719.08	1979 - 1997
30	23K/01H	VENDINHA	GUADIANA	RIO DEGEBE	39722	-134039	821.31	1981 - 2001
31	24L/01H	AMIEIRA	GUADIANA	RIO DEGEBE	50657	-151739	1477.15	1979 - 2002

ID	Code	Name	Watershed	River	LON ETRS	LAT ETRS	Drained Area (KM²)	Period
32	02G/01H	PONTILHÃO DE CELEIROS	LIMA	RIO VEZ	-23818	244320	170.8	1979 - 1990
33	11H/01H	ALMAÇA	MONDEGO	RIBEIRA DE MORTAGUA	-8063	74591	204.08	1979 - 1980
34	12I/01H	FRONHAS (RIO)	MONDEGO	RIO ALVA OU RIBEIRA DA FERVENÇA	-2628	64149	640.85	1979 - 1997
35	12I/01A	FRONHAS (EDP)	MONDEGO	RIO ALVA OU RIBEIRA DA FERVENÇA	-2033	63594	640.93	1997 - 2010
36	12H/03H	PONTE MUCELA	MONDEGO	RIO ALVA OU RIBEIRA DA FERVENÇA	-5776	65039	662.76	1979 - 1990
37	13F/04H	PONTE MOCATE	MONDEGO	RIO ARUNCA	-42978	46060	465.61	1979 - 1999
38	12G/02H	PONTE CABOUCO	MONDEGO	RIO CEIRA	-20347	56626	502.81	1979 - 1999
39	10J/01H	CALDAS DE SÃO GEMIL	MONDEGO	RIO DÃO	13737	94920	619.42	1979 - 1990
40	11I/01H	FERREIRÓS	MONDEGO	RIO DÃO	8151	88582	713.94	1979 - 1992
41	10K/01H	PONTE SANTA CLARA DÃO	MONDEGO	RIO DÃO	38145	110885	174.64	1979 - 1990
42	11I/06H	PONTE TÁBUA	MONDEGO	RIO MONDEGO	6294	78143	1543.6	1979 - 1979
43	12G/04H	PONTE SANTA CLARA COIMBRA	MONDEGO	RIO MONDEGO	-25362	59750	4915.04	1979 - 1985
44	12H/01A	RAIVA (EDP)	MONDEGO	RIO MONDEGO	-10022	71151	3294.37	1997 - 2010
45	11H/01A	AGUIEIRA (EDP)	MONDEGO	RIO MONDEGO	-5404	74669	3069.08	1997 - 2010
46	10K/03H	NELAS	MONDEGO	RIO MONDEGO	26286	92733	1125.54	1979 - 2004
47	10L/01H	PONTE JUNCAIS	MONDEGO	RIO MONDEGO	51801	104971	606.6	1979 - 2001
48	12G/01AE	AÇUDE PONTE COIMBRA	MONDEGO	RIO MONDEGO	-26124	60863	4918.53	1989 - 2009
49	31H/02H	PONTE RODOVIÁRIA	RIBEIRAS DO ALGARVE	RIBEIRA DA QUARTEIRA OU DE ALTE	-3634	-282422	324.58	1979 - 2001
50	31K/03H	BODEGA	RIBEIRAS DO ALGARVE	RIBEIRA DE ALPORTEL	38559	-278117	133.64	1979 - 1990
51	26G/04H	PONTE ALVALADE CAMPILHAS	SADO	RIBEIRA DE CAMPILHAS	-23815	-192710	698.32	1980 - 2001
52	25G/02H	MOINHO DO BRAVO	SADO	RIBEIRA DE CORONA	-24388	-178390	219.82	1979 - 1990
53	24H/03H	TORRÃO DO ALENTEJO	SADO	RIBEIRA DO XARRAMA	-8388	-152004	468.35	1979 - 2001
54	26G/05H	PONTE ALVALADE SADO	SADO	RIO SADO	-21966	-191717	669.75	1980 - 2001
55	25G/03H	MOINHO DA GAMITINHA	SADO	RIO SADO	-23773	-178170	2713.16	1979 - 2000
56	18L/01H	COUTO DE ANDREIROS	TEJO	RIBEIRA DA RAIA OU DE SEDA	45661	-44194	244.53	1979 - 1994
57	20I/04H	PAVIA	TEJO	RIBEIRA DE TERA	11287	-85729	616.63	1979 - 1992
58	19M/01H	MONFORTE	TEJO	RIBEIRA GRANDE OU DE AVIZ	59476	-67861	141.46	1979 - 1990
59	15G/02H	AGROAL	TEJO	RIO NABÃO	-26072	1237	608.49	1979 - 2001
60	16G/01H	FÁBRICA DA MATRENA	TEJO	RIO NABÃO	-21140	-15099	1047.15	1979 - 2002
61	16K/01A	PRACANA (EDP)	TEJO	RIO OCREZA	27249	-11083	1413.45	1997 - 2010
62	14H/01A	BOUÇÃ (EDP)	TEJO	RIO ZÊZERE	-7778	20849	2601.73	1997 - 2010
63	16H/01A	CASTELO DE BODE (EDP)	TEJO	RIO ZÊZERE	-16323	-13668	3964.56	1984 - 2010

ID	Code	Name	Watershed	River	LON ETRS	LAT ETRS	Drained Area (KM²)	Period
64	14I/01A	CABRIL (EDP)	TEJO	RIO ZÊZERE	522	28950	2416.32	1984 - 2010
65	10F/02H	PONTE REQUEIXO (CÉRTIMA E ÁGUEDA)	VOUGA/RIBE IRAS COSTEIRAS	RIO ÁGUEDA	-33065	102671	966.36	1979 - 1984
66	10G/02H	PONTE ÁGUEDA	VOUGA/RIBE IRAS COSTEIRAS	RIO ÁGUEDA	-26665	100285	404.28	1979 - 1990
67	10G/05H	PONTE REDONDA	VOUGA/RIBE IRAS COSTEIRAS	RIO ÁGUEDA	-20745	97490	151.6	1979 - 2000
68	10G/03H	RIBEIRO	VOUGA/RIBE IRAS COSTEIRAS	RIO ALFUSQUEIRO	-22432	99716	204.67	1979 - 2000
69	09G/01H	PONTE VALE MAIOR	VOUGA/RIBE IRAS COSTEIRAS	RIO CAIMA	-27715	113837	189.7	1979 - 2000
70	09H/01H	PEDRE RIBEIRADIO	VOUGA/RIBE IRAS COSTEIRAS	RIO VOUGA	-13757	119906	926.92	1979 - 1980
71	09I/02H	PONTE VOUZELA	VOUGA/RIBE IRAS COSTEIRAS	RIO VOUGA	1783	118228	648.84	1979 - 2001

8.3 Water budget per basin

Table 20 – Water budget per Basin

Hydrographic Region	Watershed	PRECIP [mm]	ET [mm]	DA_RCHG [mm]	REVAP [mm]	LATQ [mm]	GW_Q [mm]	SURQ [mm]
Algarve	Arade	662	368	11	178	10	32	63
Algarve	Barlavento	624	350	11	176	6	26	53
Algarve	Sotavento	599	372	8	133	6	18	62
Cavado e Leça	Ave	1524	332	43	193	18	620	318
Cavado e Leça	Cavado	1620	320	48	186	40	719	308
Cavado e Leça	Coastal Areas between Ave and Leca	1284	360	32	230	2	382	279
Cavado e Leça	Coastal Areas between Cavado and Ave	1357	401	32	227	2	381	315
Cavado e Leça	Coastal Areas between Leça and Douro	1187	253	17	138	1	185	541
Cavado e Leça	Coastal Areas between Neiva and Cavado	1481	349	46	219	3	658	205
Cavado e Leça	Leça	1339	321	35	199	5	470	301
Douro	Agueda	717	284	20	202	8	184	17

Hydrographic Region	Watershed	PRECIP [mm]	ET [mm]	DA_RCHG [mm]	REVAP [mm]	LATQ [mm]	GW_Q [mm]	SURQ [mm]
Douro	Coa	802	295	23	205	18	233	26
Douro	Coastal Areas between Douro and Vouga	1210	310	30	193	2	386	276
Douro	Douro	965	300	25	176	32	307	122
Douro	Macas	530	313	9	120	8	46	32
Douro	Paiva	1194	275	38	194	32	520	134
Douro	Rabacal	972	312	25	177	26	304	125
Douro	Sabor	600	288	12	139	14	89	54
Douro	Tamega	1364	291	41	180	28	593	232
Douro	Tua	745	302	17	159	29	162	74
Douro	Tuela	874	306	22	188	22	233	101
Guadiana	Alcarrache	466	371	3	61	1	2	28
Guadiana	Ardila	469	351	5	80	1	6	26
Guadiana	Caia	622	323	12	175	5	49	58
Guadiana	Chanca	470	331	5	93	1	7	32
Guadiana	Cobres	551	354	7	126	1	14	48
Guadiana	Degebe	586	355	9	147	1	25	49
Guadiana	Guadiana	534	366	6	106	3	14	38
Guadiana	Murtega	485	342	6	98	2	10	25
Guadiana	Xevora	631	327	11	163	9	44	74
Lima e Minho	Coastal Areas between Minho and Lima	1495	359	47	216	24	668	180
Lima e Minho	Lima	1641	325	50	192	45	760	268
Lima e Minho	Minho	1677	315	53	189	43	815	261
Lima e Minho	Neiva and Coastal Areas between Lima and Neiva	1550	349	47	208	14	690	241
Mondego e Vouga	Alva	1072	272	33	217	52	408	90
Mondego e Vouga	Coastal Areas between Mondego and Lis	969	418	20	186	5	195	130
Mondego e Vouga	Coastal Areas between Vouga and Mondego	964	482	23	219	3	214	21
Mondego e Vouga	Dao	1124	271	38	203	26	521	63

Hydrographic Region	Watershed	PRECIP [mm]	ET [mm]	DA_RCHG [mm]	REVAP [mm]	LATQ [mm]	GW_Q [mm]	SURQ [mm]
Mondego e Vouga	Lis	953	430	24	236	11	223	26
Mondego e Vouga	Mondego	1019	347	29	211	28	331	70
Mondego e Vouga	Vouga	1090	340	32	209	14	397	96
Mondego e Vouga	West 1	944	452	24	236	5	224	0
Sado e Mira	Alcacovas	650	316	13	198	3	45	73
Sado e Mira	Coastal Areas between Mira and Barlavento	623	419	9	143	4	26	21
Sado e Mira	Coastal Areas between Sado and Mira	603	399	9	139	2	30	21
Sado e Mira	Coastal Areas between Tagus and Sado 2	764	473	13	176	9	79	12
Sado e Mira	Mira	633	390	9	149	5	25	53
Sado e Mira	Roxo	548	403	6	96	1	10	32
Sado e Mira	Sado	610	379	9	146	2	31	41
Tejo	Almansor	666	346	13	194	3	60	48
Tejo	Aviz	656	344	12	188	1	48	62
Tejo	Coastal Areas between Tagus and Sado 1	764	363	18	222	5	123	33
Tejo	Divor	659	351	13	190	3	65	34
Tejo	Erges	683	317	15	179	6	104	60
Tejo	Macico Calcario	871	350	23	250	9	182	56
Tejo	Maior	765	492	11	151	6	59	45
Tejo	Nabao	926	408	23	223	15	209	45
Tejo	Ocreza	812	335	20	215	19	162	57
Tejo	Ponsul	757	310	19	206	7	153	59
Tejo	Raia	660	369	12	178	3	53	44
Tejo	Sever	659	326	15	198	12	84	22
Tejo	Sor	671	384	13	178	5	77	11
Tejo	Sorraia	673	422	11	156	3	55	24
Tejo	Tejo	723	415	13	171	6	74	41
Tejo	West 2	810	466	15	188	12	90	39

Hydrographic Region	Watershed	PRECIP [mm]	ET [mm]	DA_RCHG [mm]	REVAP [mm]	LATQ [mm]	GW_Q [mm]	SURQ [mm]
Tejo	Zezere	934	327	25	224	32	256	67

8.4 Monthly flows calibration

8.4.1 ARADE

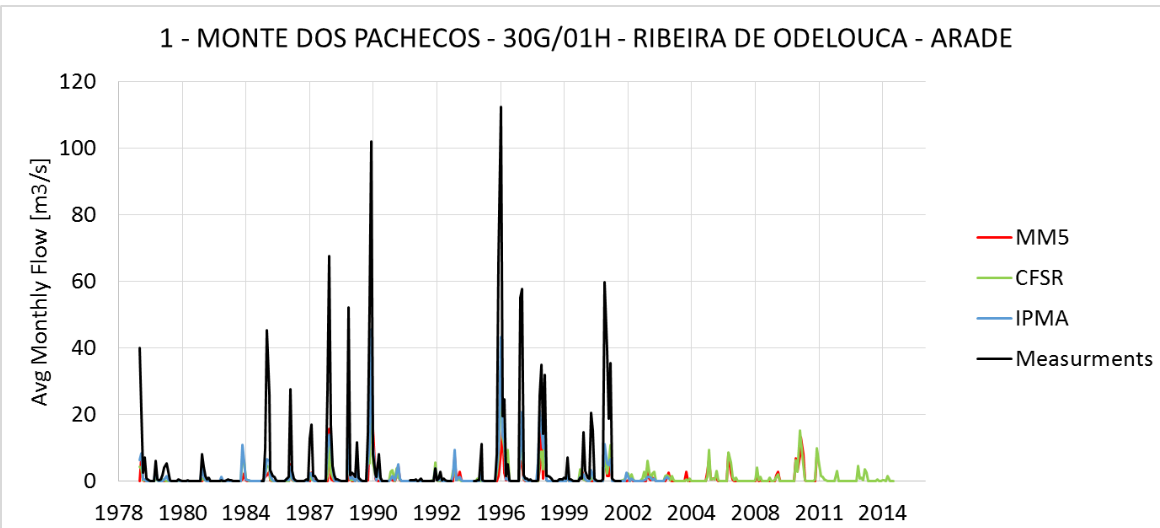

8.4.2 AVE

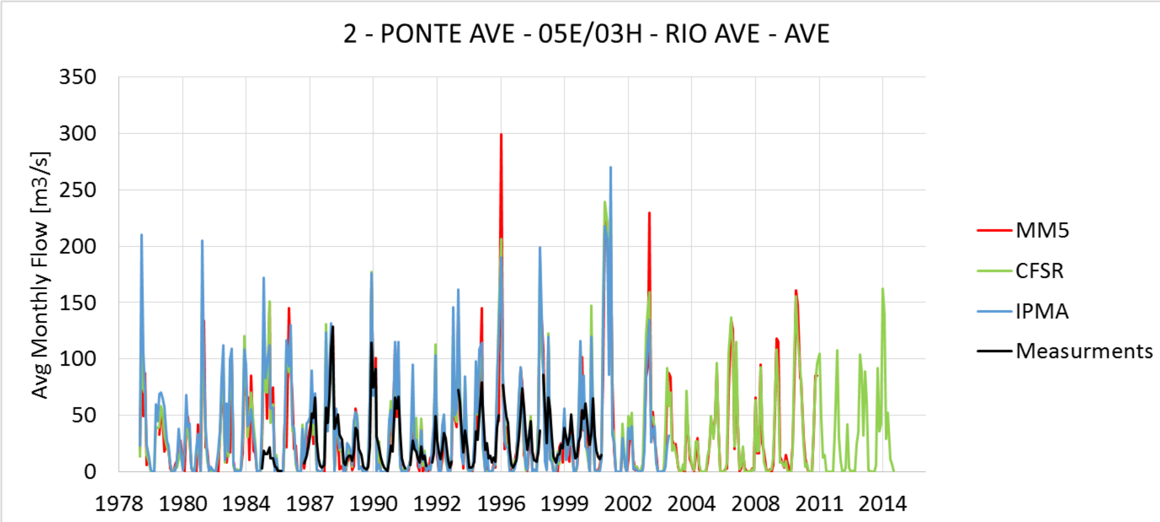
2 - PONTE AVE - 05E/03H - RIO AVE - AVE
Avg Monthly Flow [m3/s]
350
300
250
200
150
100
50
0
1978
1980
1984
1987
1990
1992
1996
1999
2002
2004
2008
2011
2014
MM5
CFSR
IPMA
Measurments

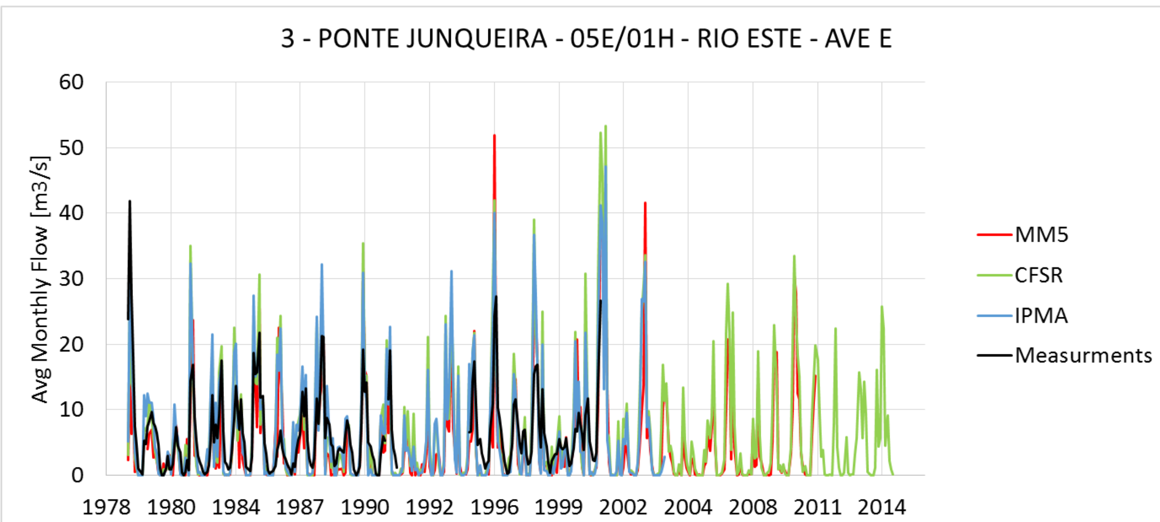
3 - PONTE JUNQUEIRA - 05E/01H - RIO ESTE - AVE E
Avg Monthly Flow [m3/s]
60
50
40
30
20
10
0
1978
1980
1984
1987
1990
1992
1996
1999
2002
2004
2008
2011
2014
MM5
CFSR
IPMA
Measurments

8.4.3 CÁVADO

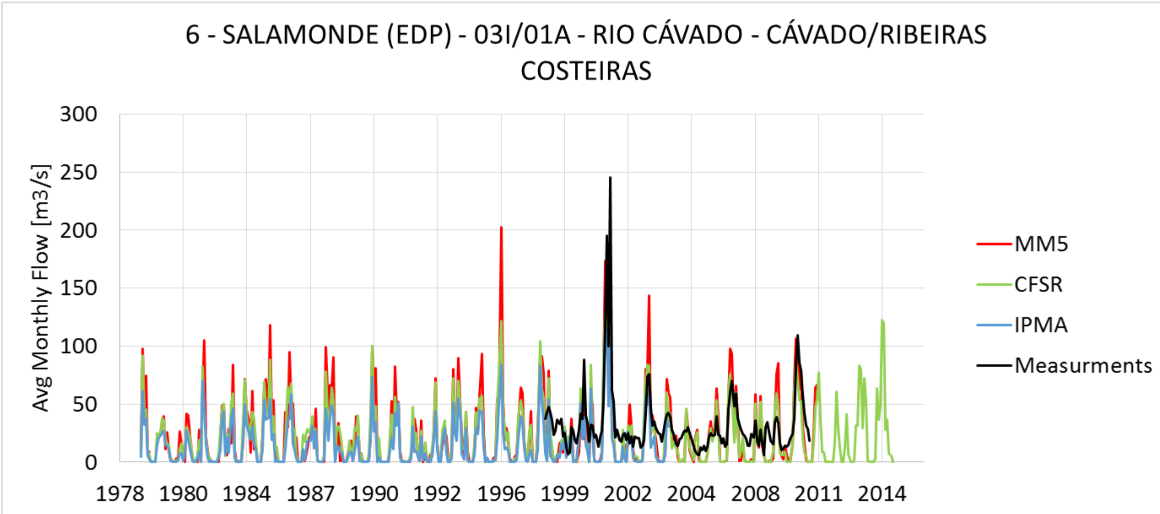
6 - SALAMONDE (EDP) - 03I/01A - RIO CÁVADO - CÁVADO/RIBEIRAS COSTEIRAS
Avg Monthly Flow [m3/s]
300
250
200
150
100
50
0
1978 1980 1984 1987 1990 1992 1996 1999 2002 2004 2008 2011 2014
MM5
CFSR
IPMA
Measurments

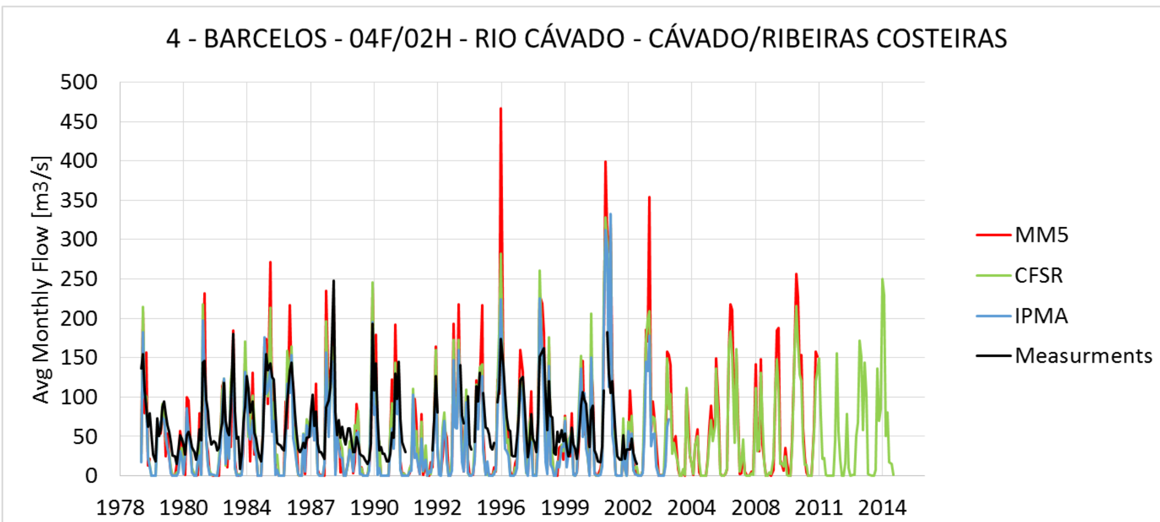
4 - BARCELOS - 04F/02H - RIO CÁVADO - CÁVADO/RIBEIRAS COSTEIRAS
Avg Monthly Flow [m3/s]
500
450
400
350
300
250
200
150
100
50
0
1978 1980 1984 1987 1990 1992 1996 1999 2002 2004 2008 2011 2014
MM5
CFSR
IPMA
Measurments

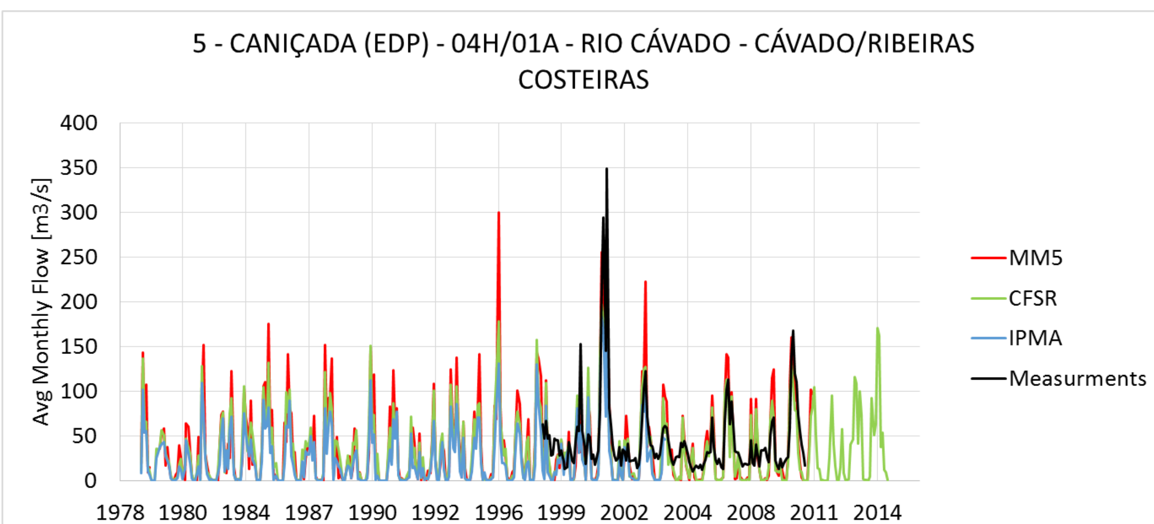
5 - CANIÇADA (EDP) - 04H/01A - RIO CÁVADO - CÁVADO/RIBEIRAS COSTEIRAS
Avg Monthly Flow [m3/s]
400
350
300
250
200
150
100
50
0
1978 1980 1984 1987 1990 1992 1996 1999 2002 2004 2008 2011 2014
MM5
CFSR
IPMA
Measurments

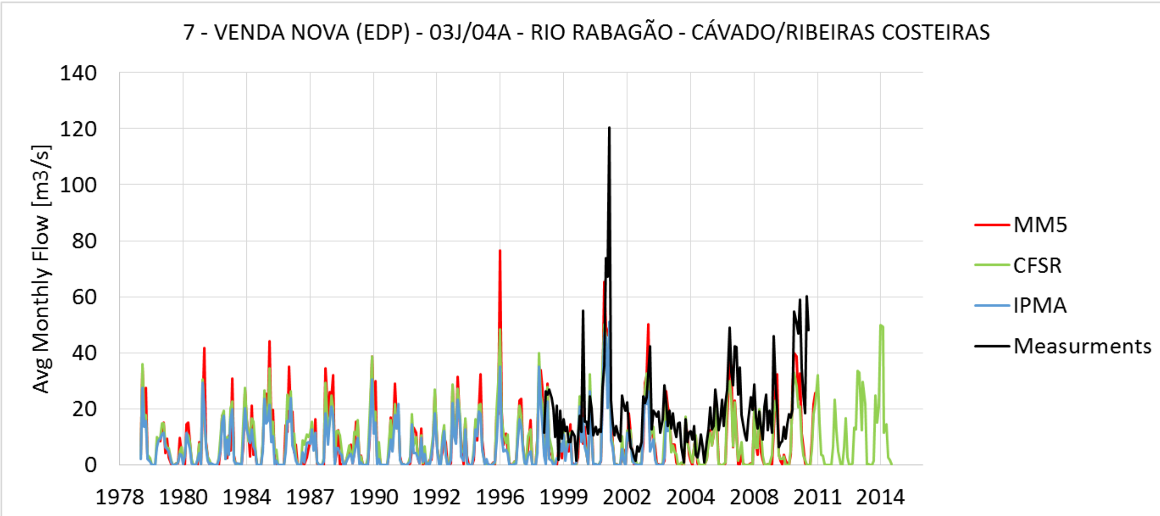
7 - VENDA NOVA (EDP) - 03J/04A - RIO RABAGÃO - CÁVADO/RIBEIRAS COSTEIRAS
Avg Monthly Flow [m3/s]
140
120
100
80
60
40
20
0
1978
1980
1984
1987
1990
1992
1996
1999
2002
2004
2008
2011
2014
MM5
CFSR
IPMA
Measurments

8.4.4 DOURO

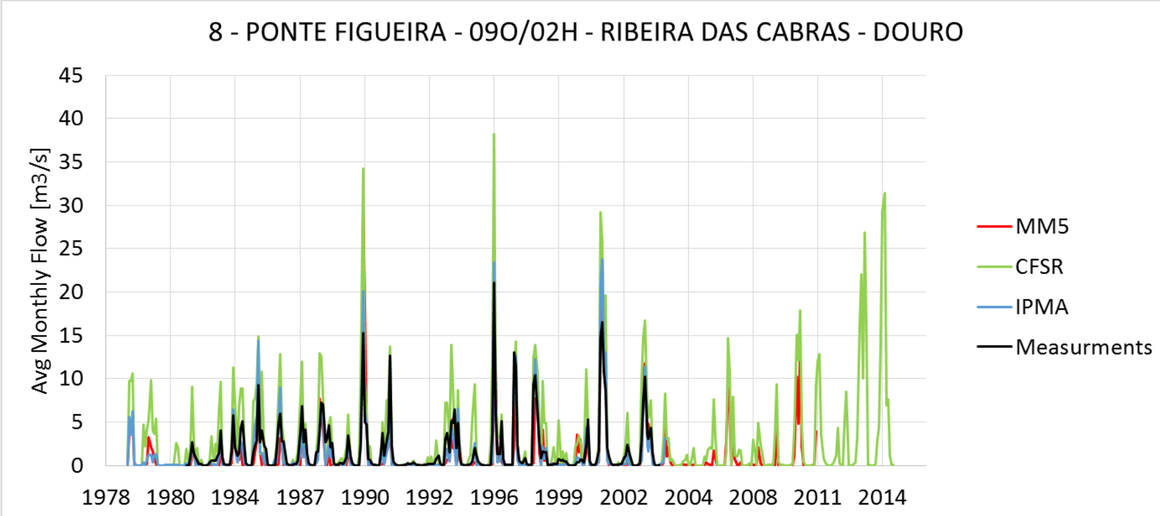
8 - PONTE FIGUEIRA - 09O/02H - RIBEIRA DAS CABRAS - DOURO
Avg Monthly Flow [m3/s]
MM5
CFSR
IPMA
Measurments

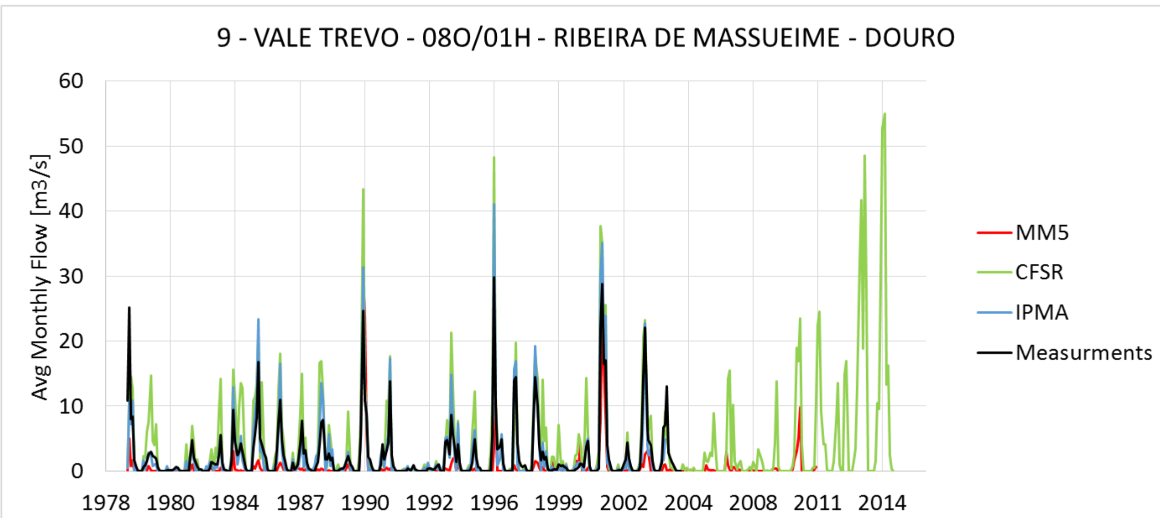
9 - VALE TREVO - 08O/01H - RIBEIRA DE MASSUEIME - DOURO
Avg Monthly Flow [m3/s]
MM5
CFSR
IPMA
Measurments

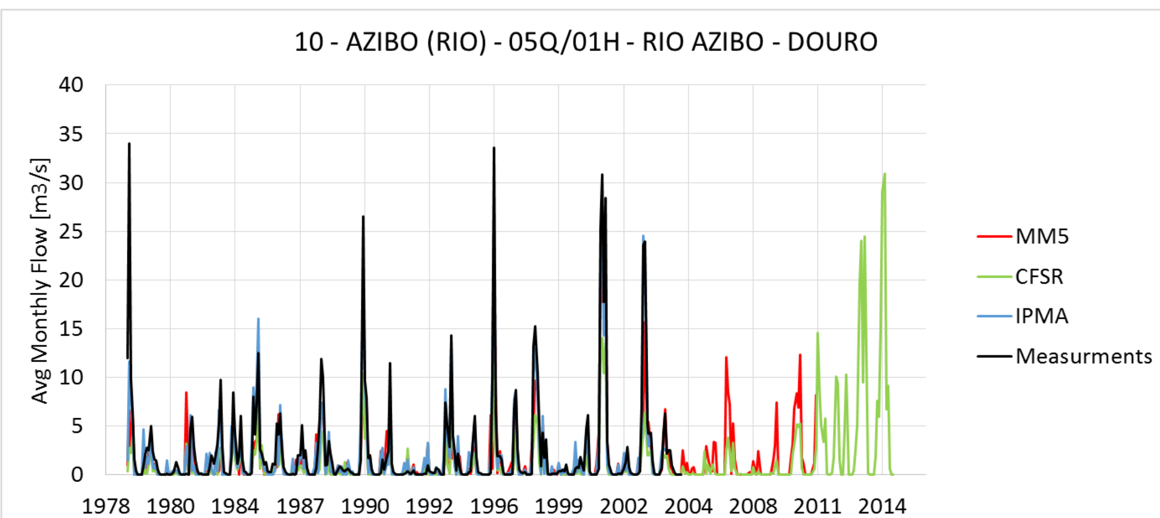
10 - AZIBO (RIO) - 05Q/01H - RIO AZIBO - DOURO
Avg Monthly Flow [m3/s]
MM5
CFSR
IPMA
Measurments

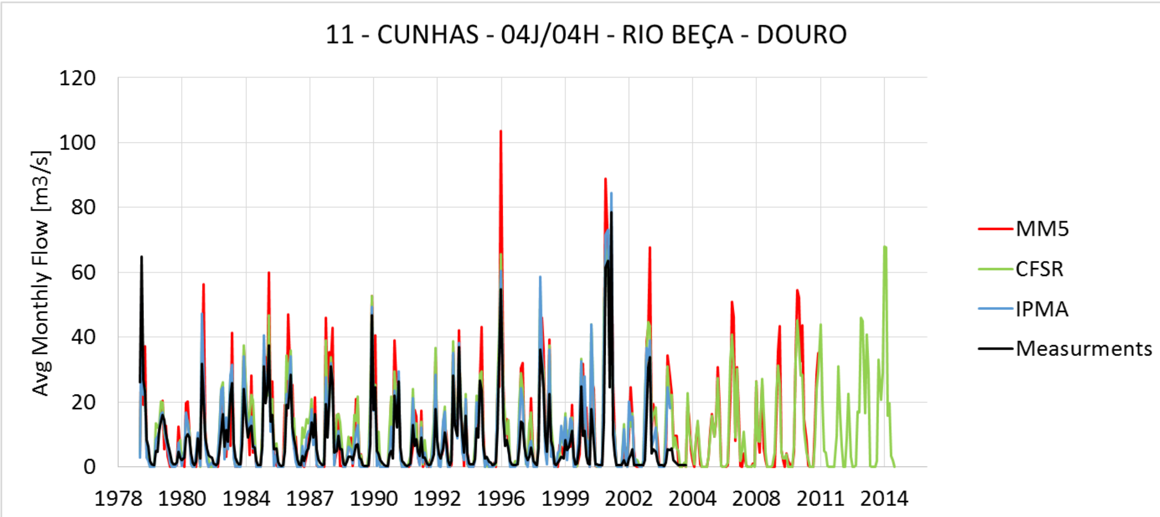
11 - CUNHAS - 04J/04H - RIO BEÇA - DOURO
Avg Monthly Flow [m3/s]
0
20
40
60
80
100
120
1978
1980
1984
1987
1990
1992
1996
1999
2002
2004
2008
2011
2014
MM5
CFSR
IPMA
Measurments

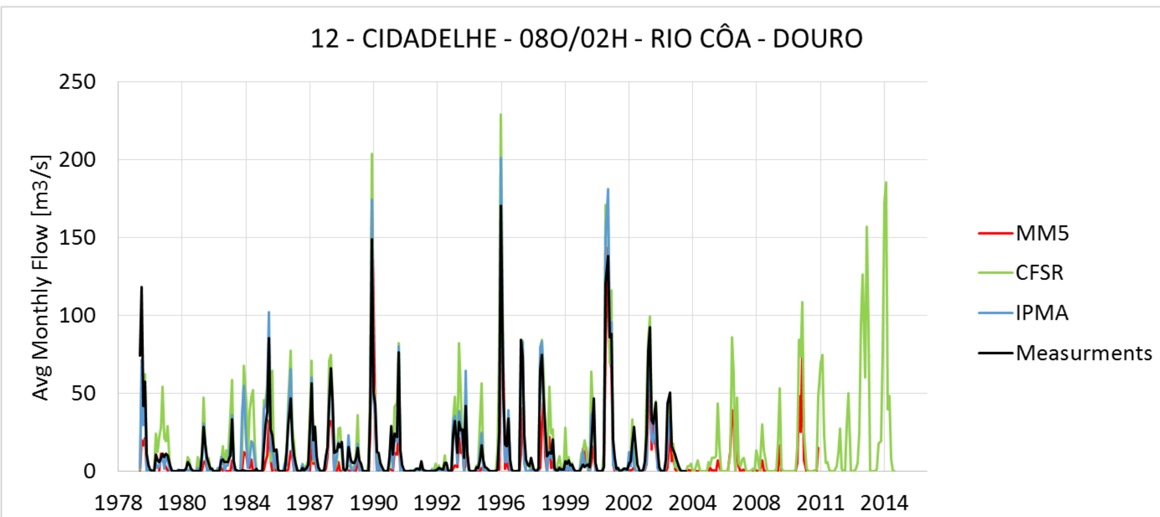
12 - CIDADELHE - 08O/02H - RIO CÔA - DOURO
Avg Monthly Flow [m3/s]
0
50
100
150
200
250
1978
1980
1984
1987
1990
1992
1996
1999
2002
2004
2008
2011
2014
MM5
CFSR
IPMA
Measurments

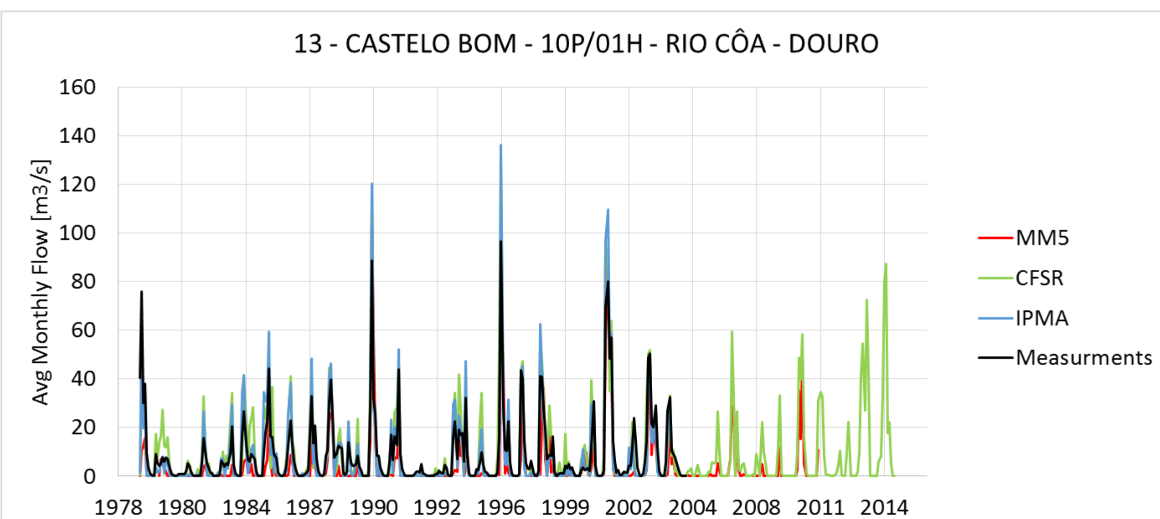
13 - CASTELO BOM - 10P/01H - RIO CÔA - DOURO
Avg Monthly Flow [m3/s]
0
20
40
60
80
100
120
140
160
1978
1980
1984
1987
1990
1992
1996
1999
2002
2004
2008
2011
2014
MM5
CFSR
IPMA
Measurments

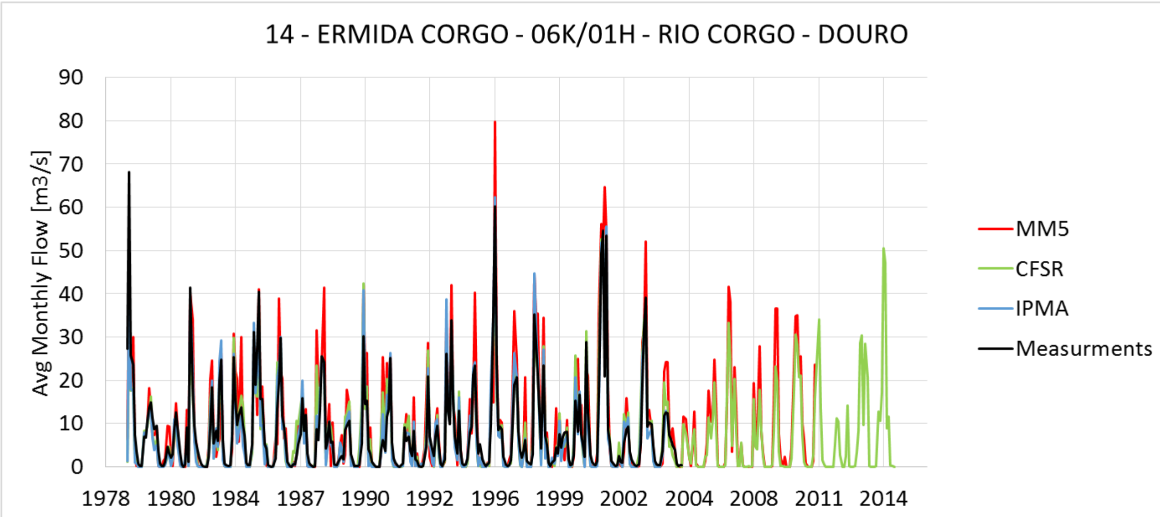
14 - ERMIDA CORGO - 06K/01H - RIO CORGO - DOURO
Avg Monthly Flow [m3/s]
0
10
20
30
40
50
60
70
80
90
1978
1980
1984
1987
1990
1992
1996
1999
2002
2004
2008
2011
2014
MM5
CFSR
IPMA
Measurments

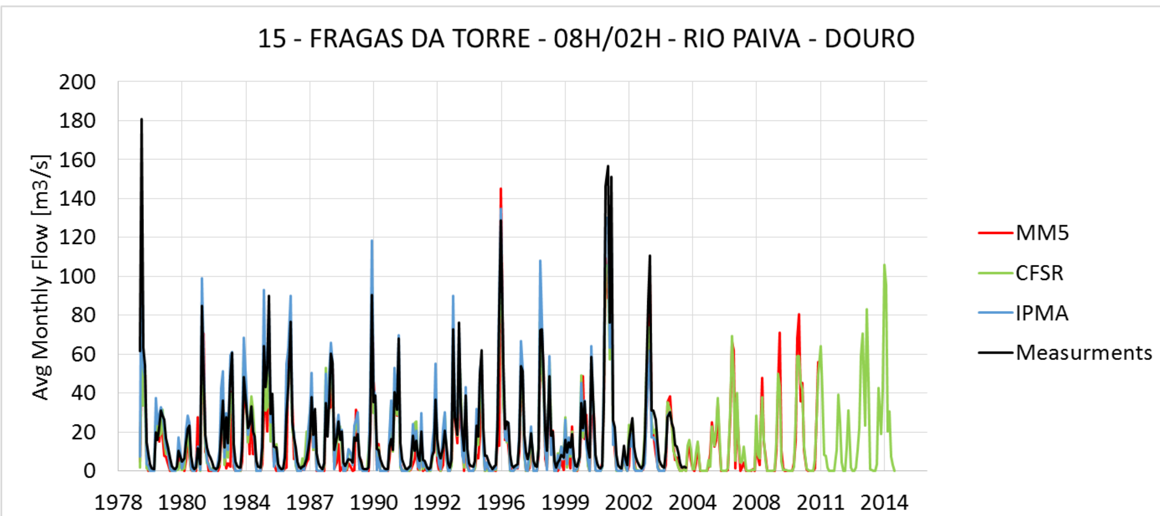
15 - FRAGAS DA TORRE - 08H/02H - RIO PAIVA - DOURO
Avg Monthly Flow [m3/s]
0
20
40
60
80
100
120
140
160
180
200
1978
1980
1984
1987
1990
1992
1996
1999
2002
2004
2008
2011
2014
MM5
CFSR
IPMA
Measurments

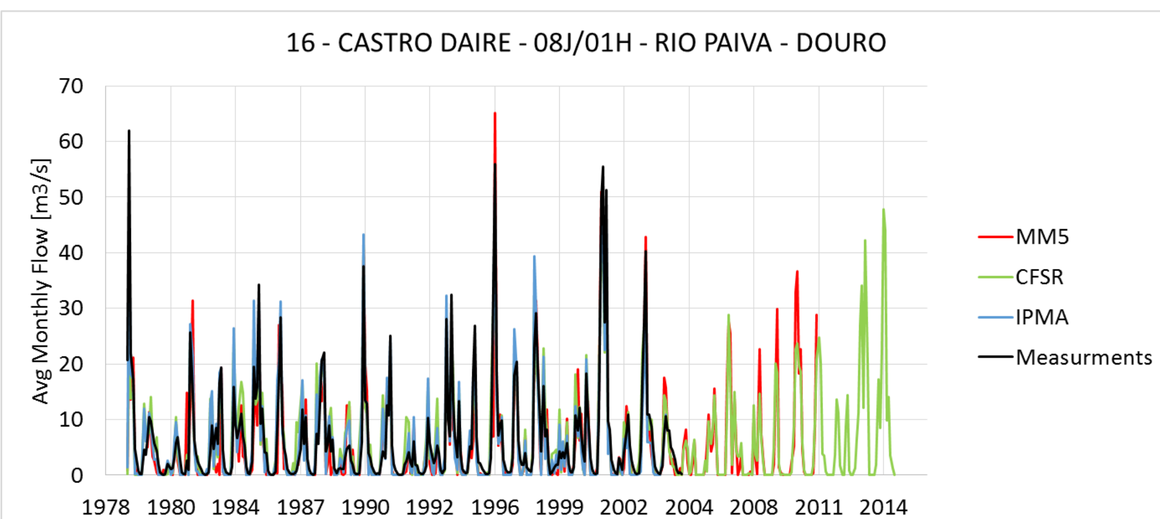
16 - CASTRO DAIRE - 08J/01H - RIO PAIVA - DOURO
Avg Monthly Flow [m3/s]
0
10
20
30
40
50
60
70
1978
1980
1984
1987
1990
1992
1996
1999
2002
2004
2008
2011
2014
MM5
CFSR
IPMA
Measurments

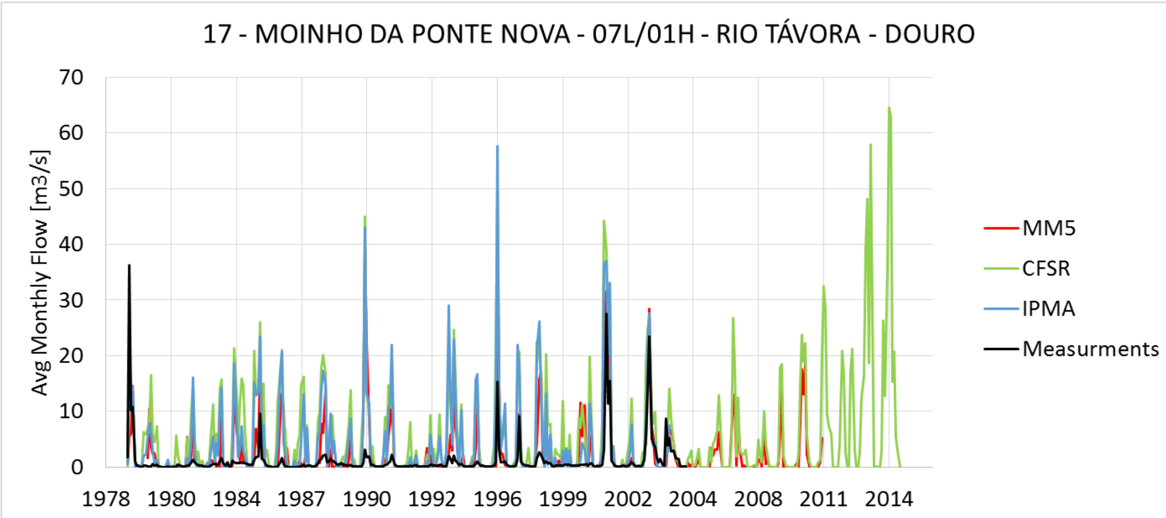
17 - MOINHO DA PONTE NOVA - 07L/01H - RIO TÁVORA - DOURO
Avg Monthly Flow [m3/s]
0
10
20
30
40
50
60
70
1978
1980
1984
1987
1990
1992
1996
1999
2002
2004
2008
2011
2014
MM5
CFSR
IPMA
Measurments

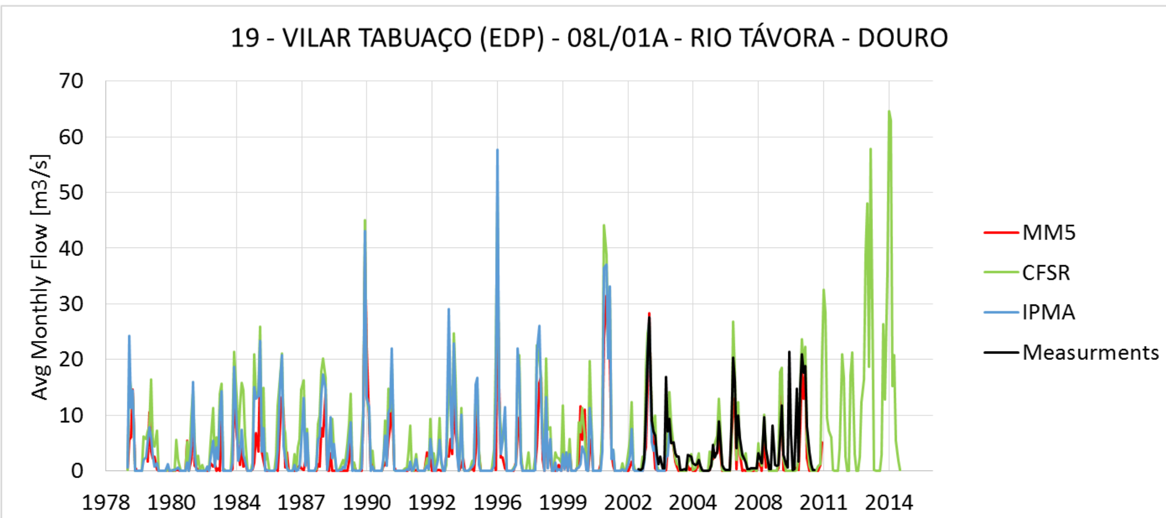
19 - VILAR TABUAÇO (EDP) - 08L/01A - RIO TÁVORA - DOURO
Avg Monthly Flow [m3/s]
0
10
20
30
40
50
60
70
1978
1980
1984
1987
1990
1992
1996
1999
2002
2004
2008
2011
2014
MM5
CFSR
IPMA
Measurments

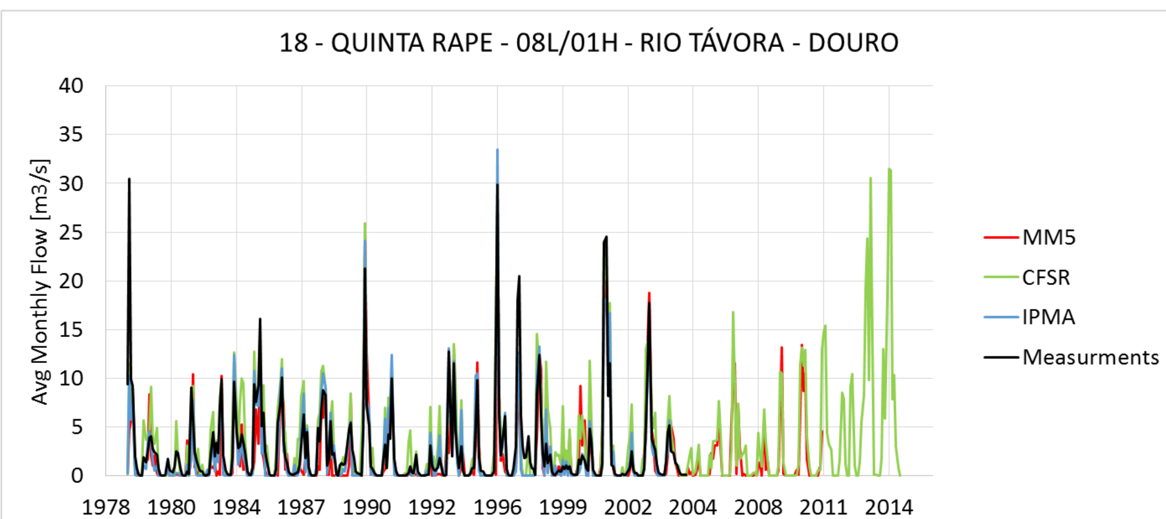
18 - QUINTA RAPE - 08L/01H - RIO TÁVORA - DOURO
Avg Monthly Flow [m3/s]
0
5
10
15
20
25
30
35
40
1978
1980
1984
1987
1990
1992
1996
1999
2002
2004
2008
2011
2014
MM5
CFSR
IPMA
Measurments

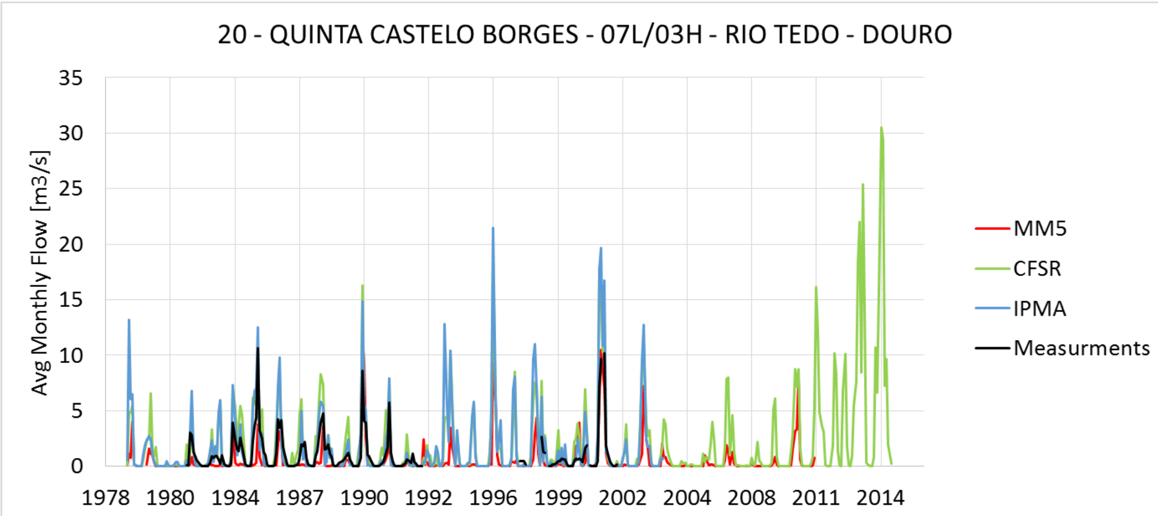
20 - QUINTA CASTELO BORGES - 07L/03H - RIO TEDO - DOURO
Avg Monthly Flow [m3/s]
0
5
10
15
20
25
30
35
1978
1980
1984
1987
1990
1992
1996
1999
2002
2004
2008
2011
2014
MM5
CFSR
IPMA
Measurments

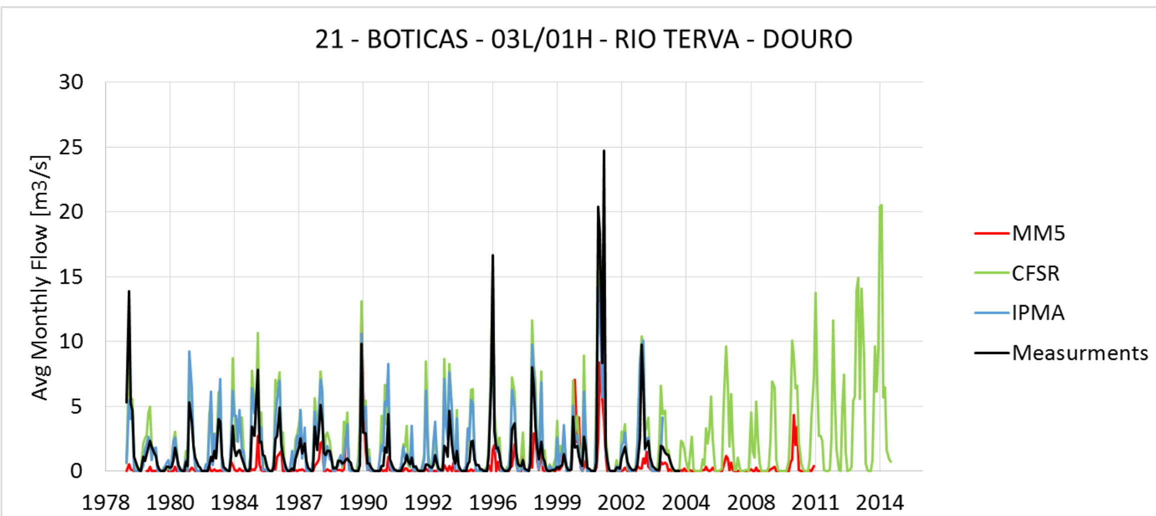
21 - BOTICAS - 03L/01H - RIO TERVA - DOURO
Avg Monthly Flow [m3/s]
0
5
10
15
20
25
30
1978
1980
1984
1987
1990
1992
1996
1999
2002
2004
2008
2011
2014
MM5
CFSR
IPMA
Measurments

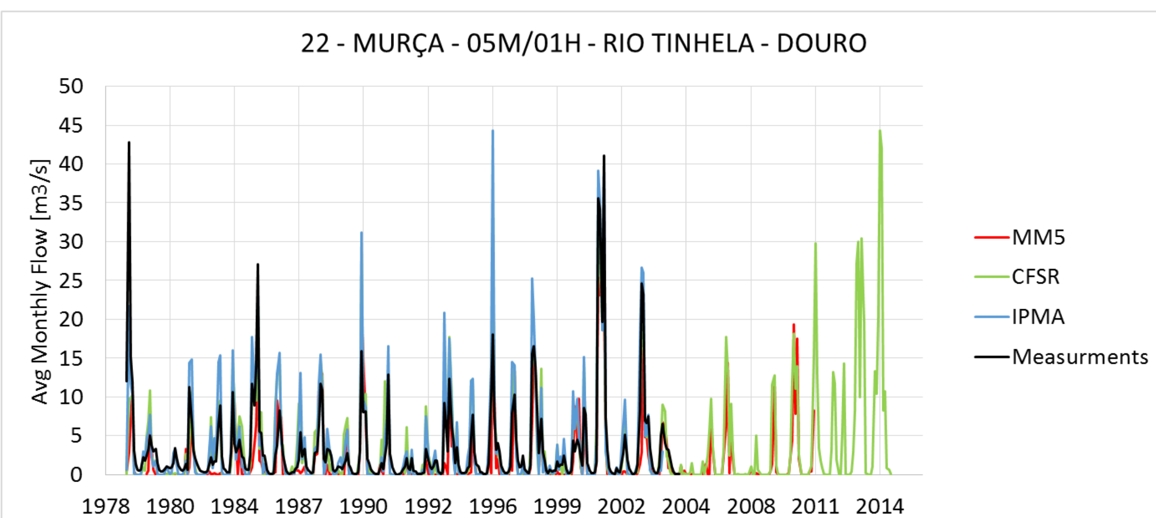
22 - MURÇA - 05M/01H - RIO TINHELA - DOURO
Avg Monthly Flow [m3/s]
0
5
10
15
20
25
30
35
40
45
50
1978
1980
1984
1987
1990
1992
1996
1999
2002
2004
2008
2011
2014
MM5
CFSR
IPMA
Measurments

8.4.5 GUADIANA

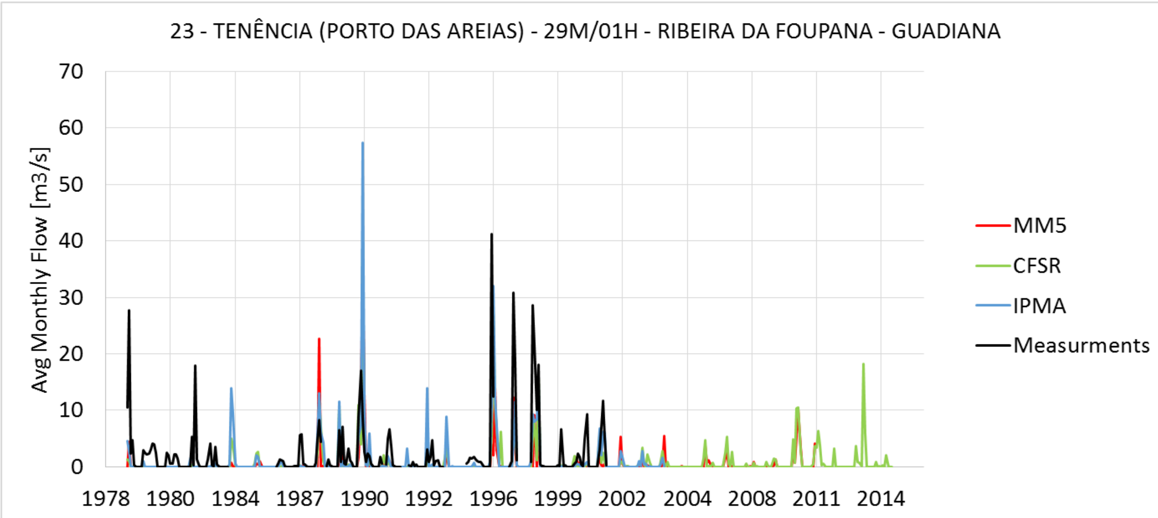

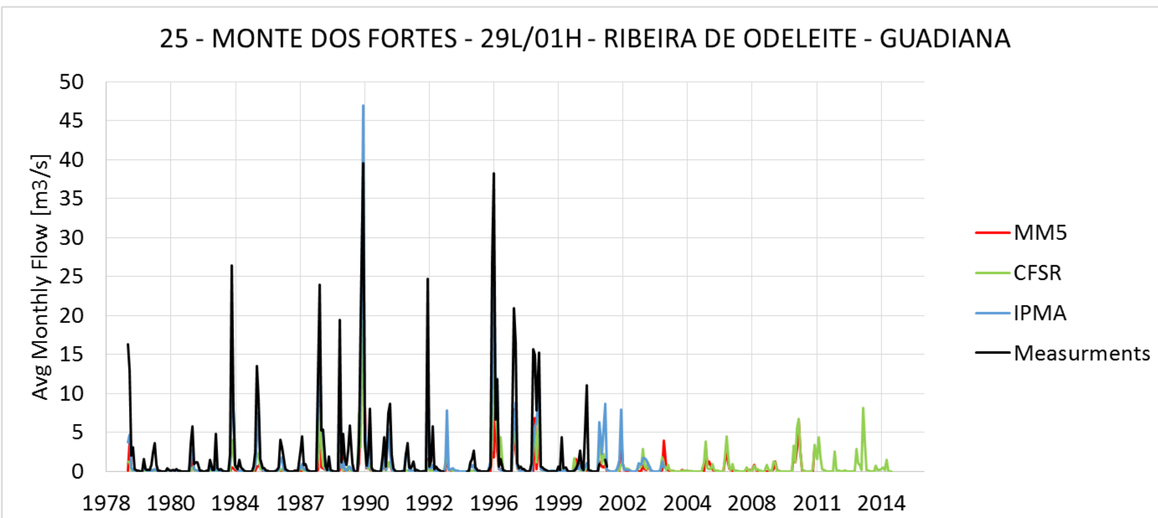

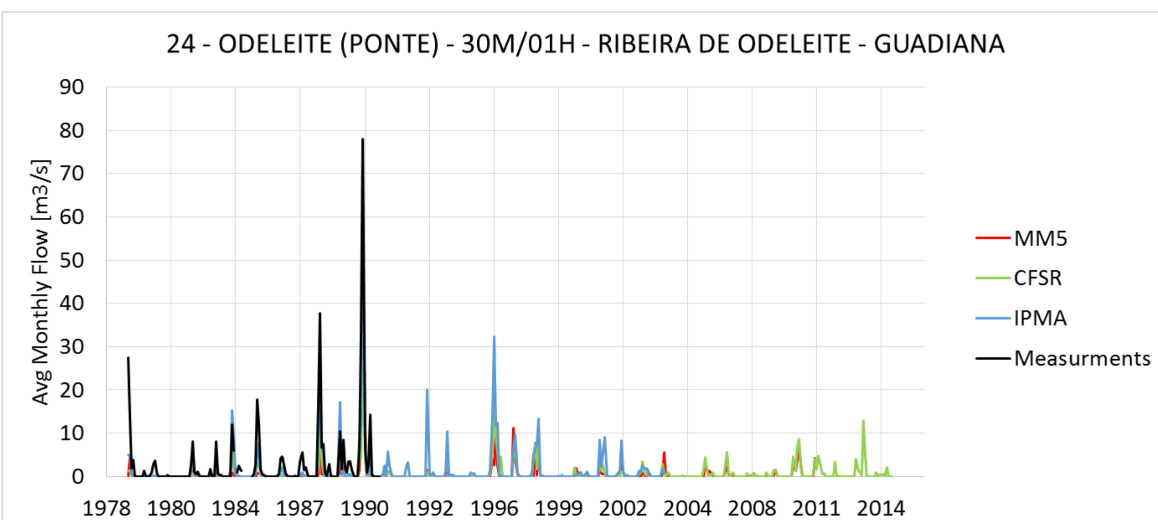

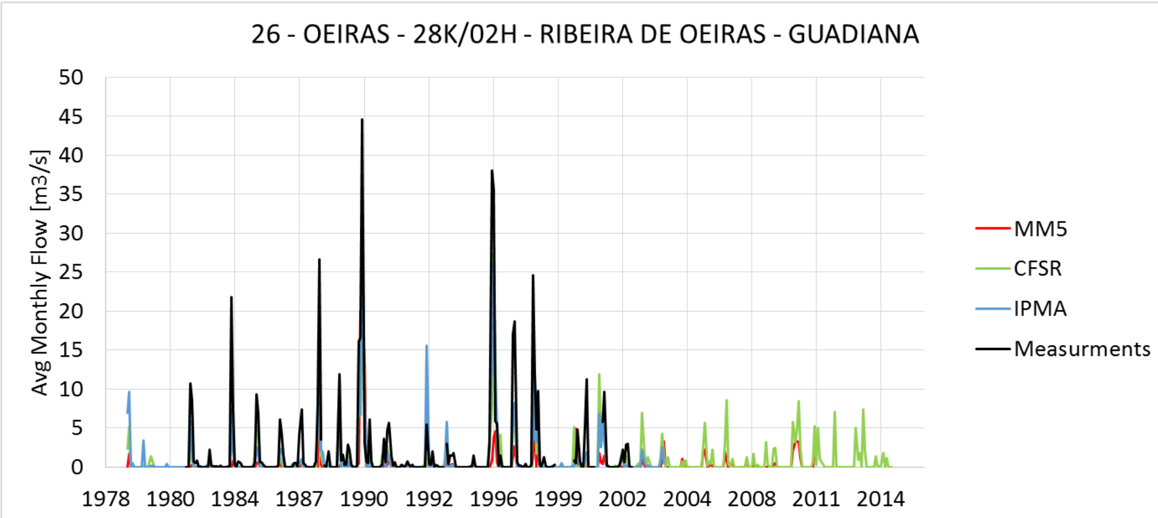
26 - OEIRAS - 28K/02H - RIBEIRA DE OEIRAS - GUADIANA
Avg Monthly Flow [m3/s]
0
5
10
15
20
25
30
35
40
45
50
1978
1980
1984
1987
1990
1992
1996
1999
2002
2004
2008
2011
2014
MM5
CFSR
IPMA
Measurments

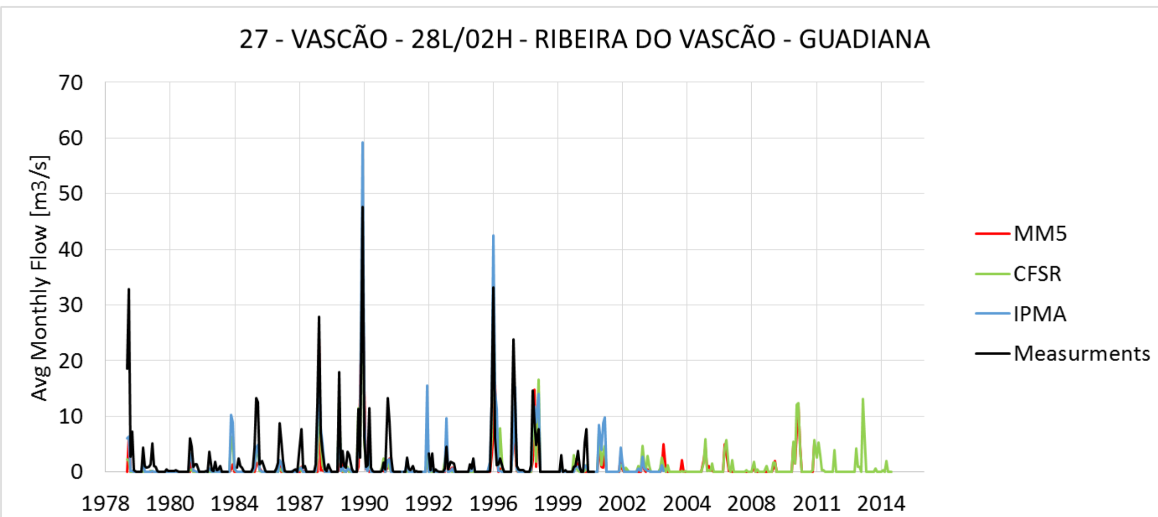
27 - VASCÃO - 28L/02H - RIBEIRA DO VASCÃO - GUADIANA
Avg Monthly Flow [m3/s]
0
10
20
30
40
50
60
70
1978
1980
1984
1987
1990
1992
1996
1999
2002
2004
2008
2011
2014
MM5
CFSR
IPMA
Measurments

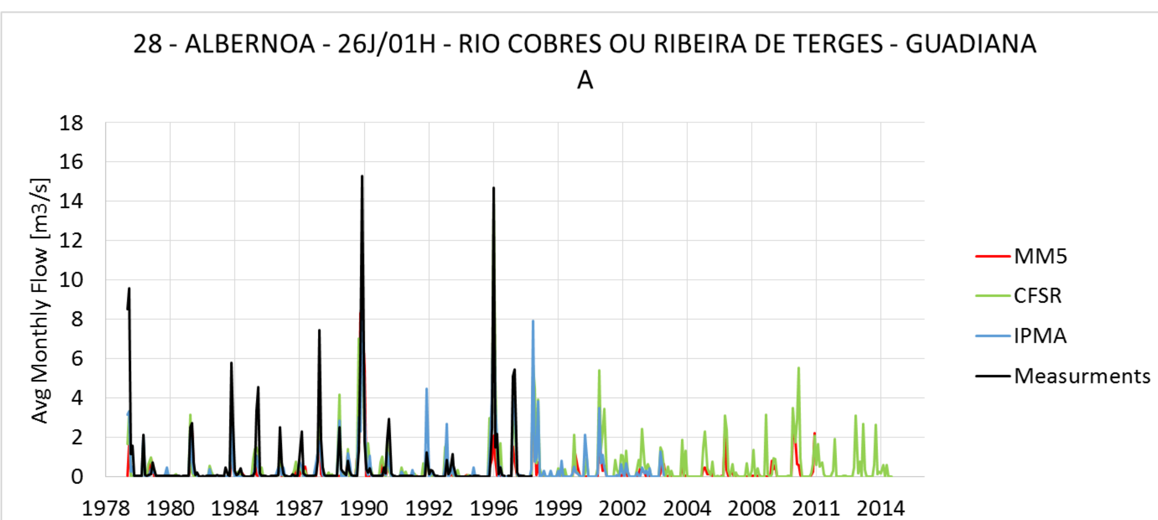
28 - ALBERNOA - 26J/01H - RIO COBRES OU RIBEIRA DE TERGES - GUADIANA
A
Avg Monthly Flow [m3/s]
0
2
4
6
8
10
12
14
16
18
1978
1980
1984
1987
1990
1992
1996
1999
2002
2004
2008
2011
2014
MM5
CFSR
IPMA
Measurments

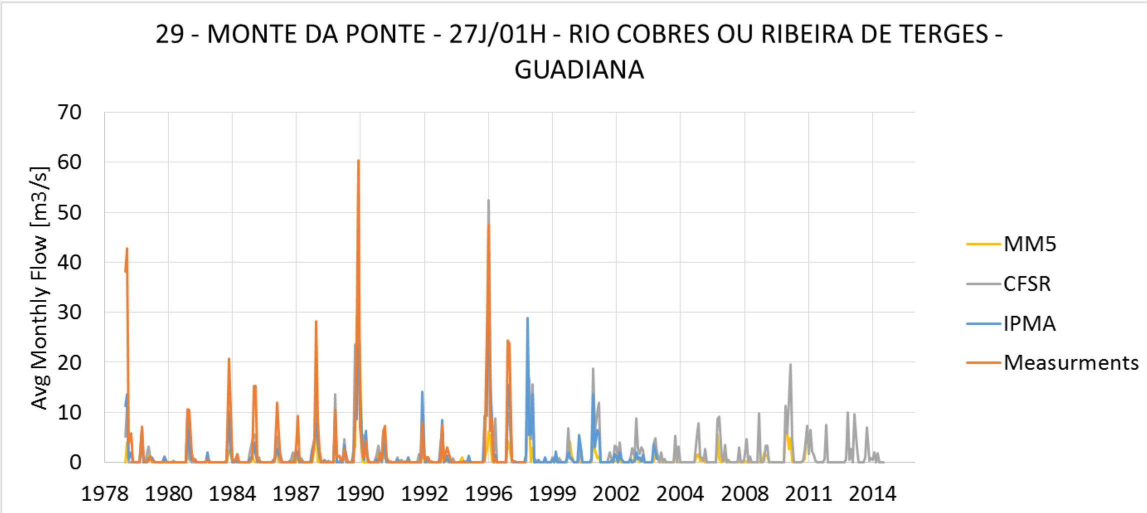
29 - MONTE DA PONTE - 27J/01H - RIO COBRES OU RIBEIRA DE TERGES - GUADIANA
Avg Monthly Flow [m3/s]
0
10
20
30
40
50
60
70
1978
1980
1984
1987
1990
1992
1996
1999
2002
2004
2008
2011
2014
MM5
CFSR
IPMA
Measurments

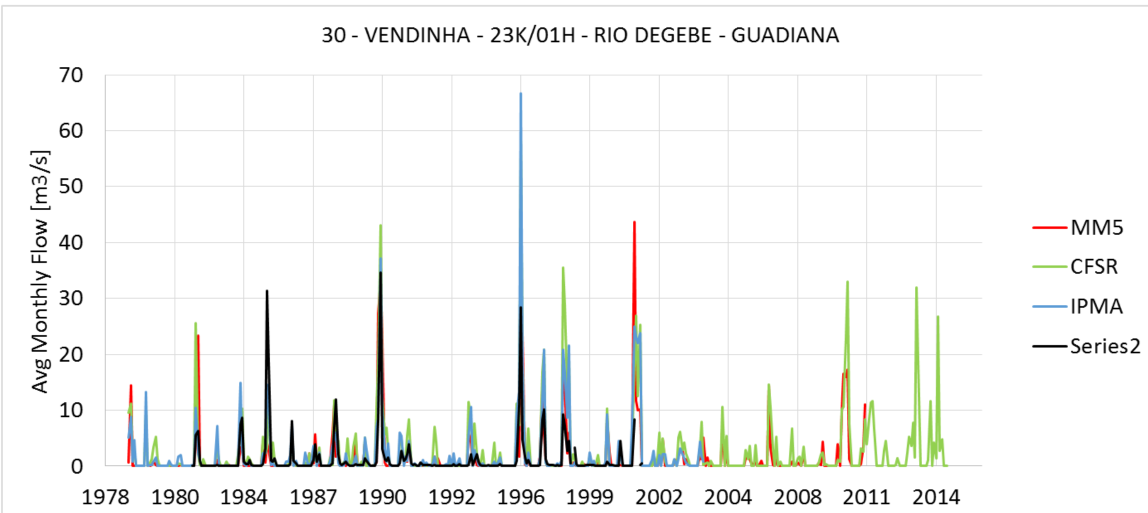
30 - VENDINHA - 23K/01H - RIO DEGEBE - GUADIANA
Avg Monthly Flow [m3/s]
0
10
20
30
40
50
60
70
1978
1980
1984
1987
1990
1992
1996
1999
2002
2004
2008
2011
2014
MM5
CFSR
IPMA
Series2

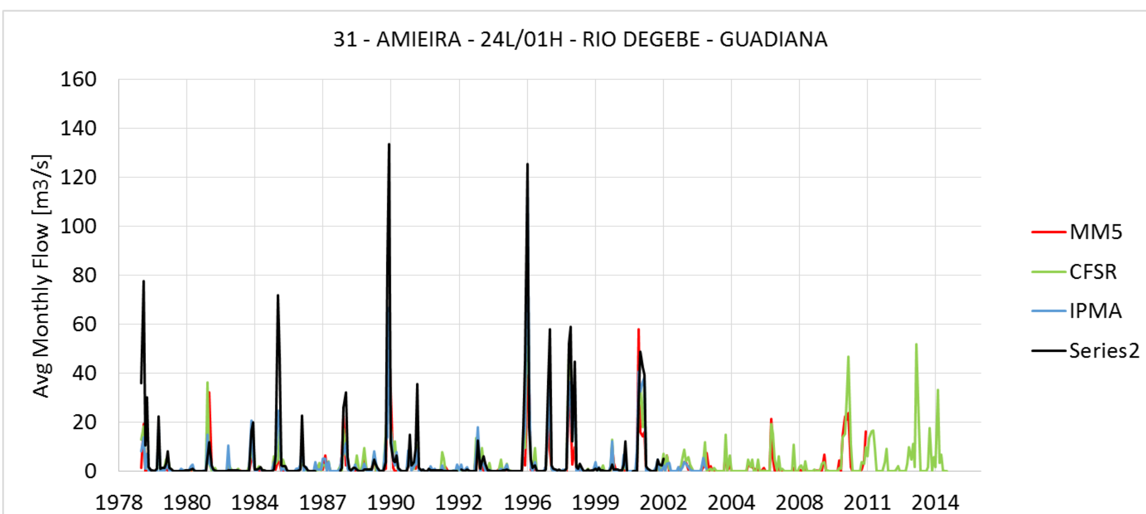
31 - AMIEIRA - 24L/01H - RIO DEGEBE - GUADIANA
Avg Monthly Flow [m3/s]
0
20
40
60
80
100
120
140
160
1978
1980
1984
1987
1990
1992
1996
1999
2002
2004
2008
2011
2014
MM5
CFSR
IPMA
Series2

8.4.6 LIMA

8.4.7 MONDEGO

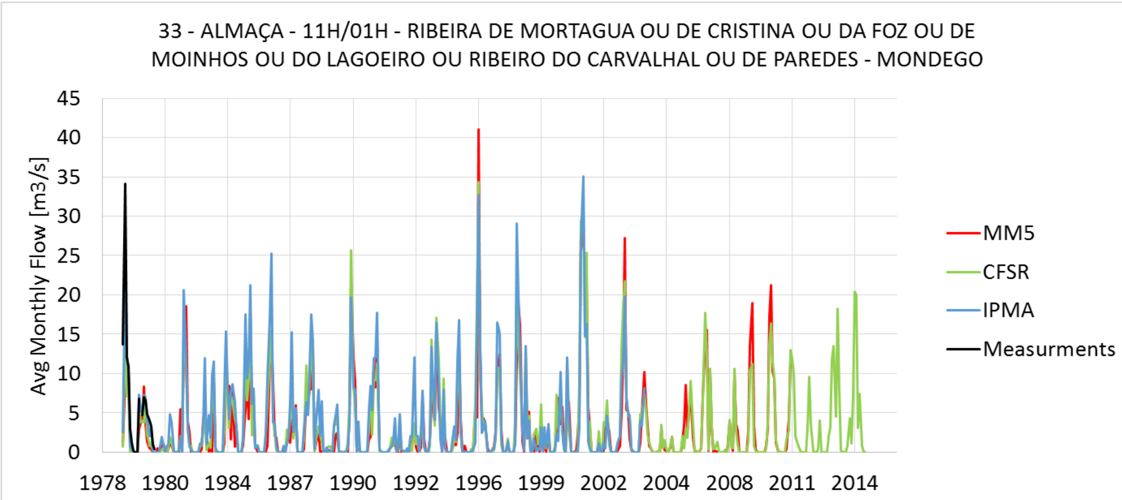

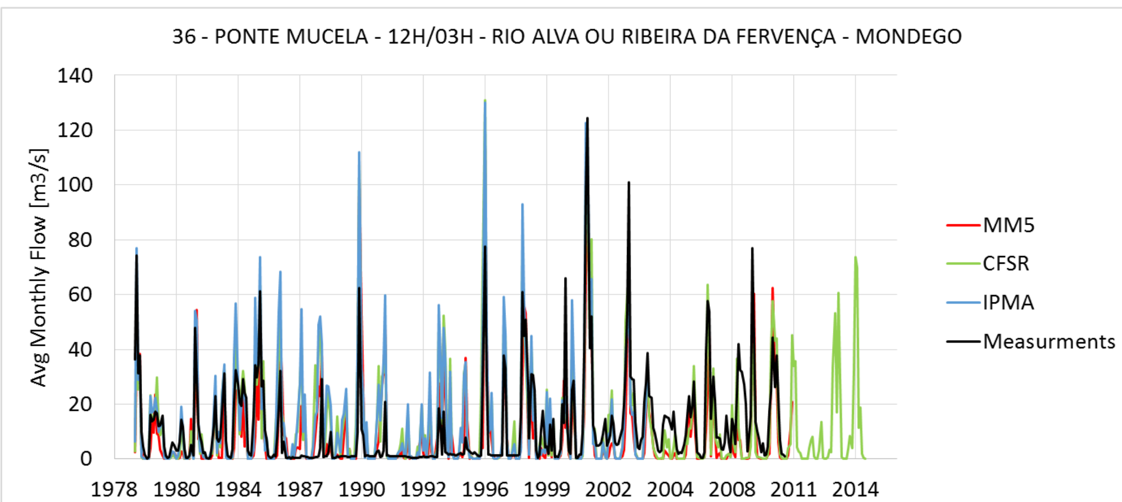

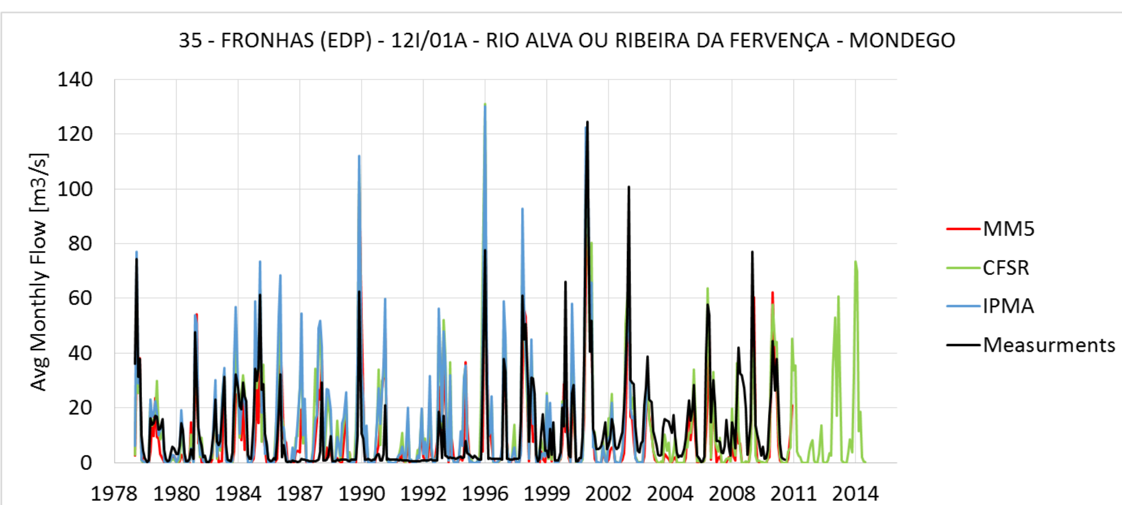

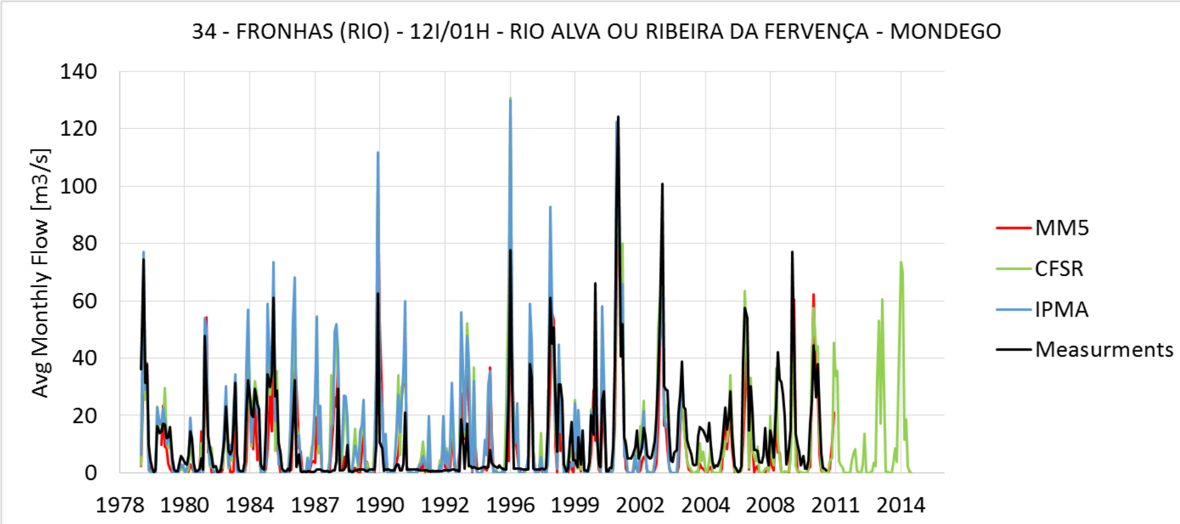
34 - FRONHAS (RIO) - 12I/01H - RIO ALVA OU RIBEIRA DA FERVENÇA - MONDEGO
Avg Monthly Flow [m3/s]
0
20
40
60
80
100
120
140
1978
1980
1984
1987
1990
1992
1996
1999
2002
2004
2008
2011
2014
MM5
CFSR
IPMA
Measurments

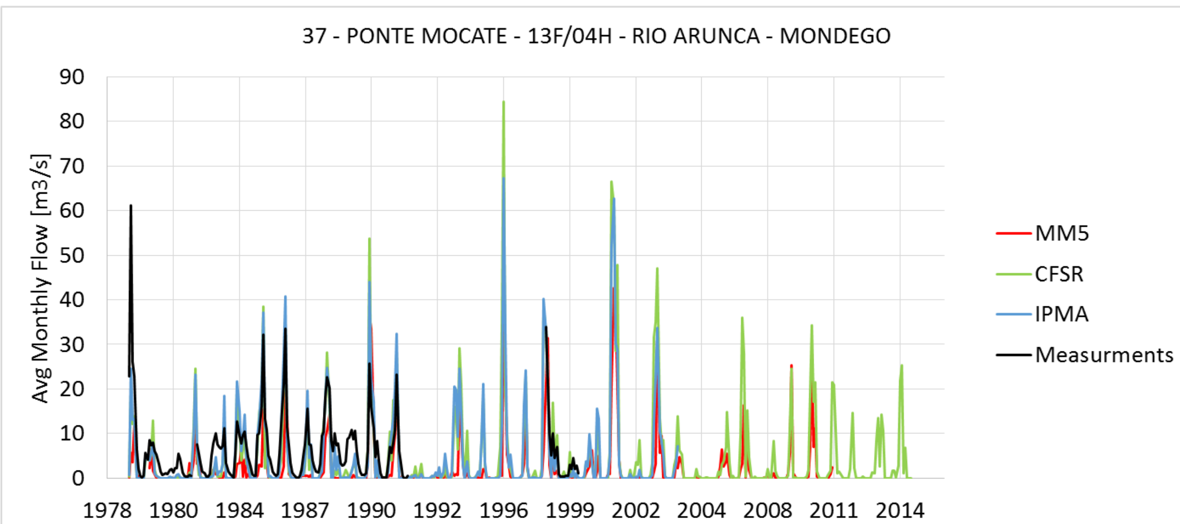
37 - PONTE MOCATE - 13F/04H - RIO ARUNCA - MONDEGO
Avg Monthly Flow [m3/s]
0
10
20
30
40
50
60
70
80
90
1978
1980
1984
1987
1990
1992
1996
1999
2002
2004
2008
2011
2014
MM5
CFSR
IPMA
Measurments

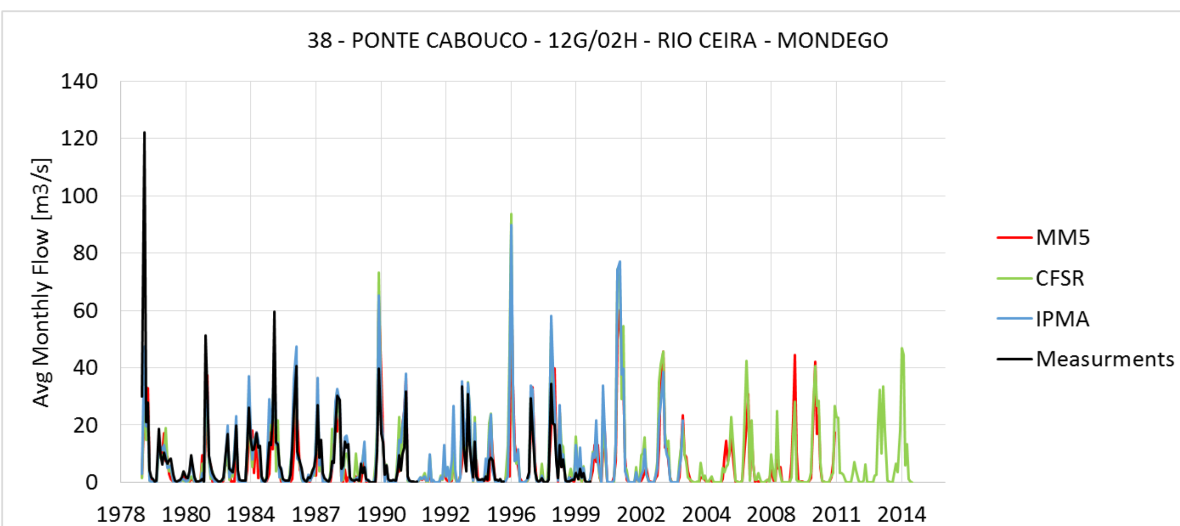
38 - PONTE CABOUCO - 12G/02H - RIO CEIRA - MONDEGO
Avg Monthly Flow [m3/s]
0
20
40
60
80
100
120
140
1978
1980
1984
1987
1990
1992
1996
1999
2002
2004
2008
2011
2014
MM5
CFSR
IPMA
Measurments

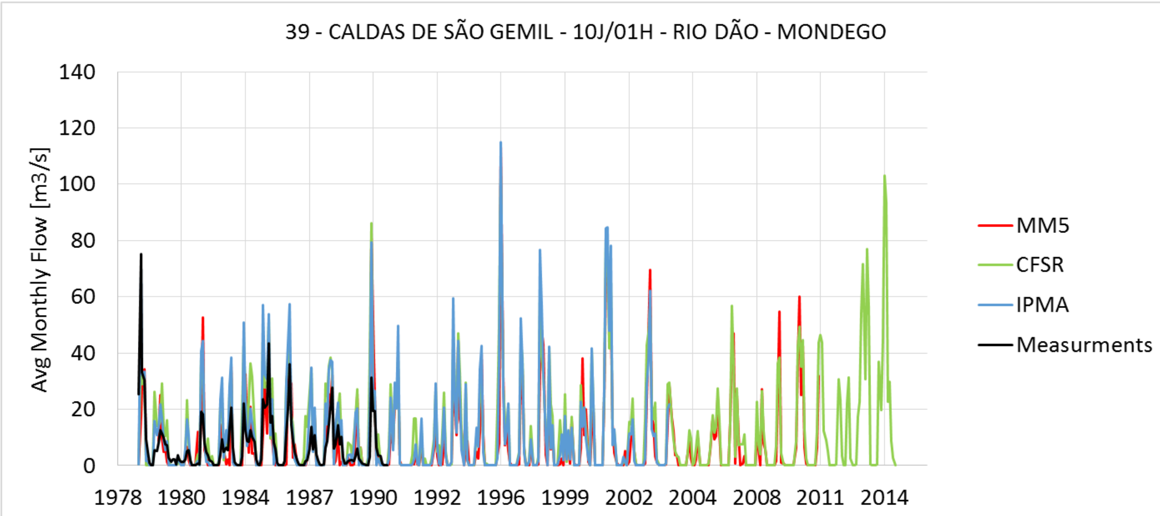
39 - CALDAS DE SÃO GEMIL - 10J/01H - RIO DÃO - MONDEGO
Avg Monthly Flow [m3/s]
0
20
40
60
80
100
120
140
1978
1980
1984
1987
1990
1992
1996
1999
2002
2004
2008
2011
2014
MM5
CFSR
IPMA
Measurments

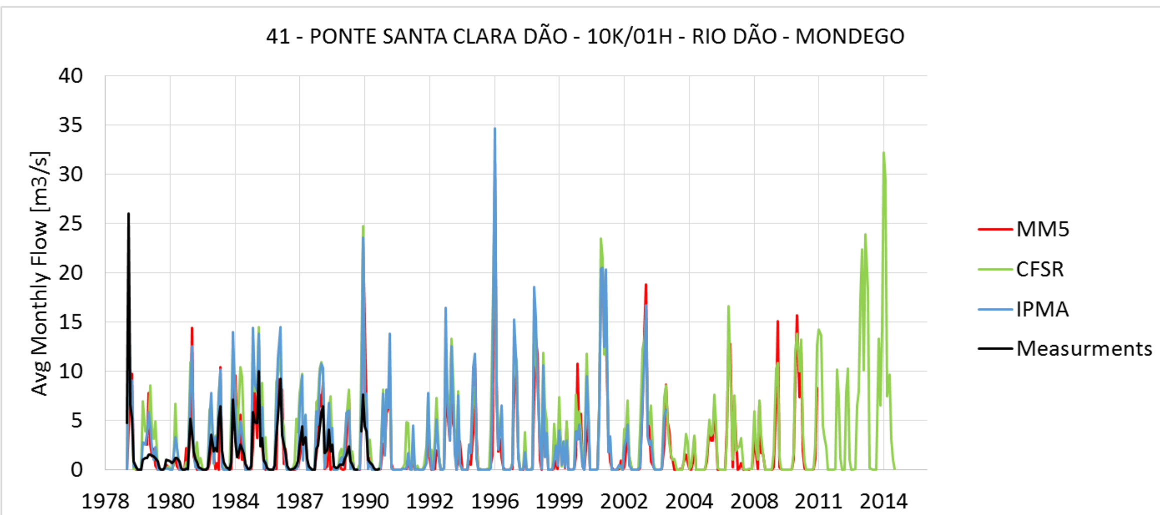
41 - PONTE SANTA CLARA DÃO - 10K/01H - RIO DÃO - MONDEGO
Avg Monthly Flow [m3/s]
0
5
10
15
20
25
30
35
40
1978
1980
1984
1987
1990
1992
1996
1999
2002
2004
2008
2011
2014
MM5
CFSR
IPMA
Measurments

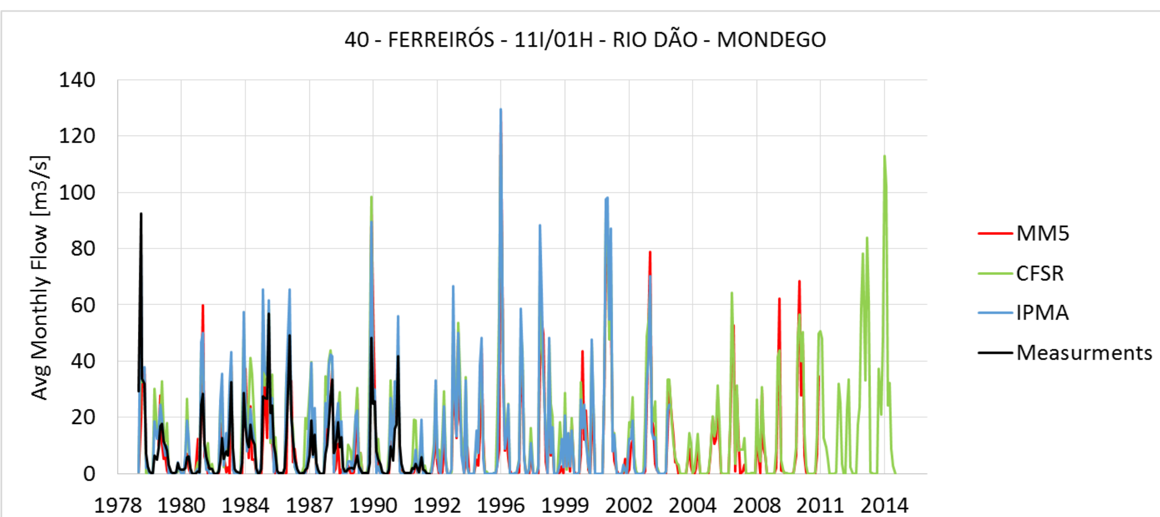
40 - FERREIRÓS - 11I/01H - RIO DÃO - MONDEGO
Avg Monthly Flow [m3/s]
0
20
40
60
80
100
120
140
1978
1980
1984
1987
1990
1992
1996
1999
2002
2004
2008
2011
2014
MM5
CFSR
IPMA
Measurments

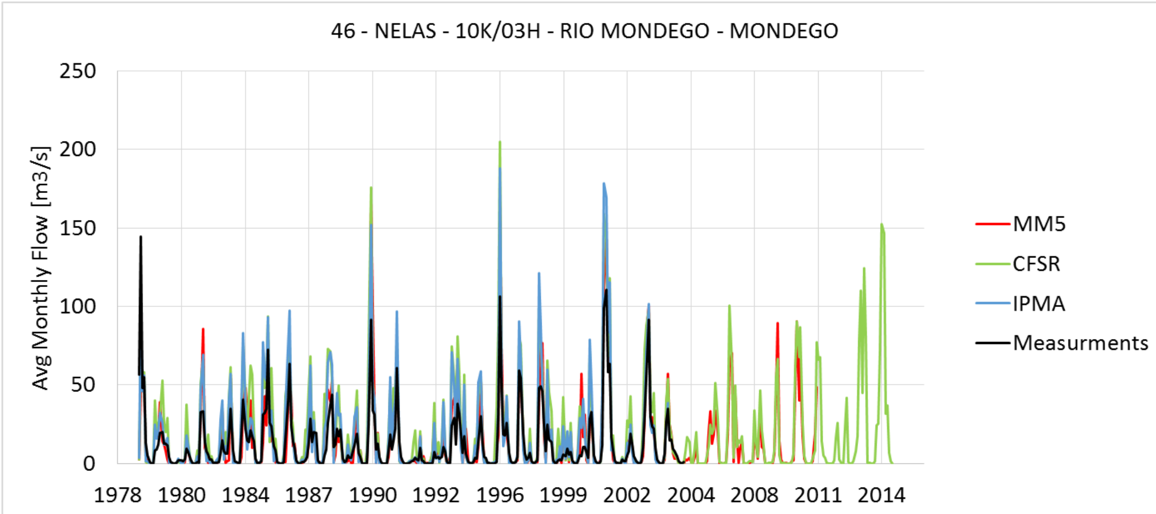
46 - NELAS - 10K/03H - RIO MONDEGO - MONDEGO
Avg Monthly Flow [m3/s]
250
200
150
100
50
0
1978 1980 1984 1987 1990 1992 1996 1999 2002 2004 2008 2011 2014
MM5
CFSR
IPMA
Measurments

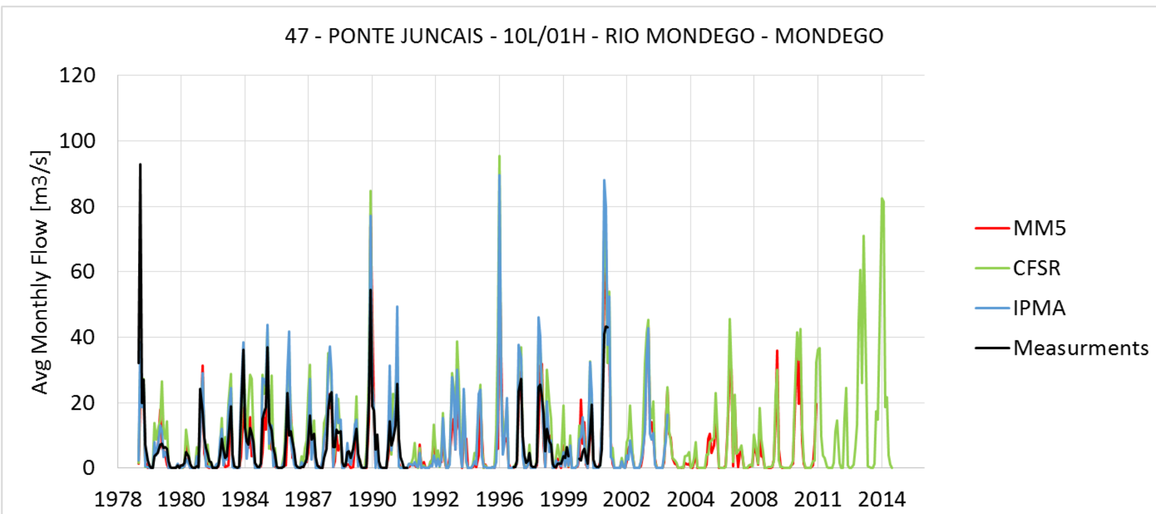
47 - PONTE JUNCAIS - 10L/01H - RIO MONDEGO - MONDEGO
Avg Monthly Flow [m3/s]
120
100
80
60
40
20
0
1978 1980 1984 1987 1990 1992 1996 1999 2002 2004 2008 2011 2014
MM5
CFSR
IPMA
Measurments

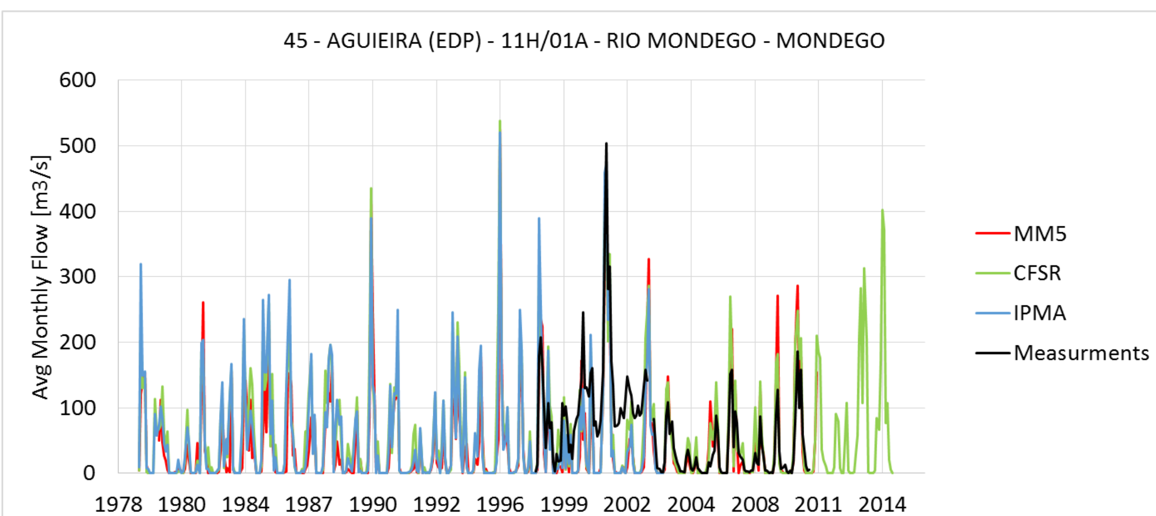
45 - AGUIEIRA (EDP) - 11H/01A - RIO MONDEGO - MONDEGO
Avg Monthly Flow [m3/s]
600
500
400
300
200
100
0
1978 1980 1984 1987 1990 1992 1996 1999 2002 2004 2008 2011 2014
MM5
CFSR
IPMA
Measurments

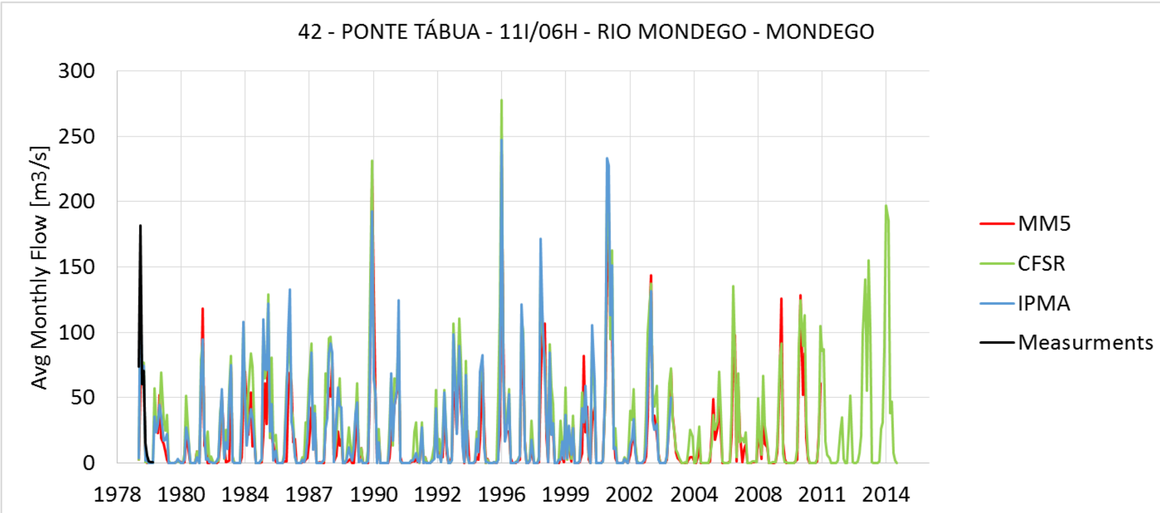
42 - PONTE TÁBUA - 11I/06H - RIO MONDEGO - MONDEGO
Avg Monthly Flow [m3/s]
300
250
200
150
100
50
0
1978 1980 1984 1987 1990 1992 1996 1999 2002 2004 2008 2011 2014
MM5
CFSR
IPMA
Measurments

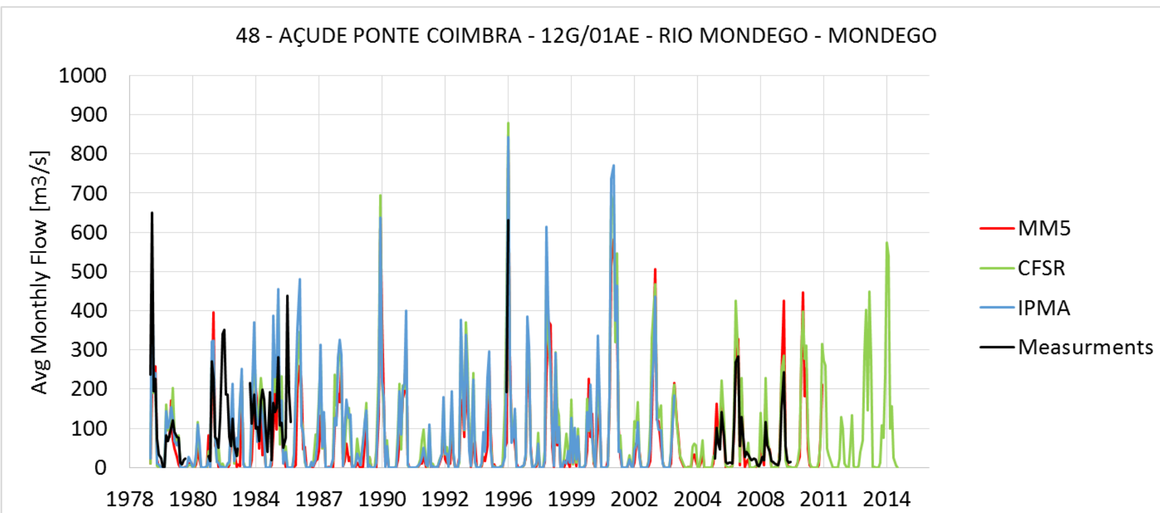
48 - AÇUDE PONTE COIMBRA - 12G/01AE - RIO MONDEGO - MONDEGO
Avg Monthly Flow [m3/s]
1000
900
800
700
600
500
400
300
200
100
0
1978 1980 1984 1987 1990 1992 1996 1999 2002 2004 2008 2011 2014
MM5
CFSR
IPMA
Measurments

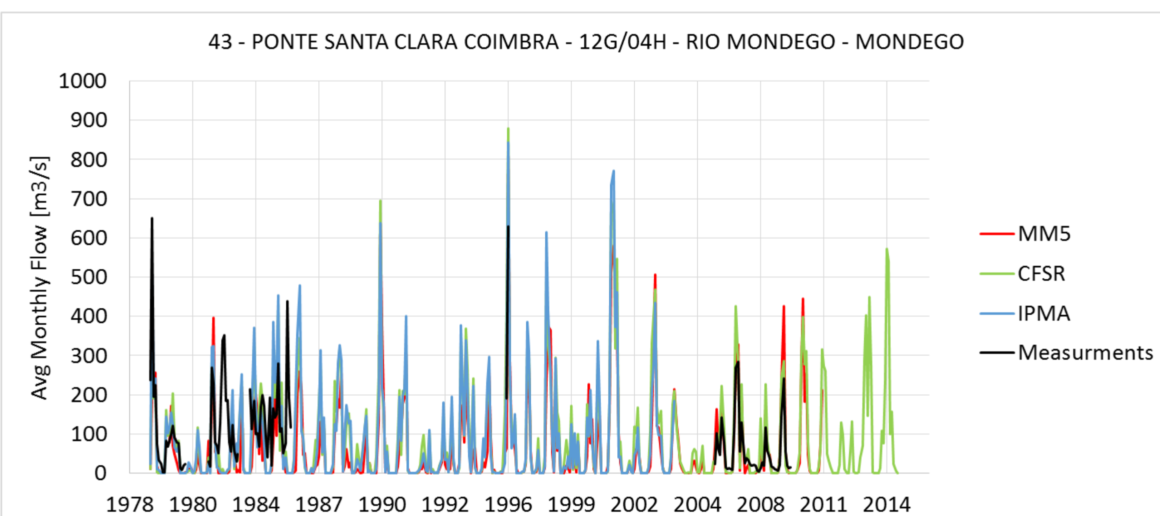
43 - PONTE SANTA CLARA COIMBRA - 12G/04H - RIO MONDEGO - MONDEGO
Avg Monthly Flow [m3/s]
1000
900
800
700
600
500
400
300
200
100
0
1978 1980 1984 1987 1990 1992 1996 1999 2002 2004 2008 2011 2014
MM5
CFSR
IPMA
Measurments

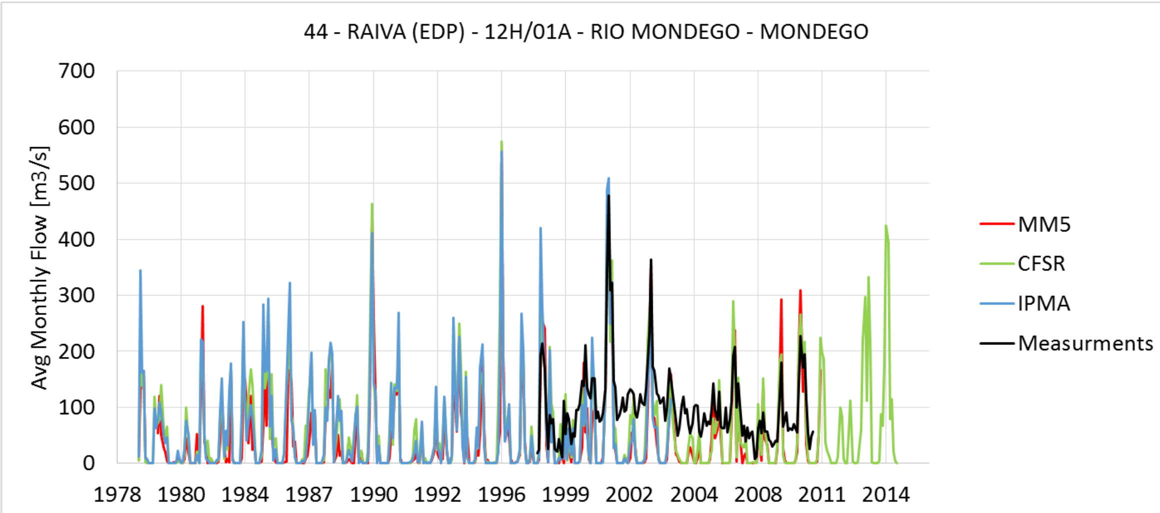

8.4.8 RIBEIRAS DO ALGARVE

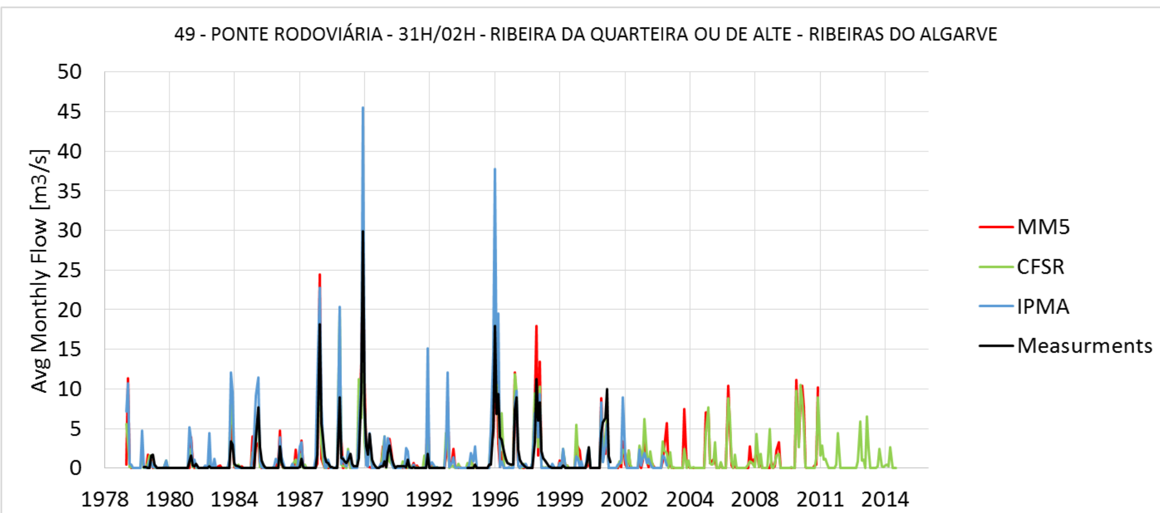

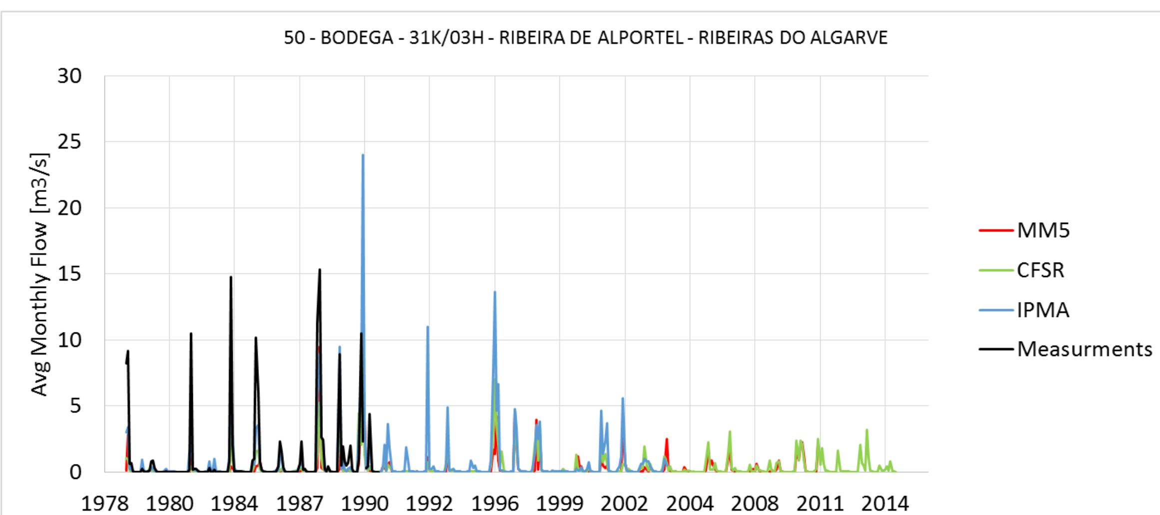

8.4.9 SADO

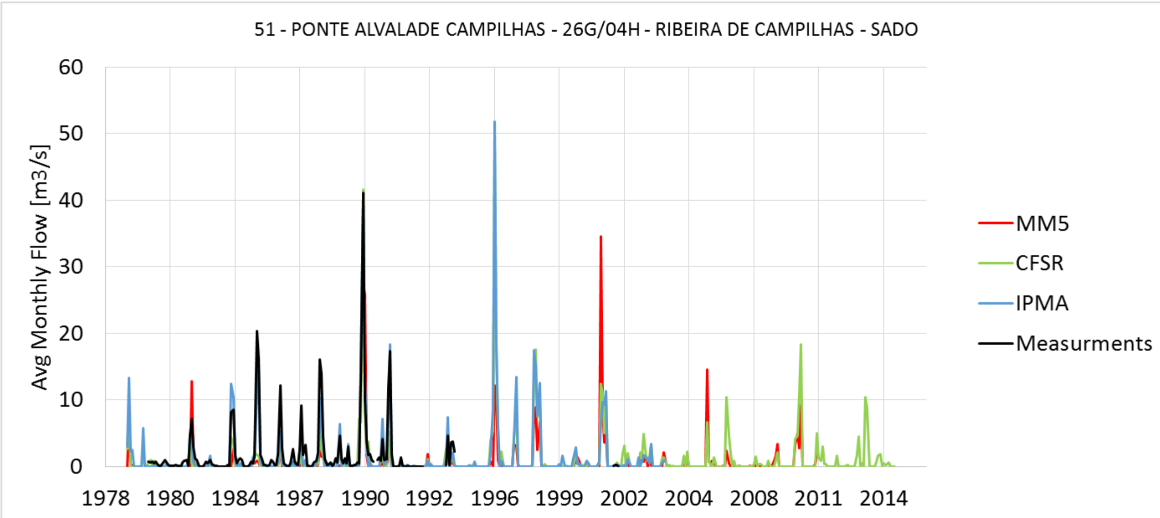
51 - PONTE ALVALADE CAMPILHAS - 26G/04H - RIBEIRA DE CAMPILHAS - SADO
Avg Monthly Flow [m3/s]
60
50
40
30
20
10
0
1978 1980 1984 1987 1990 1992 1996 1999 2002 2004 2008 2011 2014
MM5
CFSR
IPMA
Measurments

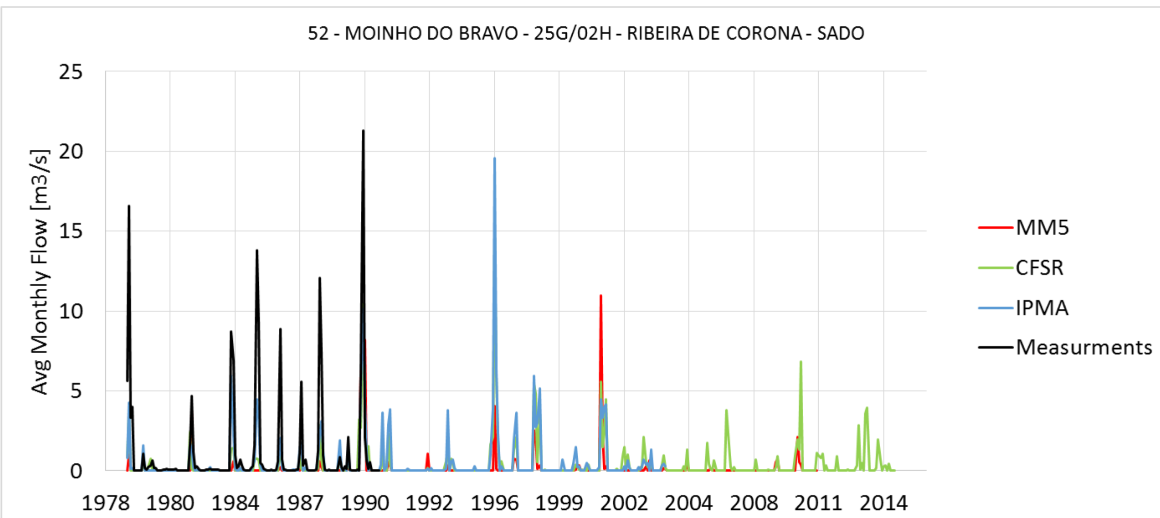
52 - MOINHO DO BRAVO - 25G/02H - RIBEIRA DE CORONA - SADO
Avg Monthly Flow [m3/s]
25
20
15
10
5
0
1978 1980 1984 1987 1990 1992 1996 1999 2002 2004 2008 2011 2014
MM5
CFSR
IPMA
Measurments

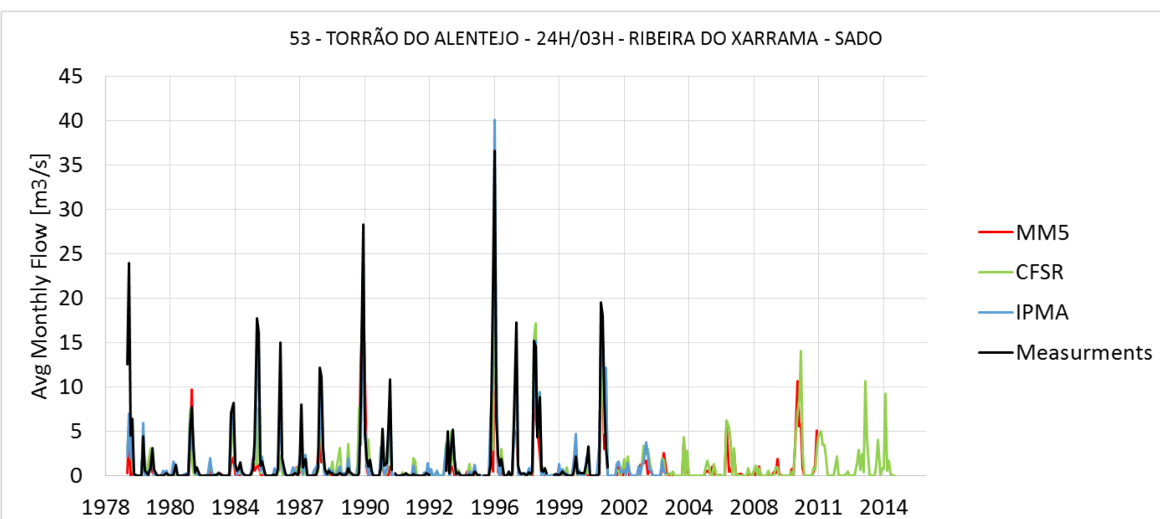
53 - TORRÃO DO ALENTEJO - 24H/03H - RIBEIRA DO XARRAMA - SADO
Avg Monthly Flow [m3/s]
45
40
35
30
25
20
15
10
5
0
1978 1980 1984 1987 1990 1992 1996 1999 2002 2004 2008 2011 2014
MM5
CFSR
IPMA
Measurments

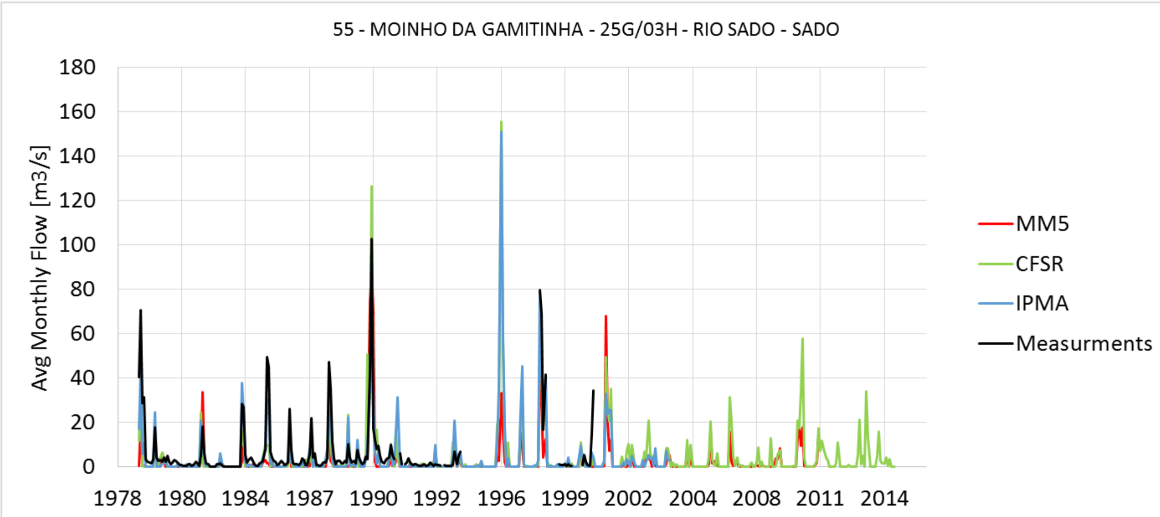
55 - MOINHO DA GAMITINHA - 25G/03H - RIO SADO - SADO
Avg Monthly Flow [m3/s]
180
160
140
120
100
80
60
40
20
0
1978 1980 1984 1987 1990 1992 1996 1999 2002 2004 2008 2011 2014
MM5
CFSR
IPMA
Measurments

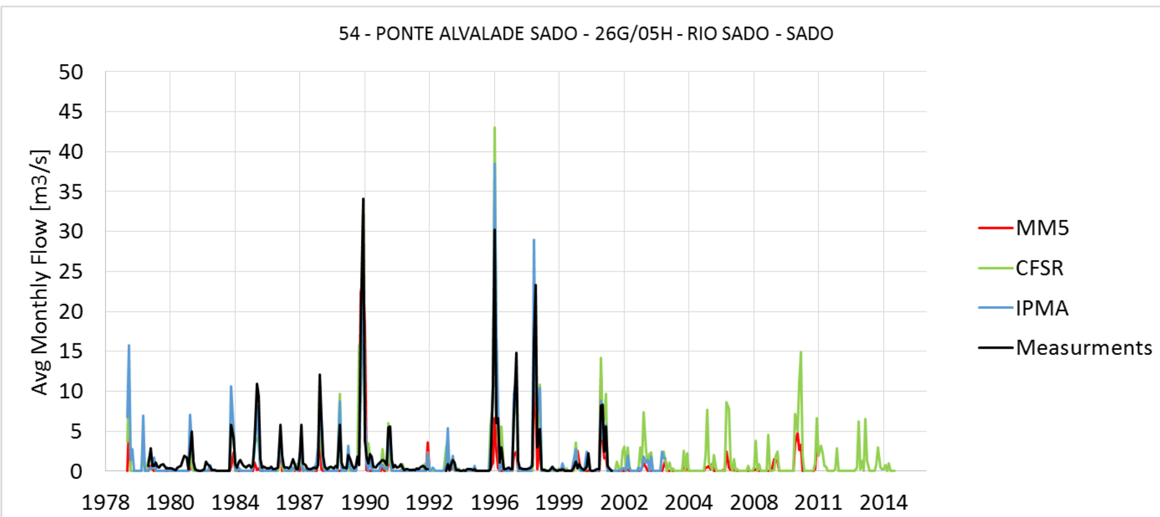
54 - PONTE ALVALADE SADO - 26G/05H - RIO SADO - SADO
Avg Monthly Flow [m3/s]
50
45
40
35
30
25
20
15
10
5
0
1978 1980 1984 1987 1990 1992 1996 1999 2002 2004 2008 2011 2014
MM5
CFSR
IPMA
Measurments

8.4.10 TEJO

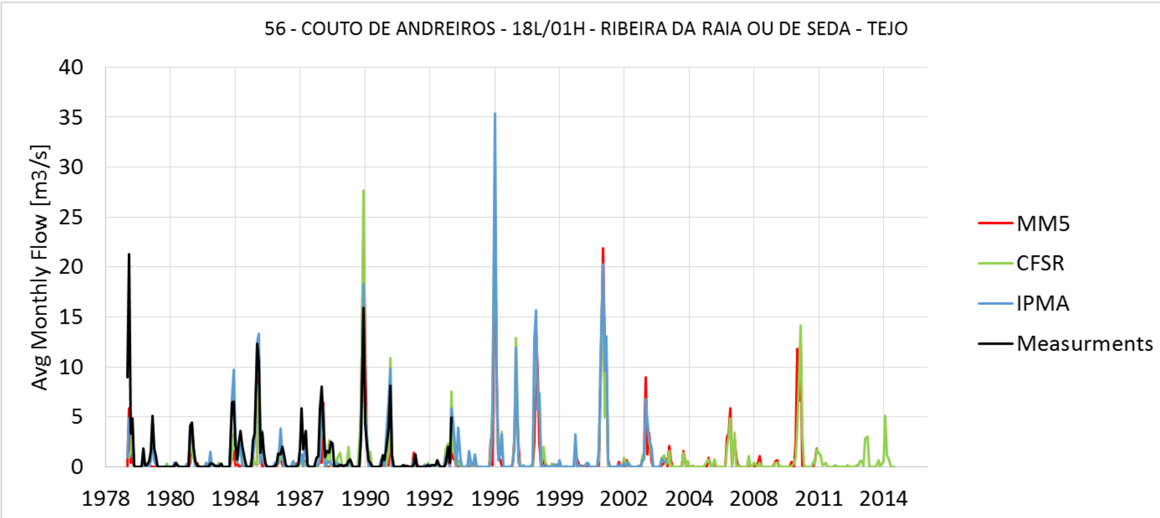
56 - COUTO DE ANDREIROS - 18L/01H - RIBEIRA DA RAIA OU DE SEDA - TEJO
Avg Monthly Flow [m3/s]
MM5
CFSR
IPMA
Measurments

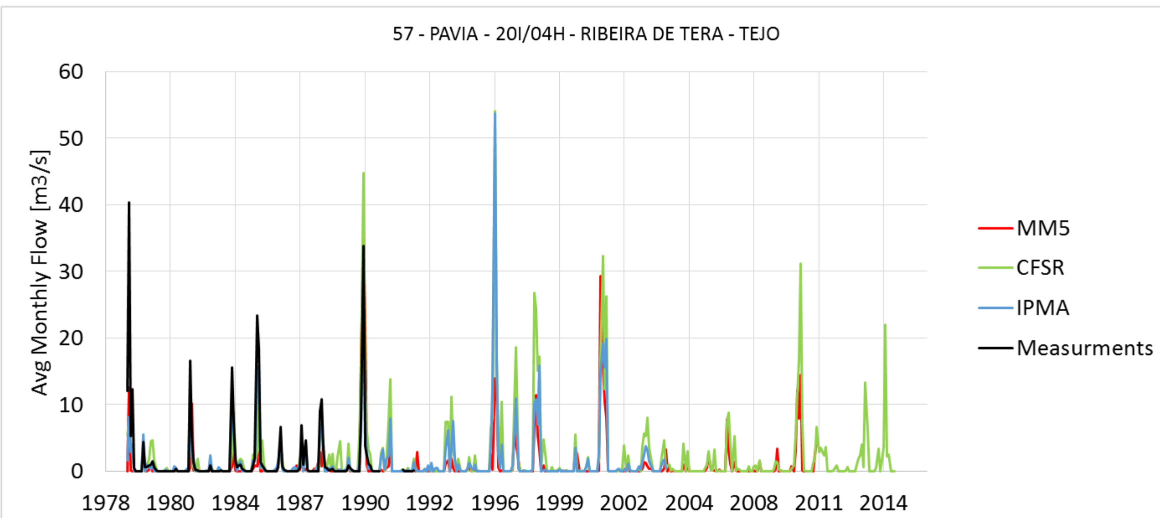
57 - PAVIA - 20I/04H - RIBEIRA DE TERA - TEJO
Avg Monthly Flow [m3/s]
MM5
CFSR
IPMA
Measurments

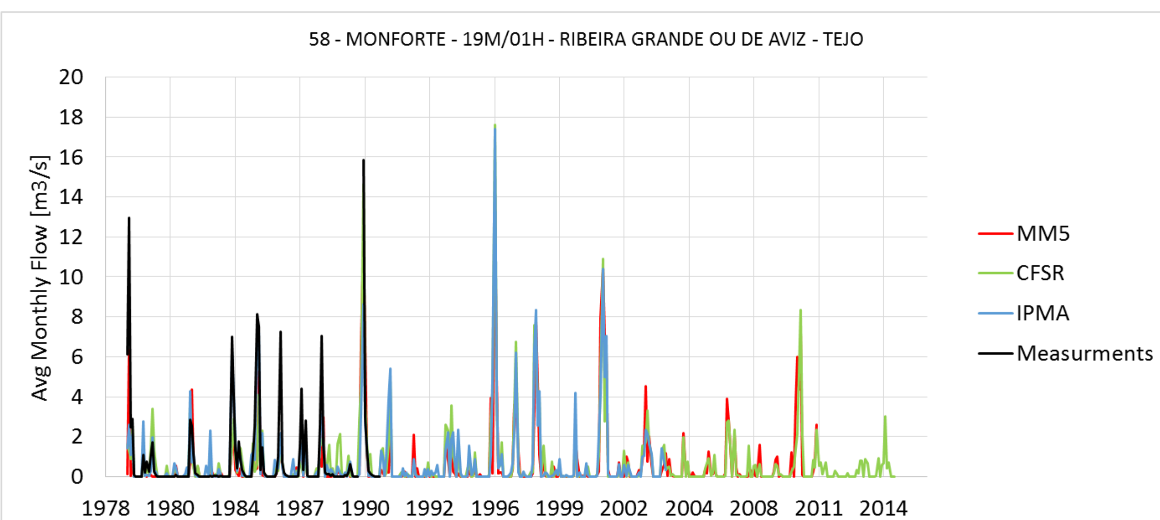
58 - MONFORTE - 19M/01H - RIBEIRA GRANDE OU DE AVIZ - TEJO
Avg Monthly Flow [m3/s]
MM5
CFSR
IPMA
Measurments

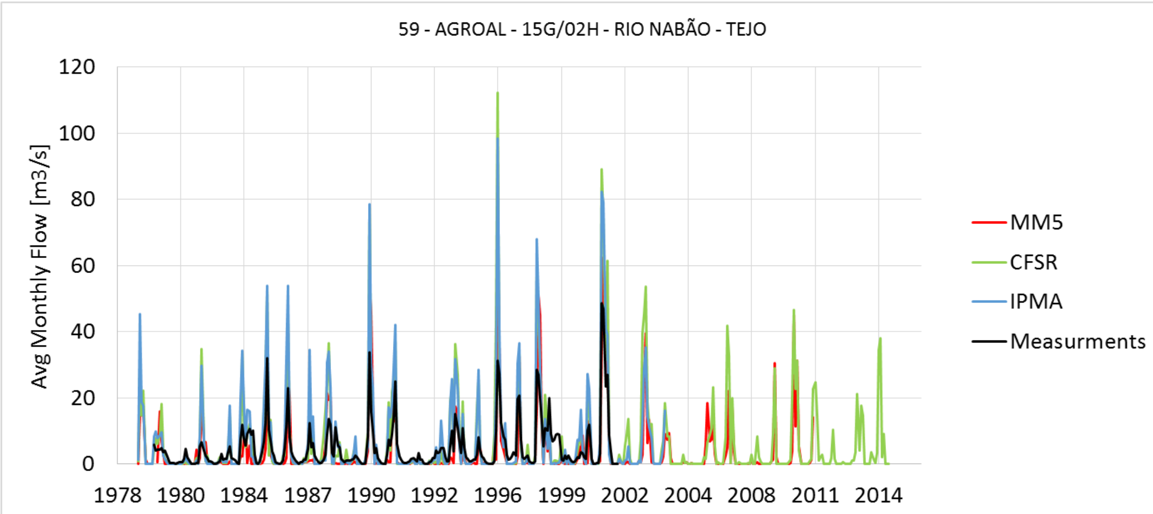
59 - AGROAL - 15G/02H - RIO NABÃO - TEJO
Avg Monthly Flow [m3/s]
0
20
40
60
80
100
120
1978 1980 1984 1987 1990 1992 1996 1999 2002 2004 2008 2011 2014
MM5
CFSR
IPMA
Measurments

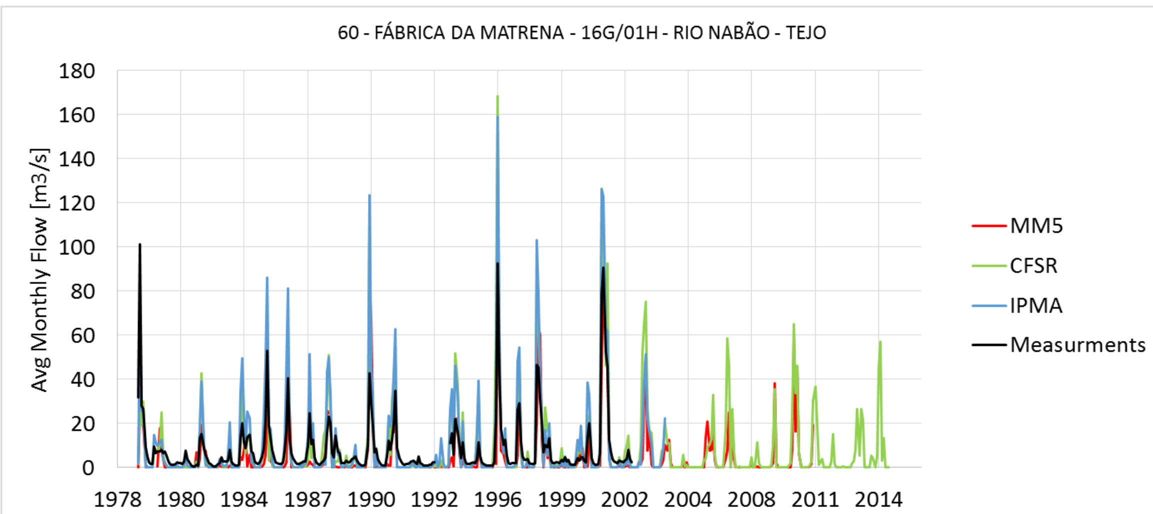
60 - FÁBRICA DA MATRENA - 16G/01H - RIO NABÃO - TEJO
Avg Monthly Flow [m3/s]
0
20
40
60
80
100
120
140
160
180
1978 1980 1984 1987 1990 1992 1996 1999 2002 2004 2008 2011 2014
MM5
CFSR
IPMA
Measurments

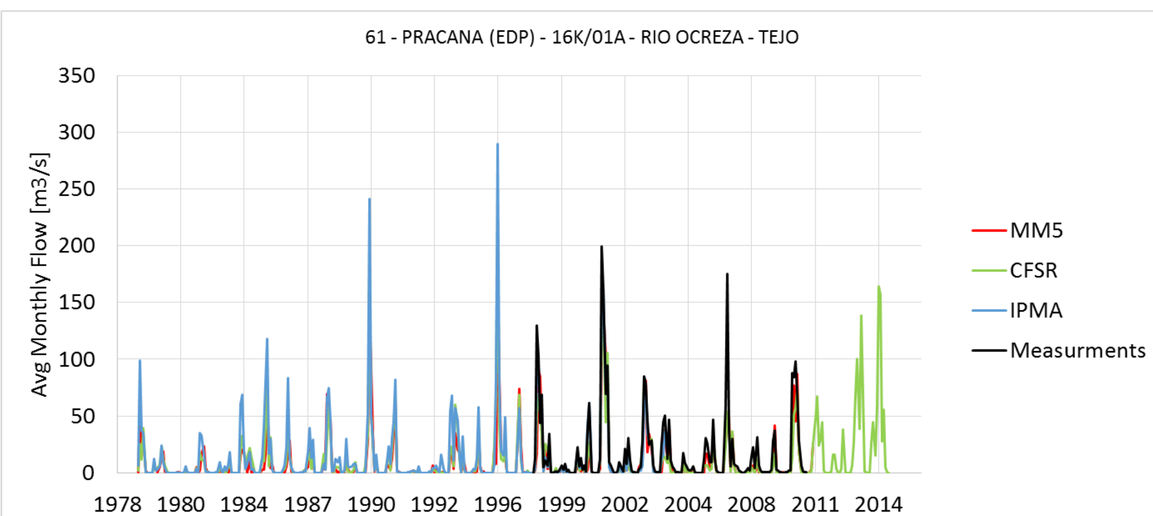
61 - PRACANA (EDP) - 16K/01A - RIO OCREZA - TEJO
Avg Monthly Flow [m3/s]
0
50
100
150
200
250
300
350
1978 1980 1984 1987 1990 1992 1996 1999 2002 2004 2008 2011 2014
MM5
CFSR
IPMA
Measurments

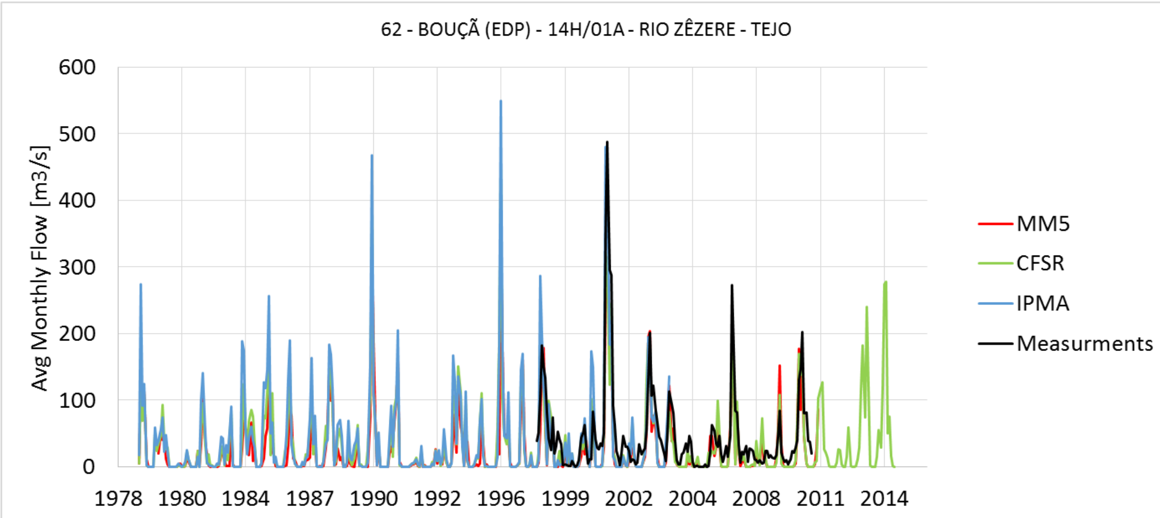

62 - BOUÇÃ (EDP) - 14H/01A - RIO ZÊZERE - TEJO
Avg Monthly Flow [m3/s]
600
500
400
300
200
100
0
1978 1980 1984 1987 1990 1992 1996 1999 2002 2004 2008 2011 2014
MM5
CFSR
IPMA
Measurments

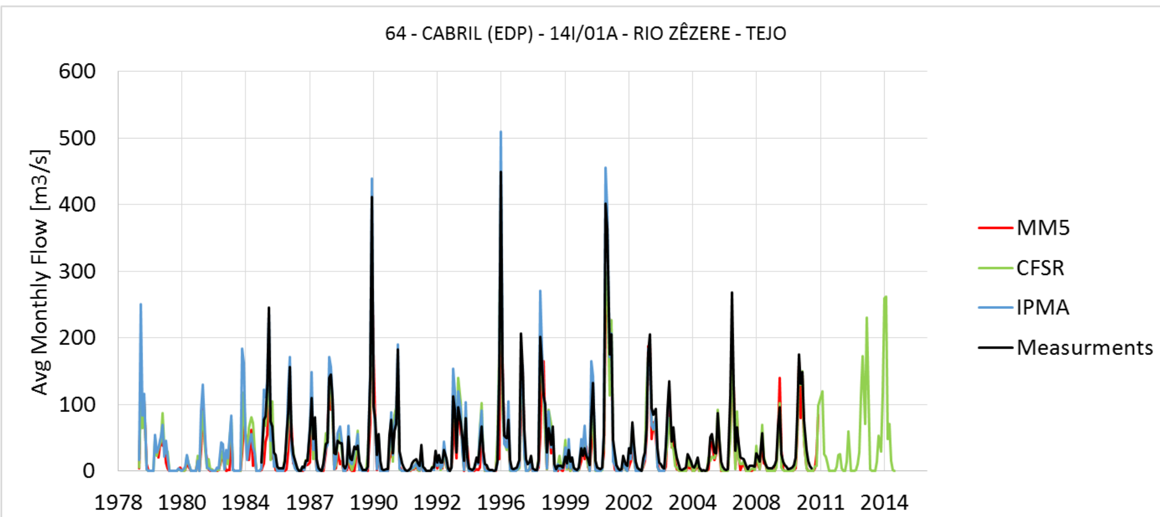

64 - CABRIL (EDP) - 14I/01A - RIO ZÊZERE - TEJO
Avg Monthly Flow [m3/s]
600
500
400
300
200
100
0
1978 1980 1984 1987 1990 1992 1996 1999 2002 2004 2008 2011 2014
MM5
CFSR
IPMA
Measurments

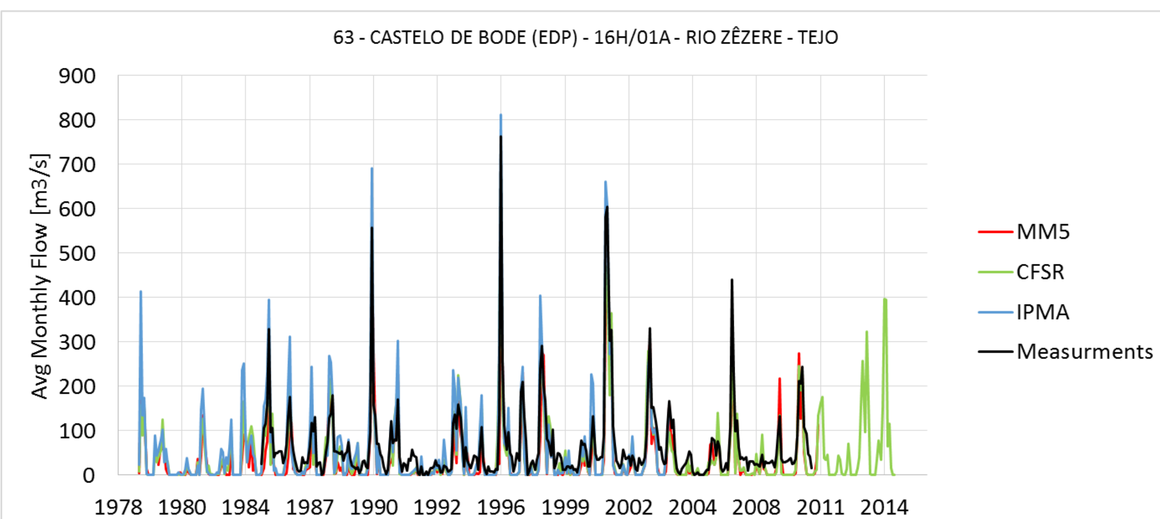

63 - CASTELO DE BODE (EDP) - 16H/01A - RIO ZÊZERE - TEJO
Avg Monthly Flow [m3/s]
900
800
700
600
500
400
300
200
100
0
1978 1980 1984 1987 1990 1992 1996 1999 2002 2004 2008 2011 2014
MM5
CFSR
IPMA
Measurments

8.4.11 VOUGA/RIBEIRAS COSTEIRAS

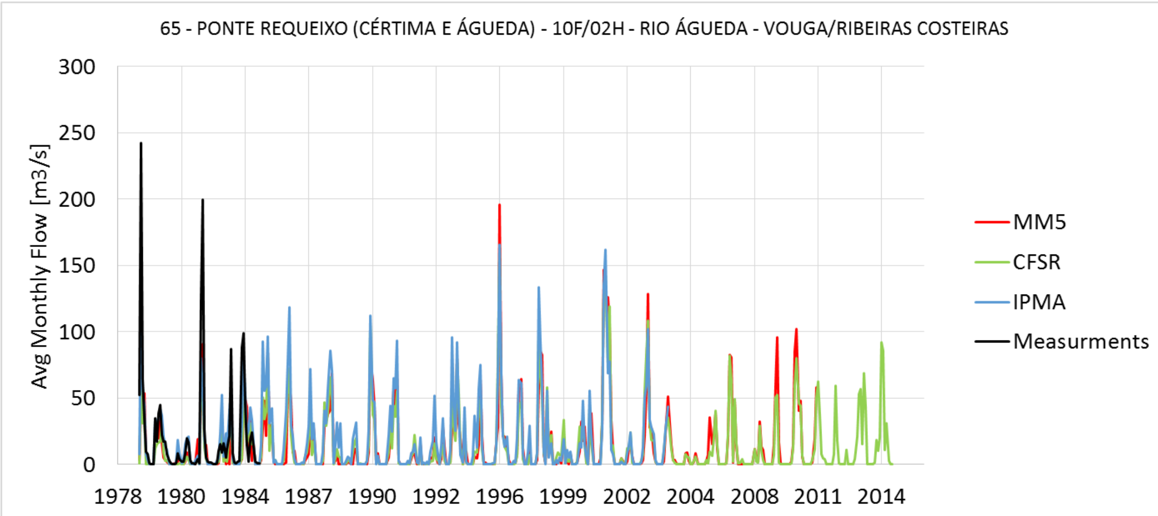

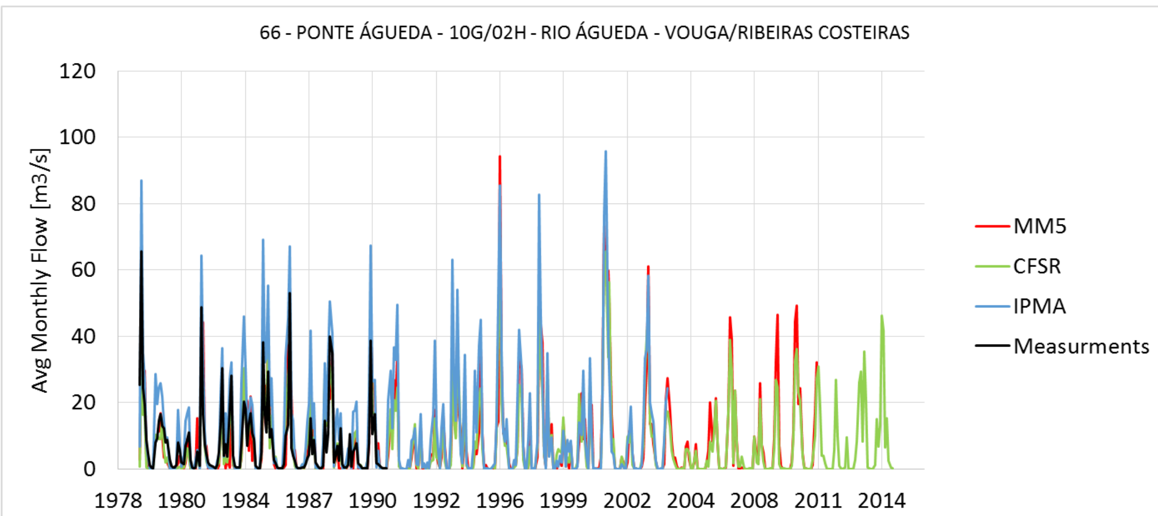

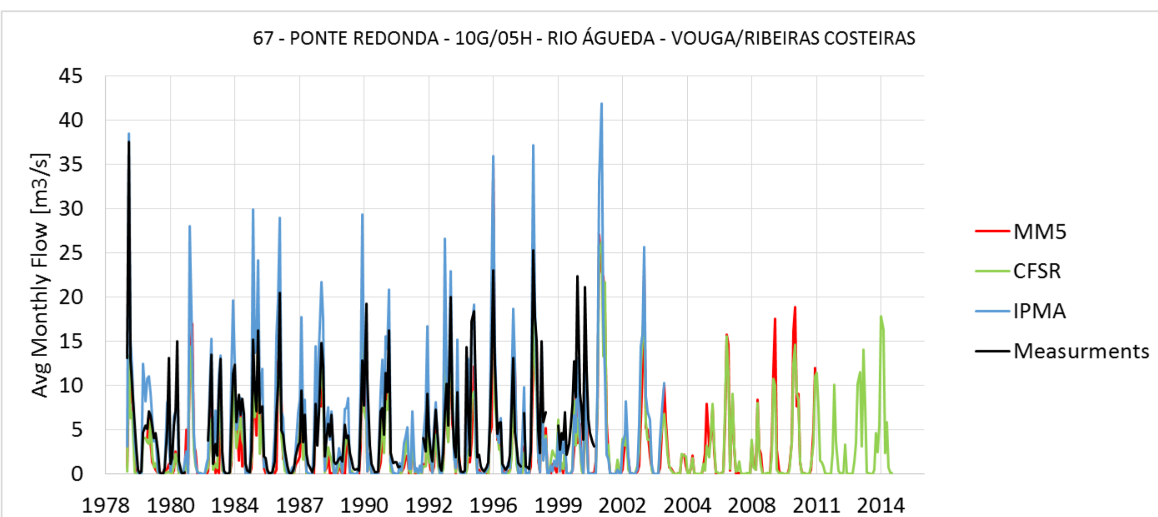

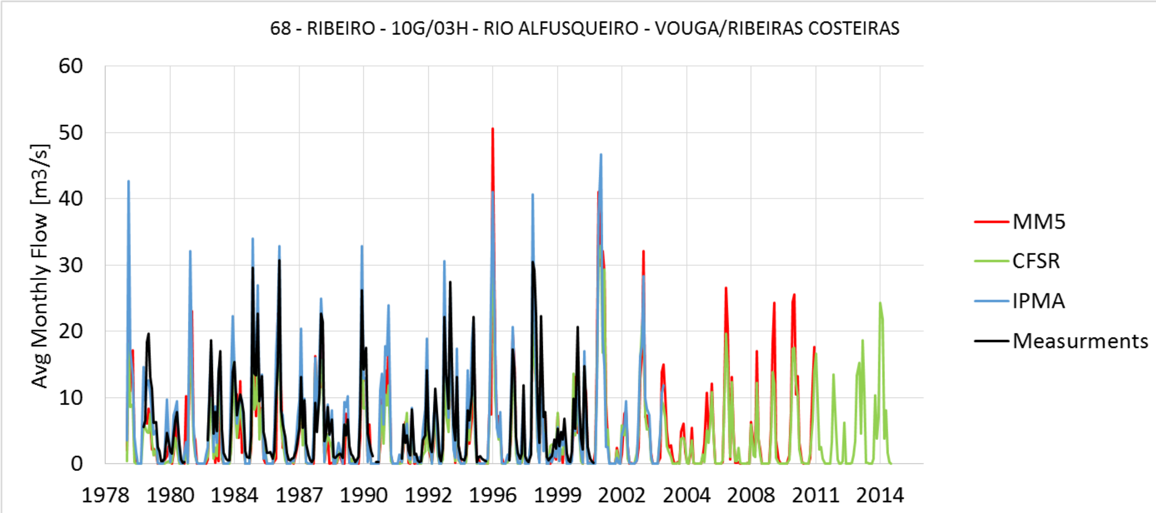
68 - RIBEIRO - 10G/03H - RIO ALFUSQUEIRO - VOUGA/RIBEIRAS COSTEIRAS
Avg Monthly Flow [m3/s]
MM5
CFSR
IPMA
Measurments

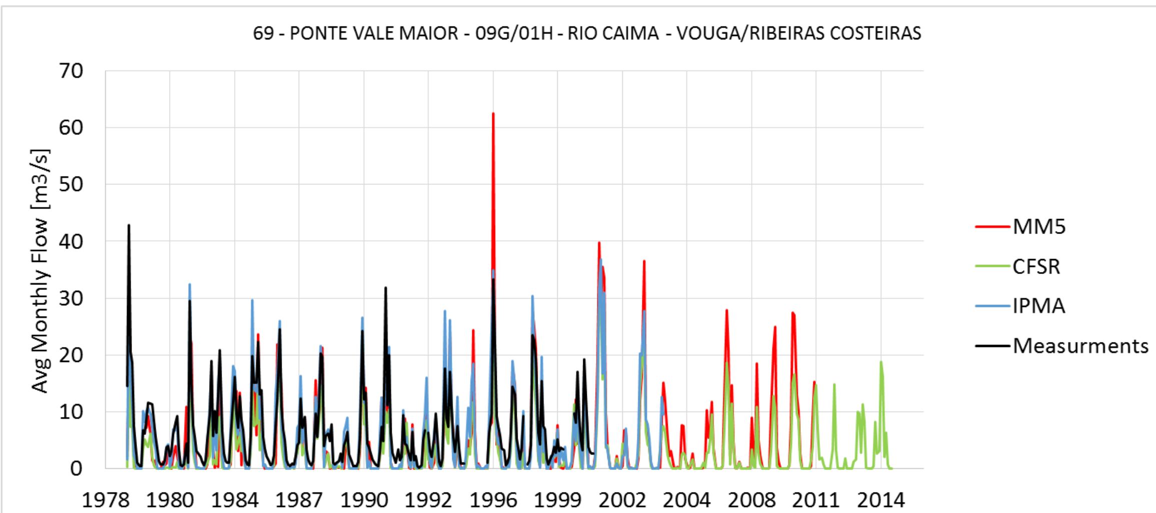
69 - PONTE VALE MAIOR - 09G/01H - RIO CAIMA - VOUGA/RIBEIRAS COSTEIRAS
Avg Monthly Flow [m3/s]
MM5
CFSR
IPMA
Measurments

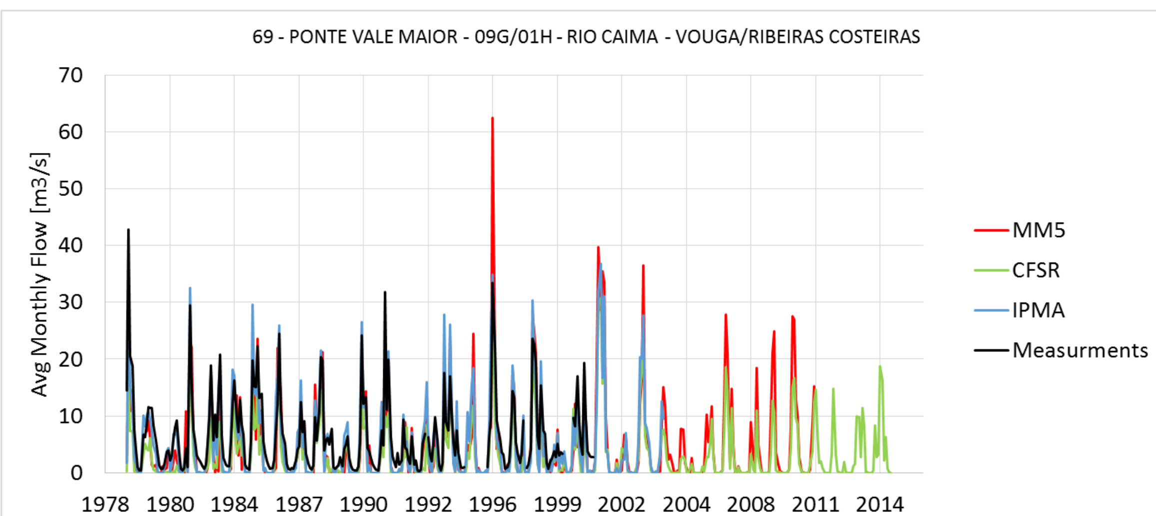
69 - PONTE VALE MAIOR - 09G/01H - RIO CAIMA - VOUGA/RIBEIRAS COSTEIRAS
Avg Monthly Flow [m3/s]
MM5
CFSR
IPMA
Measurments

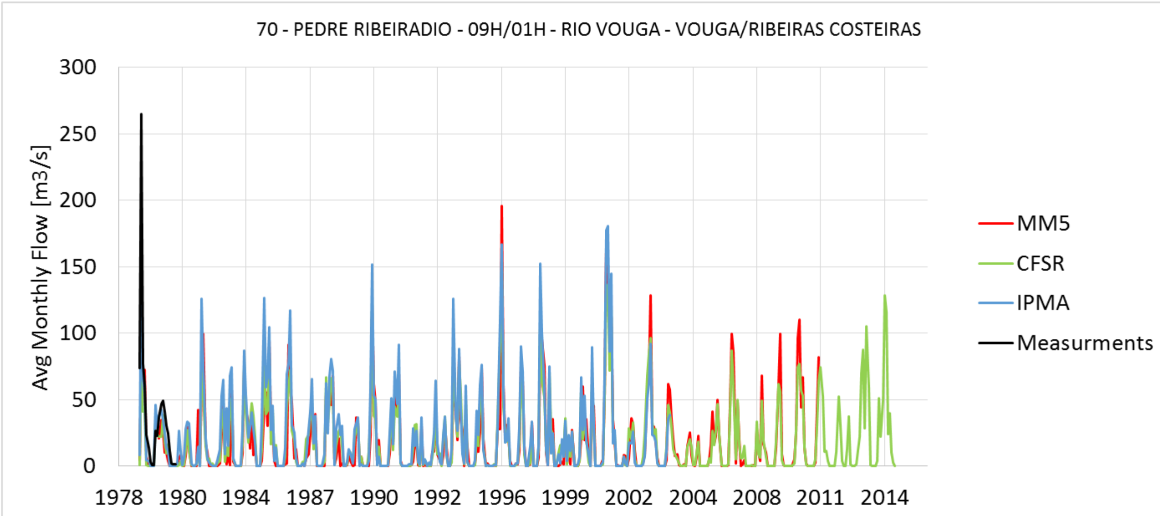

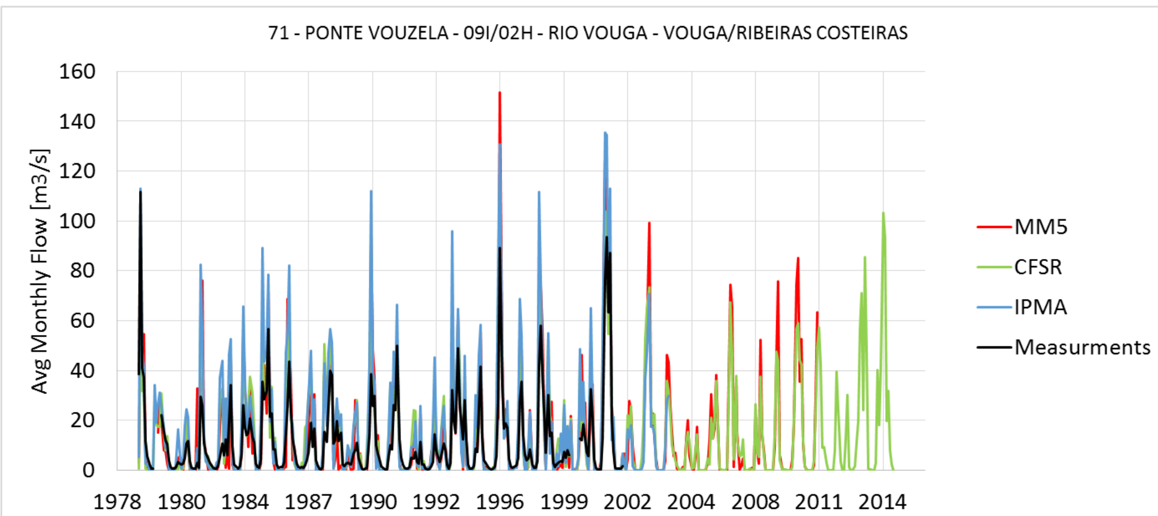

8.5 Monthly flows Validation

8.5.1 ARADE

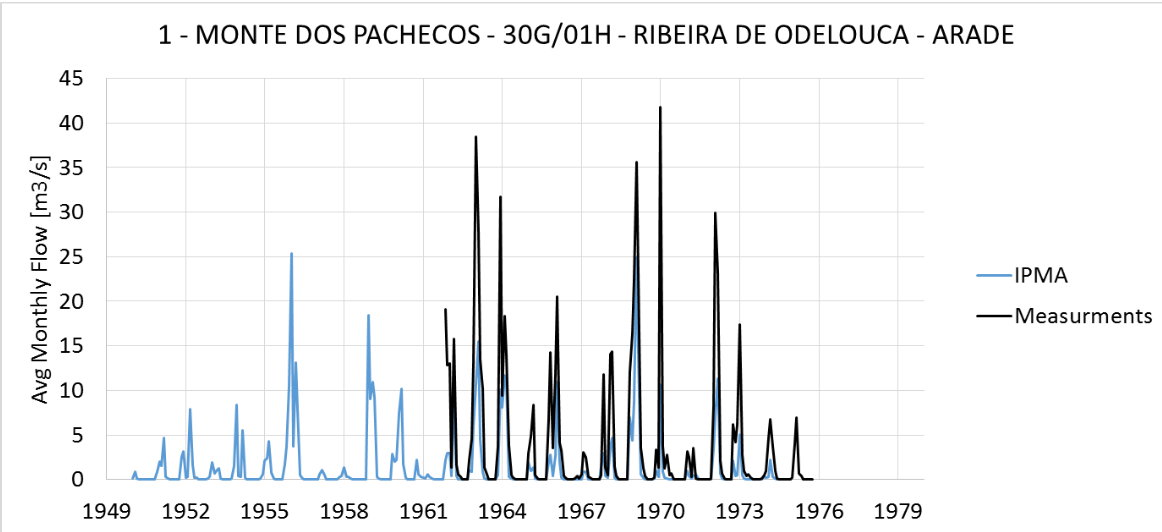
1 - MONTE DOS PACHECOS - 30G/01H - RIBEIRA DE ODELOUCA - ARADE
Avg Monthly Flow [m3/s]
45
40
35
30
25
20
15
10
5
0
1949
1952
1955
1958
1961
1964
1967
1970
1973
1976
1979
IPMA
Measurments

8.5.2 DOURO

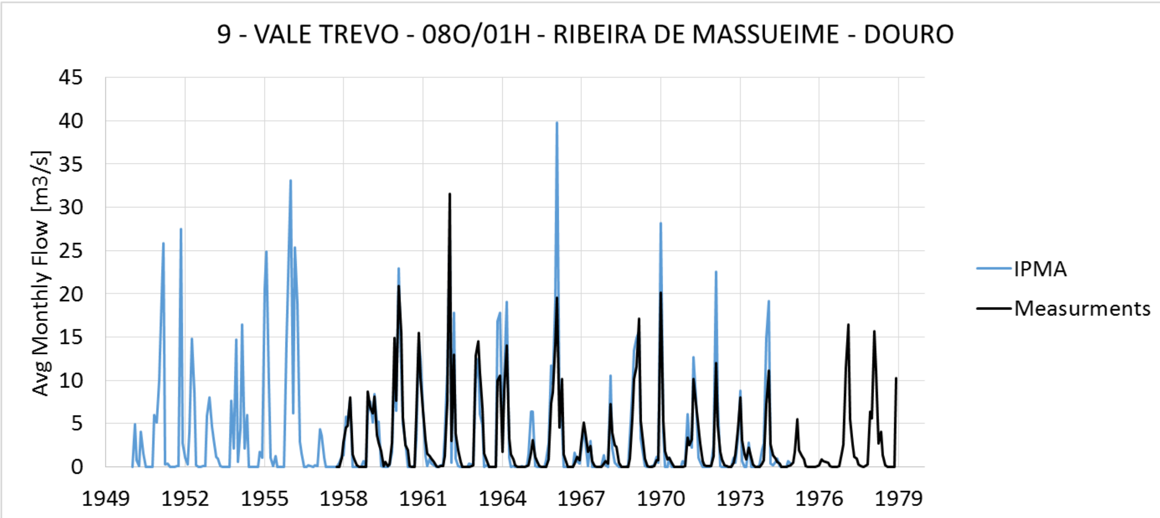
9 - VALE TREVO - 08O/01H - RIBEIRA DE MASSUEIME - DOURO
Avg Monthly Flow [m3/s]
45
40
35
30
25
20
15
10
5
0
1949
1952
1955
1958
1961
1964
1967
1970
1973
1976
1979
IPMA
Measurments

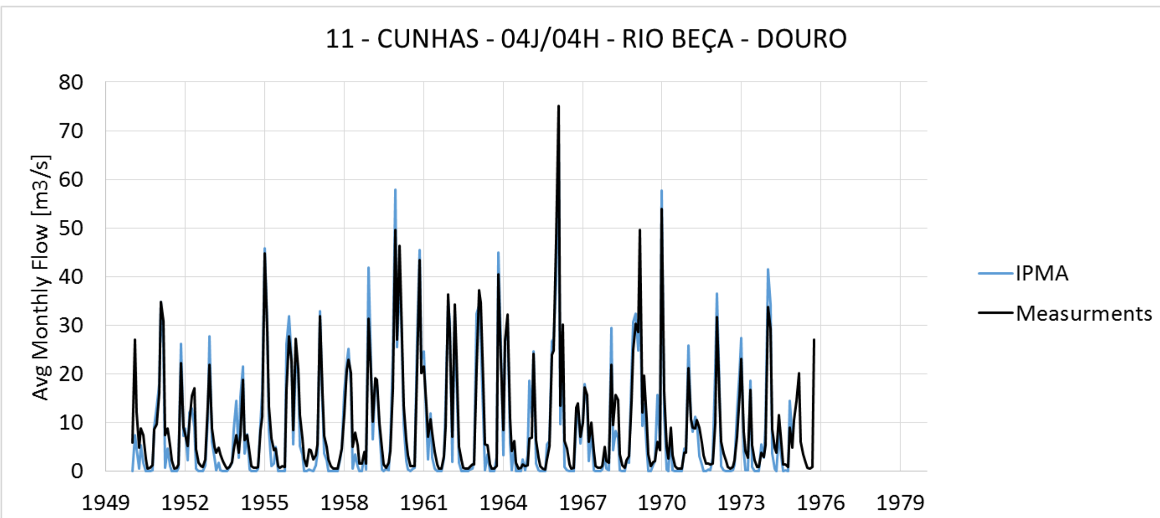
11 - CUNHAS - 04J/04H - RIO BEÇA - DOURO
Avg Monthly Flow [m3/s]
80
70
60
50
40
30
20
10
0
1949
1952
1955
1958
1961
1964
1967
1970
1973
1976
1979
IPMA
Measurments

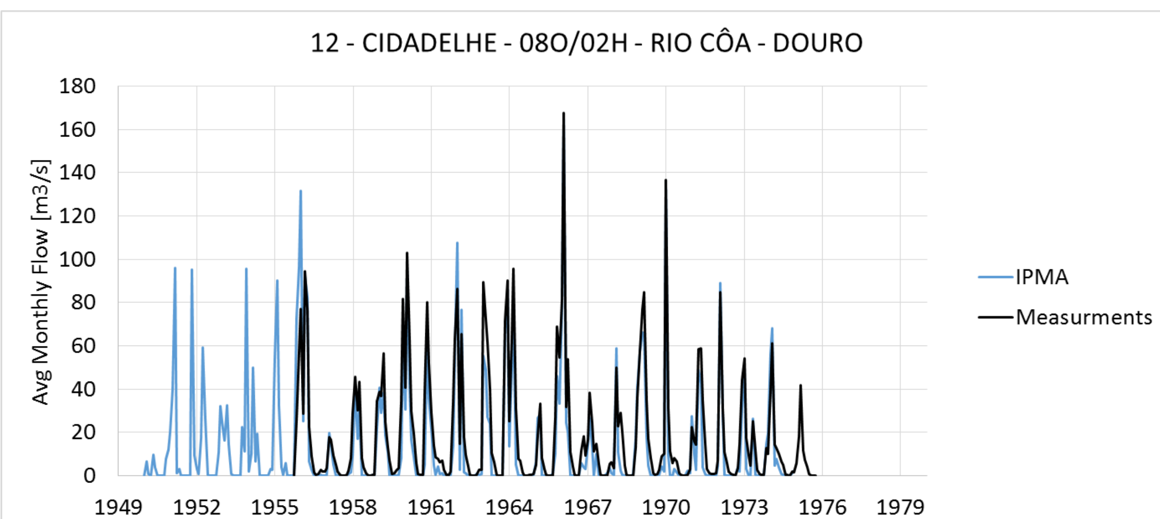
12 - CIDADELHE - 08O/02H - RIO CÔA - DOURO
Avg Monthly Flow [m3/s]
180
160
140
120
100
80
60
40
20
0
1949
1952
1955
1958
1961
1964
1967
1970
1973
1976
1979
IPMA
Measurments

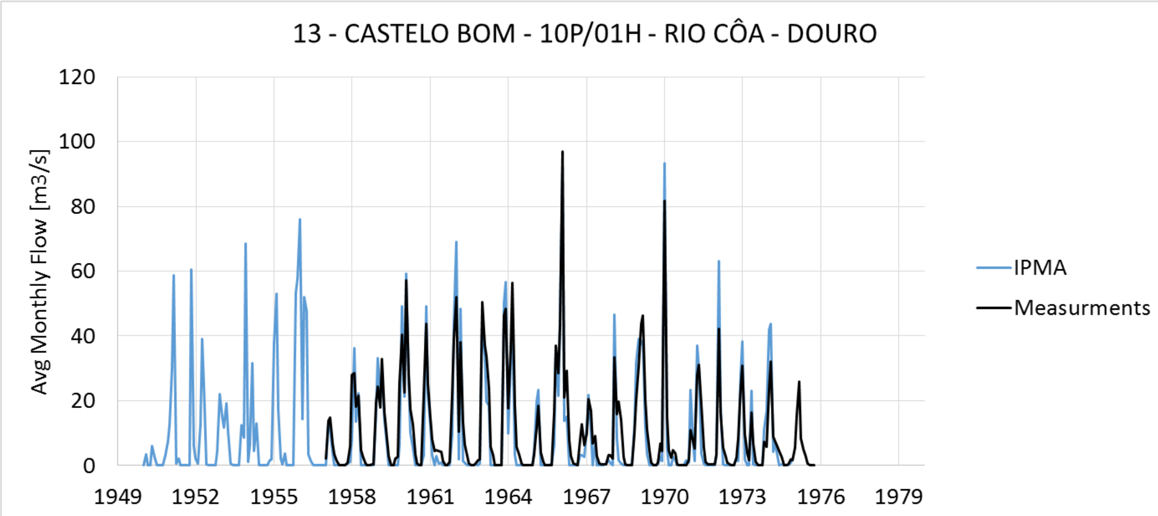
13 - CASTELO BOM - 10P/01H - RIO CÔA - DOURO
Avg Monthly Flow [m3/s]
0
20
40
60
80
100
120
1949
1952
1955
1958
1961
1964
1967
1970
1973
1976
1979
IPMA
Measurments

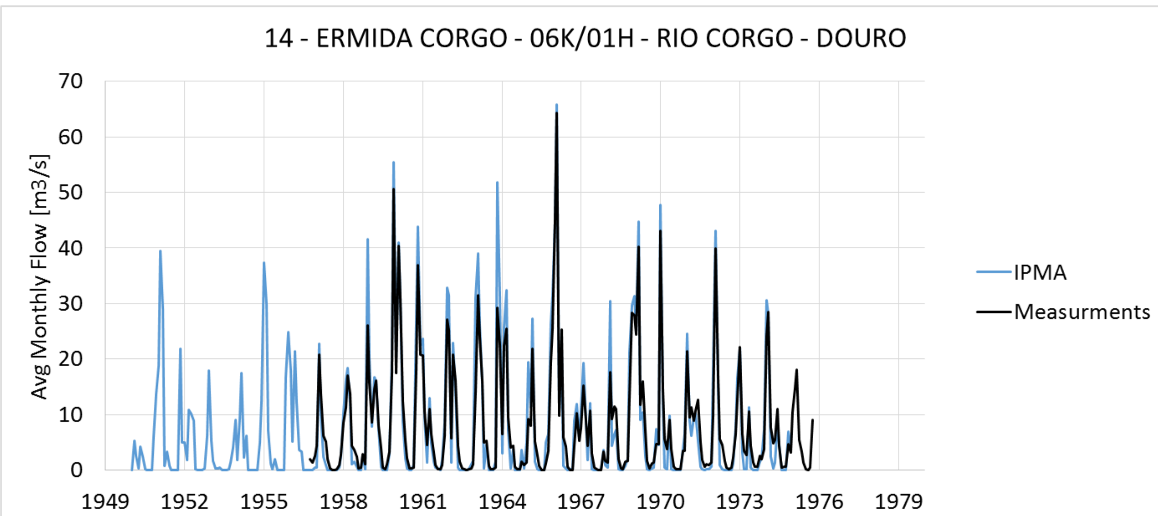
14 - ERMIDA CORGO - 06K/01H - RIO CORGO - DOURO
Avg Monthly Flow [m3/s]
0
10
20
30
40
50
60
70
1949
1952
1955
1958
1961
1964
1967
1970
1973
1976
1979
IPMA
Measurments

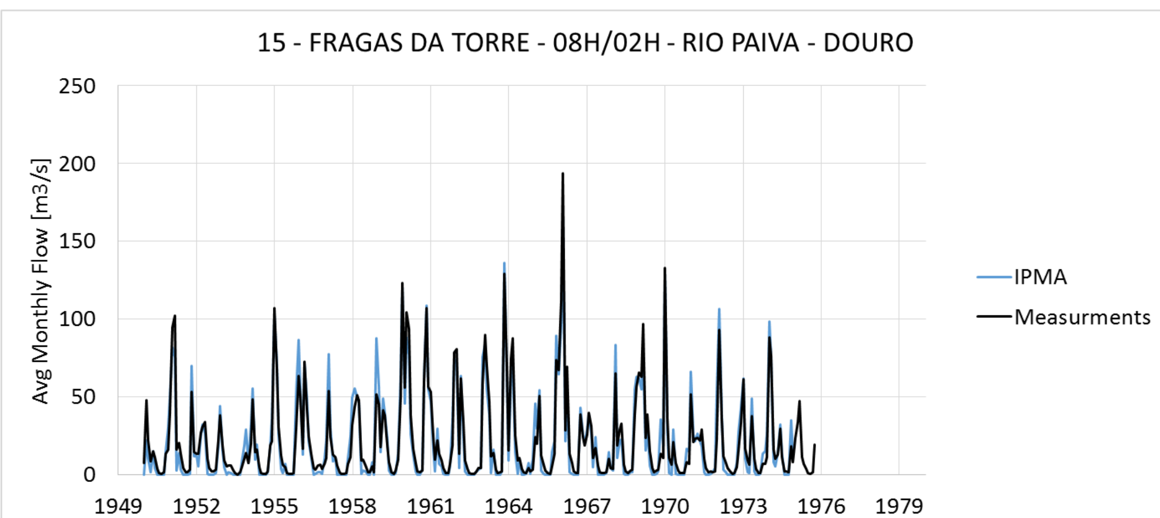
15 - FRAGAS DA TORRE - 08H/02H - RIO PAIVA - DOURO
Avg Monthly Flow [m3/s]
0
50
100
150
200
250
1949
1952
1955
1958
1961
1964
1967
1970
1973
1976
1979
IPMA
Measurments

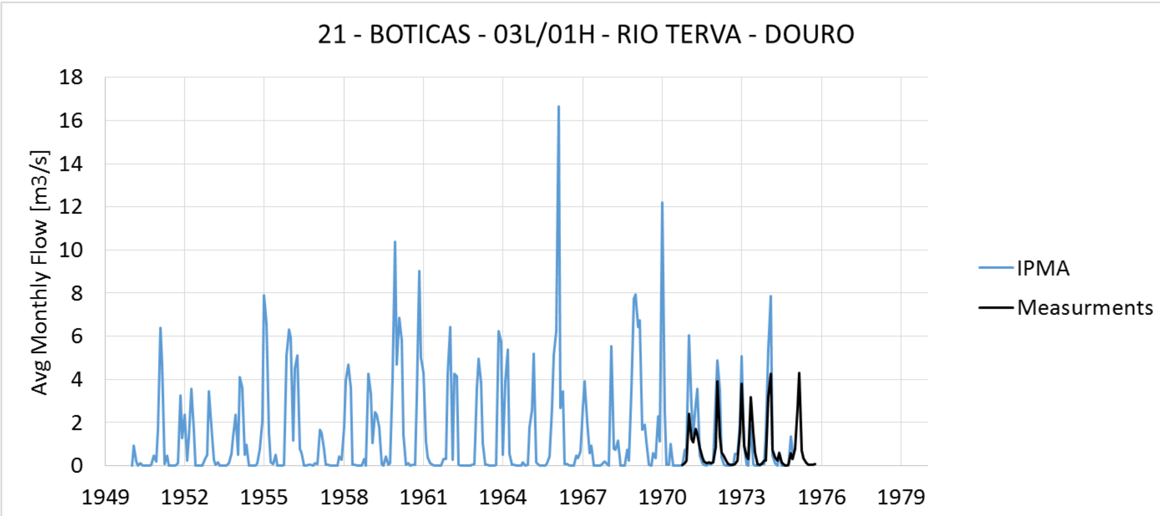
21 - BOTICAS - 03L/01H - RIO TERVA - DOURO
Avg Monthly Flow [m3/s]
0
2
4
6
8
10
12
14
16
18
1949
1952
1955
1958
1961
1964
1967
1970
1973
1976
1979
IPMA
Measurments

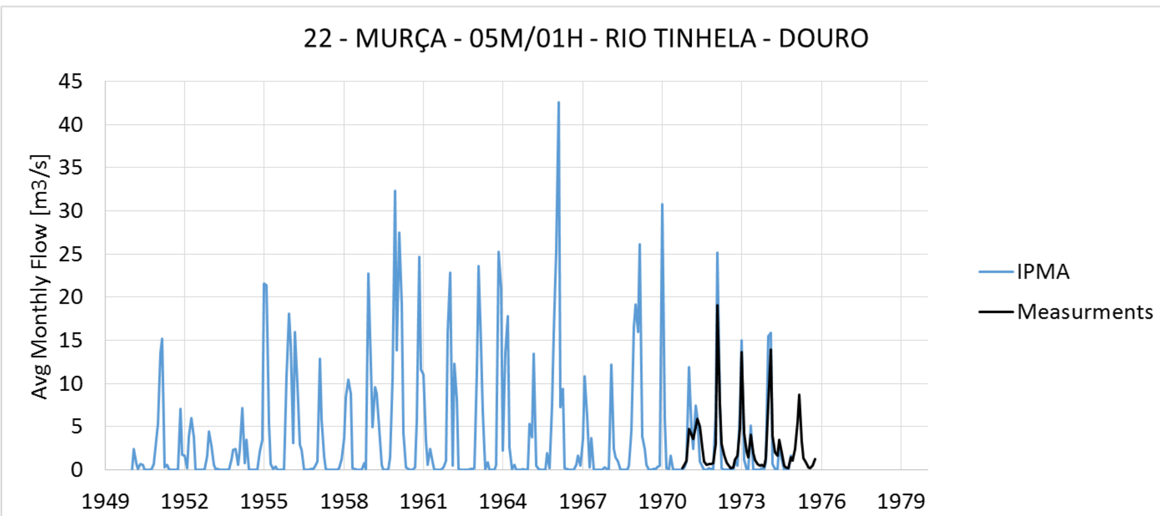
22 - MURÇA - 05M/01H - RIO TINHELA - DOURO
Avg Monthly Flow [m3/s]
0
5
10
15
20
25
30
35
40
45
1949
1952
1955
1958
1961
1964
1967
1970
1973
1976
1979
IPMA
Measurments

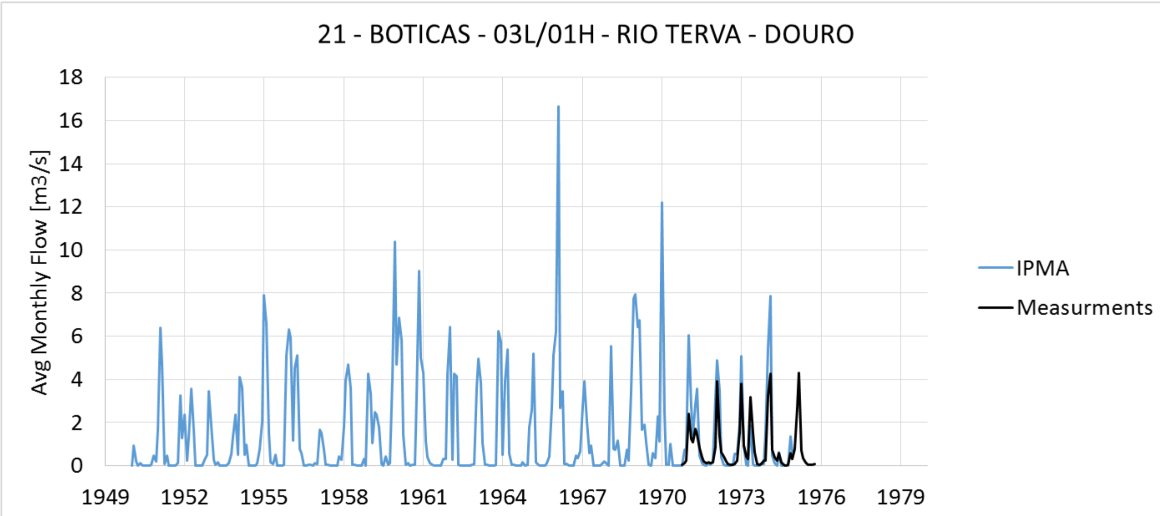
21 - BOTICAS - 03L/01H - RIO TERVA - DOURO
Avg Monthly Flow [m3/s]
18
16
14
12
10
8
6
4
2
0
1949
1952
1955
1958
1961
1964
1967
1970
1973
1976
1979
IPMA
Measurments

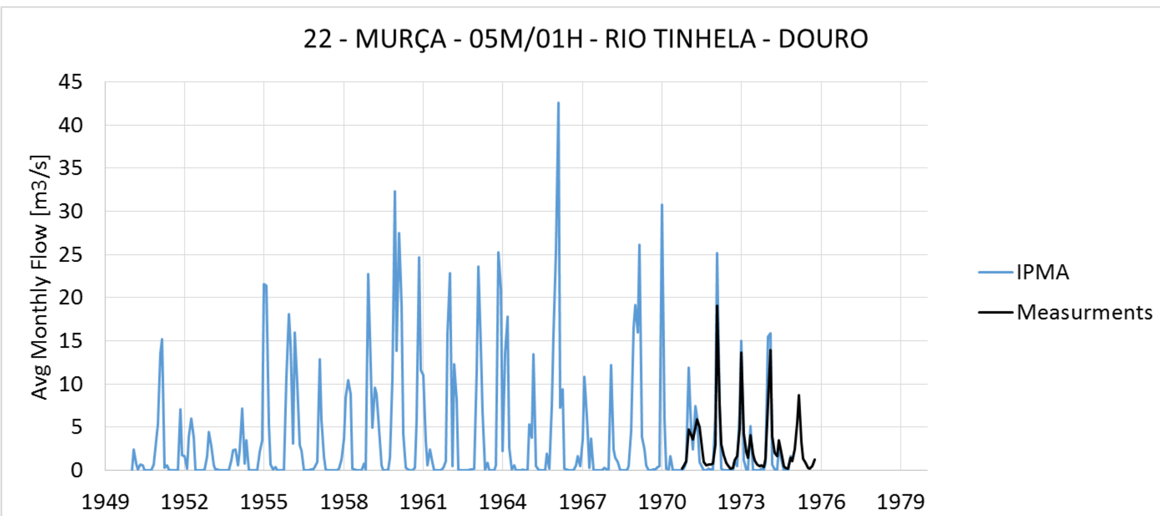
22 - MURÇA - 05M/01H - RIO TINHELA - DOURO
Avg Monthly Flow [m3/s]
45
40
35
30
25
20
15
10
5
0
1949
1952
1955
1958
1961
1964
1967
1970
1973
1976
1979
IPMA
Measurments

8.5.3 GUADIANA

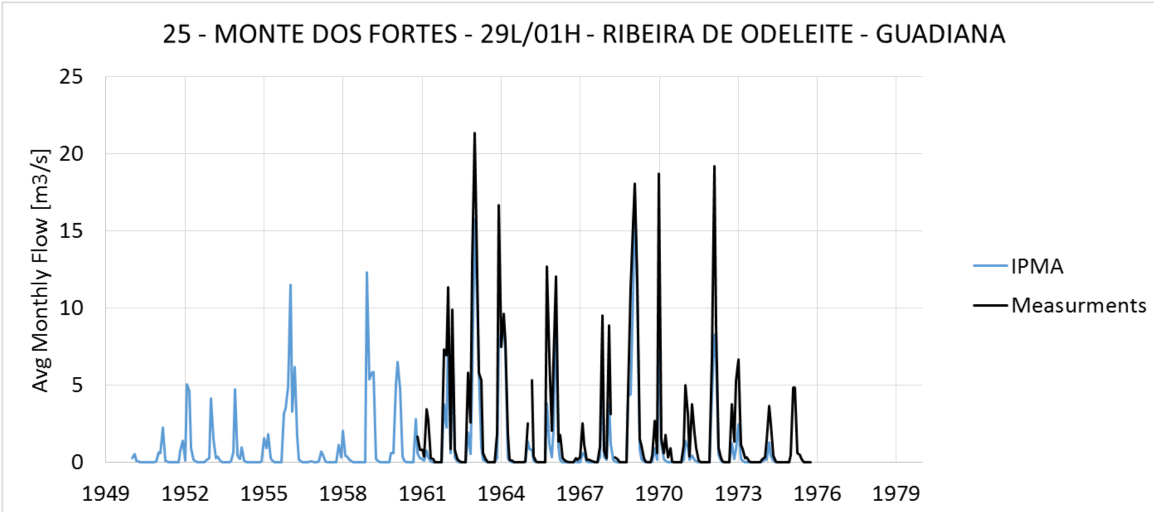

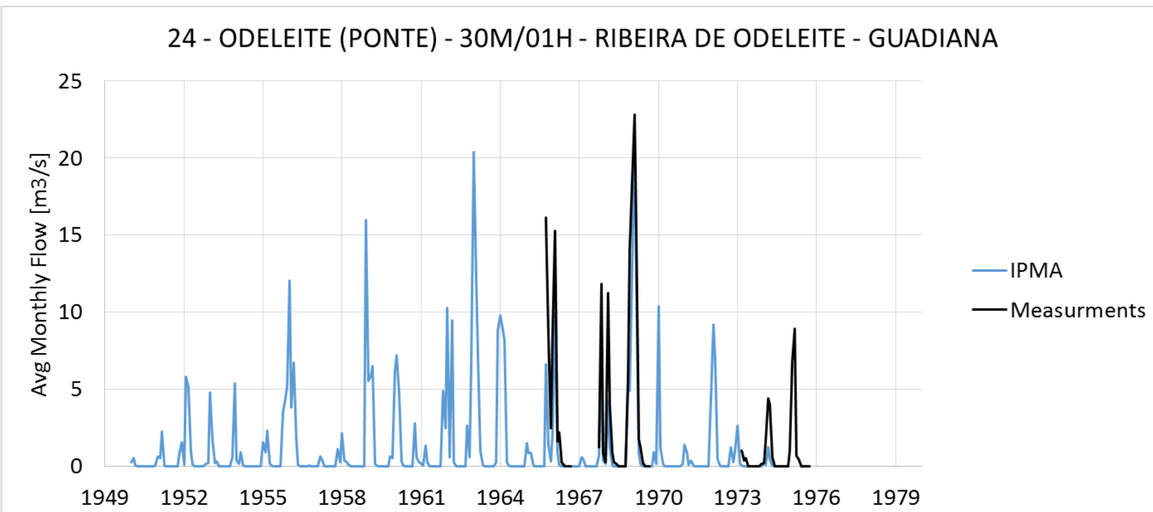

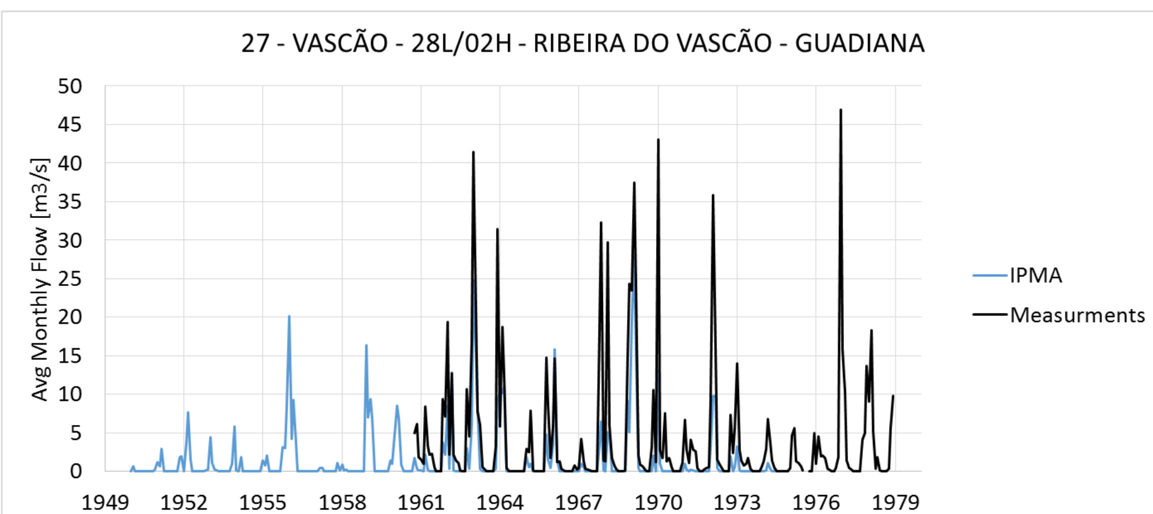

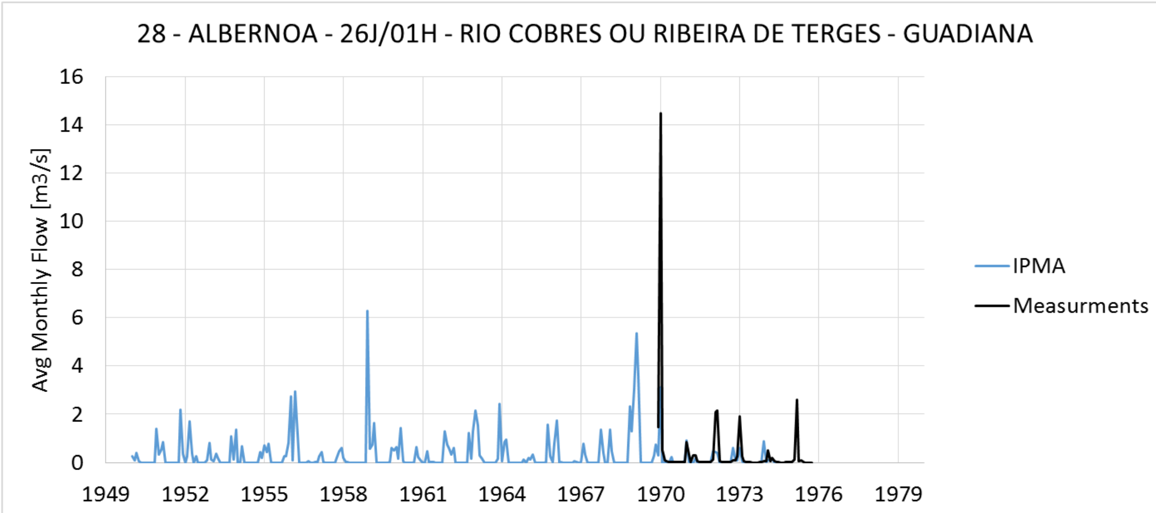
28 - ALBERNOA - 26J/01H - RIO COBRES OU RIBEIRA DE TERGES - GUADIANA
Avg Monthly Flow [m3/s]
0
2
4
6
8
10
12
14
16
1949
1952
1955
1958
1961
1964
1967
1970
1973
1976
1979
IPMA
Measurments

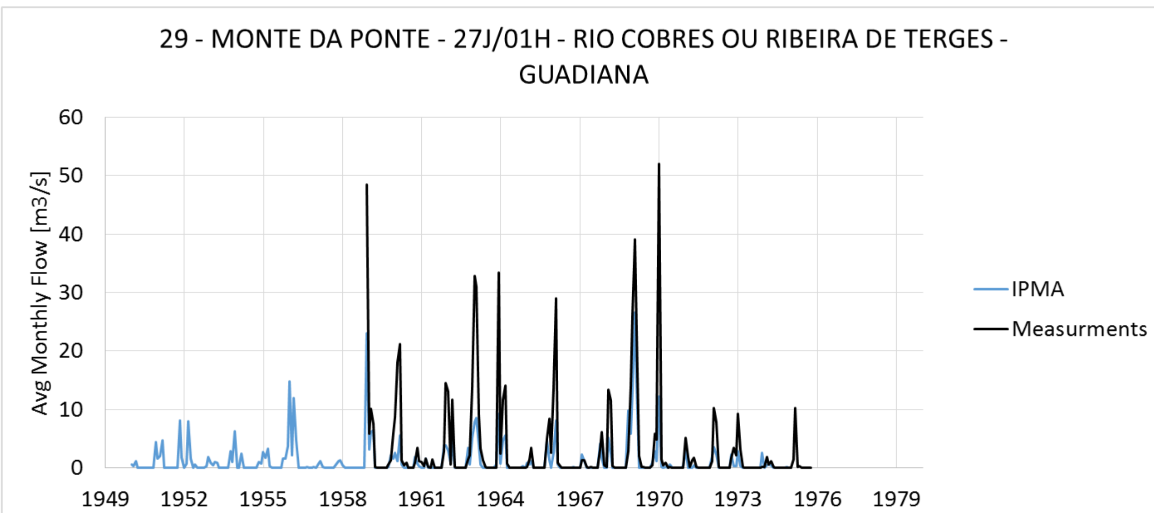
29 - MONTE DA PONTE - 27J/01H - RIO COBRES OU RIBEIRA DE TERGES - GUADIANA
Avg Monthly Flow [m3/s]
0
10
20
30
40
50
60
1949
1952
1955
1958
1961
1964
1967
1970
1973
1976
1979
IPMA
Measurments

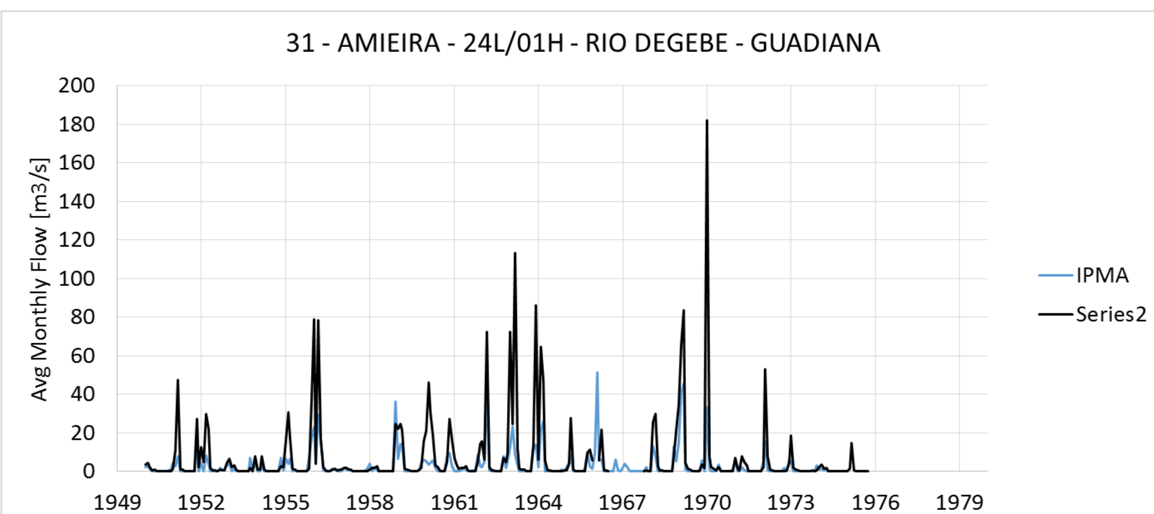
31 - AMIEIRA - 24L/01H - RIO DEGEBE - GUADIANA
Avg Monthly Flow [m3/s]
0
20
40
60
80
100
120
140
160
180
200
1949
1952
1955
1958
1961
1964
1967
1970
1973
1976
1979
IPMA
Series2

8.5.4 LIMA

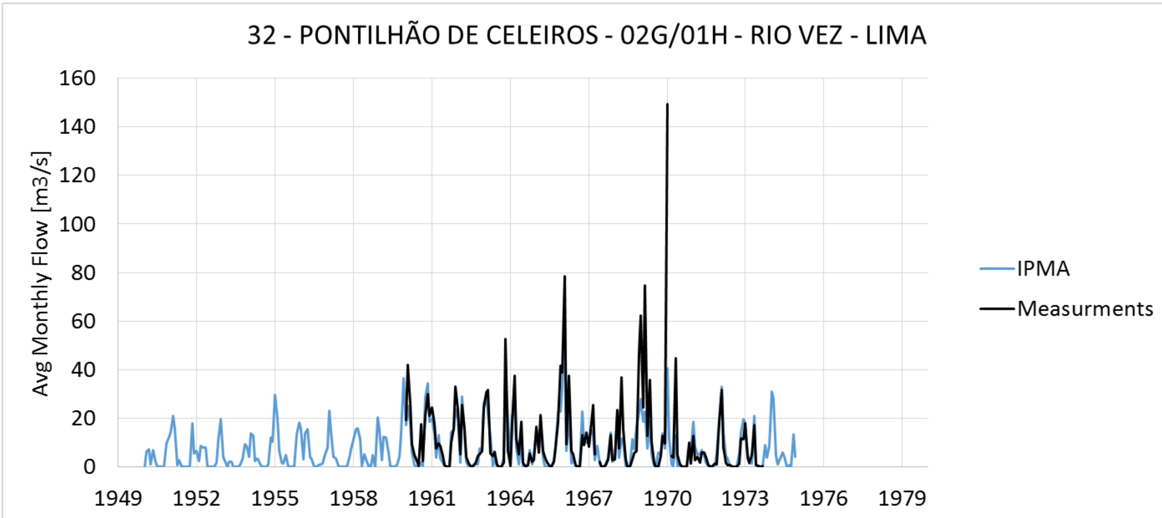
32 - PONTILHÃO DE CELEIROS - 02G/01H - RIO VEZ - LIMA
Avg Monthly Flow [m3/s]
0
20
40
60
80
100
120
140
160
1949
1952
1955
1958
1961
1964
1967
1970
1973
1976
1979
IPMA
Measurments

8.5.5 MONDEGO

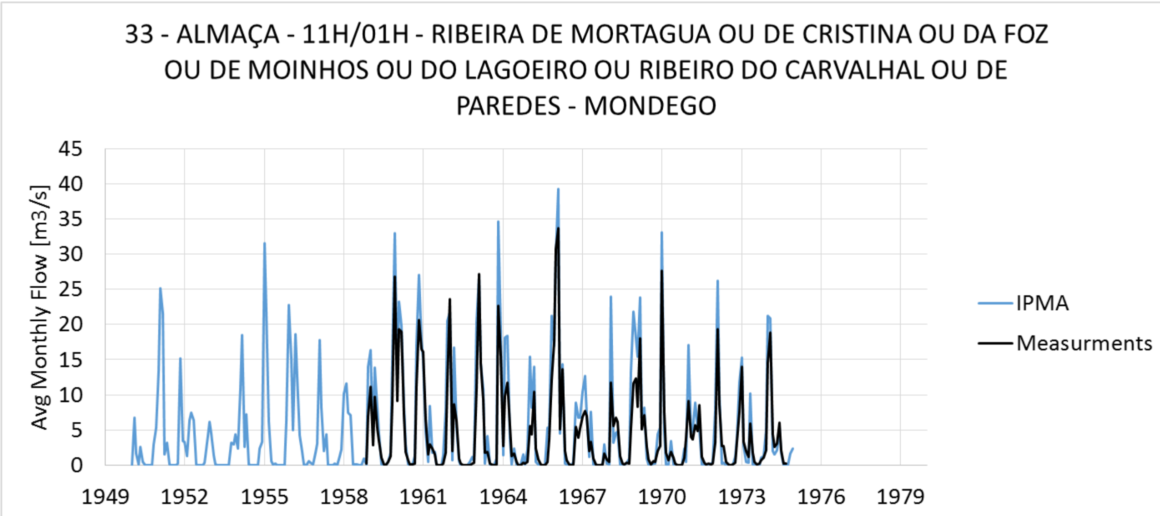
33 - ALMAÇA - 11H/01H - RIBEIRA DE MORTAGUA OU DE CRISTINA OU DA FOZ OU DE MOINHOS OU DO LAGOEIRO OU RIBEIRO DO CARVALHAL OU DE PAREDES - MONDEGO
Avg Monthly Flow [m3/s]
IPMA
Measurments
1949 1952 1955 1958 1961 1964 1967 1970 1973 1976 1979

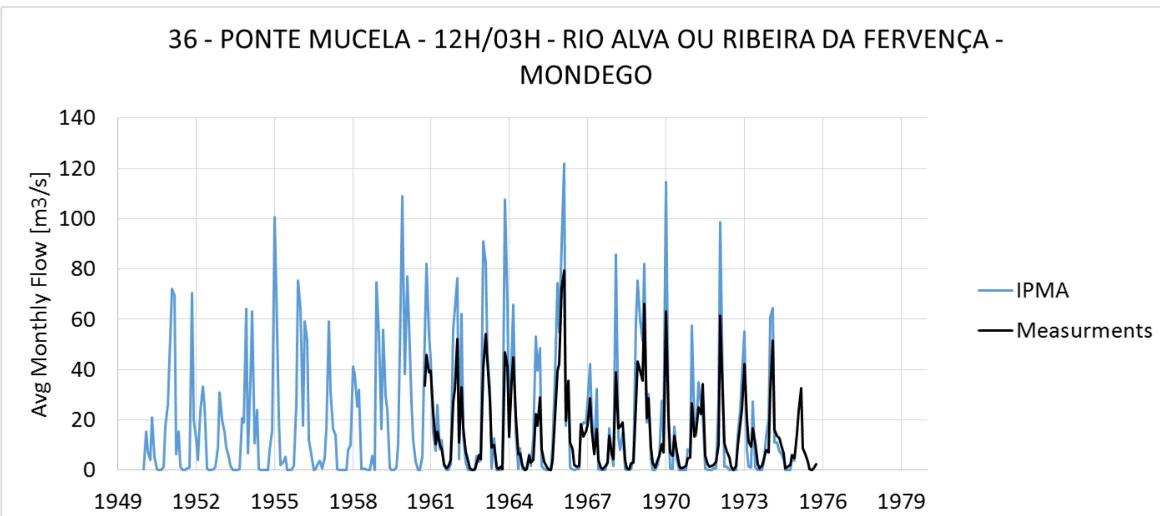
36 - PONTE MUCELA - 12H/03H - RIO ALVA OU RIBEIRA DA FERVENÇA - MONDEGO
Avg Monthly Flow [m3/s]
IPMA
Measurments
1949 1952 1955 1958 1961 1964 1967 1970 1973 1976 1979

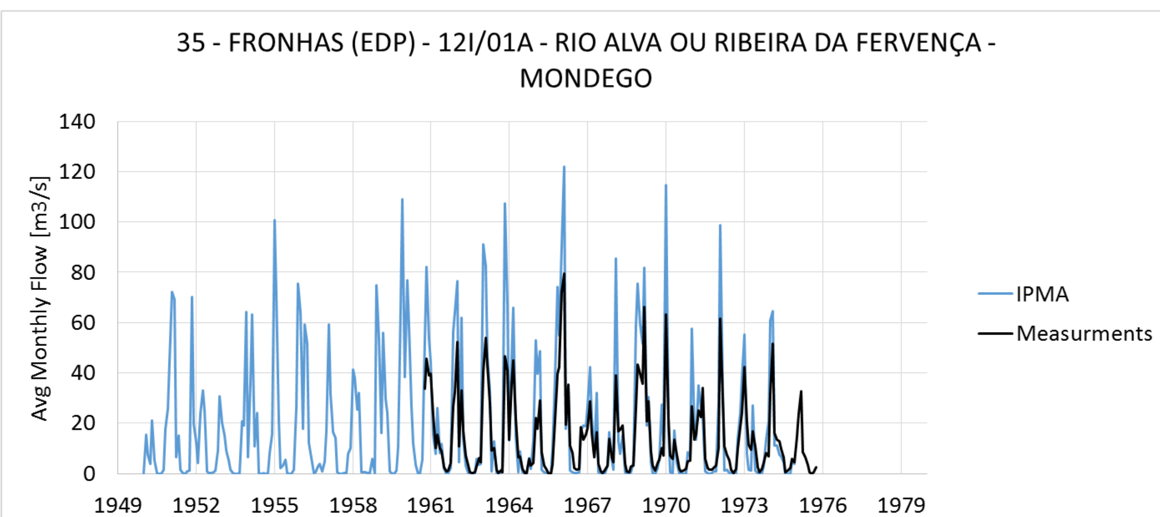
35 - FRONHAS (EDP) - 12I/01A - RIO ALVA OU RIBEIRA DA FERVENÇA - MONDEGO
Avg Monthly Flow [m3/s]
IPMA
Measurments
1949 1952 1955 1958 1961 1964 1967 1970 1973 1976 1979

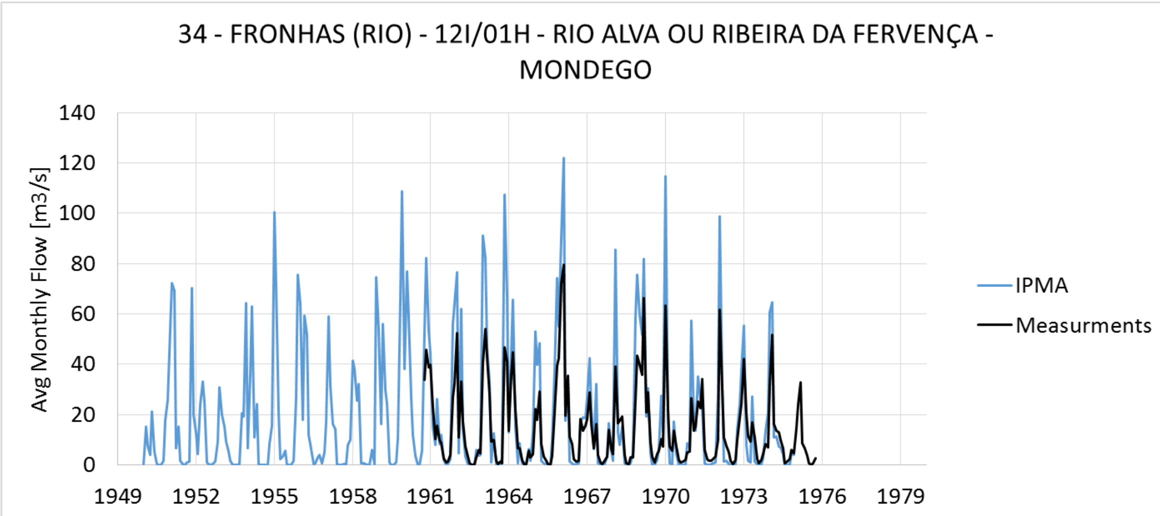
34 - FRONHAS (RIO) - 12I/01H - RIO ALVA OU RIBEIRA DA FERVENÇA - MONDEGO
Avg Monthly Flow [m3/s]
0
20
40
60
80
100
120
140
1949
1952
1955
1958
1961
1964
1967
1970
1973
1976
1979
IPMA
Measurments

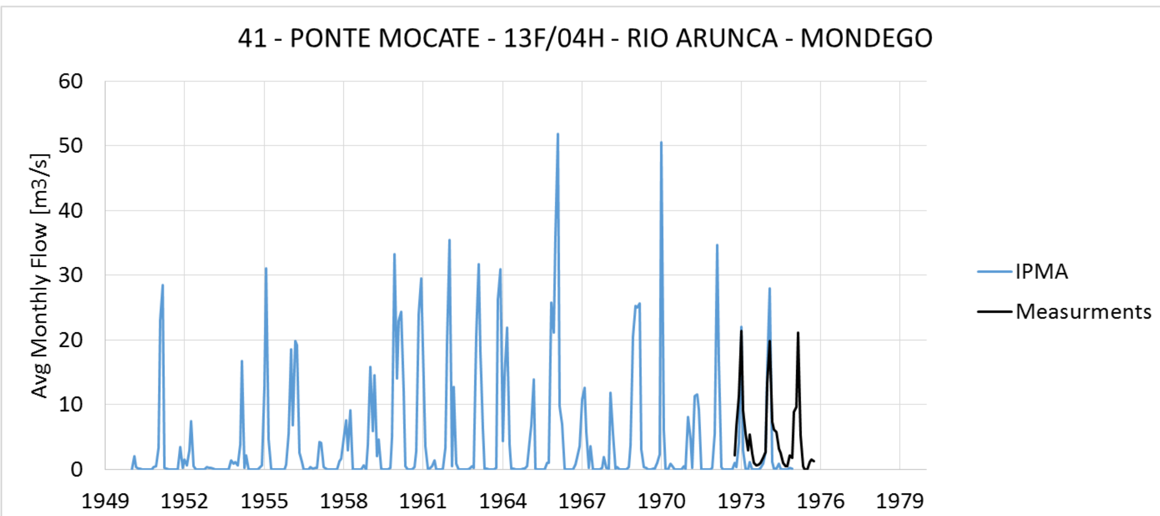
41 - PONTE MOCATE - 13F/04H - RIO ARUNCA - MONDEGO
Avg Monthly Flow [m3/s]
0
10
20
30
40
50
60
1949
1952
1955
1958
1961
1964
1967
1970
1973
1976
1979
IPMA
Measurments

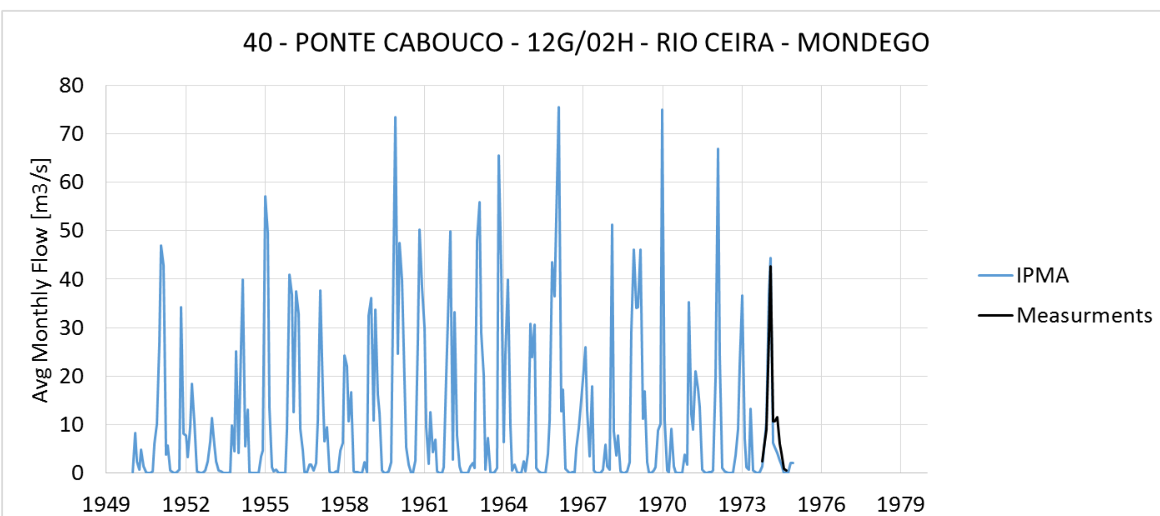
40 - PONTE CABOUCO - 12G/02H - RIO CEIRA - MONDEGO
Avg Monthly Flow [m3/s]
0
10
20
30
40
50
60
70
80
1949
1952
1955
1958
1961
1964
1967
1970
1973
1976
1979
IPMA
Measurments

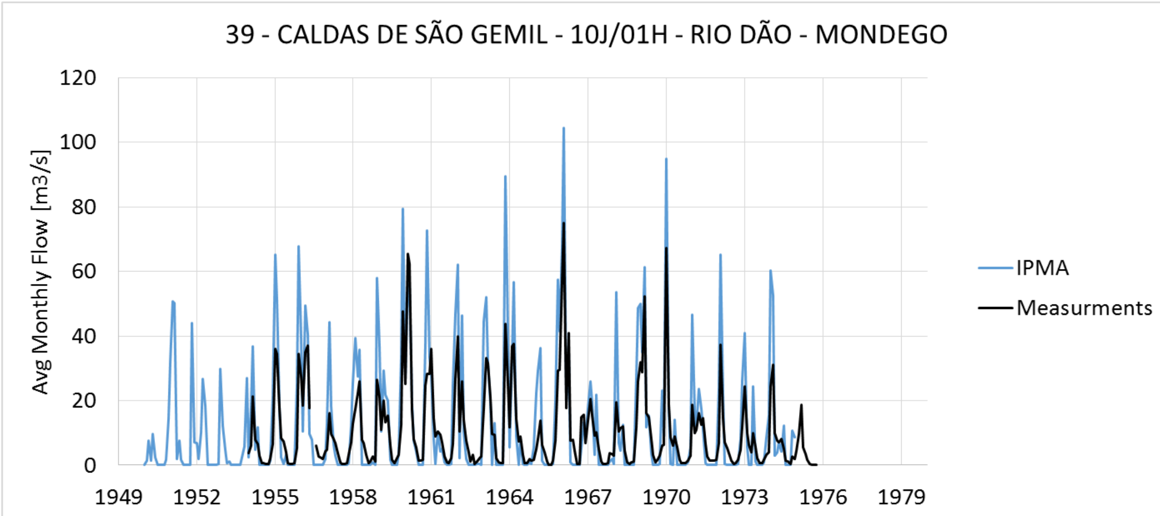
39 - CALDAS DE SÃO GEMIL - 10J/01H - RIO DÃO - MONDEGO
Avg Monthly Flow [m3/s]
0
20
40
60
80
100
120
1949
1952
1955
1958
1961
1964
1967
1970
1973
1976
1979
IPMA
Measurments

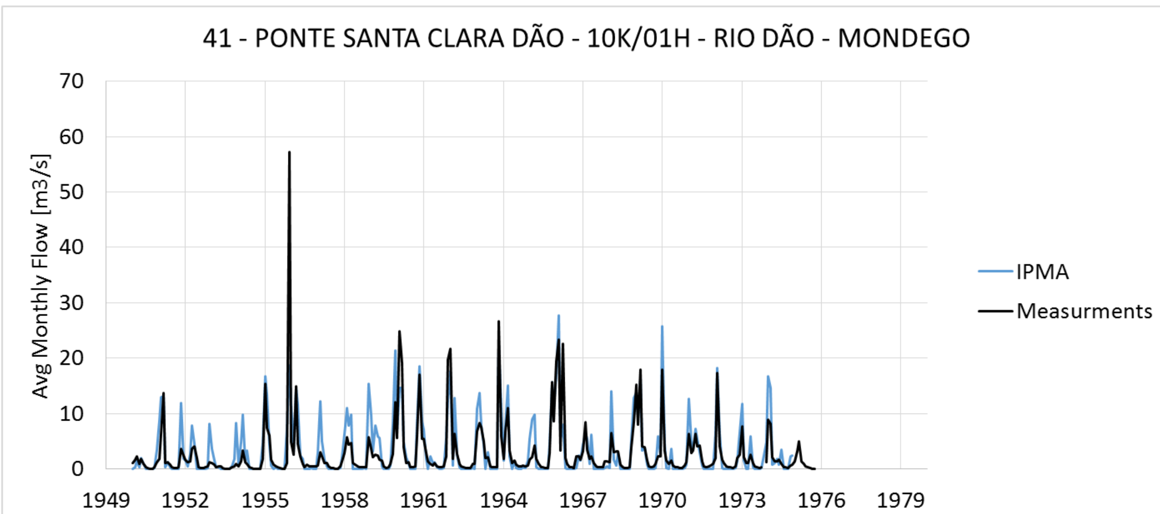
41 - PONTE SANTA CLARA DÃO - 10K/01H - RIO DÃO - MONDEGO
Avg Monthly Flow [m3/s]
0
10
20
30
40
50
60
70
1949
1952
1955
1958
1961
1964
1967
1970
1973
1976
1979
IPMA
Measurments

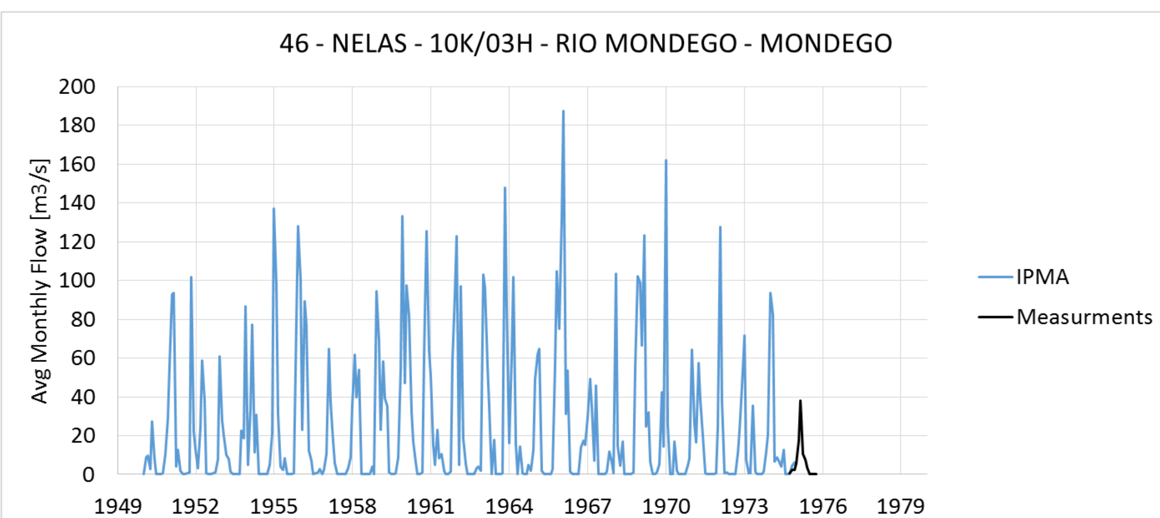
46 - NELAS - 10K/03H - RIO MONDEGO - MONDEGO
Avg Monthly Flow [m3/s]
0
20
40
60
80
100
120
140
160
180
200
1949
1952
1955
1958
1961
1964
1967
1970
1973
1976
1979
IPMA
Measurments

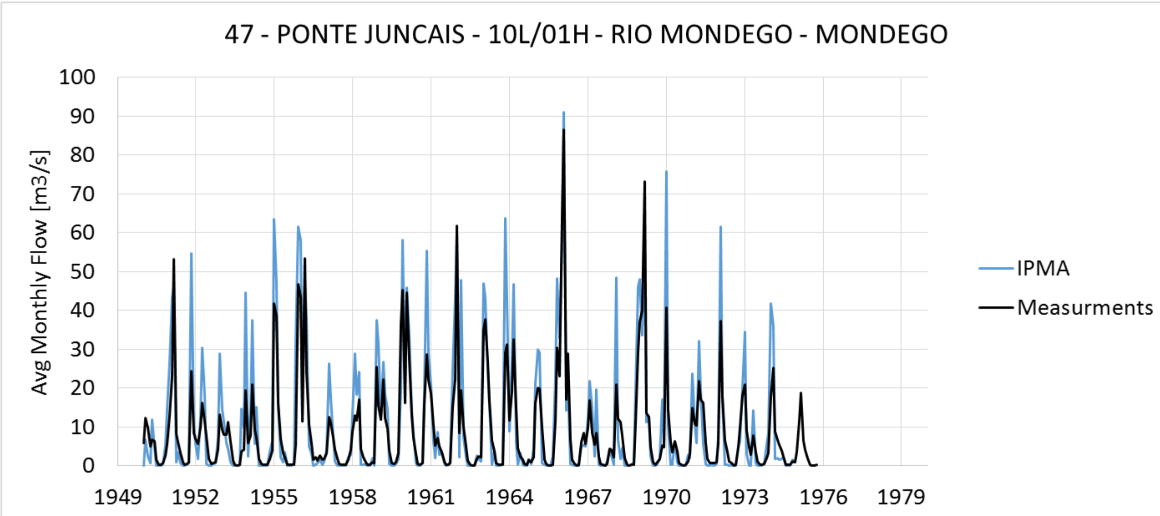
47 - PONTE JUNCAIS - 10L/01H - RIO MONDEGO - MONDEGO
Avg Monthly Flow [m3/s]
100
90
80
70
60
50
40
30
20
10
0
1949
1952
1955
1958
1961
1964
1967
1970
1973
1976
1979
IPMA
Measurments

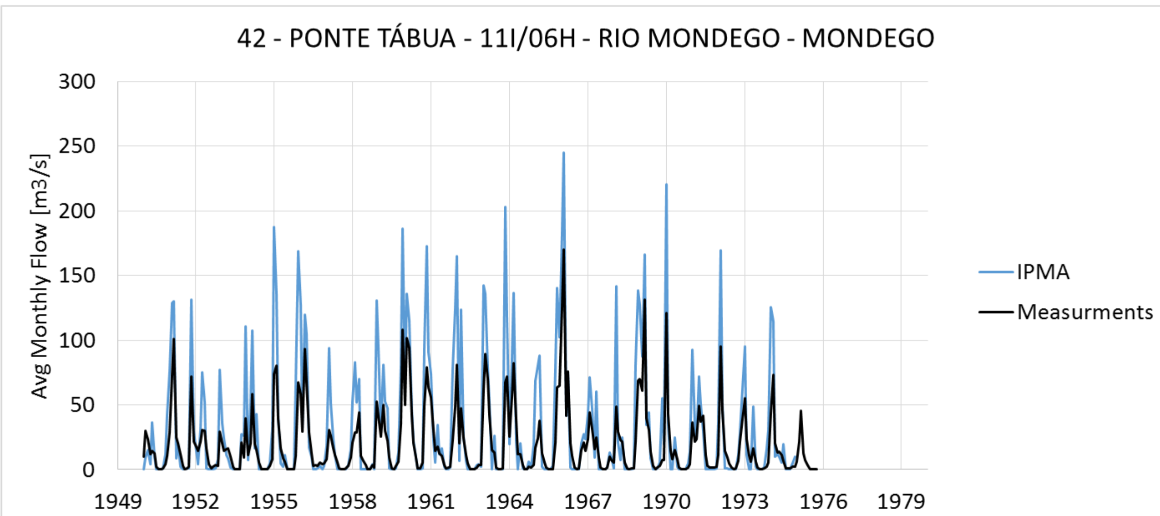
42 - PONTE TÁBUA - 11I/06H - RIO MONDEGO - MONDEGO
Avg Monthly Flow [m3/s]
300
250
200
150
100
50
0
1949
1952
1955
1958
1961
1964
1967
1970
1973
1976
1979
IPMA
Measurments

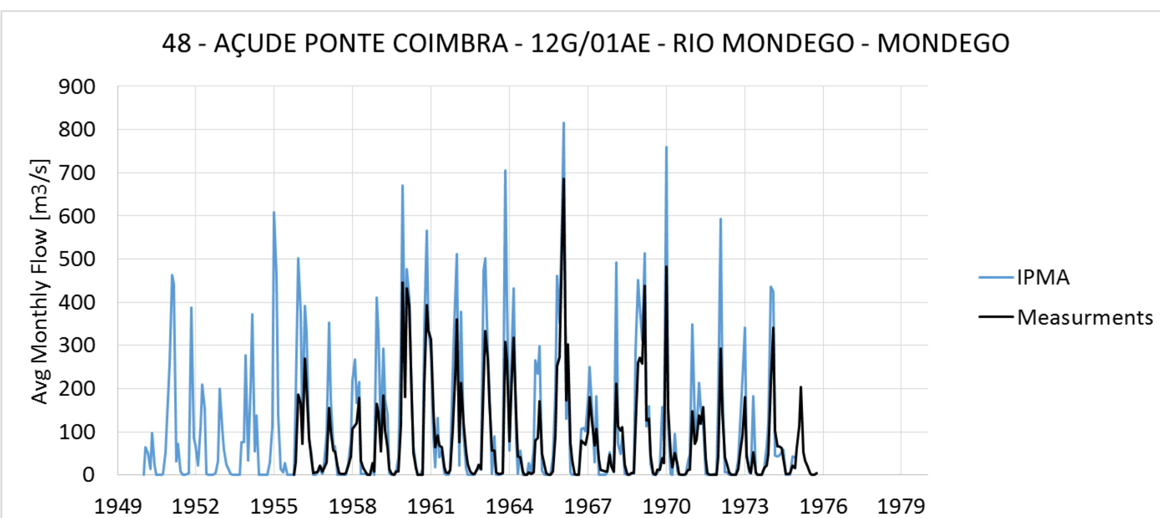
48 - AÇUDE PONTE COIMBRA - 12G/01AE - RIO MONDEGO - MONDEGO
Avg Monthly Flow [m3/s]
900
800
700
600
500
400
300
200
100
0
1949
1952
1955
1958
1961
1964
1967
1970
1973
1976
1979
IPMA
Measurments

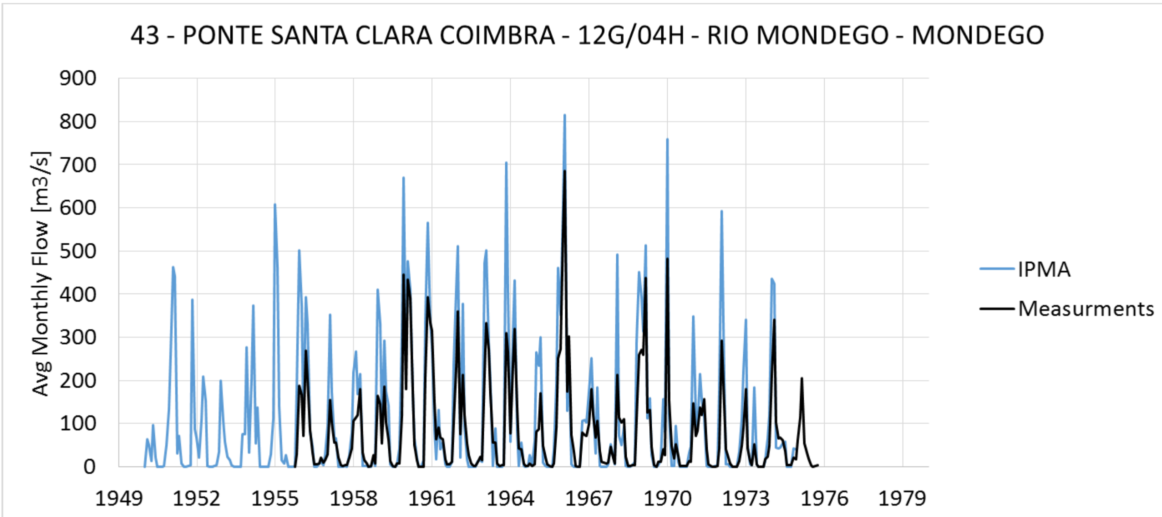
43 - PONTE SANTA CLARA COIMBRA - 12G/04H - RIO MONDEGO - MONDEGO
Avg Monthly Flow [m3/s]
900
800
700
600
500
400
300
200
100
0
1949
1952
1955
1958
1961
1964
1967
1970
1973
1976
1979
IPMA
Measurments

8.5.6 SADO

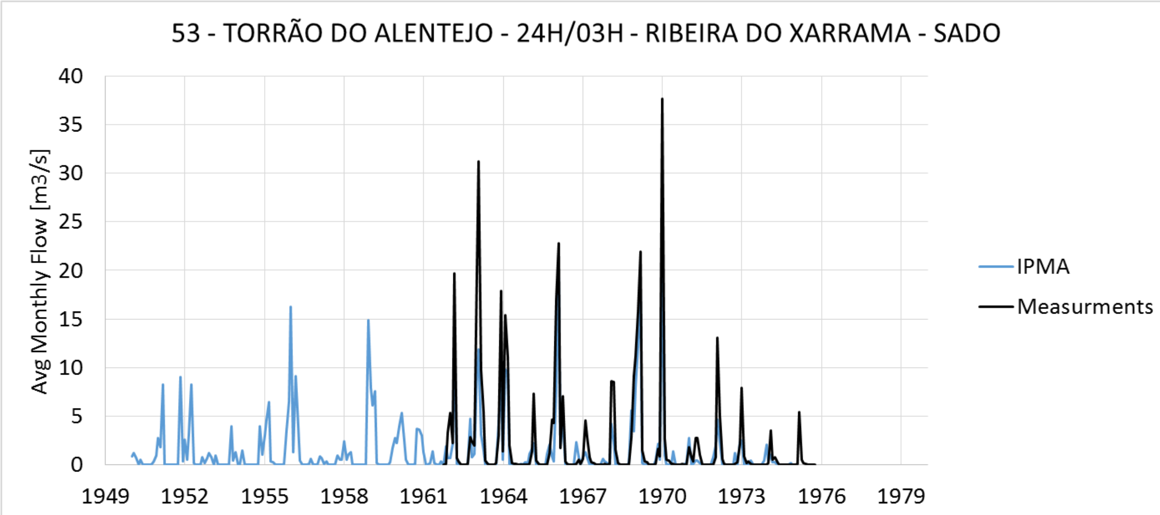
53 - TORRÃO DO ALENTEJO - 24H/03H - RIBEIRA DO XARRAMA - SADO
Avg Monthly Flow [m3/s]
0
5
10
15
20
25
30
35
40
1949
1952
1955
1958
1961
1964
1967
1970
1973
1976
1979
IPMA
Measurments

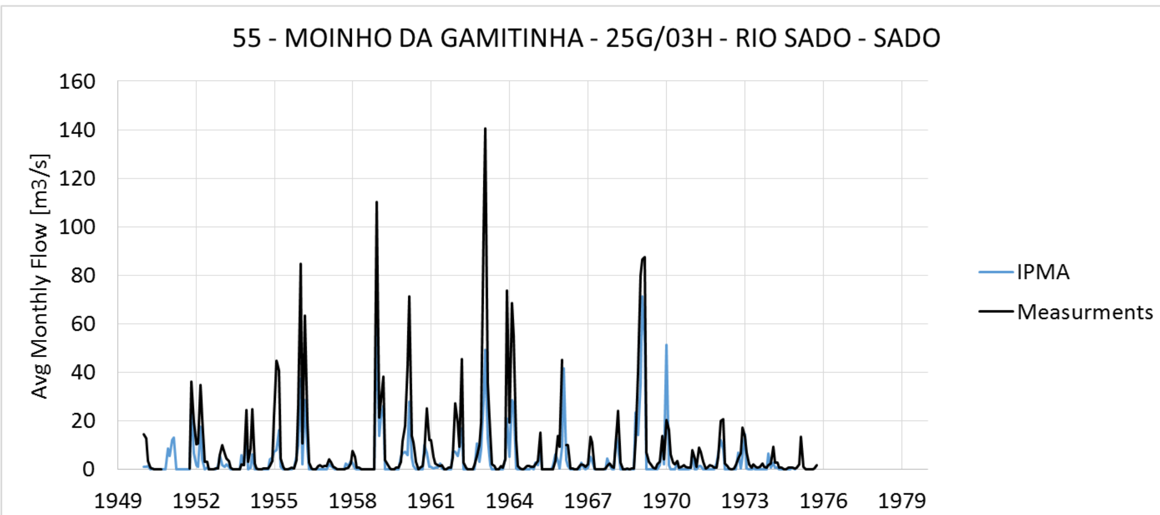
55 - MOINHO DA GAMITINHA - 25G/03H - RIO SADO - SADO
Avg Monthly Flow [m3/s]
0
20
40
60
80
100
120
140
160
1949
1952
1955
1958
1961
1964
1967
1970
1973
1976
1979
IPMA
Measurments

8.5.7 TEJO

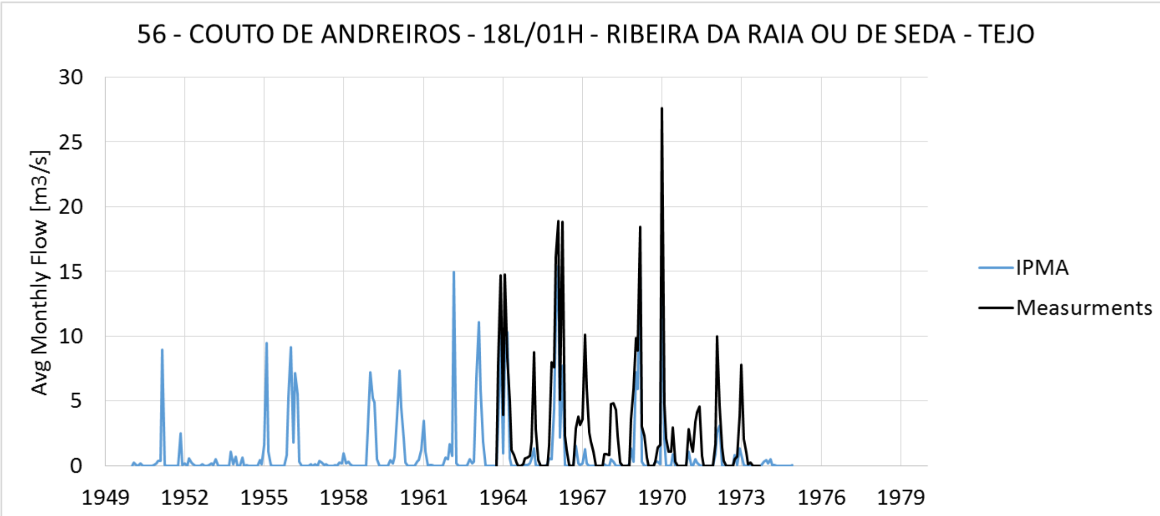
56 - COUTO DE ANDREIROS - 18L/01H - RIBEIRA DA RAIA OU DE SEDA - TEJO
Avg Monthly Flow [m3/s]
30
25
20
15
10
5
0
1949
1952
1955
1958
1961
1964
1967
1970
1973
1976
1979
IPMA
Measurments

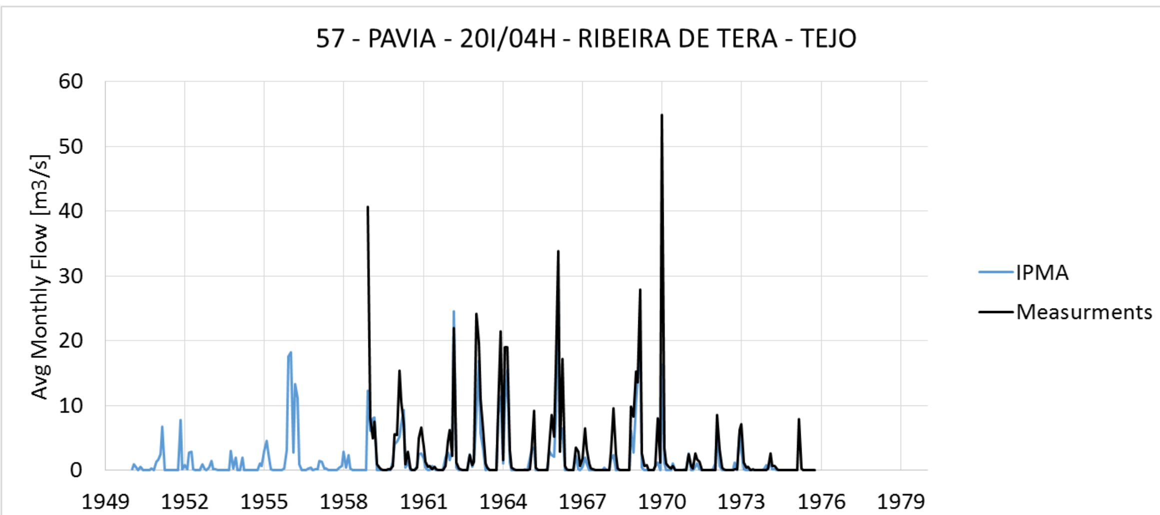
57 - PAVIA - 20I/04H - RIBEIRA DE TERA - TEJO
Avg Monthly Flow [m3/s]
60
50
40
30
20
10
0
1949
1952
1955
1958
1961
1964
1967
1970
1973
1976
1979
IPMA
Measurments

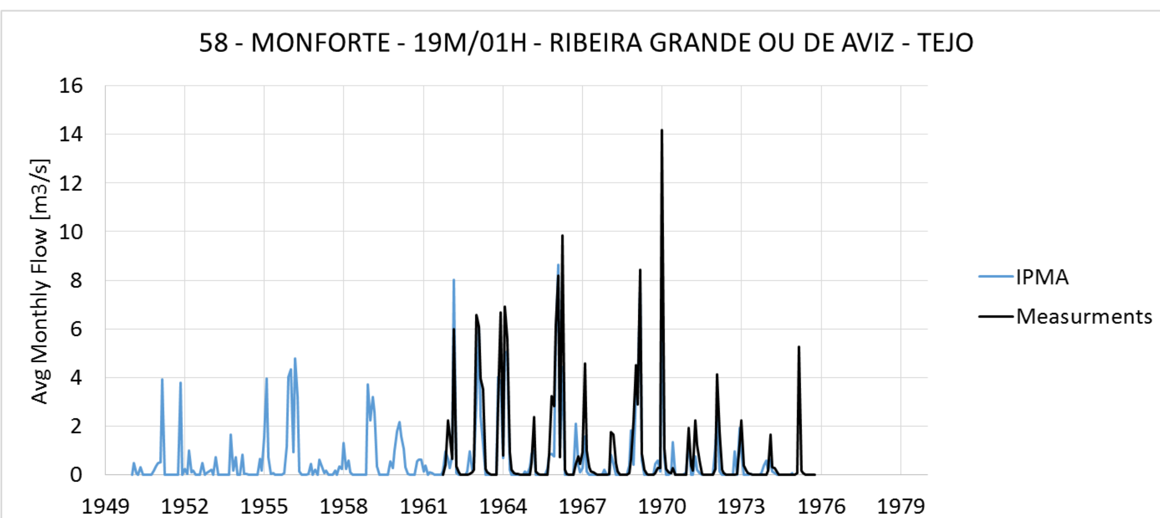
58 - MONFORTE - 19M/01H - RIBEIRA GRANDE OU DE AVIZ - TEJO
Avg Monthly Flow [m3/s]
16
14
12
10
8
6
4
2
0
1949
1952
1955
1958
1961
1964
1967
1970
1973
1976
1979
IPMA
Measurments

8.5.8 VOUGA/RIBEIRAS COSTEIRAS

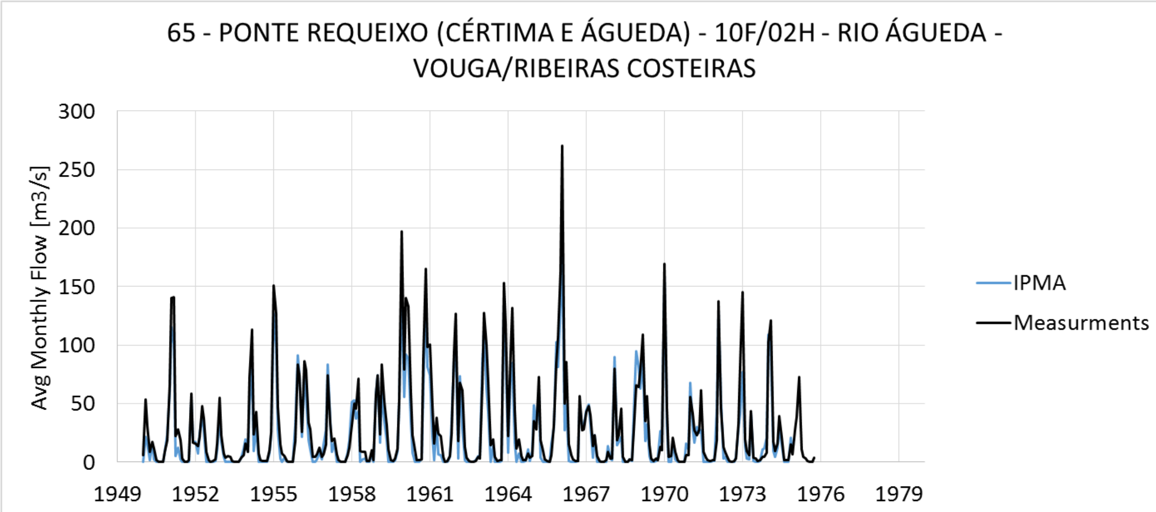

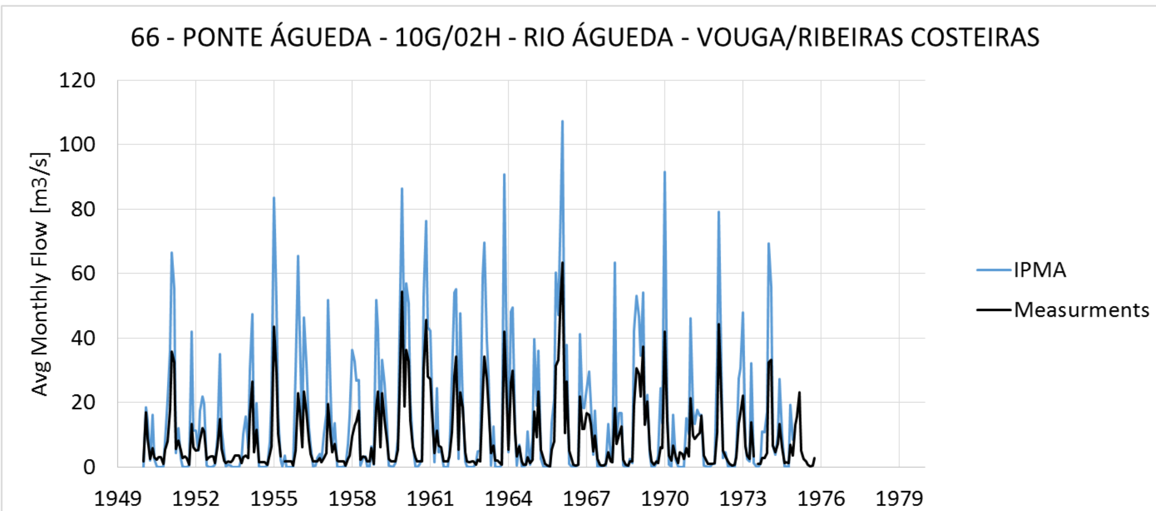

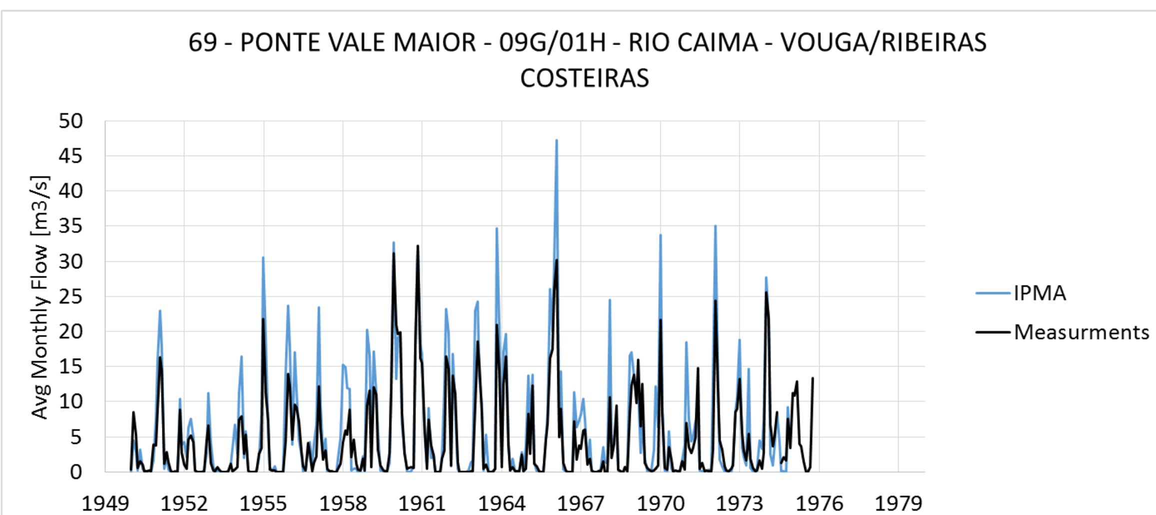

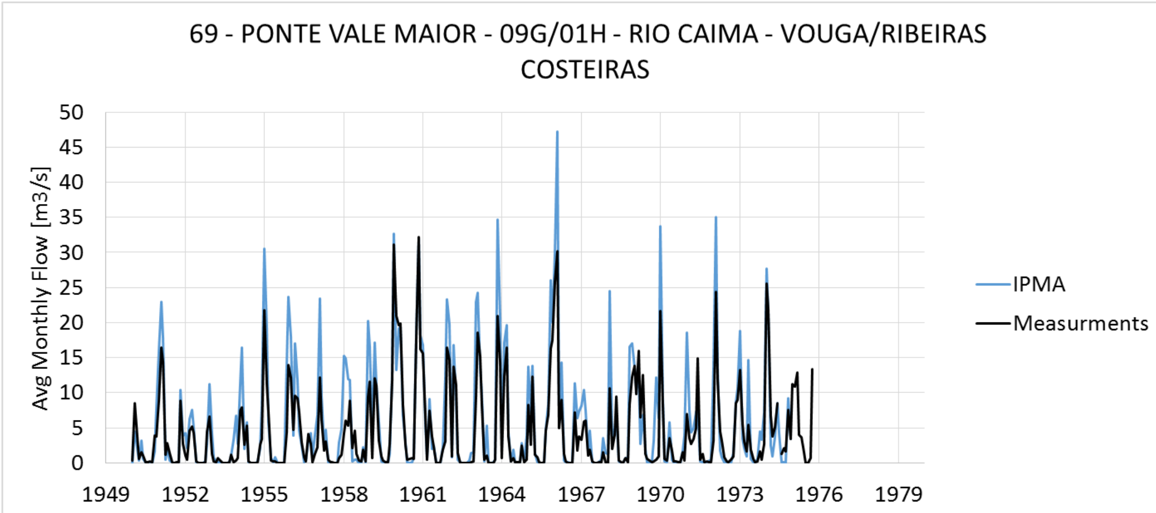
69 - PONTE VALE MAIOR - 09G/01H - RIO CAIMA - VOUGA/RIBEIRAS COSTEIRAS
Avg Monthly Flow [m3/s]
0
5
10
15
20
25
30
35
40
45
50
1949
1952
1955
1958
1961
1964
1967
1970
1973
1976
1979
IPMA
Measurments

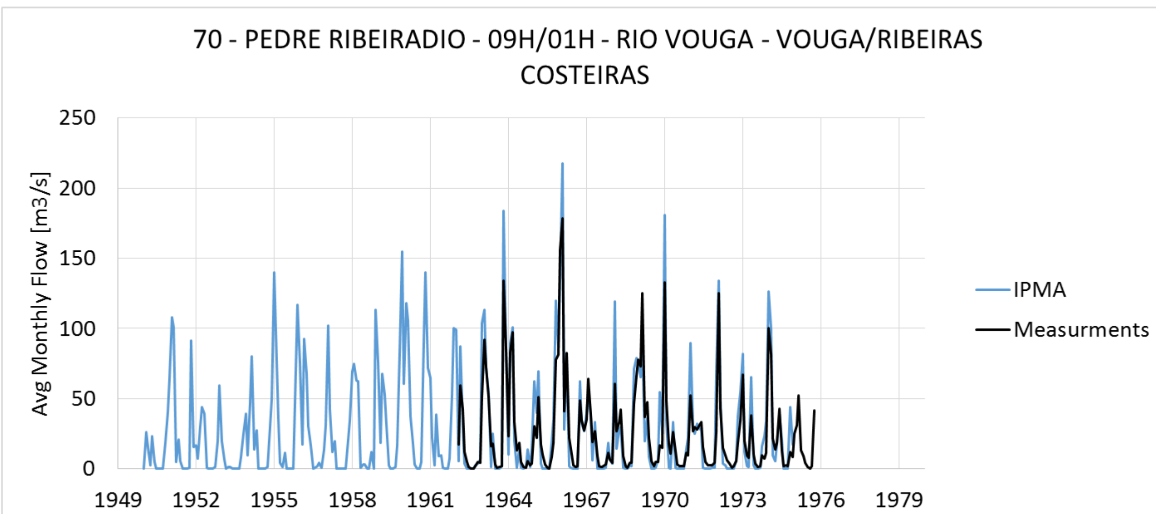
70 - PEDRE RIBEIRADIO - 09H/01H - RIO VOUGA - VOUGA/RIBEIRAS COSTEIRAS
Avg Monthly Flow [m3/s]
0
50
100
150
200
250
1949
1952
1955
1958
1961
1964
1967
1970
1973
1976
1979
IPMA
Measurments

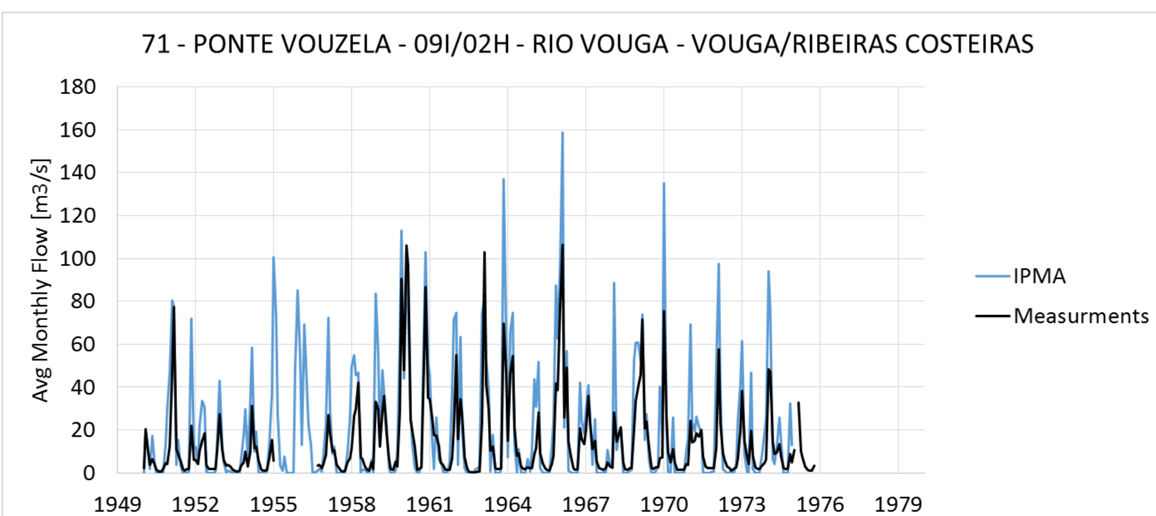
71 - PONTE VOUZELA - 09I/02H - RIO VOUGA - VOUGA/RIBEIRAS COSTEIRAS
Avg Monthly Flow [m3/s]
0
20
40
60
80
100
120
140
160
180
1949
1952
1955
1958
1961
1964
1967
1970
1973
1976
1979
IPMA
Measurments

8.6 Database description

A data base was developed as a Microsoft Access® database application to facilitate storage, handling, and use of hydrologic datasets with a simple graphical user interface.

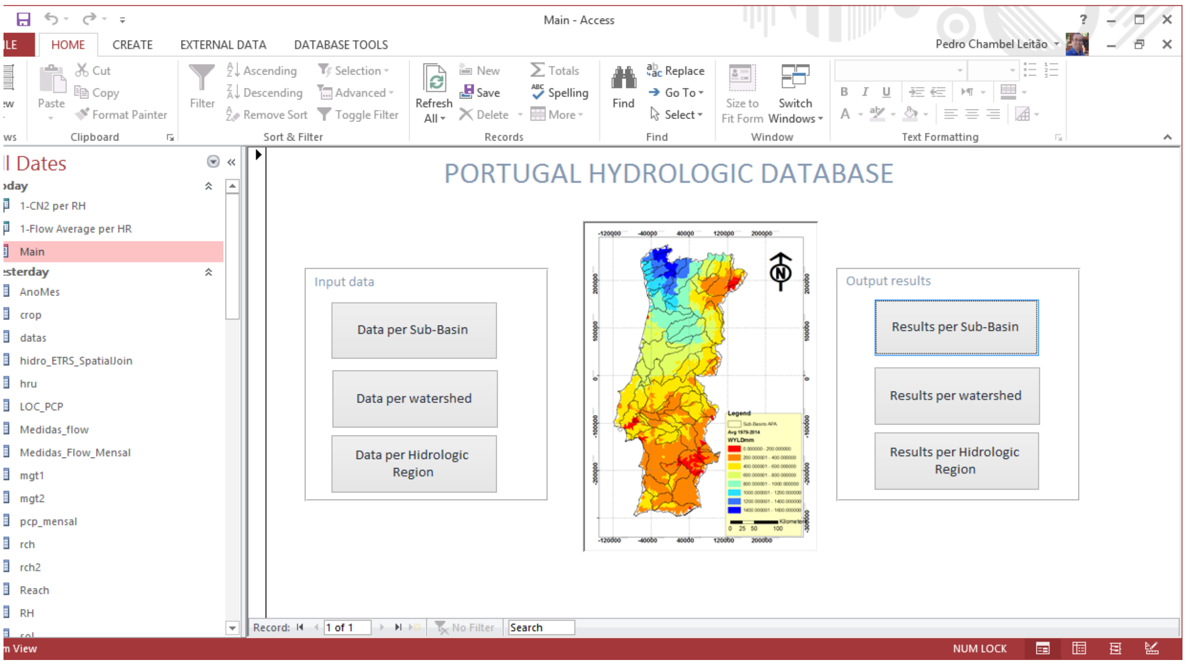

Figure 87 – Interface of Portugal Hydrological database

The database tables are described in Table 21. The presented data shows the most important model inputs per sub-basin: soil, management, geometry (of sub-basin and reaches). It also shows flows in the reach and major fluxes at the HRU level. All this information is related at sub-basin/HRU level with rivers, watersheds and gage stations. This type of setup allows any water manager in Portugal to relate information of the model with their area of interest. This database is complemented with three shape files that allow to see results distributed in space. These shapefiles are sub-basins and reach (Figure 12) and main watersheds and rivers (Figure 10).

The database produced can be considered a relational database. This model organizes data into one or more tables (or "relations") of rows and columns, with a unique key for each row. This allows properly maintenance of data integrity and eases the process of working with other objects in a database. To do this one had to define relationships among the tables in a database (Figure 88).

Table 21 – Database table description

Table name	Description
Crop	Crop parameters per Land Use
Dates	Correspondence of dates with hydrologic year
Gage correspondence to Sub	Location of gage station in relation to the model sub-basins
Gage station	Gage stations from SNIRH with more than 15 years of data and with areas between 100 and 5000 km^2
HRU	Monthly water balance results per HRU
HRU_yearly	Yearly water balance results per HRU
mgt1	CN2 values per HRU
rch_total	Results of modelled flow per reach
Reach	Characterization of reach geometry
RH	Portugal hydrographic regions
Selected gage stations	Gage stations selected (see Appendix 8.2 or Figure 34)
sol	Soil properties per HRU
Sub1	Characterization of reach geometry
tblHruDef	Definition of variables from table HRU
tblRchDef	Definition of variables from table Reach
tblSub1Def	Definition of variables from table Sub1
urban	Crop parameters per urban Land Use
Hydrographic areas	Main watersheds and rivers

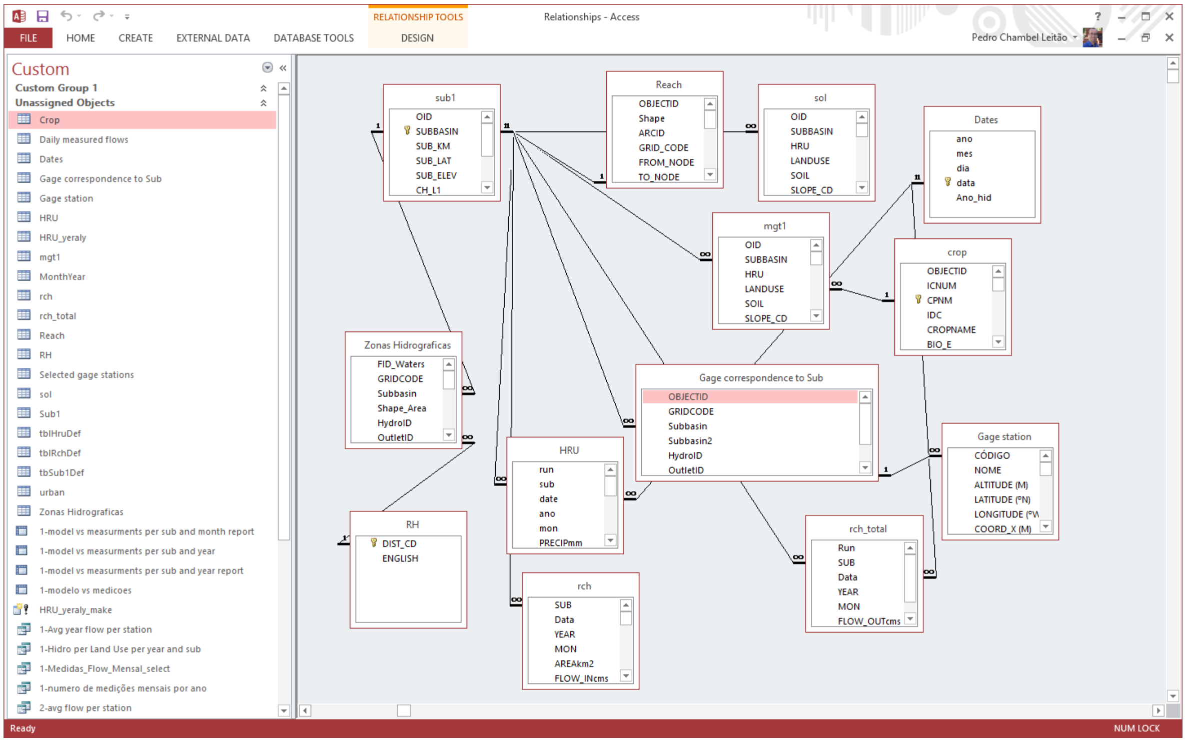

Figure 88 – Table structure of Portugal Hydrological database

In this database the CFSR data has the advantage of being continuously updated. This means that the hydrologic results presented in this thesis can be continuously updated. On the other hand the MM5-R and IPMA-GRID data sets are static in time and do not allow this continuous update. Finally, there are the IPMA-GRID results, based on which the model was calibrated.

The type of results we can get from the database are shown for CFSR in Figure 89, Table 18 and Table 20.

More information on database available in: https://sites.google.com/site/portugalhydrology/

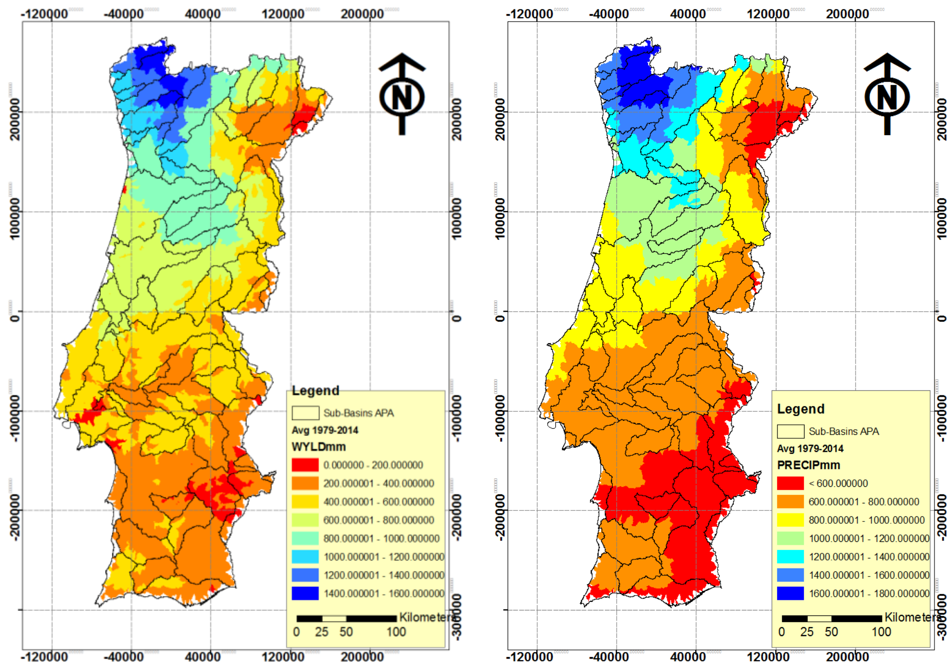

Figure 89 –Flow and precipitation per subbasin using CFSR model (36-year average - 1979-2014)

9 Appendix B

Appendix B is an extended Appendix including brief description of MOHID LAND and two papers related with Hydrologic Modeling in Portugal using MOHID LAND.

The first paper has the following title: "MOHID LAND - Porous Media, a tool for modelling soil hydrology at plot scale and watershed scale". It describes MOHID LAND Porous Media, which was the component of the model where the author of this dissertation was mostly involved. Paper compares soil moisture results with results from Hydrus model. Simulation is made in an agriculture field in Sorraia Basin.

The second paper was presented in the 13º Congresso da Água (Lisboa 2016) with the flowing title: "Operational System for Streamflow Forecasting to Support Hydroelectric Production Management". It presents an operational system to generate flows based on MOHID LAND and SWAT model.

9.1 MOHID LAND

MOHID LAND is a newer model compared to SWAT. It started being developed by the author of this thesis, reusing the code that was written for MOHID Water (Miranda et al., 2000b), in the year 2000 (Neves et al., 2000a). This model has some when compared to SWAT. For example, it enables a wide range of spatial and temporal scales, allowing the simulation of a one square metre plot or a 5000 km^2 watershed, with time steps that can range from seconds to hours. The modular design of MOHID LAND facilitates the integration of other models (Miranda et al., 2000b). Different water quality modules are available for in stream water. Furthermore, this approach minimizes the maintenance costs and allows the development of integrated models of soil water flow and surface water flow.

Table 22 – Comparison between MOHID LAND and SWAT Characteristics and Features

Model	MOHID LAND	SWAT
Suited Applications	Wide range of spatial and temporal scales; modular design facilitates integration of other models; advanced capabilities for water quality and water budget analysis	Watersheds; excellent for calculating TMDLs and simulating a wide variety of conservation practices and other BMPs; successfully applied across watersheds in several countries
Main Components	Hydrology, weather, soil properties, crop growth, nutrients, pesticides, agricultural management and channel routing, overland/channel flow, unsaturated/saturated zone, snowmelt; aquifer/rivers exchange, advection/dispersion of solutes, geochemical processes	Hydrology, weather, sedimentation, soil temperature and properties, crop growth, nutrients, pesticides, agricultural management and channel & reservoir routing
Runoff on Overland	2-D diffusive wave and dynamic wave equations	CN for runoff
Subsurface Flow	3-D groundwater and unsaturated flow	Lateral subsurface flow/ground flow
Chemical Simulation	N, P, pesticides, C, Dissolved conservative solutes in surface, soil, & ground waters	N, P, pesticides, C
Spatial Scale	Distributed (D)	Semi-Distributed (SD)
Temporal Scale	Event-base (E); Continuous (C); variable steps	Continuous (C); daily steps
Watershed Representation	2-D rectangular/square overland grids; 1-D channels; 3-D unsaturated/3-D saturated flow	Sub-basins based on topography, HRU, ponds, groundwater, & main channel
Availability	Public (Pu)	Public (Pu)

The MOHID Water Modelling System allows the connection of different models joining various water pathways and water masses. This system has produced a set of coupling between models (Chambel-

Leitão et al., 2007a). This approach was important to accomplish the European TempQSim (www.tempqsim.net) aims for adapting models to temporary waters in Southern European catchments (Obermann, 2007, Trancoso et al., 2009). MOHID River Network (MRN) was one of the main outputs of this project. When MRN is coupled to MOHID LAND, river channels can lose or gain water, depending on the hydraulic gradient between the water level in the channel bed (or Mediterranean temporary ponds) and the level of the aquifer. This approach is possible because MOHID LAND explicitly simulates the level of the aquifer (Trancoso et al., 2009). When running MRN as standalone, water from the channels (or from ponds) can infiltrate the river bed at a constant user-established rate, defined as the saturated conductivity of the sediment in the channel bed.

MOHID is an integrated system for water flow, consisting of three main modules: Water for three-dimensional fluid dynamics, Land for hydrology and Soil for groundwater flow. The MOHID LAND module is a watershed mathematical model — or hydrological transport model — designed to simulate the flow of water in a drainage basin and aquifer. The processes which are simulated include two-dimensional overland runoff, infiltration into the ground, one-dimensional drainage network flow through rivers and canals, as well as (saturated and unsaturated) porous medium transport. The interactions between the different processes (like water exchange between aquifer and river) are calculated dynamically by the model, using the hydraulic gradients. The different processes occurring in a basin are programmed in different modules. The user can choose which modules to activate, allowing simulation of the desired ones only.

MOHID LAND model has been used to study the water and nitrogen dynamics in Portuguese corn fields. The model has been validated for soil moisture, nitrogen dynamics and plant growth (Trancoso et al., 2009, Barão, 2007, Gonçalves et al., 2007). MOHID LAND was developed within the framework of three EU-funded projects: EcoRiver, TempQsim and ICReW for the simulation of water flow in watersheds with pathways for rivers and groundwater flows. The soil and plant modules were developed in close collaboration with soil scientists from EAN-INIA (Gonçalves et al., 2007).

The MOHID system is divided into three major classes: (i) flow properties, (ii) property transport by flow and (iii) transformations in transported properties. The flow properties are the base of the entire system, computing, in the case of soils, water content, pressure, water fluxes and hydraulic conductivity at each point of the grid. The transport – Eulerian or Lagrangian – uses these properties for simulating advection diffusion of solutes (and of particulate material in surface flows). The transformations that occur in properties are treated as a specific class, which includes all biological and chemical properties. In the case of soils, this class includes the microbiological activity and adsorption/desorption processes. Root activity will also be implemented in this class and will be included in an atmospheric forcing module. The fertilization process is treated as boundary condition as well as the irrigation.

9.2 Open Hydrology paper

MOHID LAND - Porous Media, a tool for modelling soil hydrology at plot scale and watershed scale

Chambel-Leitão, P., Ramos, T.B., Domingos, T., Neves, N.

MARETEC, Instituto Superior Técnico, Universidade de Lisboa, Av. Rovisco Pais, 1049-001, Lisboa, Portugal; e-mail: chambelpc@tecnico.ulisboa.pt

9.2.1 Abstract

Hydrological modelling is becoming more important in water management. Soil hydrological models are increasingly being used to provide services to farmers and to water supply managers. This study tests the stability and effectiveness of MOHID LAND-PM in modelling soil water dynamics. Soil water flow and content were simulated in five soils with different soil textures (sand, sandy loam, clay, loam, and silt). The results were then compared with HYDRUS-1D simulations using the same input data. The soil domain was divided into 100 layers up to a depth of 2 m. Five additional simulations were carried out in MOHID LAND-PM in order to quantify the error of reducing the number of layers to 10 (instead of 100) when discretizing the soil profile. This is relevant in a watershed model like MOHID LAND-PM since the computing time is greatly reduced. MOHID LAND-PM results were compared with those of HYDRUS using Nash-Sutcliffe model efficiency (NSE) and Percent bias (PBIAS). Soil volumetric water content, pressure heads, and soil water velocity were compared for 4 depths. For the water contents, NSE was above 0.87 for sand and above 0.97 for all other soils and layers except for the clay soil (NSE ≥ 0.01). For pressure heads, NSE > 0.46 for sand and > 0.98 for all other soils and layers except clay (NSE ≥ -23.95). Statistical analysis shows a soil water velocity of NSE below 0.0 for most sand and clay depths, and above 0.58 NSE for all other soils. PBias shows that in general, MOHID LAND-PM tends to underestimate HYDRUS soil water content and velocities.

KEYWORDS: Infiltration; HYDRUS; MOHID LAND-PM; Richards equation; soil water content; soil layer discretization.

9.2.2 Introduction

The entire world is experiencing changing water use patterns as a result of changes in land use (Foley et al., 2005). In developing countries, the occupation of natural landscapes by agriculture is a major cause, and developed countries are facing changing cropping patterns. In both cases economic factors driven by the globalisation of world trade are involved. In both cases further global movement is expected as a result of climate change.

Water availability is essential for socio-economic activities and citizens expect water supply managers to take the necessary measures for assuring quantity and quality for direct and indirect human consumption. Some authors are raising the possibility of transforming water into a commodity (Kaufman, 2012). From this perspective the share of the worldwide soil water balance can become a measure of the prosperity of a country, and evapotranspiration can become an expense to a country. The knowledge of the processes determining water's end use, actual reserves and the capacity to forecast water consumption are essential for catchment managers' decision making. For this it is essential to have the possibility of making operational a watershed model capable of modelling all fluxes in the global water cycle (precipitation, evapotranspiration, infiltration, aquifer recharge, etc.).

The estimation of evapotranspiration is very important for any hydrologic simulation. Reference evapotranspiration is normally calculated using FAO-56 method (Allen et al., 1998) (Allen et al., 2006). Mohid_land uses the same formulation. However, more recent papers point out that newer, more accurate methods exist to calculate evapotranspiration (Valipour, 2015, Valipour, 2014). However, this is not the focus of this paper, but it should be in future papers, due to the importance of evapotranspiration calculations.

MOHID LAND is a watershed model developed within the MOHID WATER framework (Braunschweig et al., 2004, Miranda et al., 2000a). It has the advantage of being an open integrated watershed model, using an easy to read Fortran code developed for Windows and Linux environments. MOHID LAND can use standard hdf format to generate results or read input information. It has a set of tools to generate continuous grid data, based on netcdf dat and ESRI ascii data. The model is parallelized using open MP allowing a reduction in computing time. It is fully compliant with the operational Aquasafe system (Leitão et al., 2012b) and the Art system (Campuzano et al., 2012)

MOHID LAND - Porous Media (PM) was the first component of MOHID LAND, developed in 2000 using the MOHID philosophy and implicitly solved the Richards equation using "θ-modified Picard method". In its first version, MOHID LAND-PM could be used to carry out 1D, 2D or 3D simulations (Neves et al., 2000b). Later, methods to solve the Richards equation were improved and compared with field measurements and Hydrus simulations in a single soil (Galvão et al., 2004). Later "θ-modified Picard method" was replaced by the use of the Richards Equation. After these changes, MOHID LAND-PM was again compared with soil moisture measurements and soil moisture simulations using the Hydrus and RZWQM models (Barão et al., 2010). Comparisons were made only for one soil type and had no statistical analysis. This study presents the results for 5 different soil types and provides a statistical analysis for water content, pressure head and soil water velocity.

Simultaneously, Mohid River Network (MRN) was added and MOHID LAND RunOff (RO) were included, and the first model validation of the watershed scale was made (Trancoso et al., 2009). Both MRN and MOHID LAND-RO can run as standalone models. The first is suited for river simulations and the second is more appropriate for flood simulation.

No previous works with MOHID LAND-PM have tested stability and effectiveness of the current version of MOHID LAND-PM in modelling soil water dynamics. This study analyses the MOHID LAND-Porous Media (PM) component of MOHID LAND catchment model (Trancoso et al., 2009). We present a few test cases which may help model stability and effectiveness in future irrigation and watershed modelling studies.

9.2.3 Methods

9.2.3.1 The MOHID LAND-PM model

In MOHID LAND-PM, flow is calculated based on mass and momentum conservation equations. It is assumed that the inertial forces are nil. This generates equilibrium between pressure, gravity, and viscous forces. Using the concept of conductivity, the momentum conservation equation becomes the Darcy equation, which when replaced in the mass conservation equation becomes the Richards equation (Celia and Binning, 1992):

$$\frac{\partial}{\partial t}\iiint \theta dV = \iint \left(-k\vec{\nabla}(h+z)\cdot\vec{n}\right)dA + S \qquad (9)$$

where θ [-] is the soil volumetric water content, V [m³] is the volume of integration whose surface is A [m²], $\vec{n}$ is the exterior unit normal to the volume surface, k [m/s] is the hydraulic conductivity, h [m] is the pressure head, z [m] is the vertical coordinate, t [s] is time and S [m³] represents the addition or extraction of water in the control volume (e.g. extraction by roots).

The relation between the pressure head (h) and the volumetric water content (θ) is given by the van Genuchten model (Vangenuchten, 1980):

$$h(\theta) = -\left|\frac{\left(S_e^{-\frac{1}{m}}-1\right)^{\frac{1}{n}}}{\alpha}\right| \qquad (10)$$

$$m = 1 - 1/n \quad , \quad n>1 \qquad (11)$$

$$S_e = \frac{\theta - \theta_r}{\theta_s - \theta_r} \qquad (12)$$

where θ_s and θ_r (m^3/m^3) are the saturated and residual water contents, respectively, and α (1/m) and n (-) are empirical shape parameters.

Equation (10) is non-linear, requiring an iterative process to solve a non-stationary, unsaturated flow. Hydraulic conductivity is calculated according to (Vangenuchten, 1980):

$$k(\theta) = k_S S_e^L \left(1 - \left(1 - S_e^{\frac{1}{m}}\right)^m\right)^2 \qquad (13)$$

where L is an empirical shape parameter (-) and k_S the saturated hydraulic conductivity (m/s).

The main difficulty in solving these equations is the non-linearity of the hydraulic soil properties and the definition of the calculation grid. The difficulty increases in tri-dimensional grids. MOHID is based on the finite volumes method. Thus, the simulation domain is divided into a group of control volumes of finite sizes (hence the name "finite volumes"). In MOHID LAND-PM these volumes are called cells. Cells are defined in the vertical direction using layer depth. In the horizontal direction the cells are defined using a cell corner and cell length from the east-west and north-south directions.

Figure 90 shows the calculation points for each of the state variables in an Arakawa C-grid (Arakawa and Lamb, 1977). θ, h and k are calculated in the centre of the volumes and the fluxes are calculated in the faces of the volumes. The k that are necessary to calculate the fluxes in the faces are obtained normally by averaging values in the adjacent cells. The hydraulic gradients of equation (9) ($\vec{\nabla}(h+z)$)are calculated with the h values of the cells adjacent to the face.

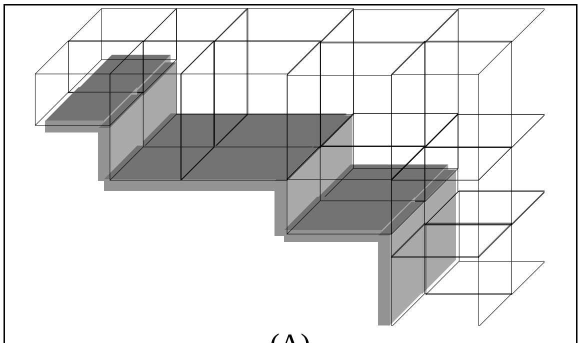

(A)

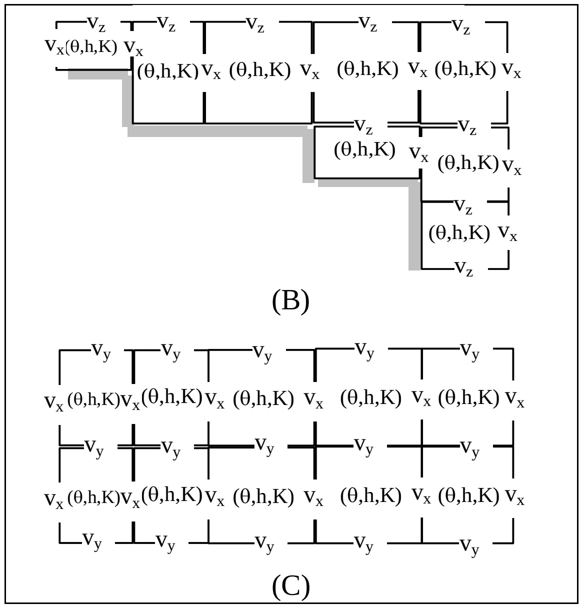

Figure 90 – Different perspectives of a MOHID LAND-PM grid: (A) tri-dimensional view (B) profile view and (C) top view. Also the location of the state variables of the model, where θ [-] is the soil volumetric water content, k [m/s] is the hydraulic conductivity, h [m] is the pressure head in the centre of the cells and V_x, V_y,V_z [m³] are the water velocities in the cell faces in the three directions

The source code and additional documentation for MOHID LAND can be accessed at the MOHID code repository website (http://mohid.codeplex.com). Modelling was done using version 88294 (http://mohid.codeplex.com/SourceControl/changeset/88294) of MOHID LAND, released on 28.02.2014. Two interfaces are available to prepare inputs and to analyse model results: (i) MOHID GIS and MOHID GUI (Braunschweig et al., 2004), free and available at www.mohid.com; and (ii) MOHID Studio, which is the commercial interface available at www.actionmodulers.com.

9.2.3.2 The HYDRUS Model

HYDRUS is as a reference model used in vadose zone modelling (Martinez et al., 2013, Simunek and van Genuchten, 2008). It has been often used in irrigation management (Ramos et al., 2012, Ramos et al., 2009, Forkutsa et al., 2009) and aquifer recharge modelling (Vithanage et al., 2010). HYDRUS also solves the Richard equation. However, HYDRUS uses nodes (finite elements) to describe the geometry of the soil in opposition to the finite volumes available in MOHID LAND-PM. The van Genuchten model is also available to describe the soil hydraulic properties (Vangenuchten, 1980).

HYDRUS-1D model version 4.16 used was retrieved from the HYDRUS site (http://www.pc-progress.com/en/Default.aspx?h1d-downloads).

9.2.3.3 General Model Setup

A vertical 1D geometry was defined In MOHID LAND-PM. The soil was divided into 100 layers up to a depth of 2 m (Table 23). The time step was variable, with a maximum of 3600 and a minimum of

0.001 seconds. The average time step was 50 seconds. The average number of iterations, for convergence in each time step, was 5. Simulations were carried out between 2013-05-01 and 2013-10-15 (168 days). The model was run on a CPU Intel® Core™ i7-2600 Processor with 8 GB RAM. The simulation took 63.76 seconds with a total CPU time of 62.70 seconds. The results of the simulation occupied 1.5 MB of disk space (excluding the 50 MB of the DT log).

Atmosphere boundary conditions were defined using historical hourly data from the meteorological model available at http://meteo.tecnico.ulisboa.pt/. Atmospheric properties used were precipitation (mm), air temperature (ºC), solar radiation (W/m2), relative humidity (-) and wind modulus (m/s). The model also included values of irrigation, measured in a field test located in the same region where the meteorological data was obtained Figure 92. Figure 91 presents the meteorological data used in this study. Hourly reference evapotranspiration was calculated using the FAO-56 method (Allen et al., 1998) (Allen et al., 2006) and used in model simulations, i.e., crop coefficients were set to 1. No plant growth was considered effectively assuming that all water evaporated was taken from the surface soil layer (and not from different layers as is the case when roots are calculated). No evaporation was computed from the water column. The lowest boundary condition was set to zero flux. Output of the model was set to daily. The accumulated error was 2.9E-11 m^3 after the 168 days of simulation. This corresponds to 3.9E-09% of the total soil water available in the end of the simulation.

Models were run for soils with five different soil textures: sand, sandy loam, clay, loam and silt. Soil hydraulic properties were obtained from (Carsel and Parrish, 1988). The soil hydraulic properties used are shown in Table 25.

In HYDRUS-1D, geometry was defined with 101 nodes (Table 24). Time step was variable and had a maximum time step of 3600 and minimum of 0.001 seconds. The average time step was 1600 seconds and the average number of iterations, for convergence in each time step, was 3. The period of simulation was the same as that used in MOHID LAND-PM simulations. The simulation took 2.6 seconds with a total CPU time of 2.6 seconds. HYDRUS output files occupied 6 MB of space. Output of the model was set to daily. The accumulated error was 1.6E-06 m^3 after the 168 days of simulation. This corresponds to 3.9E-09% of the total soil water available in the end of the simulation.

As HYDRUS-1D does not calculate reference evapotranspiration, the same atmospheric input data used in MOHID LAND-PM was used as input in HYDRUS-1D simulations. This means that it provided the same precipitation and evaporation to both models. Evaporation was that calculated by the MOHID-LAND model. The option used on the surface boundary of HYDRUS-1D was

"Atmospheric Boundary Condition with surface layers". This means that a water column can be formed on the surface when precipitation plus irrigation flux exceeds infiltration flux. Bottom boundary condition was set to zero flux. Both model outputs were set at 8, 18, 36, and 70 cm depth.

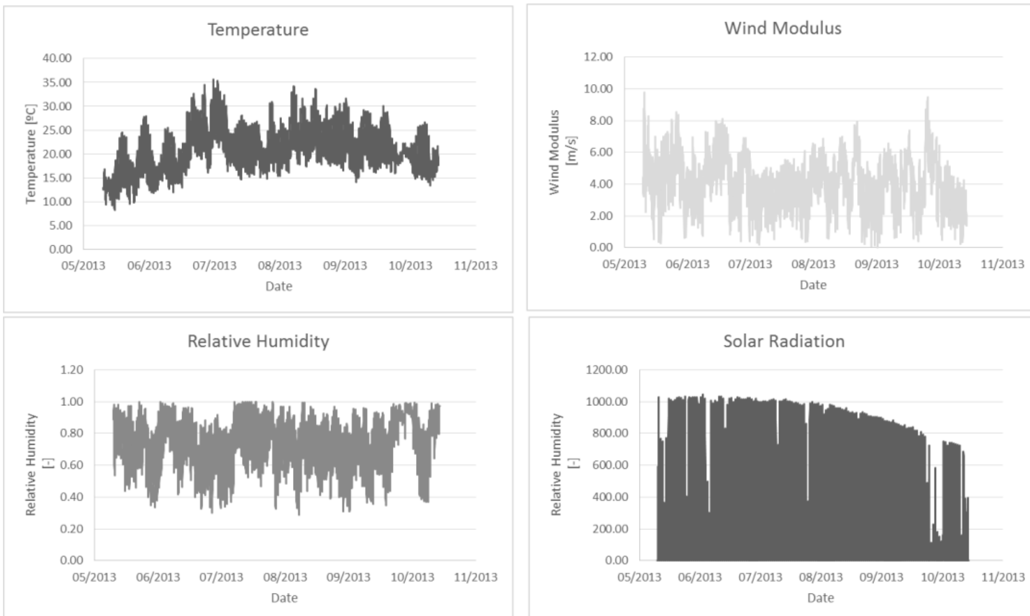

Figure 91 - Meteorological data for the simulated period

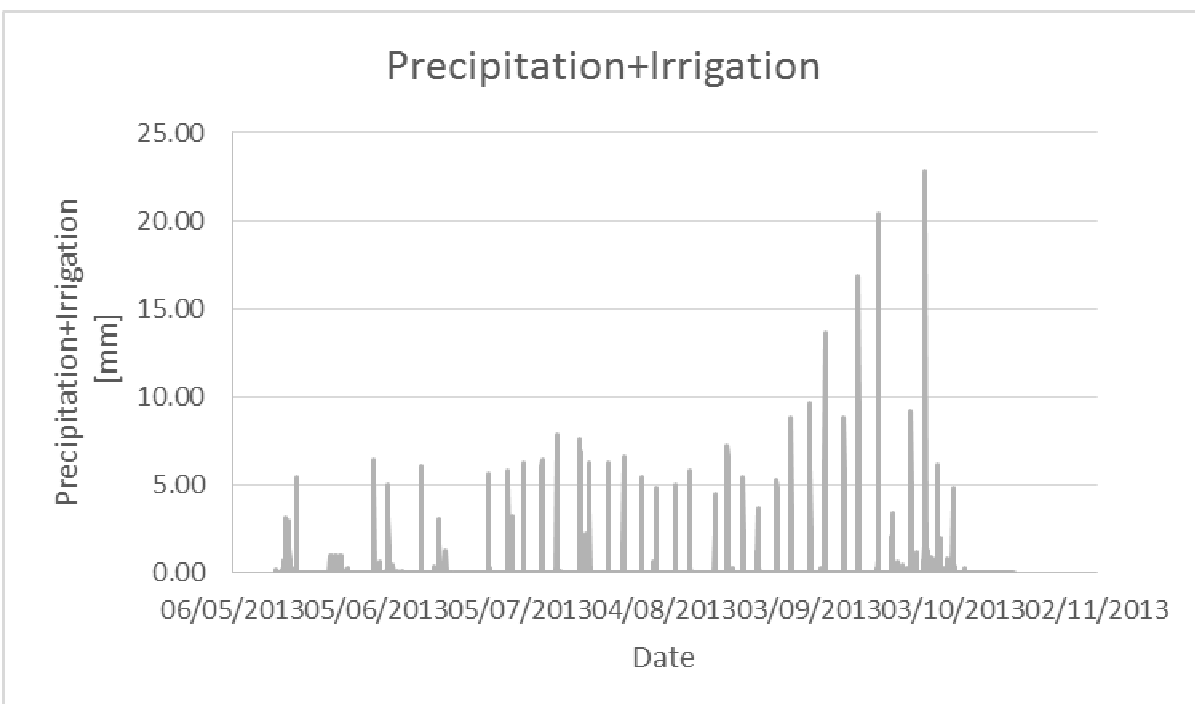

Figure 92 – Precipitation + irrigation for simulated Period

Table 23 – Layers in MOHID LAND model

Layer number	1	2	65	82	91	(...) 95	96	97	98 (...)	100
Depth of the centre of layer [cm]	198.5	196	70	36	18	10	8	6.5	5	1
Depth of layer bottom [cm]	200	197	71	37	19	11	90	7	6	2

Table 24 – Layers in HYDRUS model

Node number	101	100	36	19	10	6	5	4	3	2	1
Node depth [cm]	200	198	70	36	18	12	8	5	3	1	0

Table 25 – Van Genuchten soil hydraulic properties used to run models

Texture	ThR (-)	ThS (-)	Alfa (1/m)	N (-)	Ks (m/s)	L (-)
Clay	0.068	0.38	0.8	1.09	5.56E-07	0.5
Loam	0.078	0.43	3.6	1.56	2.89E-06	0.5
Sand	0.045	0.43	14.5	2.68	8.25E-05	0.5
Sandy loam	0.065	0.41	7.5	1.89	1.23E-05	0.5
Silt	0.034	0.46	1.6	1.37	6.94E-07	0.5

Model simulation results were compared on an hourly basis. All comparisons were carried out for 4000 instants, except for the clay soil texture. HYDRUS-1D was unable to converge after 2600 instants were considered, because of a 40 mm irrigation in one day. This was expected to happen due to the low velocities considered the in clay soil texture and due to the large pressure head variations. We made many changes to the convergence criteria but they were all unsuccessful in achieving a complete HYDRUS run. In MOHID LAND-PM there was no need to change the convergence criteria to have a complete run.

9.2.3.4 10-layer simulations

In watershed modelling it is necessary to reduce the number of layers in the soil in order to reduce the computing time. This results in an increased error. To quantify this error the same simulations were produced assuming 10 layers in MOHID LAND-PM (Table 26). The 10-layer simulation of MOHID LAND-PM was compared with the 100-layer simulation of MOHID LAND-PM.

Table 26 – Layers in MOHID LAND model with 10 layers

Layer number	1	2	3	4	5	6	7	8	9	10
Depth of the centre of layer [cm]	170	115	70	36	18	12	8	5	3	1
Depth of layer bottom [cm]	200	140	90	50	22	14	10	6	4	2

9.2.3.5 Statistical Analysis

The Nash-Sutcliffe model efficiency (NSE) (Nash and Sutcliffe, 1970) was used to evaluate the performance of the MOHID LAND-PM in reproducing HYDRUS-1D simulations of the soil water dynamics. NSE indicates how well the plot of observed versus simulated data fits the 1:1 line (trends) and it is determined as follows:

$$NSE = 1 - \left[\sum_{i=1}^{n} (Y^{obs}{}_i - Y^{sim}{}_i)^2 / \sum_{i=1}^{n} (Y^{obs} i - Y^{mean})^2 \right] \qquad (1)$$

where $Y^{obs}{}_i$ = i[th] observation for the constituent being evaluated, $Y^{sim}{}_i$ = i[th] simulated value for the constituent being evaluated, Y^{mean} = mean of observed data for the constituent being evaluated, and n = total number of observations. NSE ranges between -∞ and 1.0 (1 inclusive) with NSE = 1 being the optimal value. Values ≤ 0.0 indicate that the mean observed value is a superior predictor than the simulated value, which indicates unacceptable performance.

Percent bias (PBIAS) measures the average tendency of the simulated data to be larger or smaller than their observed counterparts (Gupta et al., 1999). The optimal value of PBIAS is 0.0 with low magnitude values indicating accurate model simulation. Positive values indicate model underestimation bias, and negative values indicate model overestimation bias. PBIAS is computed as:

$$PBIAS = \left[\sum_{i=1}^{n} (Y^{obs}{}_i - Y^{sim}{}_i) * (100) / \sum_{i=1}^{n} (Y^{obs}{}_i) \right] \qquad (2)$$

where PBIAS = deviation of data being evaluated, expressed as a percentage.

9.2.4 Results

Model simulations were compared for soil water content (Table 27), soil pressure head (Table 28) and vertical velocity (Table 29). In HYDRUS-1D, soil water content and soil pressure head were calculated per node (finite element), while in MOHID LAND-PM they were calculated per cell (finite volume). In HYDRUS, water velocity was calculated in the nodes but in MOHID LAND-PM it was calculated in the faces of the cells. This means that velocities presented for MOHID LAND-PM refer to depth plus 1 cm (i.e., 9, 19, 37 and 71 cm). As a consequence the compared velocities are 1 cm deeper in MOHID LAND-PM than in HYDRUS.

Statistical analysis shows an NSE for water content above 0.87 for sand and above 0.97 for all other soils and layers except clay (Table 27). PBias shows that MOHID LAND-PM tends to underestimate HYDRUS because all PBias are positive. PBias values are less than 6.3% in sand and less than 2.2% in the remaining soils, while for clay the maximum PBias value is 15.9%. Figure 93 shows example results for water content with MOHID LAND-PM and HYDRUS in Sandy Loam.

Table 27 – Soil water content (m^3/m^3) comparison between HYDRUS and MOHID LAND-PM

texture	depth [cm]	NSE	PBias (%)	HYDRUS [-]	Mohid [-]
sand	8	0.87	6.3	0.10	0.09
	18	0.97	4.0	0.13	0.12
	36	0.99	1.7	0.16	0.16
	70	0.99	2.1	0.20	0.20
sandy loam	8	0.99	0.5	0.16	0.16
	18	1.00	0.0	0.17	0.17
	36	1.00	0.1	0.18	0.18
	70	0.94	1.4	0.19	0.18
clay	8	0.76	5.9	0.32	0.32
	18	0.63	8.1	0.32	0.32
	36	0.45	11.1	0.29	0.30
	70	0.01	15.9	0.25	0.27
loam	8	0.99	0.7	0.23	0.23
	18	1.00	0.5	0.24	0.24
	36	1.00	0.5	0.24	0.24
	70	1.00	0.7	0.23	0.23
silt	8	0.99	1.1	0.28	0.28
	18	0.99	1.1	0.28	0.28
	36	0.99	1.5	0.27	0.26
	70	0.97	2.2	0.23	0.23

Statistical analysis shows a pressure head of above 0.46 NSE for sand and above 0.98 NSE for all other soils and layers except clay (Table 28). PBias shows that MOHID LAND-PM tends to underestimate HYDRUS because most PBias are negative. The highest absolute value of PBias is 2.6% in sandy loam, loam and silt soil. For clay, the maximum PBias value is 289.9%. High values of PBias and low values of NSE are related to the exponential variation of the head particularly in clay soils. This can be confirmed by the average values of head in each depth. It is possible to see for Hydrus that head increases one order of magnitude in each depth, while water content decreases a maximum of 0.04 between depth 36 and depth 70.

Table 28 – Soil pressure head (m) comparison between HYDRUS and MOHID LAND-PM

texture	Depth [cm]	NSE	PBias (%)	HYDRUS [m]	Mohid [m]
sand	8	0.98	0.1	-0.3	-0.3
	18	0.98	0.1	-0.2	-0.2
	36	0.83	-11.2	-0.2	-0.2
	70	0.46	-143.1	-0.1	-0.2
sandy loam	8	0.99	-0.7	-0.7	-0.7
	18	1.00	0.7	-0.5	-0.5
	36	1.00	0.6	-0.5	-0.5
	70	0.99	-0.5	-0.4	-0.4
clay	8	-23.95	-289.9	-28.0	-63.6
	18	0.98	-3.2	-155.6	-5.0
	36	0.02	-61.5	-6661.8	-7002.3
	70	0.14	-28.6	-11991.1	-10040.7
loam	8	1.00	-1.5	-1.5	-1.5
	18	1.00	-0.7	-1.2	-1.2
	36	1.00	-0.8	-1.2	-1.2
	70	1.00	-1.2	-1.3	-1.3
silt	8	1.00	-0.8	-3.9	-3.9
	18	1.00	-0.9	-3.7	-3.7
	36	1.00	-1.7	-4.5	-4.6
	70	0.98	-2.6	-6.1	-6.3

Statistical analysis shows an NSE for soil water velocity of 0.0 for sand and clay (except for first layer in sand), and above 0.58 for all other soils. In soil water velocity, negative values mean upward velocity and positive values indicate downward velocity. The average values show that velocities are mostly upwards. PBias shows that MOHID LAND-PM tends to underestimate HYDRUS soil water velocity because all PBias are positive. The worst results in depths 18, 36 and 70 are related to saturation conditions that happen at the end of a run. For saturation, MOHID LAND-PM calculates velocities, while HYDRUS assumes velocities to be zero between saturated layers. If we analyse only the velocities until 22 of August, for example for sand at 70 cm, the NSE goes from -8942.96 to 0.90.

Table 29 – Soil water velocity (m/s) comparison between HYDRUS and MOHID LAND-PM

texture	Depth [cm]	NSE	PBias (%)	HYDRUS [m/s]	Mohid [m/s]
sand	8	0.87	0.6	-3.0E-08	-3.0E-08
	18	-7827.30	-183.7	-2.9E-08	-8.3E-08
	36	-18359.59	1613.8	-2.6E-08	4.0E-07
	70	-8942.96	2517.4	-2.1E-08	5.0E-07
sandy loam	8	0.86	7.6	-1.9E-08	-1.8E-08
	18	0.94	5.4	-1.9E-08	-1.8E-08
	36	0.98	3.6	-1.9E-08	-1.8E-08
	70	0.98	2.1	-1.8E-08	-1.8E-08
clay	8	-11.13	71.0	-2.1E-08	6.1E-10
	18	-0.07	79.9	-3.8E-08	-2.5E-09
	36	0.00	99.9	-2.5E-06	3.0E-09
	70	0.00	100.1	-8.7E-07	6.0E-09
loam	8	0.87	6.0	-1.3E-08	-1.2E-08
	18	0.92	7.3	-1.2E-08	-1.1E-08
	36	0.99	5.7	-1.1E-08	-1.0E-08
	70	0.99	7.3	-9.4E-09	-8.8E-09
silt	8	0.63	27.2	-1.2E-08	-8.4E-09
	18	0.58	13.1	-1.1E-08	-9.2E-09
	36	0.95	14.4	-8.7E-09	-7.5E-09
	70	0.93	23.1	-5.1E-09	-3.9E-09

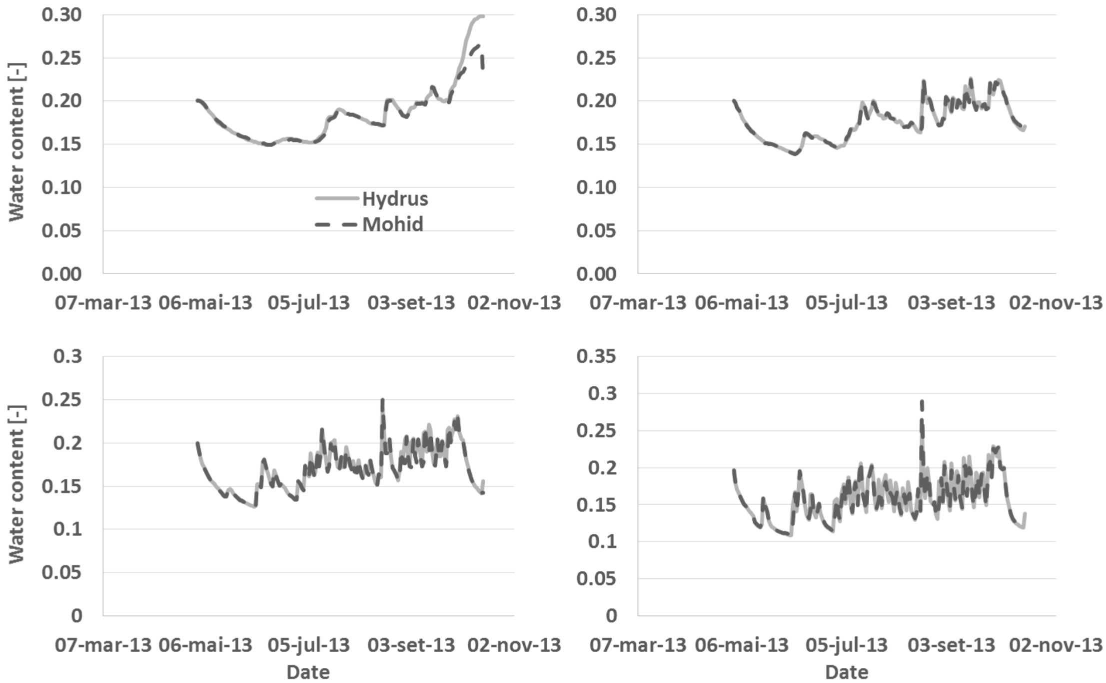

Figure 93 - Example result for water content with MOHID LAND-PM and HYDRUS in Sandy Loam

9.2.4.1 10-layer simulations

The 10-layer simulation of MOHID LAND-PM was compared with the 100-layer simulation of MOHID LAND-PM. Parameters compared were soil water content (Table 30), soil pressure head (Table 31) and vertical velocity (Table 32).

PBias shows that MOHID LAND-PM with 10 layers tends to overestimate water content when compared with MOHID LAND-PM with 100 layers because all PBias are negative.

Statistical analysis shows an NSE for water content above 0.57 for all except two layers in sandy loam and one layer in sand (Table 30). PBias values are all less than 39.4% in sand and less than 13.9% in the remaining soils.

Table 30 – Soil water content (m^3/m^3) comparison between different number of layers in MOHID LAND-PM

texture	Depth [cm]	NSE	PBias (%)	100 layers [-]	10 layers [-]
clay	8	0.96	-1.0	0.322	0.325
	18	0.96	-0.6	0.319	0.321
	36	0.85	-4.3	0.298	0.311
	70	0.72	-7.6	0.267	0.287
loam	8	0.93	-4.0	0.231	0.240

	18	0.86	-3.8	0.241	0.250
	36	0.85	-5.2	0.240	0.252
	70	0.80	-5.4	0.231	0.244
sand	8	-3.89	-39.4	0.092	0.128
	18	0.65	-13.8	0.124	0.141
	36	0.83	-6.2	0.155	0.165
	70	0.84	-3.6	0.200	0.207
sandy loam	8	0.92	-4.1	0.158	0.164
	18	0.82	-2.7	0.171	0.175
	36	0.26	-5.3	0.176	0.185
	70	-3.69	-13.9	0.183	0.208
silt	8	0.92	-4.9	0.280	0.294
	18	0.86	-6.1	0.280	0.297
	36	0.84	-7.7	0.262	0.282
	70	0.57	-9.7	0.227	0.249

Statistical analysis shows an NSE above 0.22 for all except one layer in sandy loam and one layer in sand (Table 31). PBias values are all less than 71.6% in sand and less than 44.1% in the remaining soils.

Table 31 – Soil pressure head (m) comparison between different number of layers in MOHID LAND-PM

texture	Depth [cm]	NSE	PBias (%)	100 layers [m]	10 layers [m]
clay	8	0.98	4.1	-1878.71	-1800.95
	18	0.66	36.8	-3932.67	-2487.38
	36	0.30	44.1	-7002.32	-3913.86
	70	0.22	38.0	-10040.75	-6228.00
loam	8	0.88	14.1	-1.50	-1.28
	18	0.86	10.7	-1.22	-1.09
	36	0.84	13.3	-1.21	-1.05
	70	0.81	12.2	-1.32	-1.16
sand	8	0.67	14.1	-0.30	-0.26
	18	0.83	3.7	-0.23	-0.22
	36	0.27	-10.3	-0.20	-0.22
	70	-2.10	-71.6	-0.16	-0.28
sandy loam	8	0.83	11.6	-0.66	-0.58
	18	0.84	5.4	-0.52	-0.49

	36	0.61	9.1	-0.48	-0.43
	70	0.08	11.3	-0.45	-0.40
silt	8	0.90	18.1	-3.92	-3.21
	18	0.85	18.8	-3.74	-3.04
	36	0.80	19.2	-4.57	-3.69
	70	0.35	19.9	-6.31	-5.05

Statistical analysis shows an NSE for soil water velocity below zero for 9 out of 16 depths analysed (Table 32). PBias values are all less than 35.5% for 10 out of 16 of the depths analysed. In soil water velocity, negative values mean upward velocity and positive values downward velocity. In general the 10-layer simulation tends to overestimate the soil water velocity.

Table 32 – Soil water velocity (m/s) comparison between using different number of layers in MOHID LAND-PM

texture	Depth [cm]	NSE	PBias (%)	100 layers [m/s]	10 layers [m/s]
clay	8	0.11	2171.6	6.1E-10	-1.3E-08
	18	-0.06	-559.4	-2.5E-09	-1.6E-08
	36	-0.29	614.6	3.0E-09	-1.5E-08
	70	-0.15	322.0	6.0E-09	-1.3E-08
loam	8	0.97	-31.5	-1.2E-08	-1.6E-08
	18	0.87	-34.8	-1.1E-08	-1.5E-08
	36	0.87	-30.1	-1.0E-08	-1.4E-08
	70	0.90	-28.4	-8.8E-09	-1.1E-08
sand	8	-207.82	-1837.7	-3.0E-08	-5.8E-07
	18	-0.08	-668.4	-8.3E-08	-6.4E-07
	36	-0.54	651.1	4.0E-07	-2.2E-06
	70	-2.60	1042.3	5.0E-07	-4.7E-06
sandy loam	8	0.98	-29.9	-1.8E-08	-2.3E-08
	18	0.89	-27.9	-1.8E-08	-2.2E-08
	36	0.51	-20.5	-1.8E-08	-2.2E-08
	70	-5355.01	-2279.3	-1.8E-08	-4.3E-07
silt	8	-0.15	-66.7	-8.4E-09	-1.4E-08
	18	0.34	-35.5	-9.2E-09	-1.2E-08
	36	0.90	-25.9	-7.5E-09	-9.4E-09
	70	0.91	-28.4	-3.9E-09	-5.0E-09

9.2.5 Discussion and conclusions

Results show that modelling soil water dynamics using a finite volumes model like MOHID LAND-PM and a finite elements model like HYDRUS produces similar results.

The main uncertainty in these models is the estimation of the infiltrated water. In fact, when HYDRUS calculates infiltration it returns different results from MOHID LAND-PM. The simulation in the clay soil was that which resulted in the biggest differences between models. This simulation did not manage to converge on a solution after a certain point in time. This was due to an application of about 40 mm of water in 1 day.

Some previous studies compared different models. A study carried out in Texas showed that there were differences in infiltration between the different models tested (including HYDRUS) which resulted in different soil water contents (Scanlon et al., 2002).

Infiltration is in fact one of the most critical variables in hydrology models and also one of the most difficult to determine. Infiltrated water can be evapotranspirated, percolated to the aquifer or carried laterally along the soil profile until it reaches the channel. The water that reaches the aquifer is lost to the stream, stored in deep aquifer or returned to the atmosphere through capillary rise followed by evapotranspiration. The water that is not infiltrated is converted into runoff, directed to the basin river network or it can be directly evaporated from the leaves and from the surface water column. Percolation transports nitrate to aquifer and surface waters. Runoff transports phosphorous and sediments to surface waters. Evaporated water promotes soil salinity more than transpiration. Percolation to aquifers reduces soil salinity. In this perspective, we believe that these results can have a positive impact on future infiltration assessments that can be made with the MOHID LAND model.

Accurate estimates of infiltration are paramount to knowledge of the soil water content. This paper shows that MOHID LAND calculates soil water dynamics as well as HYDRUS, which is a very well tested model in detailed percolation studies. Future studies should compare MOHID LAND infiltration with infiltration in HYDRUS-1D and other models.

This paper also evaluates the impact on the reduction of the number of layers. In watershed, simulation can be used to reduce the number of layers because of computation time. Results show that it is reasonable to make a 10-layer simulation. However, we suggest making the comparison presented here for the soils and meteorology included in a watershed simulation whenever MOHID LAND is set up.

9.2.6 References

1. Foley JA, DeFries R, Asner GP, Barford C, Bonan G, Carpenter SR, et al. Global consequences of land use. Science. 2005;309(5734):570-4.

2. Kaufman F. Wall Street's thirst for water. Nature. 2012;490(7421):469-71.

3. Allen RG, Pereira LS, Raes D, Smith M. Crop evapotranspiration-Guidelines for computing crop water requirements-FAO Irrigation and drainage paper 56. FAO, Rome. 1998;300:6541.

4. Allen RG, Pruitt WO, Wright JL, Howell TA, Ventura F, Snyder R, et al. A recommendation on standardized surface resistance for hourly calculation of reference ET< sub> o</sub> by the FAO56 Penman-Monteith method. Agricultural Water Management. 2006;81(1):1-22.

5. Valipour M. Importance of solar radiation, temperature, relative humidity, and wind speed for calculation of reference evapotranspiration. Arch Agron Soil Sci. 2015;61(2):239-55.

6. Valipour M. Investigation of Valiantzas' evapotranspiration equation in Iran. Theoretical and Applied Climatology. 2014:1-12.

7. Braunschweig F, Leitao PC, Fernandes L, Pina P, Neves RJJ. The object-oriented design of the integrated water modelling system MOHID. Dev Water Sci. 2004;55:1079-90.

8. Miranda R, Braunschweig F, Leitao P, Neves R, Martins F, Santos A. MOHID 2000 - A coastal integrated object oriented model. Wat Stud Ser. 2000;7:393-401.

9. Leitão P, Galvão P, Aires E, Almeida L, Viegas C. FECAL CONTAMINATION MODELING IN COASTAL WATERS USING A WEB SERVICE APPROACH. Environmental Engineering & Management Journal (EEMJ). 2012;11(5).

10. Campuzano F, Fernandes R, Leitão P, Viegas C, de Pablo H, Neves R. Implementing local operational models based on an offline downscaling technique: The Tagus estuary case. 2 as Jornadas de Engenharia Hidrográfica. 2012:105-8.

11. Neves R, Chambel-Leitão P, Leitão P. Numerical modeling of water circulation in the soil - MOHID model. Modelação Numérica Da Circulação Da água no solo-o modelo MOHID. Pedologia. 2000;28(1).

12. Galvão P, Chambel Leitão P, Neves R, Leitao PC. A different approach to the modified Picard method for water flow in variably saturated media. Developments in Water Science. 2004;55:557-67.

13. Barão L, Leitão PC, Braunschweig F, Neves R, Gonçalves M, Ramos T, et al. Simulation of water dynamics in two irrigated soils. Revista de Ciências Agrárias. 2010;33(1):346-57.

14. Trancoso AR, Braunschweig F, Leitao PC, Obermann M, Neves R. An advanced modelling tool for simulating complex river systems. Sci Total Environ. 2009;407(8):3004-16.

15. Celia MA, Binning P. A mass conservative numerical solution for two- phase flow in porous media with application to unsaturated flow. Water Resources Research. 1992;28(10):2819-28.

16. Vangenuchten MT. A Closed-Form Equation for Predicting the Hydraulic Conductivity of Unsaturated Soils. Soil Sci Soc Am J. 1980;44(5):892-8.

17. Arakawa A, Lamb VR. Computational design of the basic dynamical processes of the UCLA general circulation model. Methods in computational physics. 1977;17:173-265.

18. Martinez G, Pachepsky YA, Vereecken H, Hardelauf H, Herbst M, Vanderlinden K. Modeling local control effects on the temporal stability of soil water content. J Hydrol. 2013;481:106-18.

19. Simunek J, van Genuchten MT. Modeling nonequilibrium flow and transport processes using HYDRUS. Vadose Zone J. 2008;7(2):782-97.

20. Ramos TB, Simunek J, Goncalves MC, Martins JC, Prazeres A, Pereira LS. Two-dimensional modeling of water and nitrogen fate from sweet sorghum irrigated with fresh and blended saline waters. Agricultural Water Management. 2012;111:87-104.

21. Ramos TB, Goncalves MC, Castanheira NL, Martins JC, Santos FL, Prazeres A, et al. Effect of sodium and nitrogen on yield function of irrigated maize in southern Portugal. Agricultural Water Management. 2009;96(4):585-94.

22. Forkutsa I, Sommer R, Shirokova YI, Lamers JPA, Kienzler K, Tischbein B, et al. Modeling irrigated cotton with shallow groundwater in the Aral Sea Basin of Uzbekistan: I. Water dynamics. Irrigation Sci. 2009;27(4):331-46.

23. Vithanage M, Villholth K, Engesgaard P, Jensen KH. Vulnerability Analysis of the Coastal Sandy Aquifers in the East Coast of Sri Lanka with Recharge Change Consideration. Open Hydrology Journal. 2010.

24. Carsel RF, Parrish RS. Developing joint probability distributions of soil water retention characteristics. Water Resources Research. 1988;24(5):755-69.

25. Nash J, Sutcliffe J. River flow forecasting through conceptual models part I—A discussion of principles. J Hydrol. 1970;10(3):282-90.

26. Gupta HV, Sorooshian S, Yapo PO. Status of Automatic Calibration for Hydrologic Models: Comparison with Multilevel Expert Calibration. J Hydrol Eng. 1999;4(2):135-43.

27. Scanlon BR, Christman M, Reedy RC, Porro I, Simunek J, Flerchinger GN. Intercode comparisons for simulating water balance of surficial sediments in semiarid regions. Water Resources Research. 2002;38(12):59-1--16.

9.3 Congress paper

Operational System for Streamflow Forecasting to Support Hydroelectric Production Management

Pedro, CHAMBEL-LEITÃO[1]; Ana, OLIVEIRA[1]; Pedro GALVÃO[1]; José, CHAMBEL LEITÃO[1]

[1] - Hidromod - R. Rui Teles Palhinha 4, 2740-278 Porto Salvo, Tele:21 848 6013; pedrochambelleitao@hidromod.com

9.3.1 Abstract

One of the most important factors to plan the exploitation of hydropower plant cascades is the forecast of natural streamflow that arrives in each reservoir. In general, the exploitation of these systems has two main objectives: (1) to maximize the economic return obtained with hydroelectric production and (2) to minimize the flood effects along the reaches affected by hydroelectric production, particularly areas with a high flood risk. Streamflow can be estimated based on measurements (more relevant to short periods of forecast) or based on meteorological and hydrological forecasts. Among the variables that contribute to flow generation, precipitation has the greatest influence on the system. Precipitation values are available as a result of measurement stations and are simulated by meteorological models. The uncertainty in precipitation values, both measured and simulated, will affect the uncertainty in streamflow values which result from hydrological model simulations. The uncertainty introduced by a hydrological model will be added to the uncertainty mentioned above.

This paper presents an operational system for streamflow forecasting to support and optimize the exploitation of hydroelectric production in hydropower plant cascades on the Douro River. The analysis presented here takes into account different sources of precipitation predictions, the uncertainty associated with these predictions and their validation with different sources of precipitation measurements. Forecasts from the meteorological models WRF (with a resolution of 5 km and 12 km) and GFS (with a resolution of 25 km and 50 km) were used. On the other hand, for validation procedures, different sources of precipitation measurements were used. Finally, an analysis of streamflow historical data was made.

Keywords: hydrological models, meteorological models, precipitation

Topic: Evaluation of water availability, including hydrologic modelling

9.3.2 Introduction

Platforms that provide hydrologic data are very important to water resources managers. In Portugal and Spain there are two examples of this type of platform, namely the National Information System of Water Resources (Sistema Nacional de Informação de Recursos Hídricos – SNIRH) and the Automatic System of Hydrologic Information (Sistema Automático de Información Hidrológica – SAIH). The main activities of these systems are to measure, transmit, process and, in some cases, validate the data which allow the characterization of the state of rivers and some hydraulic structures. In the end they will be a tool to archive and provide long-term series of hydrological data, which helps in the management of water resources and in the prediction and monitoring of extreme climatic events, such as floods and droughts.

The SNIRH system was implemented with the goal of facilitating the usage of collected data in different studies and objectives (Santos et al., 1997). Data from SNIRH was used in many studies related to the Douro River, for example:

- SNIRH data were used to understand if anthropic activity in the Douro basin causes an increase in flood events (Rodrigues et al., 2003b).
- The application of a SWAT model to different basins on the Douro (Caetano e Pacheco, 2008, Mateus et al., 2014, Alencoão e Pacheco, 2009).
- The application of the MIKE-SHE model to the Sordo basin, which is a sub-basin of the Corgo basin (Santos, 2009).
- Neuronal networks were tested on the Côa River using only flow data of previous days as input (Pulido-Calvo e Portela, 2007).

In Portugal, SNIRH was used to develop a system of flood monitoring and alert (Sistema de Vigilância e Alerta de Cheias – SVAC) (LACERDA et al., 1997). Later, this system was updated with new features (Rodrigues et al., 2003a), becoming the system of water resources monitoring and alert of Portugal (Sistema de Vigilância e Alerta de Recursos Hídricos de Portugal – SVARH). The SVARH system is based on flow measurements and water levels measured in reservoirs and provided by National Institute of Water (Instituto Nacional da Água – INAG), Energies of Portugal (Energias de Portugal – EDP and other entities that manage these reservoirs. However, this system does not include meteorological forecasting.

SNIRH data were used in a study developed by Portela and Hora (2002) where the authors try to relate precipitation intensity with peak flood discharge using a rational method equation.

In other countries there are similar systems, such as in Brazil and the United States of America (USA). In Brazil, all hydrological information resulting from monitoring systems is available in the System of Hydrologic Information (Sistema de Informações Hidrológicas – HidroWeb) managed the by National Water Agency (Agência Natural das Águas – ANA). In the USA, the corresponding system is the National Water Information System (NWIS) which supports the acquisition, processing and storage of hydrological data. Both systems, in Brazil and the USA, provide real time information and the latter has an alert system available for the general public.

9.3.2.1 Study area

Douro basin has an area of approximately 97 000 km^2, of which 19 000 km^2 are located in Portugal (Figure 94). The availability of surface water is estimated at approximately 17 023 hm^3 in the entire basin and at 8 023 hm^3 in the Portuguese area of the basin. Of these 8 023 hm^3, about 500 hm^3 are used in agriculture and 100 hm^3 are used for urban consumption (APA, 2012). On Portuguese territory there are 67 dams with a total storage capacity of 1 594 hm^3. The availability of groundwater is estimated at about 975 hm^3/year from the three groundwater bodies (APA, 2012).

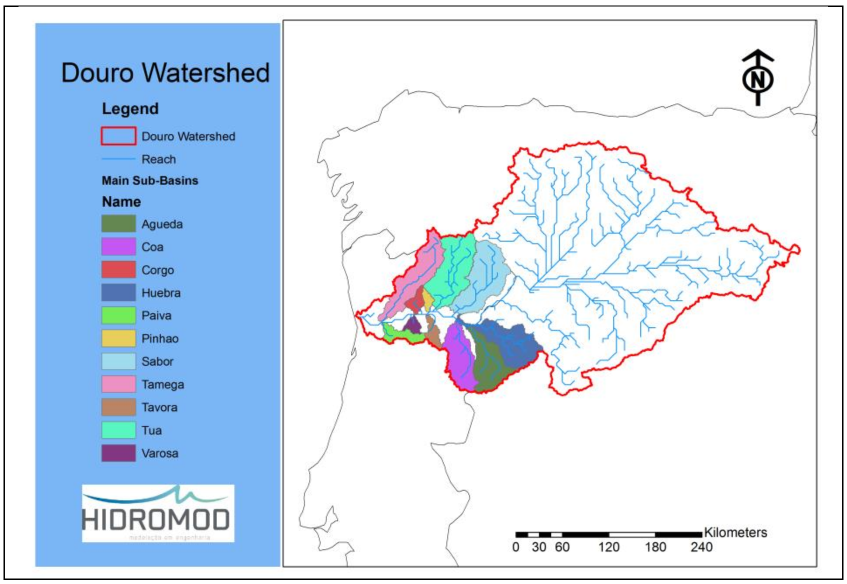

Figure 94 Douro basin and sub-basins that drain to EDP hydropower plants .

In Spain the total storage capacity for surface water is 7 500 hm^3, approximately. Of these 7 500 hm^3, 3 870 hm^3 are consumed: 3 600 hm^3 for agricultural use and 225 hm^3 for human consumption (CHD, 2016).

Miranda is the first Portuguese hydropower plant within international reach of the Douro River and is the one located further north. After this reservoir, there are two Portuguese and two Spanish hydropower plants, namely, Picote and Bemposta and Aldeadávila and Saucelle. After Saucelle, is located the cascade of hydropower plants that is subject of this paper. This cascade starts with Pocinho and ends at Crestuma-Lever, which is the last hydropower plant on the Douro River and is located immediately before the mouth of the Douro (Figure 95).

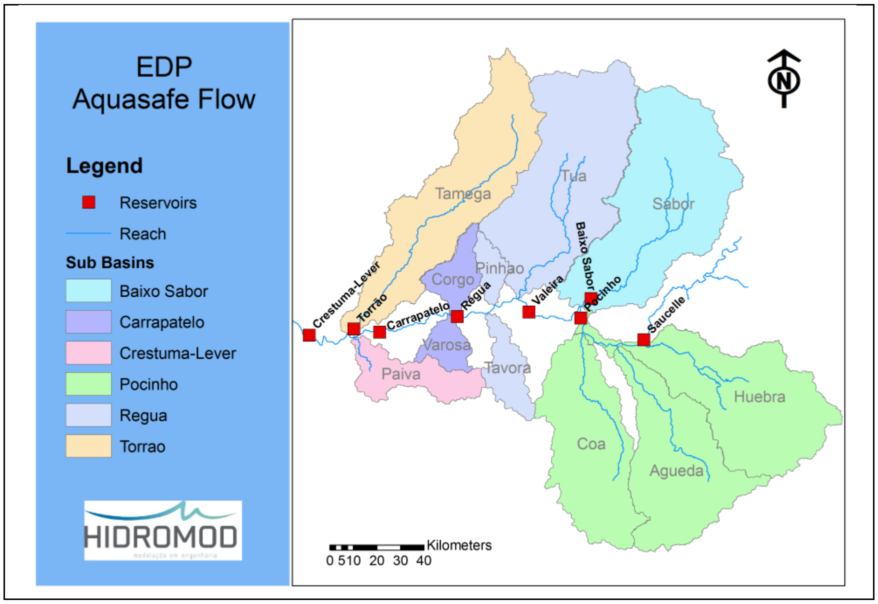

Figure 95 Main basins that drain to hydropower plants of EDP in Douro River.

This cascade is composed by five hydropower plants constructed between 1965 and 1985 to take advantage of the regularization that had previously been made in Spain (Madureira and Batista, 2002). However, none of them has a high storage capacity. In Table 33 the construction year, the storage capacity and the upstream drainage area of each hydropower plant are presented. Recently, in 2015, the Baixo Sabor dam was completed, and in 2016 it is expected that the construction of more dams will be completed.

Table 33 Reservoir characteristics (source: SNIRH).

Hydropower plant	Year of construction	Usage volume	Upstream drainage area
Carrapatelo	1972	13.8	92376
Crestuma-Lever	1985	22.5	96933
Pocinho	1982	12.2	81258
Régua	1973	12.0	91030
Torrão	1988	77.1	3268
Valeira	1975	13.0	85641
Baixo Sabor	2015	630.0	3866
Varosa	1934	12.9	307

9.3.3 Methodology

Hidromod provides daily predictions to EDP about the natural streamflow that arrives in each hydropower plant belonging to the cascade of dams located on the Douro River and operated by that entity. This system is known as "AquaSafe Douro" and is divided into two main components:

AquaSafe Server, which stores and allows the manipulation of data generated in the system (model results) or externally (SCADA systems, FTP, Open DAP, etc.), and *AquaSafe Desktop Client*, which is the user interface. The first component lets the user schedule a range of activities such as running models, publishing reports, etc., and the communication with this component is made through two web channels: i) a channel to exchange data and ii) an administration channel. On the other hand *AquaSafe Desktop Client* is the interface that assures the connection between user and server (Figure 96). This platform was designed for "operational" scenarios providing a range of features (SIG, graphs, reports, etc.) that can be grouped and accessed in workspaces. Each workspace can be available only for one user or for a group of users. Hydrologic models MOHID Land and SWAT were implemented in this system to provide daily predictions.

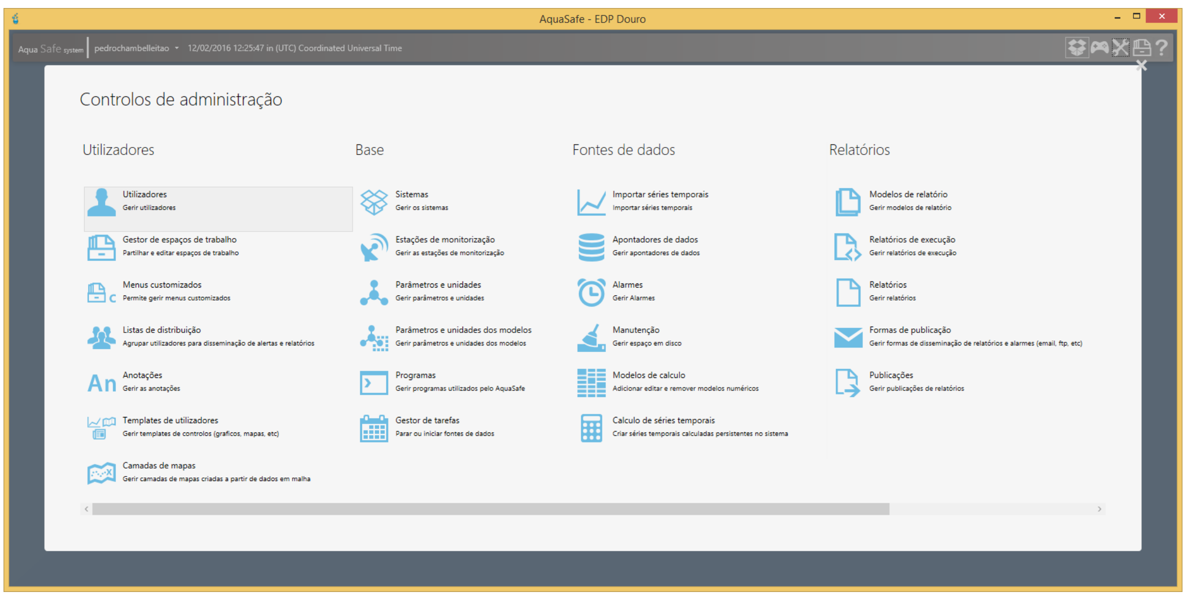

Figure 96 Administration controls of AquaSafe Client

9.3.3.1 Hydrological models

9.3.3.1.1 Mohid Land

MOHID Land is a basin model that simulates different phenomena in an integrated way: (i) superficial run-off, (ii) channel flow of drainage network, (iii) the run-off in non-saturated layer of the soil (above aquifer) and (iv) the run-off in the saturated layer of the soil (aquifer) (Chambel-Leitão et al., 2015). The integrated simulation of these interdependent phenomena eliminates the necessity to consider some hypothesis about the interaction between these domains.

The interaction of these different processes (e.g. water exchange between the aquifer and drainage network) is dynamically calculated using hydraulics gradients (Trancoso et al., 2009). Each process presents a different space scale: the run-off in drainage network is considered unidimensional (1D); the simulation of superficial run-off is bi-dimensional (2D); and the simulation of percolation is tri-dimensional (3D) (Figure 97).

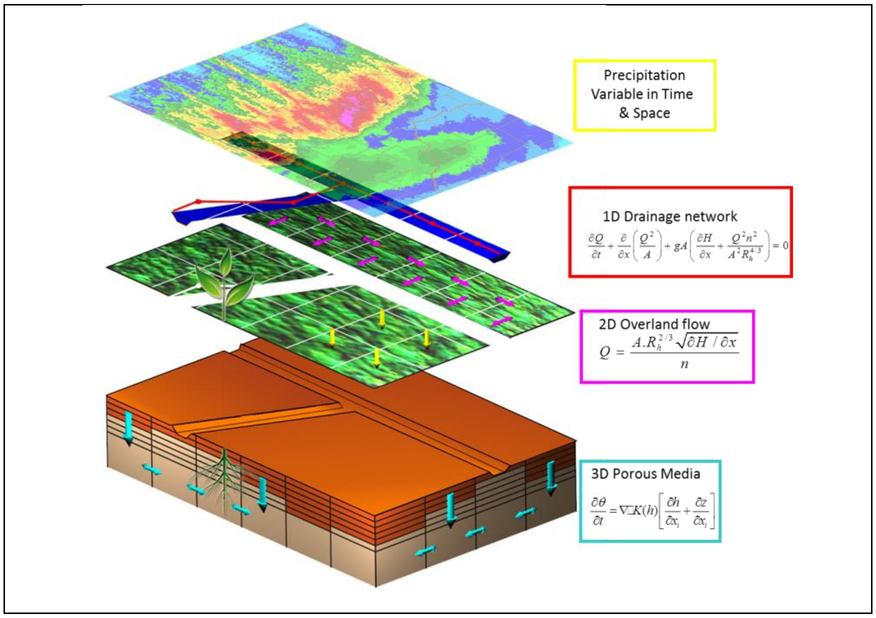

Figure 97 Conceptual model and main equations of MOHID Land.

Water flow is a result of hydraulic gradient and, for example, the elevation of a water column at the surface tends to be homogenized by the effect of thehydraulic gradient. The hydraulic gradient takes into consideration the water column and the force of gravity because the water column includes the topography. Additionally, the hydraulic gradient considers the hydraulic loss that results from the contact with the soil surface and this loss is calculated with the Manning coefficient. The channel flow is estimated with Saint Venant equations, but the user can choose another method such as diffuse wave (assuming acceleration equals 0) or kinematic wave (assuming acceleration equals 0 and the water surface is parallel to the soil surface). This module of MOHID Land can estimate flooded areas.

The channel flow estimation is based on the same concepts as superficial run-off, but considering that channel has a trapezoidal section and that the flow is unidimensional. The flow is directly proportional to hydraulic radius and to channel slope and inversely proportional to the Manning coefficient.

Real evapotranspiration is a result from the sum of three components: canopy evaporation, canopy transpiration and soil evaporation. Real evapotranspiration will always be equal or lower than potential evapotranspiration.

Flow estimation is based on equations of mass and momentum conservation. Based on the conductivity concept, momentum conservation equation turns to Darcy's law. After this equation is included in mass conservation, the Richards equation is obtained. The van Genuchten equation allows the calculation of negative hydraulic gradients of the soil, known as soil matric potential, through the relation between pressure and water content. The estimation of infiltration, percolation, evapotranspiration and capillarity is dependent on these hydraulic gradients.

9.3.3.1.2 SWAT

SWAT is a tri-dimensional model with a 1-day time step and that allows the simulation of a basin. In this model the simulation is performed by dividing the basin into different sub-basins. Each sub-basin can be considered as a single hydrologic response unit (HRU) or divided into several HRU, which are characterized by the same type of soil and land use. An HRU is characterized by a upper boundary that corresponds to the soil surface and by a lower boundary which is the aquifer. In each HRU, part of the precipitation is converted into superficial run-off and the quantity of infiltrated water results from the difference between this superficial run-off and precipitation.

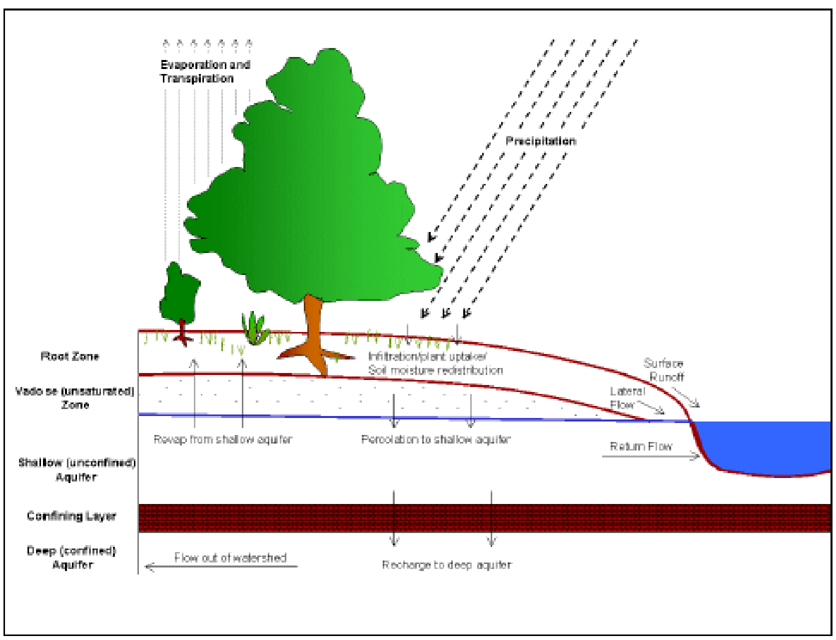

Figure 98 Conceptual model of SWAT

The simulation of percolation is based on the concepts of saturation, field capacity and wilting point, which is the minimum water content that soil can support. Each soil layer loses water by percolation to the cell below when its water content is between saturation and field capacity. Layers with a water content between field capacity and wilting point only lose water by evapotranspiration. The maximum number of soil layers that the model can simulate is 10. Percolation of the last layer flows to the aquifer and is known as groundwater recharge and is limited by a delayed factor defined by the user. The groundwater is lost to drainage network by a coefficient specified by the user.

Superficial run-off can be estimated by the curve number (CN) method developed by Soil Conservation Service (SCS) or by the Geen-Ampt method. Both of them calculate superficial run-off based on soil water content (high values of soil water content generate higher channel flows, while low values of soil water content will result in low values of channel flow). However the Green-Ampt method also uses CN curves because it does not have a way to consider the ground cover in the estimation of superficial run-off. The simulation of channel flow is based on kinematic wave equation considering a trapezoidal section. The channel flow is directly proportional to hydraulic radius and to channel slope, while it is inversely proportional to the Manning coefficient.

9.3.3.2 Implementation

SWAT implementation includes 315 sub-basins with an average area of 550 km^2, soil type and ground cover variable in space and a daily time-step. MOHID Land was implemented in a grid of 65 rows and 86 columns with a cell size of 0.03º x 0.03º (8 km^2). In this last model soil type is invariable in space and has an hourly time step.

The advantage of a sub-daily time step, such as Mohid Land provides, is that it allows a more correct and detailed simulation of the distribution of peak flows. This feature is more important when peak flow occurs at the end of the day because MOHID Land predicts if the peak flow occurs in the late hours of the night or in the first hours of the next day while SWAT estimates the accumulated daily precipitation and simulates each day according to these values. Thus, SWAT results are corrected with MOHID Land results, minimizing the errors caused by the difficulty of SWAT in estimating on what day the peak flow occurs. The SWAT model has the advantage of simulating the basin area in higher detail than MOHID Land does.

MOHID Land interpolates precipitation, while SWAT uses Thiessen polygons to distribute precipitation in the HRU. This difference gives MOHID Land higher spatial detail for precipitation.

Meteorological forcing for hydrological models is made automatically by AquaSafe and is given by different meteorological models: WRF 12 (MateoGalicia), WRF 5 km (Aveiro University) and GFS (NOAA) (Figure 99). Each hydrologic model in operation has a priority order to fill the input meteorology, enabling a redundant system that reduces the likelihood of failure of the operating system. Two meteorology fill orders of priority were established: 1st WRF 12km 2nd WRF 5 km 3rd GFS 25km 4th GFS and 1st WRF 5 km 2nd WRF 12km 3rd GFS 25km 4th GFS.

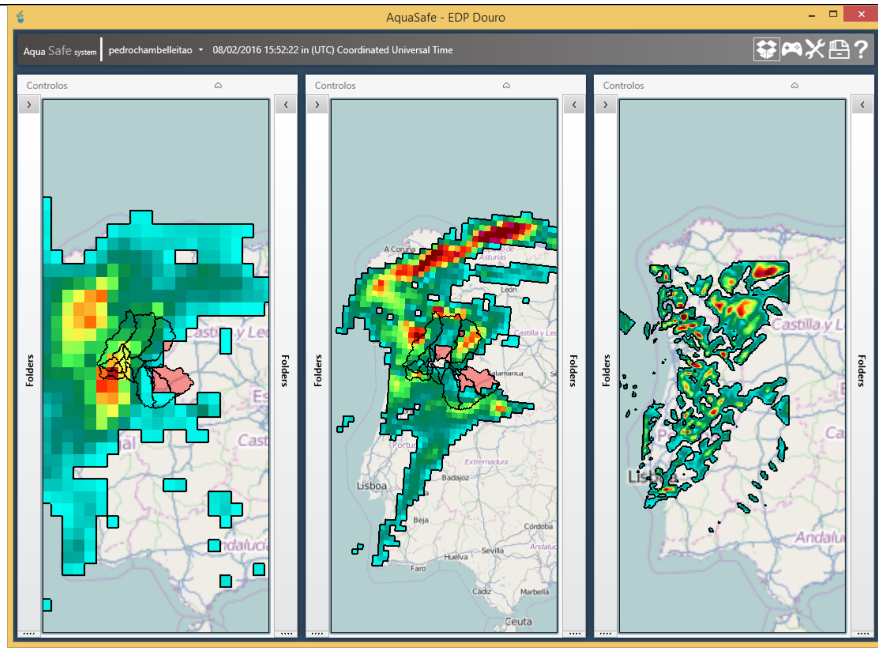

GFS25km WRF12km WRF5km

Figure 99 Precipitaiton forecasts.

Figure 100 presents drainage network and channel flow simulated by MOHID Land (rainbow scale) for one day and the spatial distribution of precipitation simulated by WRF 12 km (blue scale) that forced MOHID Land. Figure 100 shows a more detailed precipitation than Figure 99 because WRF 12 km is interpolated to the MOHID Land grid. The darkest blue band of precipitation in Figure 100 shows a precipitation front that crosses the basin from Northwest to Southeast.

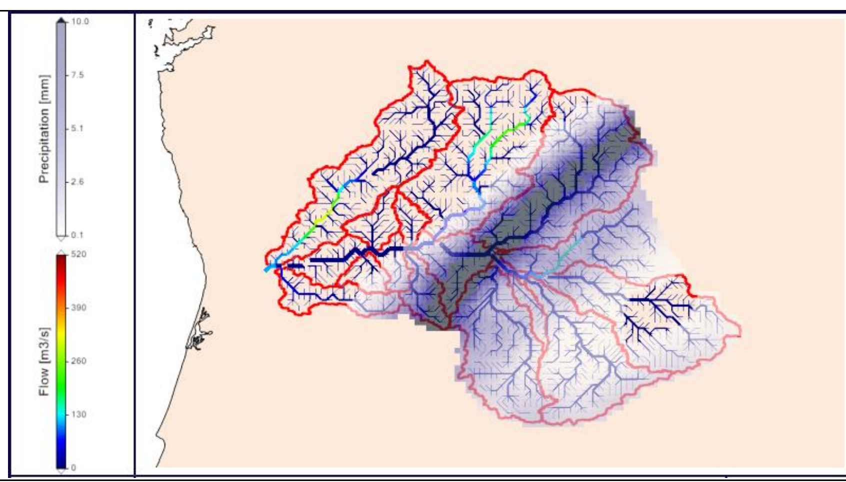

Figure 100 Hourly channel flow simulated by MOHID Land and precipitation forecasts of WRF 12 km model.

9.3.4 Results

The described system involves the prediction of two fundamental properties: precipitation and streamflow. Streamflow is the only property that has interest for the final result; however, its values are totally dependent on the quality of precipitation predictions. Thus, in the next paragraphs, first simulated precipitation and then simulated streamflow are analysed. Beyond precipitation, hydrologic models have air temperature, relative humidity, wind and solar radiation as input to estimate evapotranspiration. However, the quality of the predictions of these parameters is not analysed in this paper because evapotranspiration does not have a significant influence on streamflow estimation in the Douro basin.

9.3.4.1 Precipitation

9.3.4.1.1 Measured precipitation

To understand how correct the precipitation predictions are given by meteorological models, a validation of these values was performed. To accomplish this goal the values of meteorological models were compared with measurements available in two meteorological monitoring networks: Automatic Meteorological Stations (EMA) of the Portuguese Institute of Sea and Atmosphere (Instituto Português do Mar e da Atmosfera – IPMA) and Weather Underground.

The *IPMA*'s network stations provide automatic precipitation records on its website in an hourly time step. In the area studied there are 21 automatic stations which are presented in Table 34. This table shows the number of days, from May to November 2015, that each station has no record.

Table 34 Missing values in IPMA's network stations located in Douro basin (May – November 2015).

Station	Number of days without records
Luzim, Viseu, Guarda, Mogadouro, Moncorvo, Macedo de Cavaleiros, Vila Real, Cabril, Chaves, Mirandela, Vinhais, Bragança, Montalegre, V. Torpim, Carrazeda de Ansiães	0
Trancoso	1
Sabugal	2
Pinhão	3
Miranda do Douro	5
Arouca	7
Moimenta da Beira	25

Weather Underground provides values of precipitation rates in its website without a defined frequency and based on measurements made by particular meteorological stations. This platform receives data from 180 000 stations around the world. However, they are only responsible for the platform where data is available and not for the stations. In the area studied there are 8 active stations and these are presented in Table 35. This table also presents the number of days without any record from May to November 2015.

Table 35 Missing values in Weather Underground stations (May – November 2015).

Station	Number of days without records
Moimenta da Beira e Guarda	0
Freixo de Numão	1
Trancoso	2
IPortoLi4	4
Bragança	5
Santa Valha	20
Carrazedo de Montenegro	81

9.3.4.1.2 Simulated precipitation

The quality of precipitation predictions is evaluated by comparison of the accumulated daily values predicted and measured in each sub-basin. Measured values by sub-basin are based on both monitoring networks referred to before and are estimated by Thiessen polygons. Thiessen polygons generated for both networks are presented in Figure 101.

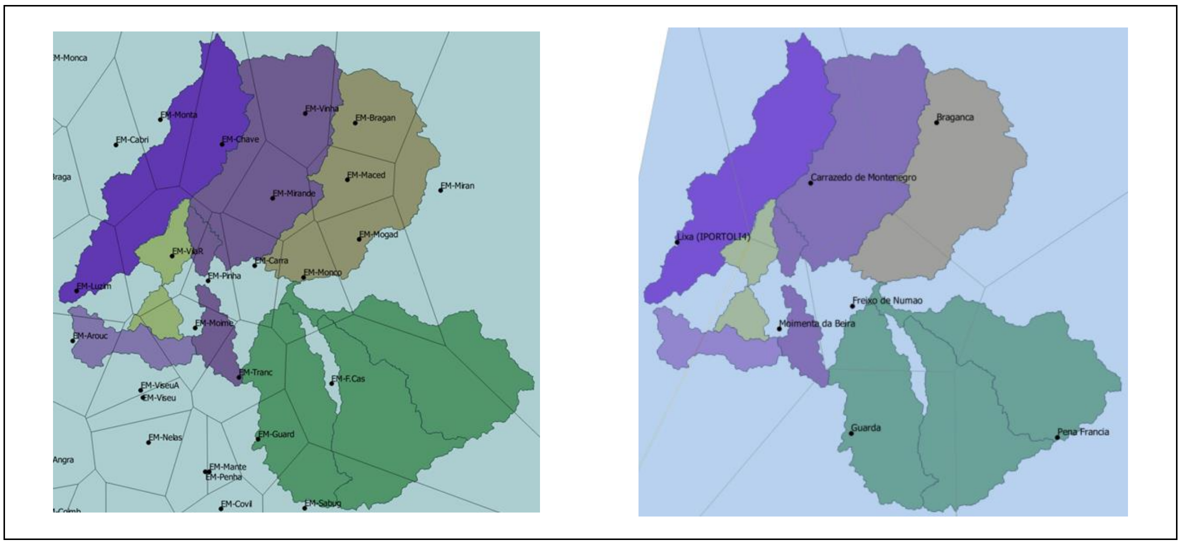

[a] [b]

Figure 101 Thiessen polygons based on monitoring stations of IPMA [a] and Weather Underground [b].

The graph of Figure 102 presents four different estimations of daily precipitation in the Tâmega basin, two of them based on Thiessen polygons as a results of monitoring stations of IPMA and Weather Undergraound (WU) and the other two resulting from simulated precipitation of WRF 12 km and WRF 5 km. The latter were obtained using HDF5Exporter, which is a tool of MOHID. Precipitation data from IPMA were available only since 1st of July of 2015.

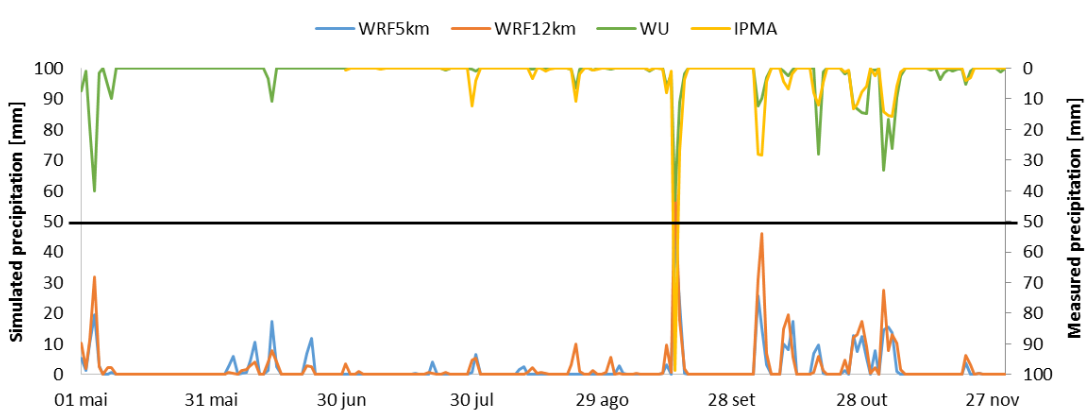

Figure 102 Comparison of forecast and measured precipitation in Tâmega basin for year 2015.

9.3.4.2 Flow

9.3.4.2.1 Measured inflow

Natural streamflow, which is the flow that arrives in a dam without suffering any anthropologic influence, was estimated based on measured values of inflow and outflow recorded at each dam. For the proposed work, only the rivers Douro, Varosa and Tâmega were considered regularized rivers. However all sub-basins have small dams in their headwaters that regularize some of the stream. Since these dams are located so far upstream, there is a significant area between them and the dams on the Douro River that is not regularized.

Based on water elevation that is stored in a dam, the variation of stored water volume is calculated. Adding the outflow of the same dam to this result and subtracting the outflow of the upstream dam, the result will be the natural streamflow that arrives in the dam for which the variation of stored water was calculated. The calculation of natural streamflow that arrives in each dam can be expressed by the following equation:

$$NS_{dam} = \frac{\Delta V_{dam}}{86400} - QO_{dam-1} + QO_{dam} - QP_{dam} \tag{1}$$

Where NS_{dam} is the natural streamflow of each dam (m³/s), ΔV_{dam} is the variation of stored water (m3), $QO_{dam-1}$is the outflow of upstream dam (m³/s), $QO_{dam}$is the outflow of the dam (m³/s) and QP_{dam} is the pumped flow (m³/s). The variation of stored water results from the difference between the stored volumes on two consecutive days and can be expressed by the following equation:

$$\Delta V_{dam} = V_{d+1} - V_d \tag{2}$$

Where V_{d+1} is the volume stored in day d+1 (m³) and V_d is the stored volume in day d (m³). The stored volume on a specific day is estimated with an expression that relates stored volume with water elevation:

$$V_d = f(E_d) \tag{3}$$

Where E_d is the water elevation in day d (m).

Equation (1) is not a direct measurement of natural streamflow and its application can result in systematic errors. Figure 103 presents a black line that results from adding natural streamflow to Saucelle outflow. This result is compared with outflow in Crestuma (the grey line in Figure 103). This graph shows that both lines have a similar behaviour; however, there are differences that can be related to the time lag of streamflow to reach the Crestuma dam and to operational decisions of this dam. This means that if a longer period is analysed both lines should be identical. In the period between May and November 2015, the analysed period, Crestuma's outflow is 7% lower than

Saucelle's outflow plus natural stream flows. This difference can be justified by an overestimation of natural stream flows or an underestimation of Saucelle's outflow.

Natural streamflow estimation has an associated uncertainty which is essentially related with the estimation of the volume of water stored in the dam. On the other hand, the uncertainty in the outflow values of Saucelle is related to missing values in the SAIH system.

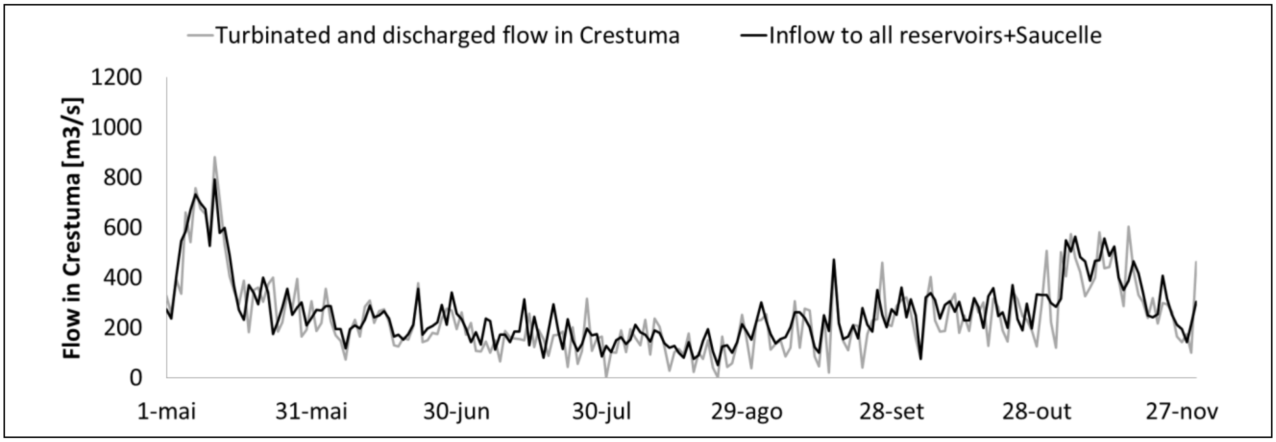

Figure 103 Comparison of natural streamflow estimated with equation (1) plus outflow in Saucelle and outflow in Crestuma (May to November 2015).

In Figure 104 the black line is the same black line of Figure 103 but now it is compared with the daily maximum and minimum simulated values which are represented by the grey area in graph of Figure 104

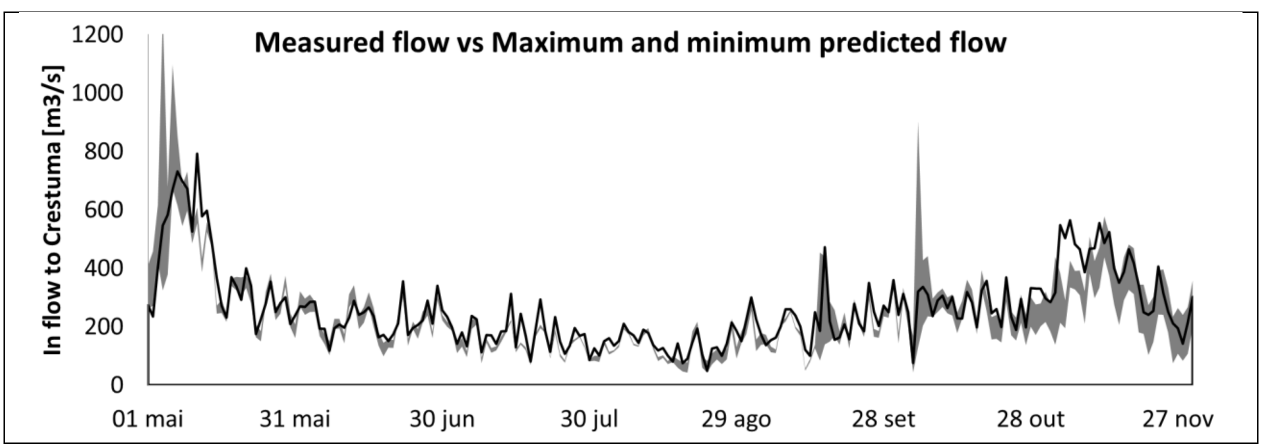

Figure 104 Comparison of simulated and measured flow.

Figure 105 presents the same analysis as Figure 104 but only for the Torrão dam. In Figure 105 it is clear that simulated values are similar to measured values. From the analysed period the peak flow of September 16 results from precipitation which occurred the day before (see Figure 102) and when seen in detail, it is possible to conclude that SWAT overestimated the flow and the peak flow occurs in September 15 while MOHID Land underestimated the flow but put it on the right day (September 16). After this event SWAT results started to be correct with MOHID Land results.

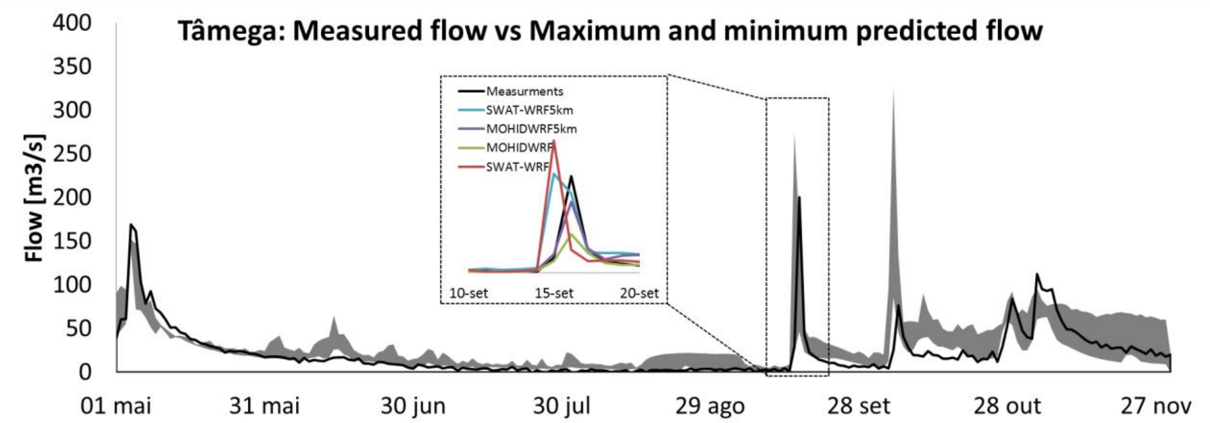

Figure 105 Comparison of flow predictions and measurement that arrive to Torrão dam.

The value of peak flow estimated to October is similar to that predicted for September which is explained by the similarity between predicted precipitations by WRF 12 km for both peak flows. However, the measured flow was lower than the simulated flow both in October and September.

9.3.5 Discussion and conclusion

The results presented here show that it is possible to implement a system that includes meteorological and hydrological models to predict natural stream flows.

This system has some uncertainty associated. The uncertainty in the system has many origins; however, the most significant sources of uncertainty are precipitation values (measured and simulated) and the uncertainty inherent to the hydrological model. All the uncertainties in the system will have an impact on the simulated streamflow values. On the other hand, streamflow values which result from streamflow measurements also have an associated uncertainty.

In general, the main problem of this system is related to the capability of predicting flow peaks. To improve this part of the system it is essential that high precipitation values are correctly and precisely simulated. However, it is also necessary to guarantee that initial conditions for water content in soil are correctly given to the model. This condition is totally dependent on what happens in the past in terms of precipitation. Presently, precipitation used to simulate the past is given by meteorological models, which are a result of the application of a range of equations and are corrected with some measurements, allowing a decrease in the uncertainty about precipitation. In the future, an alternative to this method could be to force hydrological models to run on the past only with measured precipitation. An improvement would be also the knowledge of the initial soil condition, which would be achieved using real time monitoring of soil water content.

9.3.6 References

ALENCOÃO, A. M. P. & PACHECO, F. A. L. 2009. Estimativa de parâmetros hidrológicos: dois modelos, um caso de estudo. Recursos Hídricos, 31.

APA 2012. Plano de gestão da região hidrográfica do douro. In: DHV (ed.).

CAETANO, C. & PACHECO, F. A. L. 2008. Modelação de escoamentos fluviais na região de Trás-os-Montes e Alto Douro utilizando o modelo SWAT. In: DOURO, U. D. T.-O.-M. E. A. (ed.) V Seminário de recursos geológicos ambeinete e ordenamento do território.

CHAMBEL-LEITÃO, P., RAMOS, T., DOMINGOS, T. & NEVES, R. 2015. Mohid Land-Porous Media, a Tool for Modeling Soil Hydrology at Plot Scale and Watershed Scale. The Open Hydrology Journal, 9.

CHD. 2016. Confederación Hidrográfica del Duero [Online]. Available: http://www.chduero.es [Accessed 02 de Janeiro de 2016.

EDP 2015. Declaração Ambiental Aproveitamentos Hidroelétricos da EDP Produção. In: PRODUÇÃO, E. (ed.). Lisboa: EDP.

LACERDA, M. A., RODRIGUES, C. M., RODRIGUES, R. R., RODRIGUES, A. C., RODRIGUES, A., SARAMAGO, M., BRANDÃO, C. & DIOGO, P. A. APRH-SIMPÓSIO SOBRE APROVEITAMENTOS HIDROELÉCTRICOS. APRH-SIMPÓSIO SOBRE APROVEITAMENTOS HIDROELÉCTRICOS, 1997.

MADUREIRA, C. & BATISTA, V. J. M. 2002. Hidroelectricidade em Portugal: memória e desafio. In: NACIONAL, R. R. E. (ed.). Lisboa.

MATEUS, M., ALMEIDA, C., BRITO, D. & NEVES, R. 2014. From eutrophic to mesotrophic: Modelling watershed management scenarios to change the trophic status of a reservoir. International journal of environmental research and public health, 11, 3015-3031.

PORTELA, M. M. & HORA, G. R. Aplicação da fórmula racional à analise de cheias em Portugal Continental: valores do coeficiente C". Congresso da Água, Porto, 2002.

PULIDO-CALVO, I. & PORTELA, M. M. 2007. Aproximaciones neuronales univariantes para la predicción de caudales diarios en cuencas portuguesas. Ingeniería del agua, 14, 97-111.

RODRIGUES, R., BRANDÃO, C. & COSTA, J. 2003a. Breve Nota sobre as Cheias no Tejo e o seu Sistema de Vigilância e Alerta. In: INAG (ed.). Lisboa, Instituto da Água.

RODRIGUES, R., BRANDÃO, C. & PINTO DA COSTA, J. 2003b. As cheias no Douro ontem, hoje e amanhã. In: SNIRH (ed.). INAG.

SANTOS, C. M. M. 2009. Necessidade e Disponibilidade de Água para uma Gestão Hídrica Eficiente na Bacia Hidrográfica do Sôrdo. Master, UNIVERSIDADE DE TRÁS-OS-MONTES E ALTO DOURO.

SANTOS, M. A., RODRIGUES, R. & CORREIA, F. 1997. Technical communication: on the European water resources information policy. Water resources management, 11, 305-322.

TRANCOSO, A. R., BRAUNSCHWEIG, F., CHAMBEL-LEITAO, P. C., OBERMANN, M. & NEVES, R. 2009. An advanced modelling tool for simulating complex river systems. Science of the Total Environment, 407, 3004-3016.